CRANFIELD INSTITUTE OF TECHNOLOGY

DEPARTMENT OF FLUID ENGINEERING AND INSTRUMENTATION

Ph.D Thesis

Academic Years 1980-1983

J.M. HASSAN

TRANSIENTS CAUSED BY LOAD CHANGES ON A TURBOGENERATOR SET

Supervisor: K.J. Enever

October 1983

TO MY WIFE

ACKNOWLEDGEMENTS

The work in this thesis was carried out under the supervision of Dr. K.J. Enever. I wish to express my heartfelt thanks to Dr. Enever for suggesting this interesting work and without his constant encouragement and advice throughout, this thesis would not have come to fruition.

I am grateful to the Head of the Fluid Engineering Unit, Professor R.C. Baker for his encouragement and co-operation.

I wish to acknowledge the valuable discussions I have had with Dr. J. Heritage, Mr. K. Spendel, Miss J. Deacon (FEU) and Mr. D.J. Lewis and Mr. P.S. Collins (SESD).

I would like to thank the staff of BHRA especially Mr. J. Stanton and the Instrumentation Department. Also Mr. P.R. Bull for taking the photographs of the rig.

I express my deepest gratitude to my friend Mr. A. El-Zafrany (SME) for his invaluable help by day as well as by night and, in particular, all he has taught me of computing.

Thanks are also due to John Parker and Dave Wallace who helped me in constructing and doing the heavy jobs on the rig. Without their help I would have required superhuman effort to keep the experiment going.

Finally Mrs. Mary Shields deserves special mention for converting my handwriting into this neatly typed report.

CONTENTS

		Page
CHAPTER 1	INTRODUCTION	1
	1.1 General	1
	1.2 General Description of Hydroelectric Plants	1
	1.3 Nature of the Transients Problem	2
	1.4 The Present Work	2
	1.4.1 Objective	2
	1.4.2 Layout of this work	3
CHAPTER 2	LITERATURE REVIEW	5
	2.1 Computational Methods	5
	2.2 Governing Stability	6
CHAPTER 3	THEORETICAL ANALYSIS	9
	3.1 Turbine and the Conduit System	9
	3.1.1 Representation of the conduit	9
	3.1.2 Representation of the turbine	10
	3.1.3 Turbine-Generator Torque equation	13
	3.2 Derivation of Boundary Conditions	14
	3.2.1 Upstream boundary	17
	3.2.2 Downstream conditions	18
	3.3 Proportional-Integral-Derivative Governor	20
	3.3.1 General	20
	3.3.2 Representation of the governor	20
	3.3.2.1 Phase-locked loop	20
	3.3.2.2 Analogue multiplier	23
	3.3.2.3 Controller	23
	3.3.2.4 Smoothing network	25
	3.3.2.5 Actuator	26
	3.4 Bivariate Lagrangean Interpolation	28
	3.4.1 General	28
	3.4.2 Derivation	28
	3.4.3 Piecewise Lagrangean Interpolation	30
	3.4.4 The advantage of Lagrangean Interpolation	30
CHAPTER 4	EXPERIMENTAL PROCEDURE	32
	4.1 Description of the Rig	32
	4.2 The Control Circuit	33
	4.3 Stability of the PID Controller	40
	4.4 Instrumentation	45
	4.4.1 Inlet pressure measurement	45
	4.4.2 Flowrate measurement	49
	4.4.3 Speed measurement	55
	4.4.4 Gate opening measurement	59
	4.5 Experimental Method	62

		Page
CHAPTER 5	COMPUTATIONAL PROCEDURE	64
	5.1 Introduction	64
	5.2 Functions	64
	5.2.1 Function FACT(I,J,K,L,PHIO)	64
	5.2.2 Function FLAG1(N,X,I,X_O)	65
	5.2.3 Function FLAG(I,J,PHIO)	65
	5.2.4 Function DLAG(I,J,PHIO)	66
	5.2.5 Function D2LAG(I,J,PHIO)	66
	5.2.6 Function TAUF(PHIO,QI)	66
	5.2.7 Function ZI(TAUI,PHII,Z,ID)	68
	5.3 Subroutines	69
	5.3.1 Subroutine DATA(IDATA)	69
	5.3.2 Subroutine LINEAR(TAUI,PHII,QI, AO,A1)	69
	5.3.3 Subroutine PARABOLIC(TAUI,PHII, CO,C1,C2)	70
	5.3.4 Subroutine ITER(N,QP,TAUI,PHII, HN,HP,CP,IC)	70
	5.3.5 Subroutine RUNG(PHII,TAOI,HN)	72
	5.3.6 Subroutine CHARACTER(IC,C_p)	72
	5.4 The Main Programme	73
	5.5 Summary of the Computational Procedure	73
	5.6 Flow Charts	75
CHAPTER 6	COMPUTATIONAL AND EXPERIMENTAL RESULTS	93
	6.1 Introduction	93
	6.2 Full Load Rejection	93
	6.3 Partial Load Reduction	95
CHAPTER 7	CONCLUSIONS AND FURTHER WORK	121
	7.1 Conclusions	121
	7.2 Suggestions for Further Work	122
APPENDIX A	DESIGN OF THE CONTROL CIRCUIT	123
	A.1 Phase Lock Loop	123
	A.2 Proportional Element	124
	A.3 Integrator Circuit	125
	A.4 Derivative Circuit	128
	A.5 Smoothing Network	130
APPENDIX B	EXPERIMENTAL RESULTS	131
APPENDIX C	INITIAL CONDITION DATA AND TURBINE CHARACTERISTIC DATA	136
APPENDIX D	DERIVATION OF FIRST AND SECOND ORDER LAGRANGEAN INTERPOLATION EQUATIONS	140
	Derivation of equation (5.7)	140
	Derivation of equation (5.8)	141

		Page
APPENDIX E	COMPUTER LISTING	142
REFERENCES		153

FIGURES

Number		Page
1.1	A typical Hydro-power unit	4
3.1	Characteristic of Francis turbine Unit Flow vs. Unit Speed	11
3.2	Characteristic of Francis turbine Unit Power vs. Unit Speed	12
3.3	The Turbine and Pipework	15
3.4	Block Diagram of PID Governor	21
4.1	The Control Circuit	34
4.2	Stepping motor drive (Logic Circuit)	37
4.3	Basic Stepping Motor Circuit	38
4.4	Voltage Inverting Threshold Circuit	39
4.5	Bode Magnitude Plot	42
4.6	Bode Phase-angle Plot	43
4.7	Bode Plots resultant	44
4.8	Dual range dead-weight pressure gauge tester	46
4.9	The Calibration Circuit of Pressure Transducer	47
4.10	Calibration curve of the Pressure Transducer	48
4.11	The orifice plate arrangement	50
4.12	Calibration Circuit of Differential Pressure Transducer	53
4.13	Calibration Curve of Differential Pressure Transducer	54
4.14	Variable Reluctance Tachometer	56
4.15	Calibration Curve of the Turbine speed (rpm)	58
4.16	Schematic and Block Diagram of the Potentiometer	59
4.17	Calibration Curve of the Gate opening (%)	61
6.1	Speed against Time Comparison of Experiment and Theory 100% load rejection	97
6.2	Flowrate against Time Comparison of Experiment and Theory 100% load rejection	98
6.3	Gate Opening against Time Comparison of Experiment and Theory 100% load rejection	99
6.4	Head Rise against Time Comparison of Experiment and Theory 100% load rejection	100
6.5	Speed against Time Comparison of Experiment and Theory 80% load rejection	101
6.6	Flowrate against Time Comparison of Experiment and Theory 80% load rejection	102
6.7	Head Rise against Time Comparison of Experiment and Theory 80% load rejection	103
6.8	Gate Opening against Time Comparison of Experiment and Theory 80% load rejection	104
6.9	Speed against Time Comparison of Experiment and Theory 63% load rejection	105
6.10	Flowrate against Time Comparison of Experiment and Theory 63% load rejection	106
6.11	Head Rise against Time Comparison of Experiment and Theory 63% load rejection	107
6.12	Gate Opening against Time Comparison of Experiment and Theory 63% load rejection	108

Number		Page
6.13	Speed against Time Comparison of Experiment and Theory 31% load rejection	109
6.14	Flowrate against Time Comparison of Experiment and Theory 31% load rejection	110
6.15	Head Rise against Time Comparison of Experiment and Theory 31% load rejection	111
6.16	Gate Opening against Time Comparison of Experiment and Theory 31% load rejection	112
6.17	Speed against Time Comparison of Experiment and Theory 10% load rejection	113
6.18	Flowrate against Time Comparison of Experiment and Theory 10% load rejection	114
6.19	Head Rise against Time Comparison of Experiment and Theory 10% load rejection	115
6.20	Gate Opening against Time Comparison of Experiment and Theory 10% load rejection	116
6.21	Speed against Time Comparison of Experiment and Theory full/partial load rejection	117
6.22	Flowrate against Time Comparison of Experiment and Theory full/partial load rejection	118
6.23	Head Rise against Time Comparison of Experiment and Theory full/partial load rejection	119
6.24	Gate Opening against Time Comparison of Experiment and Theory full/partial load rejection	120

PLATES

3.1	The Turbine and the Pipework	16
4.1	The Control Circuit	35
4.2	The Tachometer	57
4.3	The Stepping Motor and the Connected gears	60

NOMENCLATURE

a	Waterhammer wave velocity (m/s)
A	Cross-sectional area of pipe (m^2)
D	Pipe diameter (m)
D_R	Turbine runner diameter (m)
f	Darcy-Weisbach friction factor
g	Acceleration due to gravity (m/s^2)
H_A	Piezometric head at beginning of time step at Δx from turbine (m)
H_n	Net head (m)
H_p	Piezometric head at end of time step at turbine inlet (m)
H_t	Tailwater level above datum (m)
I	Moment of inertia of rotational parts (Kg m^2)
K_D	Gain of derivative element
K_E	Voltage constant of step motor (volts/radian)
K_I	Magnetic null displacement constant of step motor (radians/amp)
K_m	Constant of analogue multiplier
K_p	Gain of proportional element
n	N/N_r
N	Rotational speed (rpm)
N_r	Rated speed (rpm)
P_g	Power of generator (KW)
P_t	Power of turbine (KW)
p	Unit power
q	Unit flow
Q_A	Flow at beginning of time step at Δx from turbine (m^2/s)
Q_e	First estimate of Q_p (m^3/s)
Q_p	Flow at the end of time step at turbine inlet (m^3/s)
R	Resistance of step motor windings
S	Laplace operator
T_A	Smoothing network time constant
T_D	Time constant of the derivative element
T_I	Time constant of the integral element
T_s	Time constant of step motor winding
T_U	Unbalanced torque (Nm)
Δt	Time step (s)
V_A	Smoothing network output

V_D	Output of derivative element
V_I	Output of integral element
V_p	Output of proportional element
Δx	a Δt
Z	Input to derivative, integral and proportional elements
ηg	Generator efficiency
ηt	Turbine efficiency
σ	Permanent speed droop
ϕ	Unit speed
ω	Rotational speed (rads/s)
J	Total load moment of inertia referred to motor shaft
j	$\sqrt{-1}$
ζ	Damping ratio

CHAPTER 1

INTRODUCTION

1.1 GENERAL

Nearly all prime movers used in hydroelectric power systems are equipped with governors by means of which their speed can be controlled automatically. Recently the control of the proportional-integral-derivative governor for hydroelectric systems has achieved world wide interest because of its faster response, small size and higher accuracy and sensitivity than mechanical governors. In order to place the subject of this study within a somewhat more general framework, the scheme of a hydroelectric power unit must first be explained.

1.2 GENERAL DESCRIPTION OF HYDROELECTRIC PLANTS

Figure 1.1 shows the interconnection of the principal elements of a typical hydroelectric installation with a simple surge tank.

The supply reservoir stores the water which is finally delivered to the exhaust reservoir at lower elevation. The water flows from the supply reservoir to the surge tank through a supply line which may be either a free-flowing channel or a concrete aqueduct. The latter is generally called the conduit, while the supply line between the surge tank and the turbine (which must withstand higher pressure than the conduit and is therefore constructed differently) is called the penstock.

The penstock delivers the flow to the turbine from the surge tank, either as shown in the Figure or, in the case of concentrated fall (no surge tank), installations, directly from the supply reservoir. The wicket gates, or movable vanes, act as structural modulators of the turbine water consumption and thereby determine the generated power. The turbine transduces the fluid power of the supply stream to mechanical power which is in turn transduced to electrical power by the generator. The water, having spent much of its available energy, is exhausted through the draft tube into the tailrace.

1.3 NATURE OF THE TRANSIENTS PROBLEM

Change in the power demand of the load centre served by a hydroelectric power system initiates a period of complex unsteady behaviour the effects of which are transmitted to every part of the system from the load centre through the transmission system and into the various mechanical and hydraulic components of the power plants. The transients problem may be characterized by the following chain of interrelated events: the load change propagates over the transmission line (Figure 1.1), to the generator resulting in modification of the electrical resisting torque seen by the generator rotor; this results in an unbalanced torque on the turbine-generator unit which causes a change in the rotational speed of the unit; the speed variation activates the governor which alters the turbine gate opening; the changed gate position alters the amount of discharge through the gate thus initiating unsteady effects in the hydraulic system which appear as level changes in the surge tank and as rapidly propagated pressure fluctuations; these affect the turbine head and discharge thus producing new speed variations which, in turn, initiate a new sequence of transient effects throughout the entire system. At all stages of the process, reflection and dispersion of the propagating quantities and damping (electrical, mechanical and hydraulic), create interactions and forces which greatly complicate the process but which, in properly designed systems, limit the magnitude of the transient effects and prevent an unstable response to the load changes from occurring. It is the task of the designer to ensure that the magnitudes of these effects are kept within acceptable limits and that unstable response cannot occur under any possible load change conditions.

1.4 THE PRESENT WORK

1.4.1 Objective

The objective of this work can be summarized in the following points:

(a) To develop a computer program using an improved interpolation technique to deal with the turbine

boundary conditions making use of piecewise Lagrangean interpolation.

(b) To design and build a proportional plus integral plus derivative (PID) governor to control a small turbine installed in the laboratory.

(c) To study the stability of a PID governor using a Bode plot method.

1.4.2 Layout of this work

In Chapter 1 the nature of the transients problem and a scheme of a hydroelectric power plant has been described.

Chapter 2 contains a review of the works of others which is of particular relevance to this thesis.

In Chapter 3 the mathematical representation of the system and the derivation of the boundary conditions has been explained. Also a general explanation of Lagrangean interpolation technique and the derivation of the Lagrangean interpolation equations and the advantages and accuracy of this type of interpolation has been explained.

Chapter 4 explains the rig and the design of the proportional-integral-derivative governor. Also the stability limit of the governor has been found making use of the Bode plot method. All the instruments used are described together with an estimate of their accuracy.

Chapter 5 contains the description of the computer program and the computational procedure. A flow chart for each part of the program and the main program has been drawn.

Chapter 6 describes a comparison between the computational and experimental results and presents a plot for each test.

Chapter 7 contains the conclusions of the thesis and some suggestions for further work.

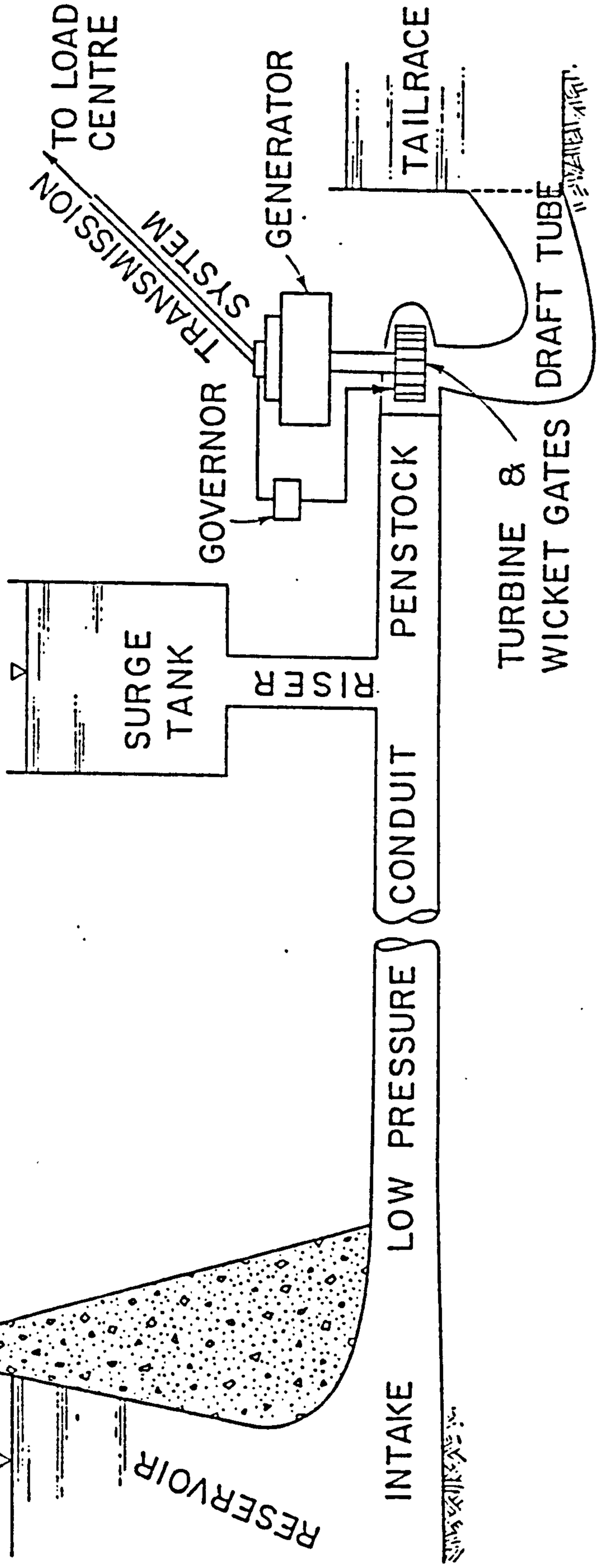

Figure 1.1 A typical hydro-power unit
(after Ref.3)

CHAPTER 2

LITERATURE REVIEW

2.1 COMPUTATIONAL METHODS

Investigation of transients caused by governed hydraulic turbines began with the advent of the turbines and Control Systems. Early methods of computation are well covered by C. Jaeger in his book "Engineering Fluid Mechanics" (Ref.1).

Swiecicki (Ref.2), 1961, investigated the regulation characteristics of a hydraulic turbine by using a step-by-step arithmetical integration. Equations were developed to calculate speed and pressure transients of a hydraulic turbine during a load change. A computer program was developed (Ref.3), in which the dynamic and continuity equations were solved by an implicit finite-difference method. The turbine characteristics were included in a simplified form and the governor was represented by a linear third-order ordinary differential equation having constant coefficients i.e. the saturation of various elements was not included. Wozniak and Fett (Ref.4) developed a computer program for closed-loop simulation of the transient behaviour of a hydroelectric power plant. In this program the governor nonlinearities were included and the conduits were represented by a Maclaurin series expansion of the closed-form solution of the linearized partial differential equations. Streeter and Wylie (Ref.5) presented a mathematical model in which a method of characteristics was used to simulate the conduit. Turbine characteristics were included and the governor was represented by a second-order ordinary differential equation. Chaudhry (Ref.6) presented another mathematical model in which turbine characteristics were globally represented. A method of characteristics was used to solve the continuity and dynamic equations representing transient flow in closed conduits. A temporary-droop governor was represented by five first-order differential equations and all major nonlinearities of the governor were included. Two iteration loops were required to solve the equations. In another computer program (Ref.7), the number of iteration loops were reduced to one by combining the equation of the

instantaneous speed change with equations of the governor and a solution was obtained by the fourth-order Runge-Kutta method. The finite difference method was used in dealing with turbine characteristics.

2.2 GOVERNING STABILITY

The speed oscillations of a turbogenerator in a hydroelectric power system are caused by load change. To control these oscillations a temporary droop governor or a PID (Proportional, Integral, Derivative) governor is usually provided. These oscillations may be either stable or unstable depending on the value of the parameters which are the temporary speed droop and the dashpot time constant in a temporary droop governor and the proportional, integral and derivative gains in a PID governor.

Paynter (Ref. 8). presented a stability limit curve and suggested optimum values of the governor settings by solving the problem on an analogue computer. Hovey (Ref. 9). derived a similar stability curve theoretically, i.e. the differential equations of the system were derived with the main parameters involved in the speed transient of the turbine following a load change. All non linear relationships were assumed to be linear and he applied his analysis to a practical power system. The work of Paynter and Hovey, which treated the case of a temporary droop governor, neglected the following factors:-

(1) The steady state speed droop.
(2) The net damping torque.
(3) The mechanical inertia of the rotating leads.

Chaudhry (Ref. 10) extended the work of Hovey to include the effects of gate feed-back and self-regulation. His work shows that the stability boundaries are greatly extended when these factors are included. Hovey and Chaudhry established the stability boundaries by first setting up a third order differential equation in speed and then applying the Routh-Hurwitz criterion.

Thorne and Hill (Ref. 11) were the first to apply the state-space approach to the study of PID governors and examined the

stability boundary as a function of proportional gain, integral gain, system damping and turbine loading. Furthermore, an operating boundary is derived from the time-response requirements of the governor. Thorne and Hill's work was undertaken with the following limiting conditions:-

(1) The unit steady state speed regulation was set at zero.
(2) The remaining equivalent system operated with a blocked governor.
(3) No account was taken of the derivative gain effect on stability.
(4) No effect of interconnection to neighbouring utilities was considered.

Dhaliwal and Wichert (Ref. 12) also used the state-space approach to study PID governors in a multi-machine system in isolated operation. While the effect of governor derivative gain on the stability was considered, no stability boundary was defined. Their work used an ideal simplified relationship between mechanical torque and gate opening and neglected damping torque due to the prime mover and generator. A high derivative gain can cause the system to go unstable.

The works of Hovey and Chaudhry are expanded to show the stability boundaries of a hydraulic turbine generating unit having a PID governor by Hagihara et al (Ref. 13). They established the stability boundaries by setting up a fourth order differential equation in speed and then applying the Routh-Hurwitz criterion. The effect of derivative gain was studied, not directly but through the intermediary of a parameter that also implicates the proportional gain and the water start time. Hagihara et al used an ideal simplified model of the hydraulic conduit, i.e. the relationship between mechanical torque and gate.

D.T. Phi et al (Ref. 14) investigated the incident of unstable frequency oscillation that occurred on March, 1977, following a major system disturbance on the New Brunswick power system. Their

work was extended and complemented by other authors (Refs. 10-13), taking into account more parameters and more varied operating conditions.

CHAPTER 3

THEORETICAL ANALYSIS

In this Chapter the mathematical representation of the system is based largely on Chaudhry (Refs. 6,7) with the exception of the method of dealing with the boundary conditions.

3.1 TURBINE AND THE CONDUIT SYSTEM

3.1.1 Representation of the Conduit

The method of characteristics and the boundary conditions presented in the standard manner, (Ref.6), was used to analyse the pipework system.

In the method of characteristics the partial differential equations are converted into ordinary differential equations which are then solved by finite-difference technique. A summary of the necessary equations is given below, for details see Ref.6.

For an intermediate section of a pipework:

$$QP_I = 0.5\ (C_p + C_n) \tag{3.1}$$

$$HP_I = 0.5\ \left(\frac{C_p - C_n}{C_a}\right) \tag{3.2}$$

in which

$$C_p = Q_{I-1} + C_a H_{I-1} - \frac{f\Delta t}{2DA} Q_{I-1}/Q_{I-1}/ \tag{3.3}$$

$$C_n = Q_{I+1} - C_a H_{I+1} - \frac{f\Delta t}{2DA} Q_{I+1}/Q_{I+1}/ \tag{3.4}$$

$$C_a = \frac{gA}{a} \tag{3.5}$$

For the upstream end

$$Q_{P_1} = C_n + C_a H_{P_1} \tag{3.6}$$

For the downstream end

$$Q_{P_{n+1}} = C_p - C_a H_{P_{n+1}} \tag{3.7}$$

In the above equations, Q is the transient flow, a is the pressure wave speed, Δt is the time-step chosen for the calculation, A is the cross-sectional area of the pipe, D is its diameter, f is its friction factor, H is the piezometric head, subscript P_I indicates conditions at Section I at the end of a time-step and the subscripts I, I-1, I+1 denote conditions at these pipe sections at the beginning of a time-step.

The unknown flowrate and piezometric head at point I are expressed in terms of their known values at points I+1 and I-1.

3.1.2 Representation of the turbine

The relationship between the net head and discharge has to be specified to simulate a turbine in a hydraulic transient model. Flow through a turbine depends upon various parameters: for example, the flow through a Francis turbine depends upon the net head, rotational speed of the unit and wicket gate opening. Curves representing the relationship between these parameters are called turbine characteristics. These curves are obtained from tests conducted on the model of the turbine runner.

The characteristic curves for the turbine used in the laboratory are shown in Figures 3.1 and 3.2. In these Figures, the abcissae are the unit speed, ϕ, and the ordinates are the unit flow q, and the unit power, p. Definitions of ϕ, q and p used are:-

$$\text{Unit speed } \phi = \frac{D_R\, N}{84.45\sqrt{H_N}} \tag{3.8}$$

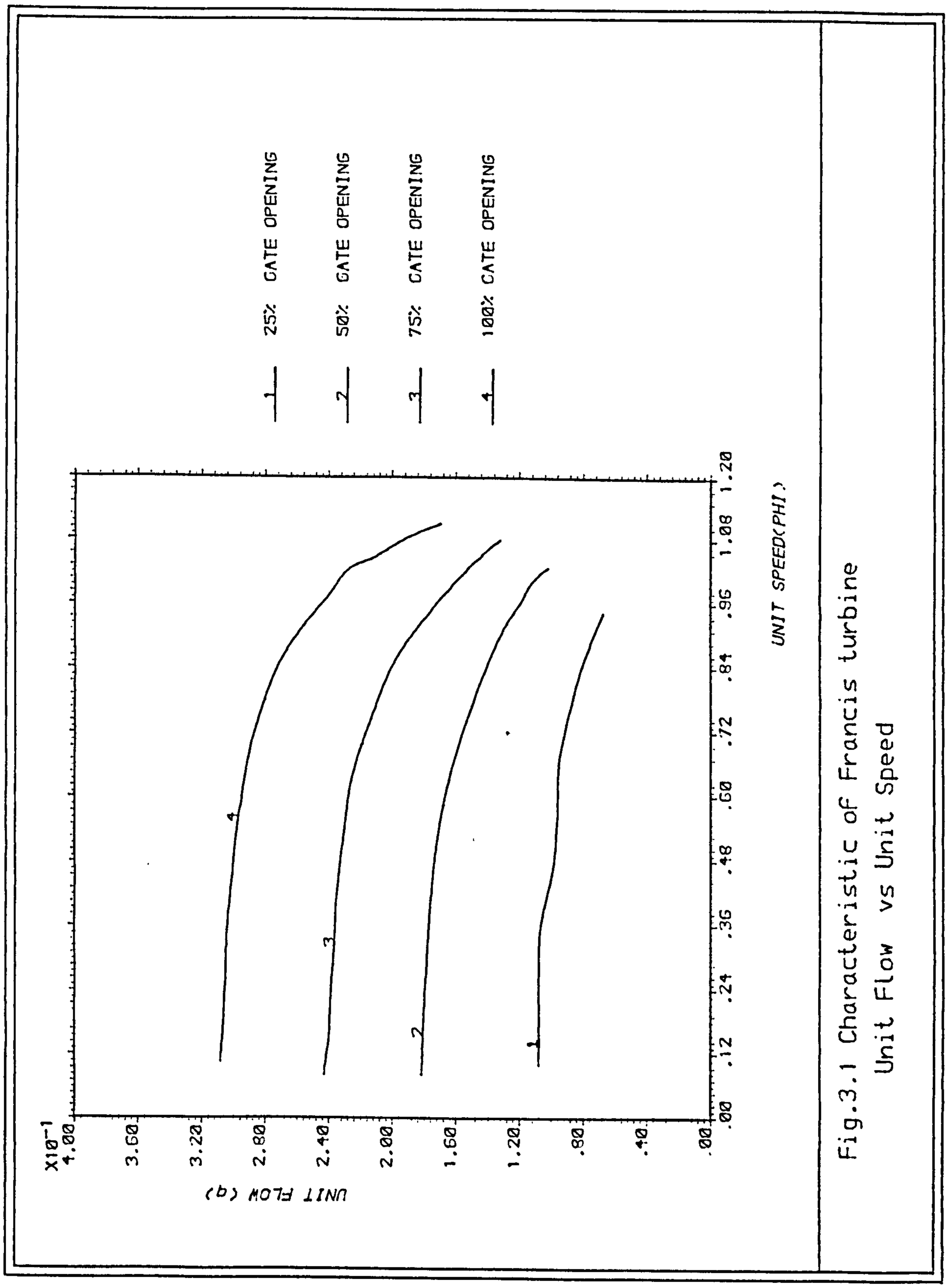

Fig.3.1 Characteristic of Francis turbine
Unit Flow vs Unit Speed

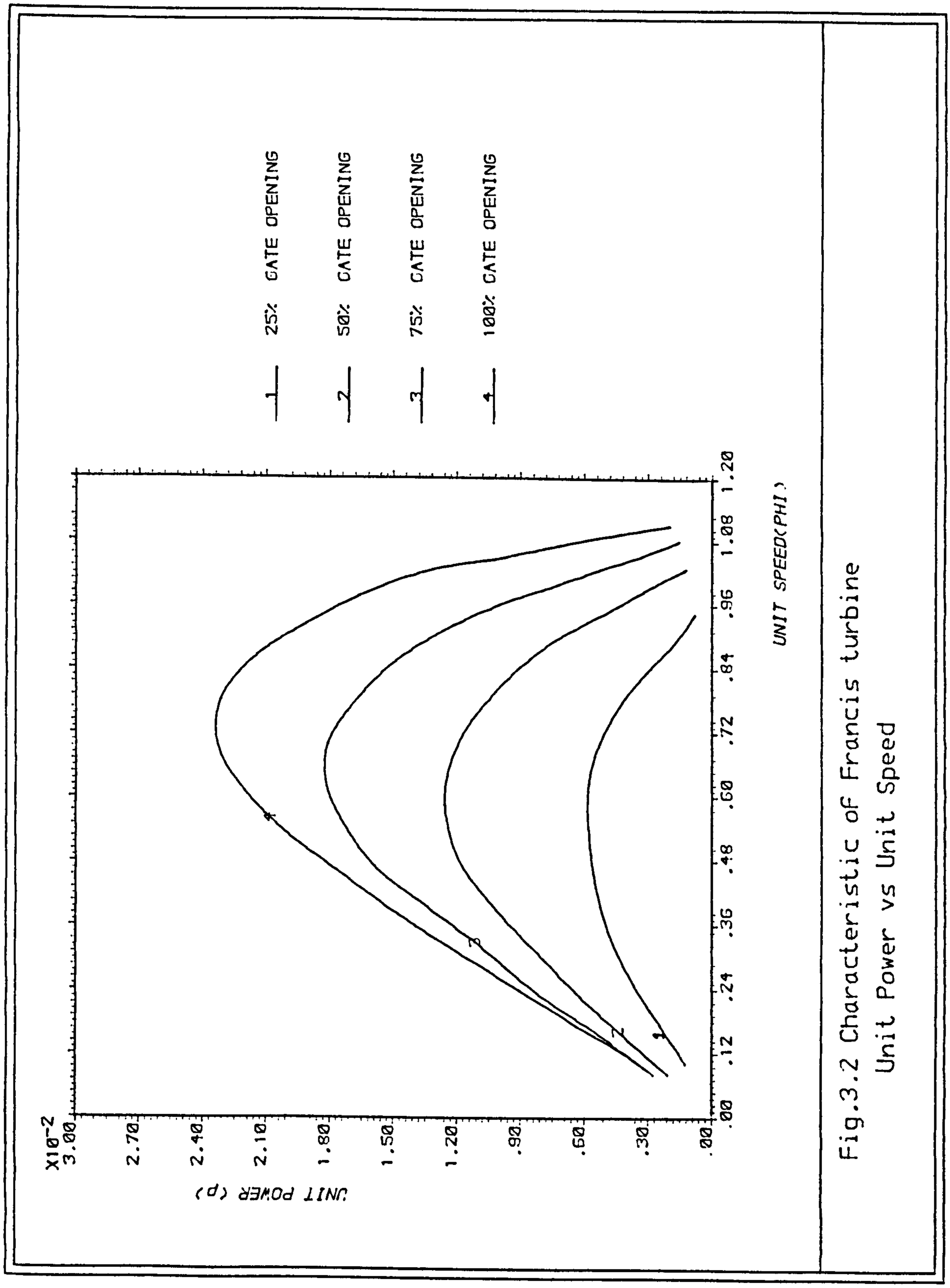

Fig.3.2 Characteristic of Francis turbine
Unit Power vs Unit Speed

$$\text{Unit flow } q = \frac{Q_p}{D_R^2 \sqrt{H_N}} \tag{3.9}$$

$$\text{Unit power } p = \frac{P_t}{D_R^2 H_N^{3/2}} \tag{3.10}$$

In these definitions D_R is the turbine runner diameter, N is the rotational speed, H_N is the net head, Q_p is the flowrate at the turbine, and P_t the power of the turbine.

A grid of points on the characteristic curves for various gate openings was stored in the computer and the unit flow, unit power and unit speed at intermediate gate opening were determined by using Bivariate Lagrangean interpolation.

3.1.3 Turbine-Generator Torque Equation

The speed of the turbogenerator set increased due to unbalanced torque (T_u) after load reduction such that:-

$$T_u = I \frac{d\omega}{dt} \tag{3.11}$$

in which I is the moment of inertia of the rotating parts of the turbo-generator set and ω is the rotational speed of the unit in radians/s. Equation (3.11) may be written as:-

$$P_t - \frac{P_g}{n_g} = I\,\omega \frac{d\omega}{dt} \tag{3.12}$$

Hence

$$\frac{dn}{dt} = \frac{91.19}{I\,N_R^2\,n}\left(P_t - \frac{P_g}{n_g}\right) \tag{3.13}$$

in which P_g is the final generator load, $n = N/N_R$ and N_R is the synchronous speed.

In equation (3.13) there are two unknowns n, P_t and we need another equation for a unique solution. This equation is provided as follows.

The characteristics for unit power (p) for a particular gate opening (τ) may be approximated by a parabola over a small speed range, so

$$p = C_0 + C_1\phi + C_2\phi^2 \tag{3.14}$$

where C_0,C_1 and C_2 can be determined by Lagrangean interpolation.

Using equations (3.8) and (3.10) into equation (3.14)

$$P_t = a_7 + a_8 n + a_9 n^2 \tag{3.15}$$

where

$$a_7 = C_0 \, D_R^2 \, H_N^{1.5}$$

$$a_8 = C_1 \, D_R^3 \, N_R \, H_N/84.45$$

$$a_9 = C_2 \, D_R^4 \, N_R^2 \, \sqrt{H_N}/(84.45)^2$$

i.e. equation (3.13) can be written as:

$$\frac{dn}{dt} = \frac{91.19}{I \, N_R^2 \, n}\left(a_7 + a_8 n + a_9 n^2 - \frac{P_g}{n_g}\right) \tag{3.16}$$

Hence equation (3.16) may be integrated by the fourth-order Runge-Kutta method (Ref.15), together with the equations of the governor given in the following section.

3.2 DERIVATION OF BOUNDARY CONDITIONS

The laboratory set up is shown in Figure 3.3 and Plate 3.1. Special boundary conditions are required to represent the conditions at the upstream and downstream ends of the system.

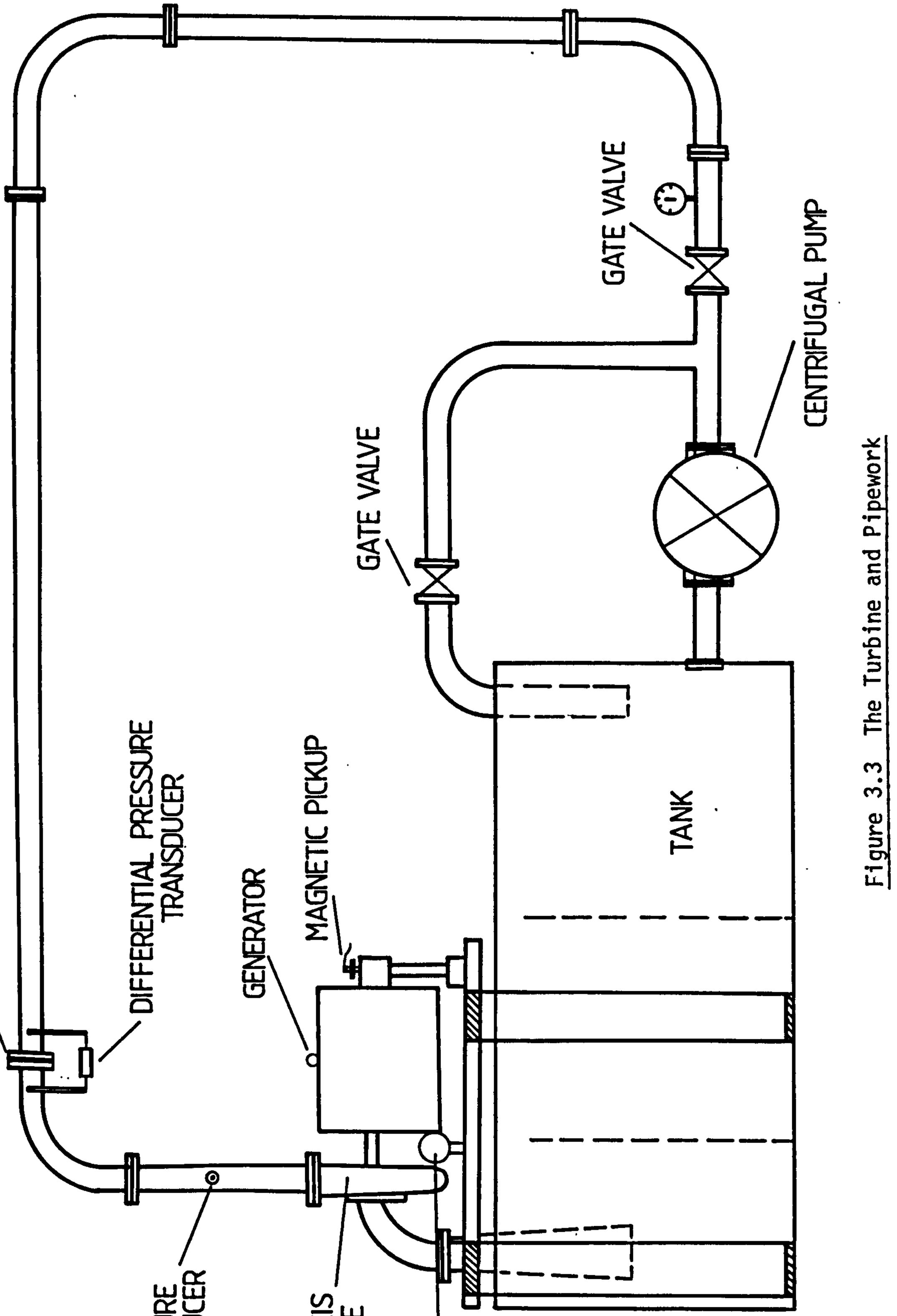

Figure 3.3 The Turbine and Pipework

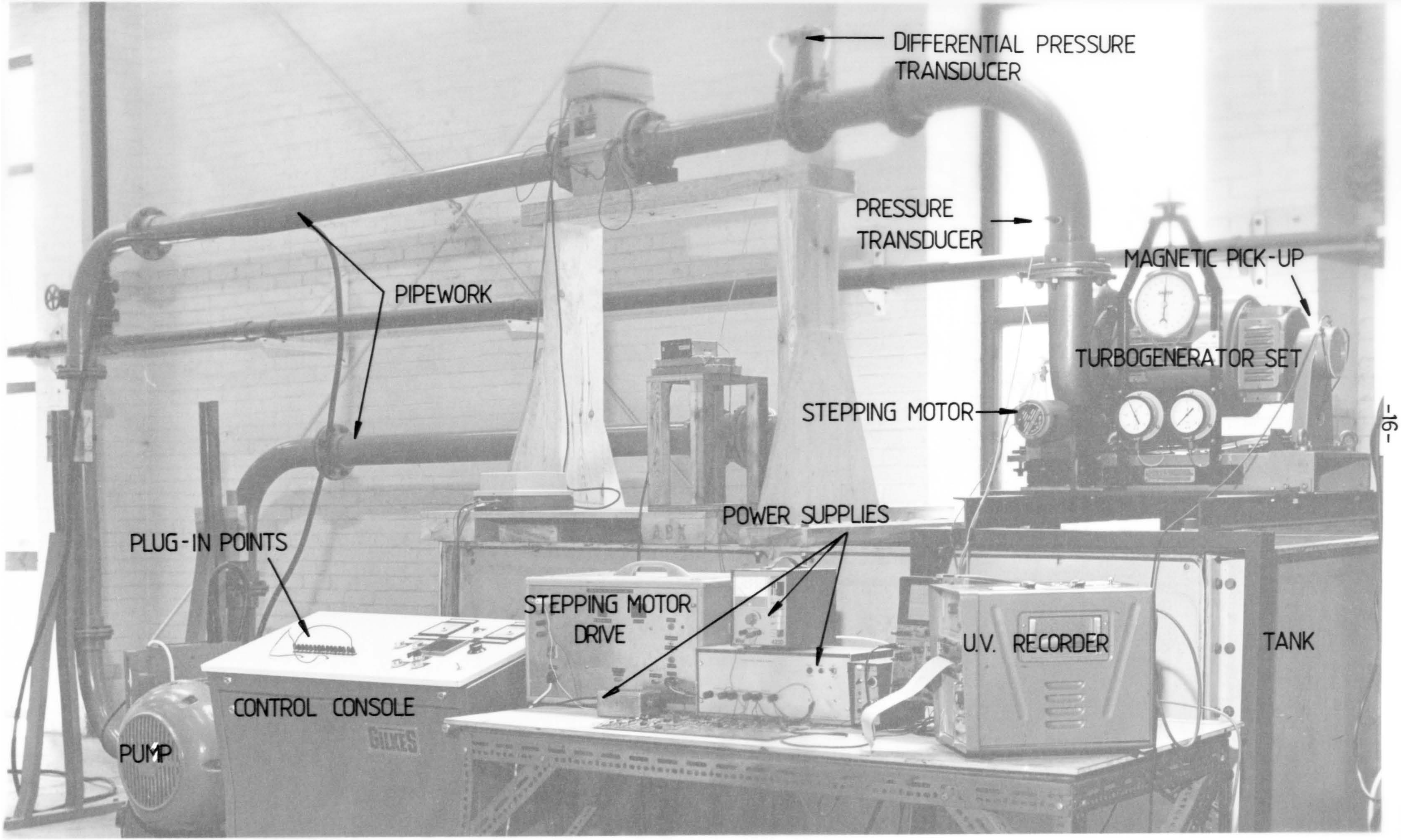

PLATE 3·1 THE TURBINE AND PIPEWORK

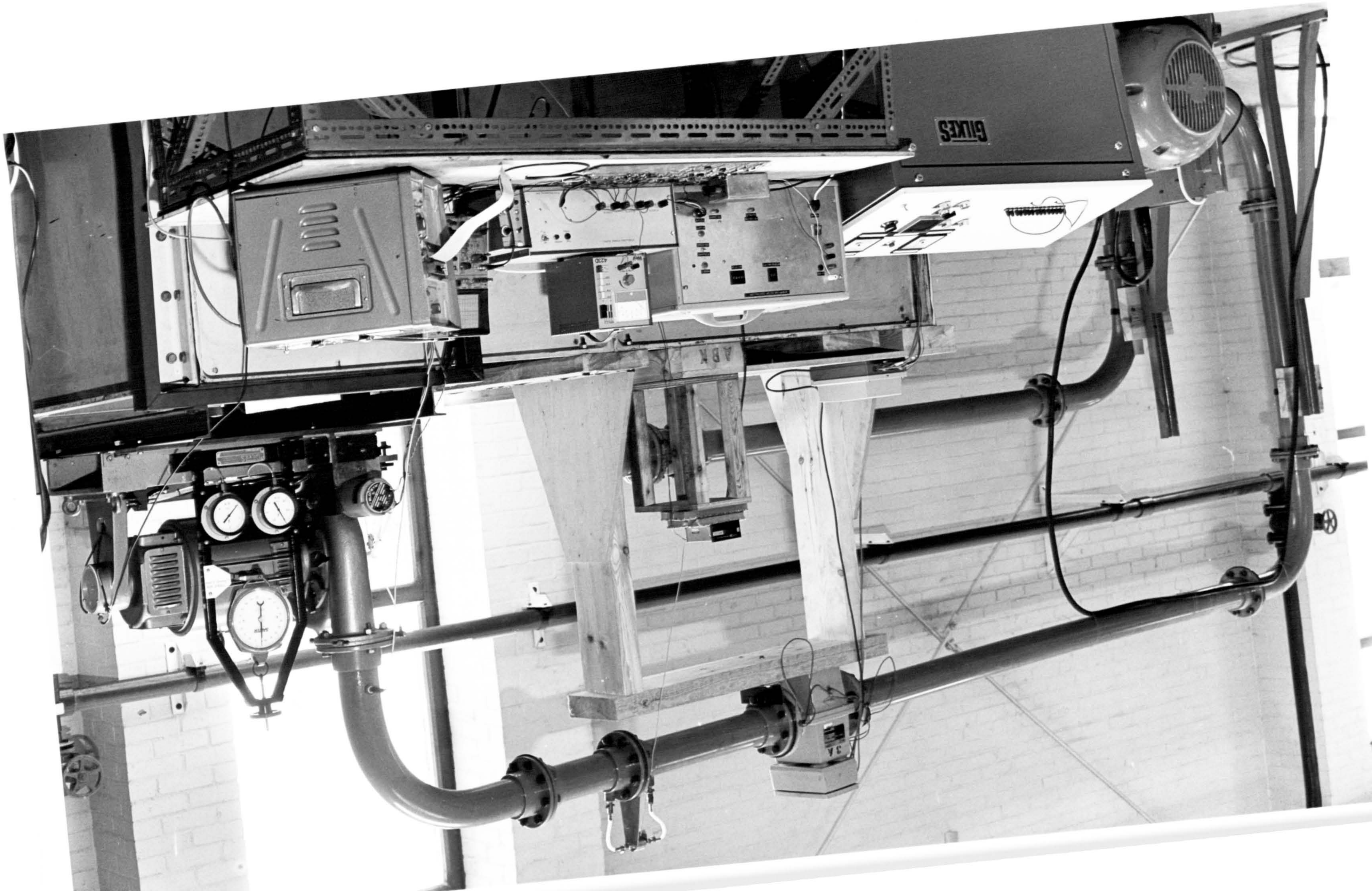
GILKES
ADK

3.2.1 Upstream Boundary

The input to the system was supplied by a pump, but a large pump with a by-pass was used so that a required combination of head and flow could be obtained without having to match the pump characteristics. As shown below the relation between the pump, the conduit and the by-pass was derived as follows.

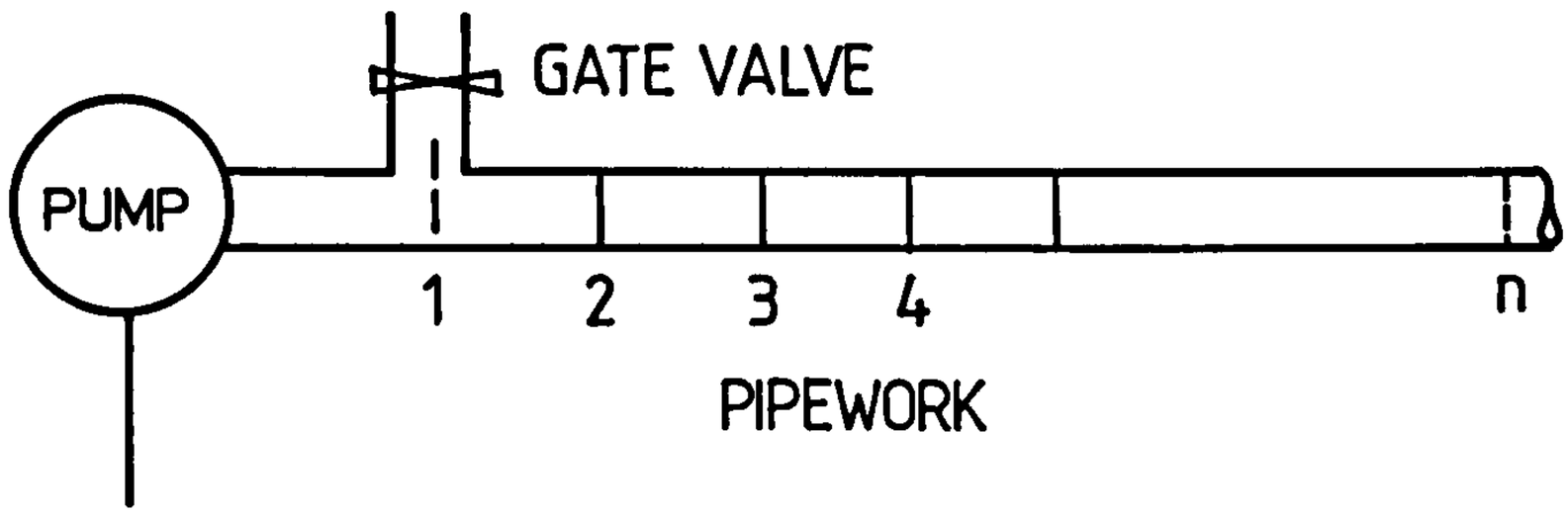

1. The relation between the head and the discharge of the pump can be approximated by the equation

$$H_p = C_7 - C_8 Q_p^2 \qquad (3.17)$$

2. The gate opening of the gate valve of the by-pass is constant for a given test so can be approximated by the equation

$$Q = K \sqrt{H_p - H_s} \qquad (3.18)$$

3. The inlet flow to the system is:

$$Q_c = Q_{pump} - Q_{by\text{-}pass} \qquad (3.19)$$

4. Equation for total head at point (1)

$$H_{pump} = H_{by\text{-}pass} = H_1 = H_p \qquad (3.20)$$

From equations (3.17) and (3.18) into equation (3.19) the flowrate at the inlet of the conduit is given by

$$Q_c = \sqrt{\frac{C_7 - H_p}{C_8}} - K\sqrt{H_p - H_s} \qquad (3.21)$$

In the above equation C_7 and C_8 are the pump constants calculated from the pump characteristics, K the orifice constant for the valve.

Equation (3.21) and the negative characteristic equation (3.6) give two equations for two unknowns, i.e. the boundary conditions at the inlet are represented by these equations.

3.2.2 Downstream Conditions

To develop the boundary conditions for the turbine end, one has to solve the positive characteristic equation (3.7) with the relationship between the flow, Q_p, and net head, H_N, imposed by the boundary. The flow through a Francis turbine depends upon the head, H_N, gate opening, τ, and the speed of the unit N. Since the gate is opened or closed under governor control depending upon the turbine speed which is also unknown, equations between these variables have to be solved simultaneously.

As shown in Ref.6 the relationship between the inlet head of the turbine and the net head H_N is:

$$H_p = H_N + H_T - \frac{Q_p^2}{2gA^2} \qquad (3.22)$$

where H_T is tailwater level above datum.

The values of the four variables namely Q_p, H_p, τ, and N are unknown at the end of each time-step during load change and may be obtained by the following procedure.

The characteristics for unit flow (q) for a particular gate opening (τ) can be approximated by a straight line over a small interval of speed. The equation of the straight line may be written as:

$$q = a_0 + a_1\phi \tag{3.23}$$

where a_0 and a_1 can be determined by Lagrangean interpolation. Substituting q and ϕ from equations (3.8) and (3.9) into equation (3.23)

$$a_2 H_N^{\frac{1}{2}} = Q_p - a_3 \tag{3.24}$$

where

$$a_2 = a_0 D_R^2$$

$$a_3 = N D_R^2 a_1/84.45$$

From equations (3.7), (3.22) and (3.24) the flowrate at the inlet to the turbine is given by:

$$Q_p = \frac{- a_5 - \sqrt{a_5^2 - 4a_4a_6}}{2 a_4} \tag{3.25}$$

where

$$a_4 = C_a/(2 g A^2) - C_a/a_2^2$$

$$a_5 = 2a_3 C_a/a_2^2 - 1$$

$$a_6 = C_p - C_a H_t - C_a a_3^2/a_2^2$$

Using equation (3.25) Q_p is found. By substituting into equations (3.24) and (3.22) H_N and H_p are found, i.e. the boundary conditions at the inlet of the turbine are known.

As discussed before the boundary conditions at the boundaries are known so we can find the conditions at time $t = \Delta t$.

To illustrate how to use the previous equations (3.1), (3.2), (3.6) and (3.7) the pipework is divided into n equal reaches and the

steady state conditions at $t = t_0$ are first obtained. Then, to determine the conditions at $t = t_0 + \Delta t$, equations (3.1) and (3.2) are used for the interior points and the boundary conditions at the upstream and downstream together with equations (3.6) and (3.7) are used to calculate the conditions at the end of the time-step. Now conditions at $t = t_0 + \Delta t$ are known and the conditions at $t = t_0 + 2\Delta t$ are determined by following the same procedure. In this manner, the computations proceed step-by-step until transient conditions for the required time are determined.

3.3 PROPORTIONAL-INTEGRAL-DERIVATIVE GOVERNOR

3.3.1 General

The governor is provided to keep the speed of the turbo-generator at the synchronous speed.

There are three types of governors used for hydraulic units.

(1) Dashpot governor
(2) Accelerometric governor
(3) Proportional-Integral-Derivative governor (PID).

The dashpot governor has been more commonly used in North America and the accelerometric in Europe, the PID has been introduced during the last ten years. In the dashpot governor the corrective action of the governor is proportional to the speed deviation, Δn; in the accelerometric governor it is proportional to dn/dt; in the PID it is proportional to Δn; dn/dt and time integral of Δn.

3.3.2 Representation of the Governor

As shown in the block diagram, Figure 3.4, the governor components are:

3.3.2.1 Phase-locked loop

A phase-locked loop contains three basic components as shown below:

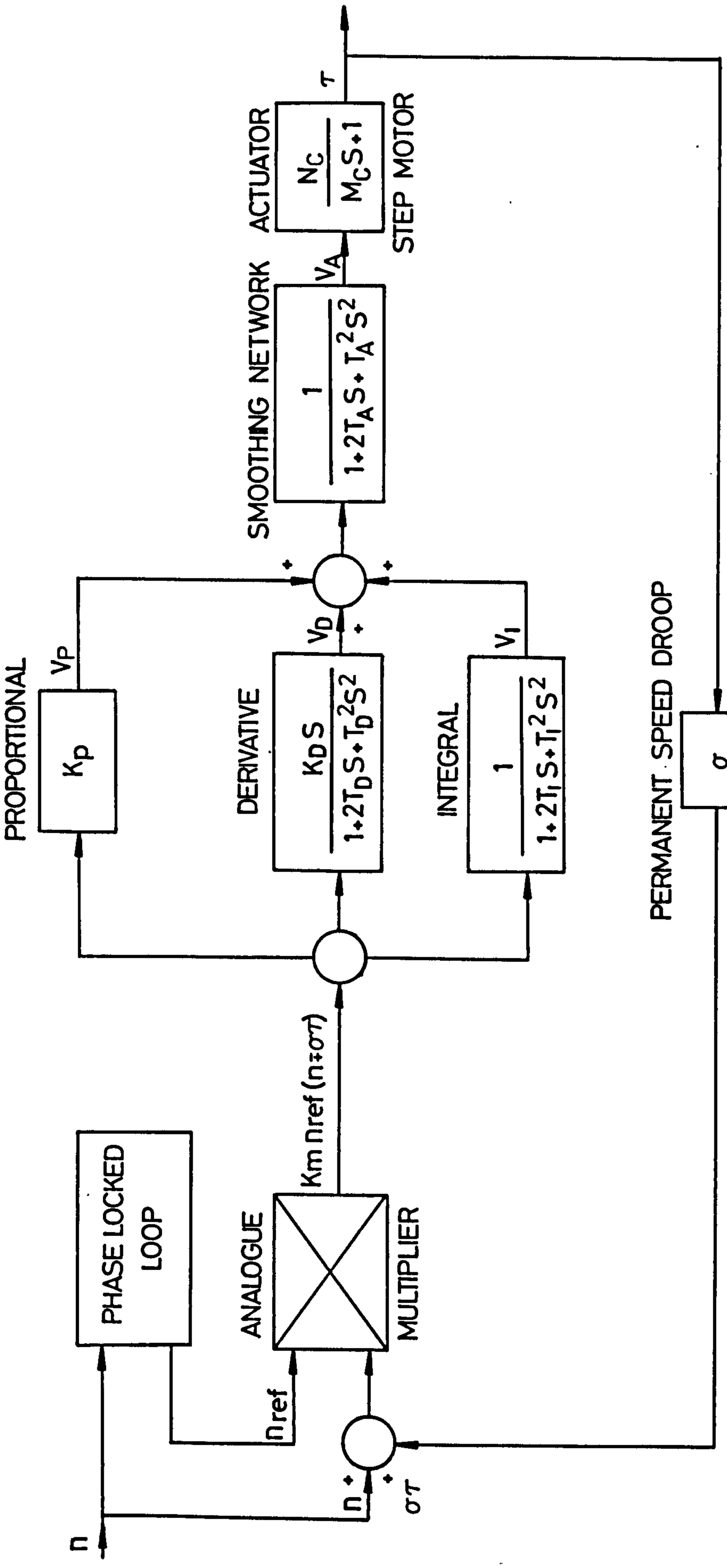

Figure 3.4 Block Diagram of PID Governor

(1) A phase detector (PD)
(2) A low-pass filter
(3) A voltage-controlled oscillator (VCO) whose frequency is controlled by an external voltage.

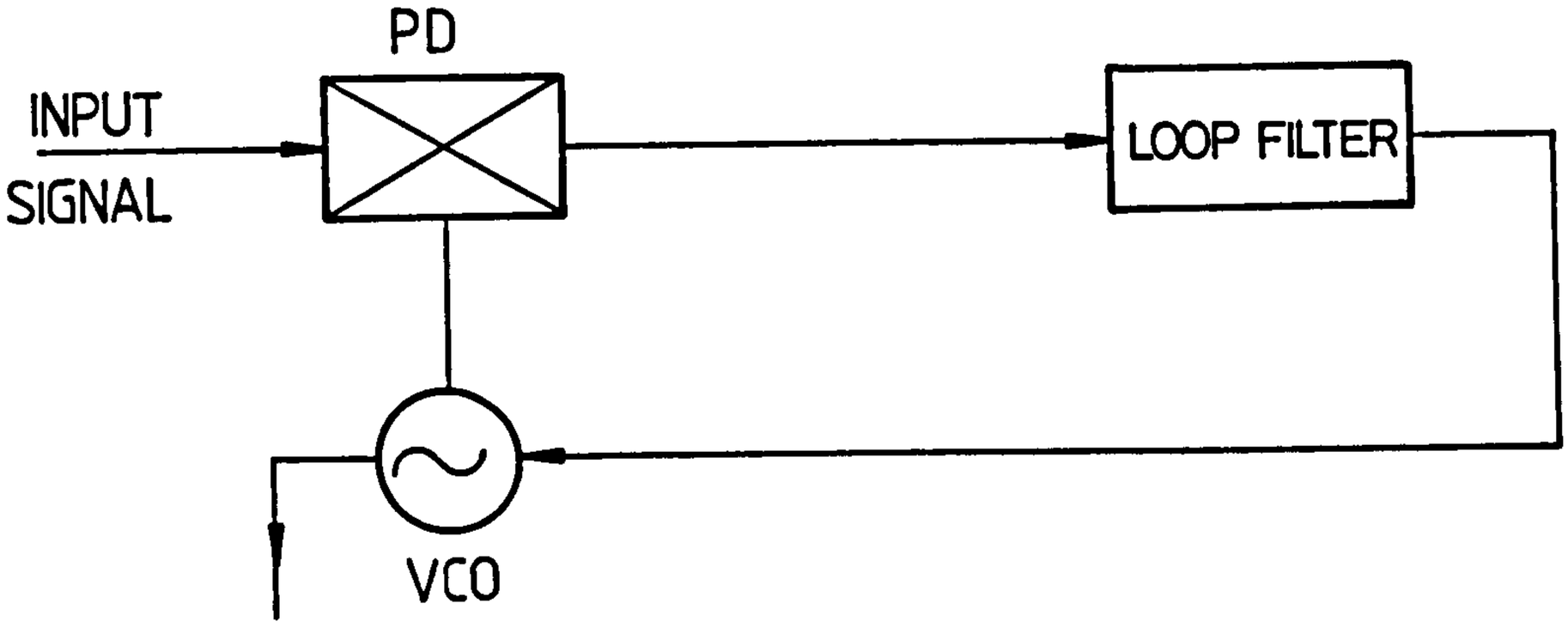

Basic Phase-locked Loop

The phase detector compares the phase of a periodic input signal against the phase of the VCO; the output of the PD is a measure of the phase difference between its two inputs. The difference in voltage is then filtered by the loop filter and applied to the VCO. Control voltage on the VCO changes the frequency in a direction that reduces the phase difference between the input signal and the local oscillator.

As shown in Figure 3.4 the input signal is

$$V_{in} = A \text{ Sin } \omega_1 t \text{ where } V_{in} \propto n \tag{3.26}$$

The output signal is:

$$V_{out} = A_1 \text{ Sin } \omega_2 t \text{ where } V_{out} \propto n_{ref} \tag{3.27}$$

where A is the amplitude of the input signal and proportional to the speed of the shaft.

A_1 is the output amplitude of the phase-locked loop, it is a constant.

The aim of PLL

1. To ensure that ω_1 and ω_2 are in the same phase and are equal.
2. To generate a constant amplitude to represent the reference speed (bias voltage) at the input of the analogue multiplier while generating an error signal to control the system operation.

3.3.2.2 Analogue multiplier

The main function of the multiplier is to compare the reference voltage which represents the reference speed (n_{ref}) and the variable voltage which is proportional to the speed (n).

$$V_{out} = A_1 \text{ Sin } \omega_2 t \tag{3.27}$$

and $$V_{in(multiplier)} = A \text{ Sin } \omega_1 t \tag{3.28}$$

Due to the feedback $V_{in(multiplier)} \propto n \pm \sigma\tau$

But $\omega_1 = \omega_2$ due to PLL

$$V_{in(multiplier)} = A_1 \text{ Sin } \omega_2 t$$

$$V_{in(multiplier)} \cdot V_{out} = A\, A_1 (\text{Sin } \omega t)^2$$

$$= \frac{A\, A_1}{2} + \frac{A\, A_1 \text{ Cos } 2\omega t}{2} \tag{3.29}$$

The output of the multiplier = $K_m \cdot V_{in(multiplier)} \cdot V_{out}$ and

$$V_{in} \cdot V_{out} \propto n_{ref} (n \pm \sigma\tau)$$

Note: If A_1 A the output signal is negative

If A_1 A the output signal is positive

i.e. the sign ($\pm$) dictates the direction of the turbine gate.

3.3.2.3 Controller

(i) Proportional

The proportional mode of control is very widely used by itself and also in conjunction with other modes which are added to obtain

certain performance improvements. The proportional element is as follows:

Let

$$Z = K_m.n_{ref}.(n\pm\sigma\tau) \tag{3.30}$$

Then

$$V_p = K_pZ \tag{3.31}$$

where Z = output of the analogue multiplier
K_p = the gain of the proportional element
V_p = the output of the proportional element.

(ii) Integral

The first order integrator $1/T_IS$ is a perfect integrator but it is unstable in nature because the root of the characteristic equation is on the imaginary axis as shown below.

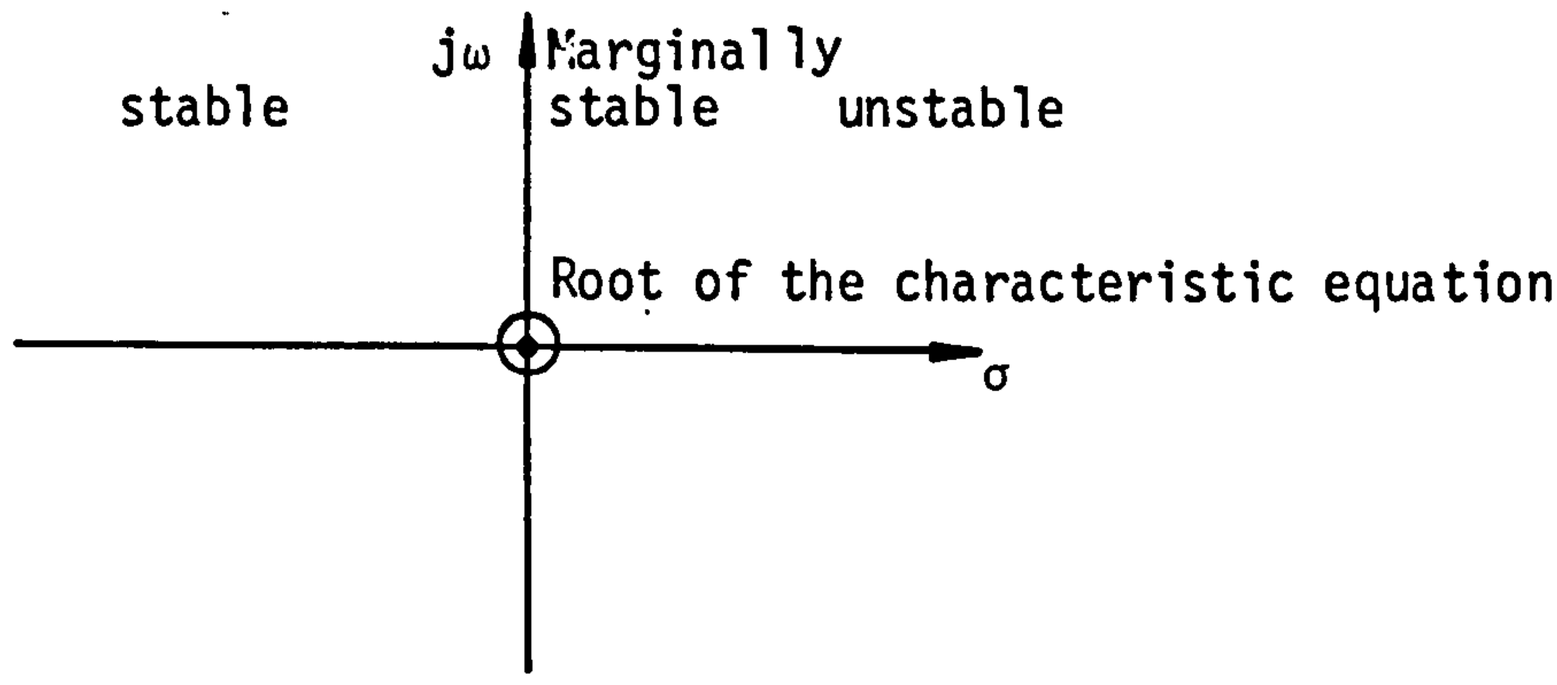

This means that it needs to be followed by a limiter as shown by Chaudhry, (Ref.7), but this limits it to dealing with low frequencies which is not suitable for a laboratory system. An improvement can be made by using an integrator with a transfer function (K/1+TS), shifting the pole to the left of the imaginary axis to the point (-1/T) which is stable but this has a low time response.

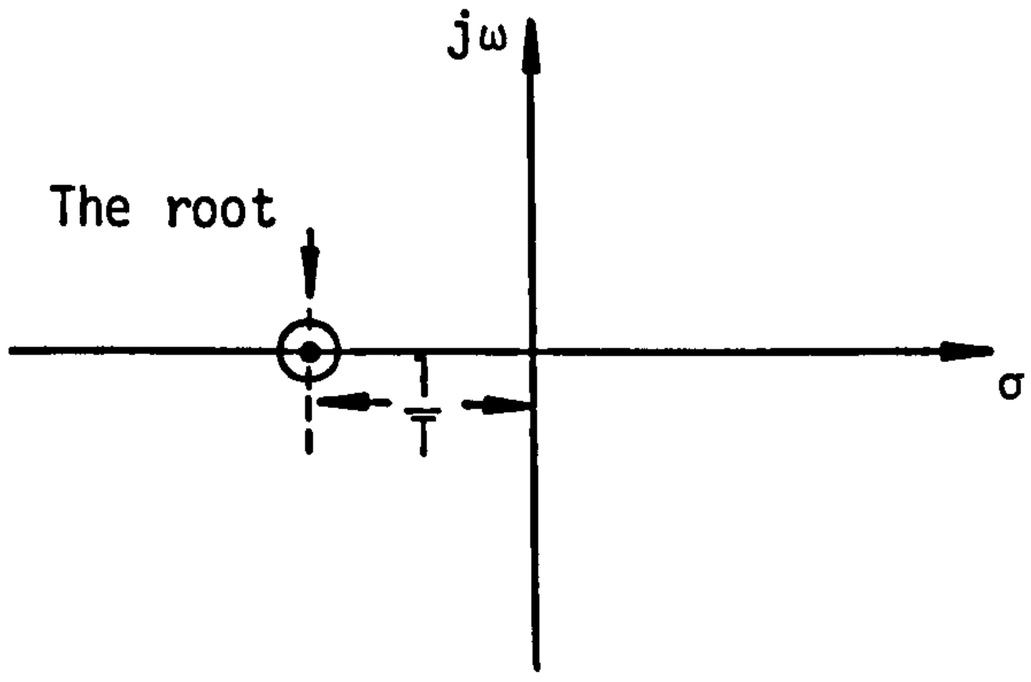

To improve this response a second order system can be designed to give faster response with lowest overshoot transient response as shown below.

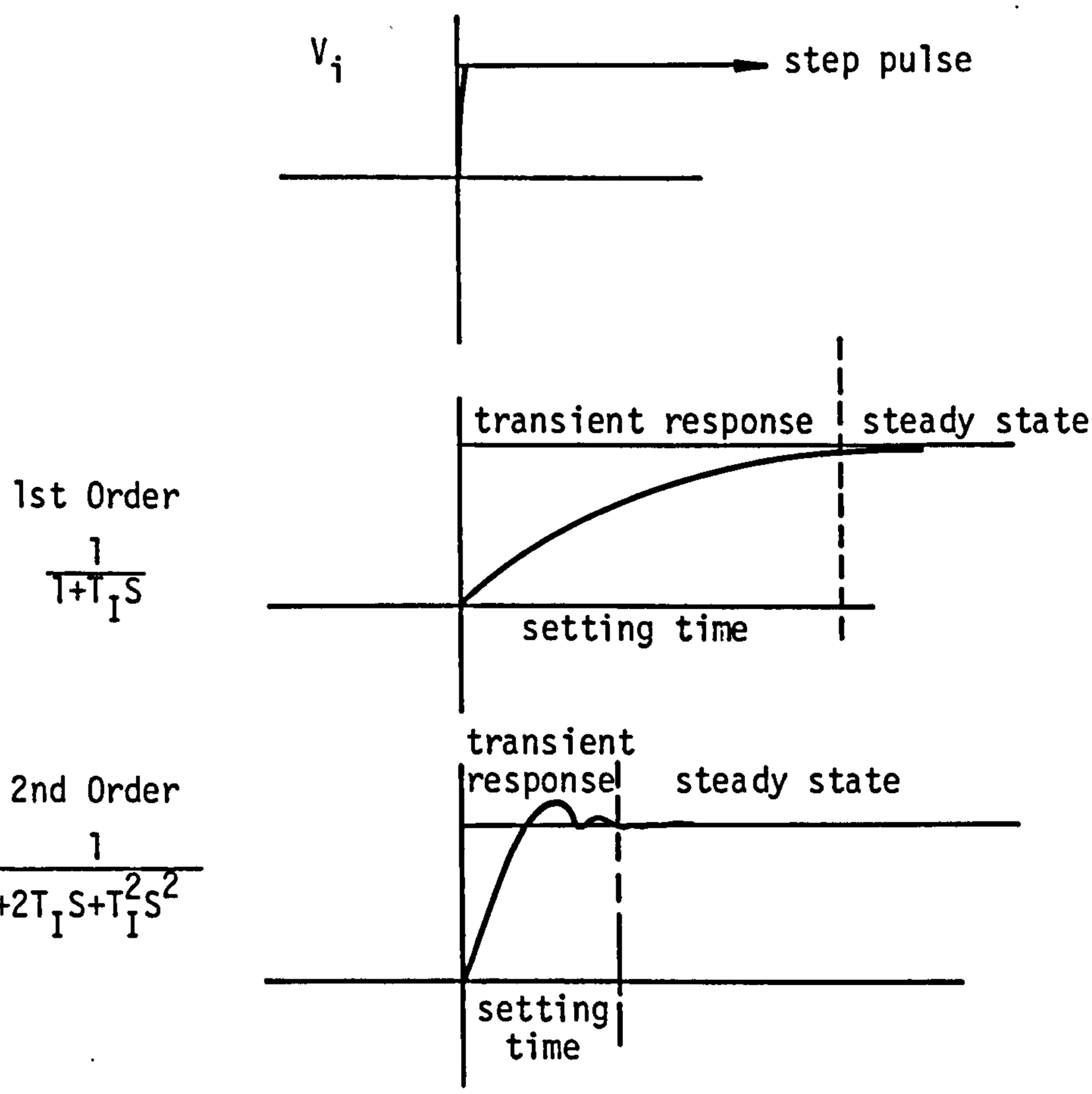

Appendix A shows the derivation and design of the second order integrator, i.e. the transfer function becomes:

$$\frac{V_{I(s)}}{Z(s)} = \frac{1}{1 + 2T_I S + T_I^2 S^2} \tag{3.32}$$

where S = Laplace operator which is equivalent to d/dt if the initial conditions are zero.

Then

$$\frac{d^2 V_I}{dt^2} = \frac{1}{T_I^2} \left| Z - V_I - 2T_I \frac{dV_I}{dt} \right| \tag{3.33}$$

where V_I is the output of the integral element and
T_I is its time constant.

(iii) Derivative

The differentiator should be compatible with the integrator and hence a second order differentiator was also used. This differentiator can be designed in two forms:

$$\text{(a)} \quad \frac{K_D S^2}{1 + T_D S + T_D^2 S^2}$$

$$\text{(b)} \quad \frac{K_D S}{1 + 2T_D S + T_D^2 S^2}$$

It was found that the first had got a limited gain but the second had unlimited gain which improved the dynamics of the system. The transfer function of the derivative elements may be written.

$$\frac{V_D(s)}{Z(s)} = \frac{K_D S}{1 + 2T_D S + T_D^2 S^2} \tag{3.34}$$

Then by substituting $S = d/dt$

$$\frac{d^2 V_D}{dt^2} = \frac{1}{T_D^2} \left| K_D \frac{dZ}{dt} - 2T_D \frac{dV_D}{dt} - V_D \right| \tag{3.35}$$

where V_D is the output of the derivative element
K_D is its gain and
T_D is its time constant.

3.3.2.4 Smoothing network

Practically the output of the controller is DC plus AC (low frequency). To filter this frequency a smoothing network is introduced to give approximated DC input to the actuator.

The general form of the transfer function is:

$$H(s) = \frac{K_0}{1 + 2\zeta S/\omega_n + S^2/\omega_n^2} \tag{3.36}$$

where K_0 is zero frequency gain
ζ is damping ratio
ω_n is the natural cut-off frequency.

Appendix A shows the derivation and design of the smoothing network, i.e. the transfer function becomes:

$$\frac{V_A(s)}{V_x(s)} = \frac{1}{1 + 2T_A S + T_A^2 S^2} \tag{3.37}$$

where $V_x = V_p + V_I + V_D$ and
$S = d/dt$.

Then

$$\frac{d^2V_A}{dt^2} = \frac{1}{T_A^2}\left|V_p + V_I + V_D - 2T_A \frac{dV_A}{dt}\right| \tag{3.38}$$

where V_A is the output of the smoothing network and
T_A is its time constant.

3.3.2.5 Actuator

In order to achieve a desired flow the wicket gate must be accurately positioned and subsequently held in position against the flow. This is the job done by the actuator. The choice of an actuator depends on the power source available, the speed of response required, the force required to move the wicket gate and hold it in position and the accuracy of position required. A stepping motor was chosen to actuate the wicket gate.

Step motor

For electric motors to generate the required power economically the rotational speed of the motor is high, the high speed low torque is converted to low speed high torque by gearing. This had advantages in an infrequent on/off operation where an impact hammer blow may be required to move the gate off its seat. It is though, a disadvantage in the control loop where the momentum will cause overrun from the desired position.

One type of electric motor which does not suffer from the problem of overrun is the DC stepping motor. This motor remains static when energised. Movement is caused by de-energising and then re-energising the stator windings in a different pattern. This sequence is controlled by drive circuitry which changes the pattern following receipt of an external pulse. The power output of a DC stepping motor is limited. One advantage which the electric motor does possess in the control loop situation, is high stiffness. That means the movement of the gate under dynamic loading resulting from pressure fluctuations in the flow is small.

Theoretical transfer function

Delgado, (Ref.16), assumed the self inductances were constant and the inertial torque included the applied torque. He also assumed there was no mutual inductance between stator phase windings. The induced voltage was assumed to be a linear function of speed and the resulting equation was a linear third order system.

$$\frac{\tau(s)}{V_A(s)} = \frac{N_c}{AS^3 + BS^2 + M_cS + 1} \qquad (3.39)$$

where $A = J\,T_s/K_r$

$B = J/K_r$

$M_c = T_s + (K_E - K_I/R)$

$N_c = K_I/R$

K_r = Restoring torque constant (N.B. usually K_r is very high)

J = Total load moment of inertia referred to motor shaft.

Practically, A and B were very small so as to simplify the transfer function

$$\frac{\tau(s)}{V_A(s)} = \frac{N_c}{M_c S + 1} \tag{3.40}$$

Then

$$\frac{d\tau}{dt} = \frac{1}{M_c} \left| N_c y_A - \tau \right| \tag{3.41}$$

3.4 BIVARIATE LAGRANGEAN INTERPOLATION

3.4.1 General

Many contributions towards representation of turbine characteristics have been published within the last few years. Wozniak, (Ref.19), used the least squares method. The turbine characteristics were globally represented by Chaudhry, (Ref.7), who used finite difference interpolation.

The use of Lagrangean polynomials, (Ref.17) is amongst the simplest and most practical methods of interpolation. The general equations of Lagrangean interpolation which are used in this work are as follows:

$$Z = \sum_{i=1}^{m} \sum_{j=1}^{n} \ell_i^m(x)\, \ell_j^n(y)\, Z_{i,j}$$

3.4.2 Derivation

Along any y line which intersects line $x=x_i$ in point $z(x_i,y)$ using one dimensional interpolation along $x=x_i$ line.

$$z(x_i,y) = \sum_{j=1}^{n} \ell_j^n(y)\, Z_{i,j} \tag{3.42}$$

Applying the same one dimensional interpolation on y line

$$z(x,y) = \sum_{i=1}^{m} \ell_j^m(x)\, Z(x_i,y) \tag{3.43}$$

Substituting equation (3.42) into equation (3.43) we get:

$$\boxed{z(x,y) = \sum_{i=1}^{m} \sum_{j=1}^{n} \ell_i^m(x)\, \ell_j^n(y)\, Z_{i,j}} \tag{3.44}$$

The first and second partial derivative of equation (3.44) will give the following equations:

$$\boxed{\begin{aligned} \frac{\partial z}{\partial x} &= \sum_{i=1}^{m} \frac{\partial \ell_i^m(x)}{\partial x} \sum_{j=1}^{n} \ell_j^n(y)\, Z_{i,j} \qquad (3.45) \\ \frac{\partial^2 z}{\partial x^2} &= \sum_{i=1}^{m} \frac{\partial^2 \ell_i^m(x)}{\partial x^2} \sum_{j=1}^{n} \ell_j^n(y)\, Z_{i,j} \qquad (3.46) \end{aligned}}$$

where $$\ell_i^m(x) = \prod_{\substack{r=1 \\ r\neq i}}^{m} \frac{x-x_r}{x_i-x_r}$$

From (Ref.18) it can be proved that the error, obtained from the following formula is

$$E = \left(\frac{\partial^m z}{\partial x^m}\right) \frac{P_m(x)}{m!} + \left(\frac{\partial^n z}{\partial y^n}\right) \frac{P_n(y)}{n!} - \left(\frac{\partial^{m+n} z}{\partial x^m \partial y^n}\right)_{\substack{x=\alpha \\ y=\beta}} \frac{P_m(x)\ P_n(y)}{m!\ .\ n!} \qquad (3.47)$$

where $P_m(x) = \prod_{r=1}^{m} (x - x_r)$

If z is a polynomial of degree m-1 in x and n-1 in y the error will be zero.

3.4.3 Piecewise Lagrangean Interpolation

Practically speaking, the general Lagrangean interpolation is more accurate than necessary and uses a considerable amount of computation time. It is important to reduce computation time without unduly affecting the accuracy. The best solution is to employ piecewise Lagrangean interpolation, (Ref.17). With this technique a specified subdomain which surrounds the interpolation point and contains a certain number of the grid points, depending on the required accuracy, can be used for the Lagrangean interpolation.

3.4.4 The Advantage of Lagrangean Interpolation

(i) A uniform grid is not required.

(ii) Given values of z tabulated for x and y it is as easy to interpolate for x or y as it is for z.

(iii) The method is more accurate than many other interpolation methods because all the points in the grid are used.

From the error analysis given in Ref.18 it can be proved that the interpolation from equations (3.44), (3.45) and (3.46) is much more accurate than the least squares method, (Ref.19), and the finite difference method, (Ref.7).

(iv) Piecewise Lagrangean interpolation has the following advantages.

(a) It saves computer time.

(b) It may even improve the accuracy by reducing rounding off errors, assuming a sufficient number of points has been used.

(c) Using a large number of values of τ (gate opening) will give greater accuracy without affecting the computer time.

CHAPTER 4

EXPERIMENTAL PROCEDURE

4.1 DESCRIPTION OF THE RIG

In order to carry out a series of tests a flow rig was built in the laboratory using 100 mm ID pipes. These tests were for a range of partial load rejections as well as for full load rejection. A plastic tube (ABS-durapipe) was used for the construction of the rig whose elements are explained below. A photograph of the rig is shown in Plate 3.1 and a diagram in Figure 3.3.

1. Pump

The input to the system was supplied by a large centrifugal pump, (Head = 29 (m), Q = 50 l/s, N = 1,450 rpm, HP = 22 KW). A large pump with a by-pass was used so that a required combination of head and flow could be obtained without having to match the pump characteristic to the system.

2. Valves

The water was controlled by two manual gate valves (100 mm diameter), one at the input of the conduit and another at the by-pass to obtain the required conditions of head and flowrate.

3. Tank

The tank which was made of plastic material was of about 3.5 m^3 capacity. The turbogenerator set was fitted on the tank with a suitable frame, thus the draft tube was immersed in the tank.

4. Turbine and generator

A Gilkes 150 mm Reversible Francis pump/turbine was used. As a Francis turbine the machine has a high efficiency (73%) and test results can be repeated without difficulty. The 150 mm pump-turbine is integrally constructed with a dynamometer type motor generator.

ABSTRACT

This work is concerned with transients caused by changes in load on a turbogenerator set governed by a proportional plus integral plus derivative (PID) governor.

A PID governor was designed and built in the laboratory to control a small turbine installed in the laboratory. Having the turbine available in the laboratory meant that a full set of tests could be carried out for a range of partial load rejections as well as for full load rejection. A computer program was developed using an improved interpolation technique to deal with the turbine boundary conditions making use of piecewise Lagrangean interpolation. The gate opening, turbine speed, pressure rise and flow rate recorded in the laboratory are presented and compared with theoretical results from the computer analysis.

There is a good measure of agreement between the experiment and computed results, particularly up to the peak of speed and pressure rise.

The motor generator is used to absorb the power developed during turbine tests and to drive the machine as a pump.

The incoming AC is converted to DC in the control console. This DC is then used to power the motor generator.

The auto-transformer with on/off switch would only give the full load. In our case we required full load and partial load. To provide this, a tap-changer and on/off switch was used. The tap-changer consists of 14 inductors connected in series as shown below. The 240V supply voltage is divided equally across each inductor.

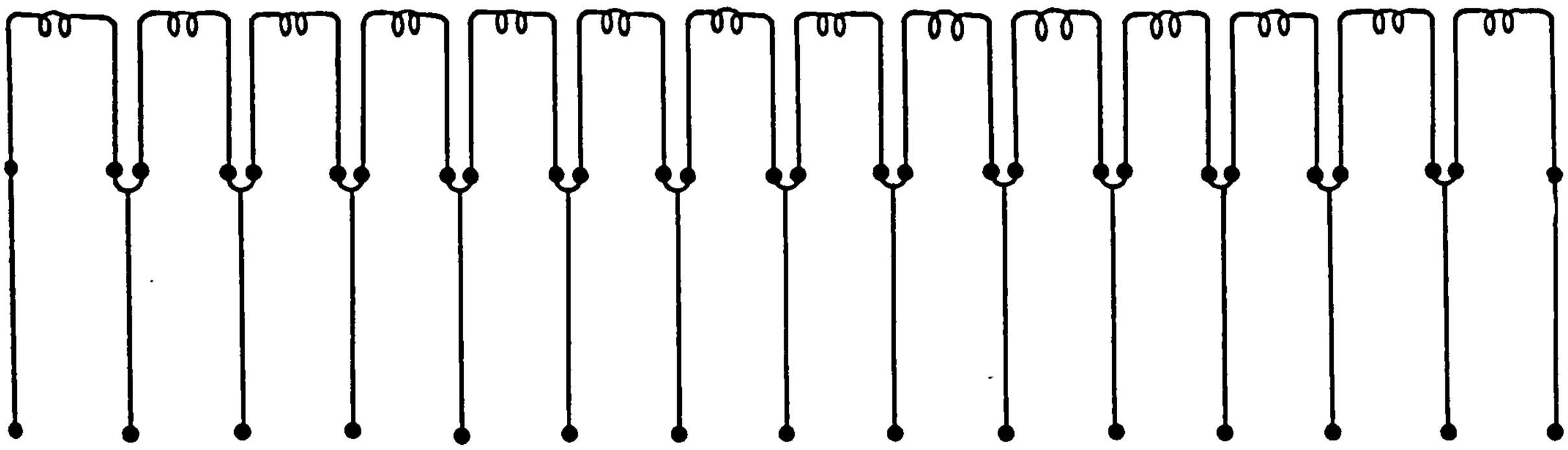

1 2 3 4 5 6 7 8 9 10 11 12 13 14 15

0V 240V

Tap-changer connection

The motor-generator operates from the DC supply provided by the control cabinet. During turbine tests resistors in the control console dissipated any power generated.

The ammeter and voltmeter indicate the power output. The turbine and motor-generator are both mounted together on a substantial cast bedplate.

4.2 THE CONTROL CIRCUIT

Figure 4.1 shows the connection diagram of the control circuit. The circuit contains different types of operational amplifiers supplied by ITT Instrument Services, RS Components Ltd. and Macro Marketing Ltd. (UK),(Plate 4.1). The magnetic pickup output signal is connected to the phase locked loop (PLL) to generate a reference voltage

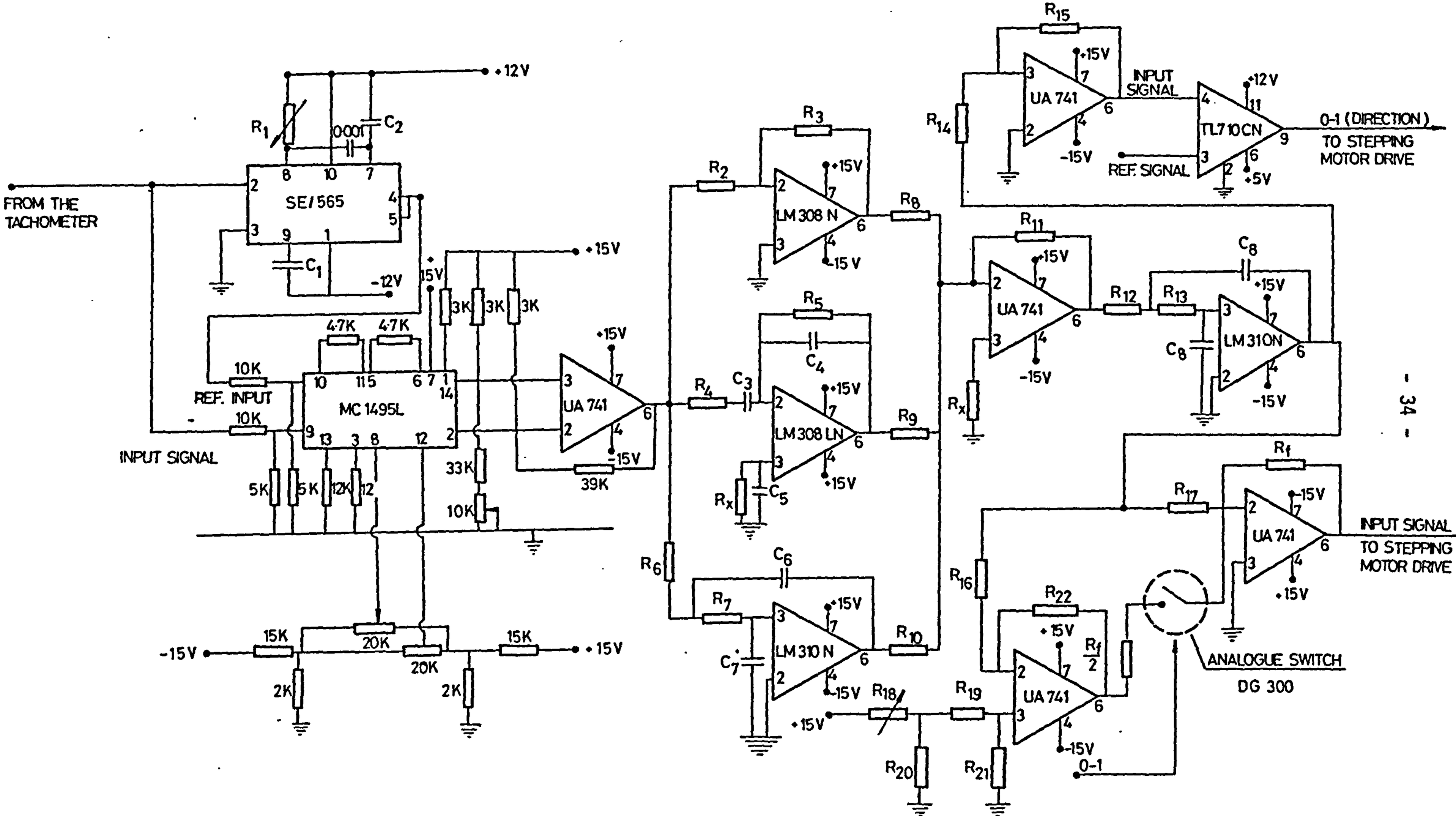

Figure 4.1 The Control Circuit

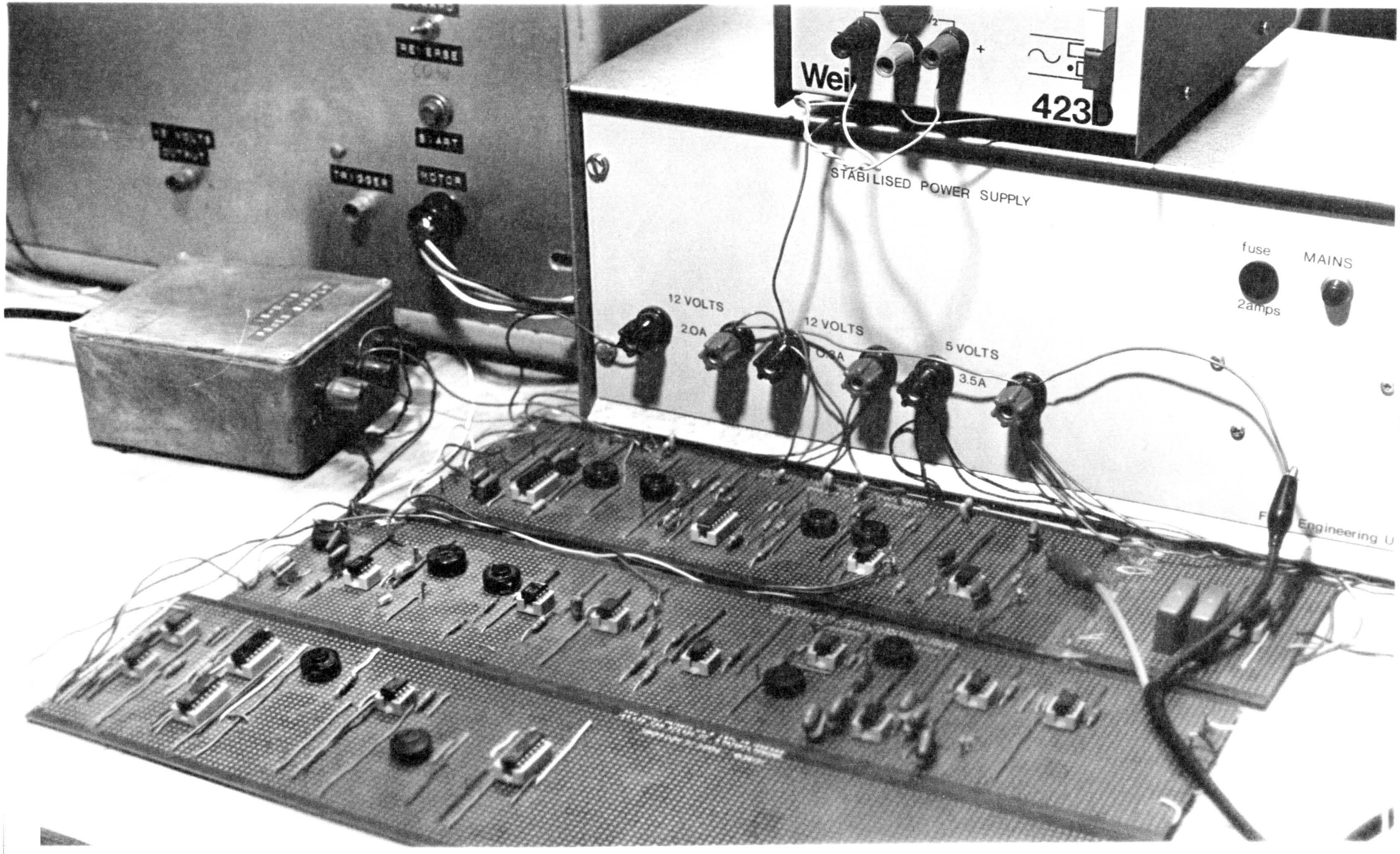

PLATE 4·1 THE CONTROL CURCUIT


REVERSE
START
MOTOR
TRIGGER
STABILISED POWER SUPPLY
423D
fuse
2amps
MAINS
12 VOLTS
2.0A
12 VOLTS
0.8A
5 VOLTS
3.5A
Engineering U

and to the analogue multiplier as discussed in the previous chapter. The output of the control circuit is connected to the stepping motor drive which consists of a power supply and a digicard (logic circuit), Figure 4.2, and dropping resistors (to make the power supply compatible with digicard) of 1 ohm 50 watts. A basic stepping motor circuit is illustrated in Figure 4.3. As shown in Figure 4.3 two inputs are needed to drive the stepping motor, one is an analogue signal to de-energise the stator windings and the second is a digital signal to control the direction of the motor. The derived analogue signal is fed through a smoothing circuit before being connected to the stepping motor drive. The digital signal is obtained by connecting the analogue signal to a voltage comparator (TL710CN). The comparator compares the instantaneous signal with the reference voltage and produces a digital one or zero at the output when the input is higher than the reference signal. This dictates the direction of the stepping motor.

When the analogue signal is 10.5 volts the speed of the motor is zero, i.e. the speed of the turbine is equal to the reference speed. When at 0 volts the motor is at a preset speed. When the load changes, the input voltage of the stepping motor drive will change. This is due to the feedback voltage (10.5-0 volts). The motor will de-energise and rotate clockwise (CW), thus closing the gate. Consequently the input flowrate will reduce as will the speed of the turbine. If the speed becomes less than synchronous speed the output signal of the control circuit becomes greater than 10.5 volts. In this case the motor should rotate counter clockwise (CCW), but due to an inherent characteristic of the stepping motor it will not rotate at all. To overcome this problem and cause a CCW rotation it was necessary to design a voltage inverting threshold circuit, Figure 4.4.

The circuit contains a summing and a subtracting amplifier (UA741CP) and an analogue switch (DG300CJ). The analogue switch is controlled by the comparator discussed earlier. When the comparator signal is logical '1' the switch is closed (indicating that the input signal on the comparator is greater than 10.5 volts).

For signals less than 10.5 volts the signal path is:-

PACK	-8V	0V	N° OFF
SN 7475	8	12	L
SN 7476	16	13	O
SN 7472	14	7	E
SN 7473	14	7	M
SN 7490	14	7	F
SN 7401	14	7	H
SN 7404	14	7	B
SN 7451	14	7	C
SN 7438	16	7	AJ

PACK	-12V	0V	N° OFF
NE 565 V	8/4	1	N
SN 15206	14	7	K

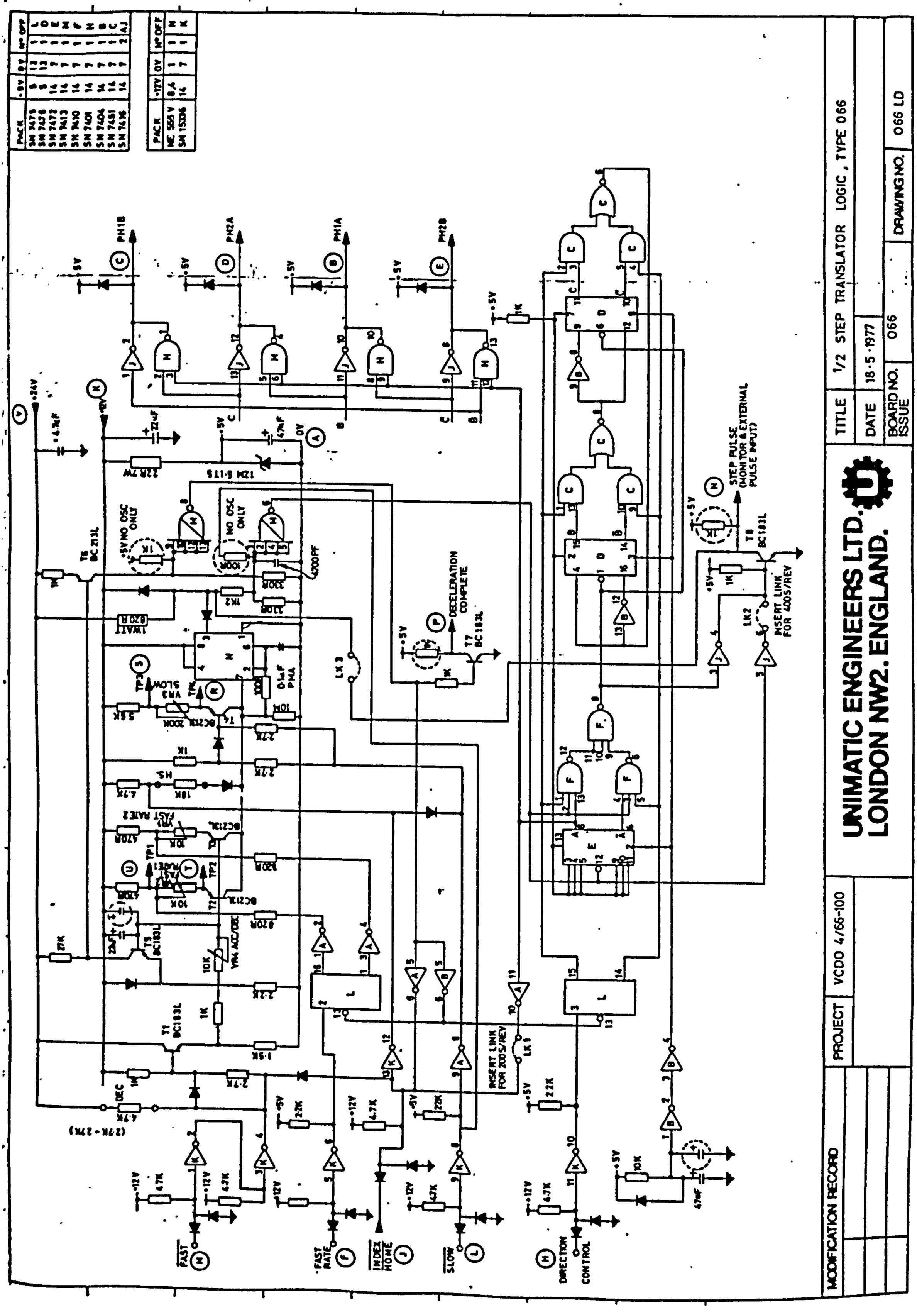

TITLE	1/2 STEP TRANSLATOR LOGIC , TYPE 066
DATE	18·5·1977
BOARD NO. ISSUE	066
DRAWING NO.	066 LD

UNIMATIC ENGINEERS LTD.
LONDON NW2. ENGLAND.

PROJECT	VCDO 4/66-100

MODIFICATION RECORD

Figure 4.2 Stepping motor drive (Logic circuit)

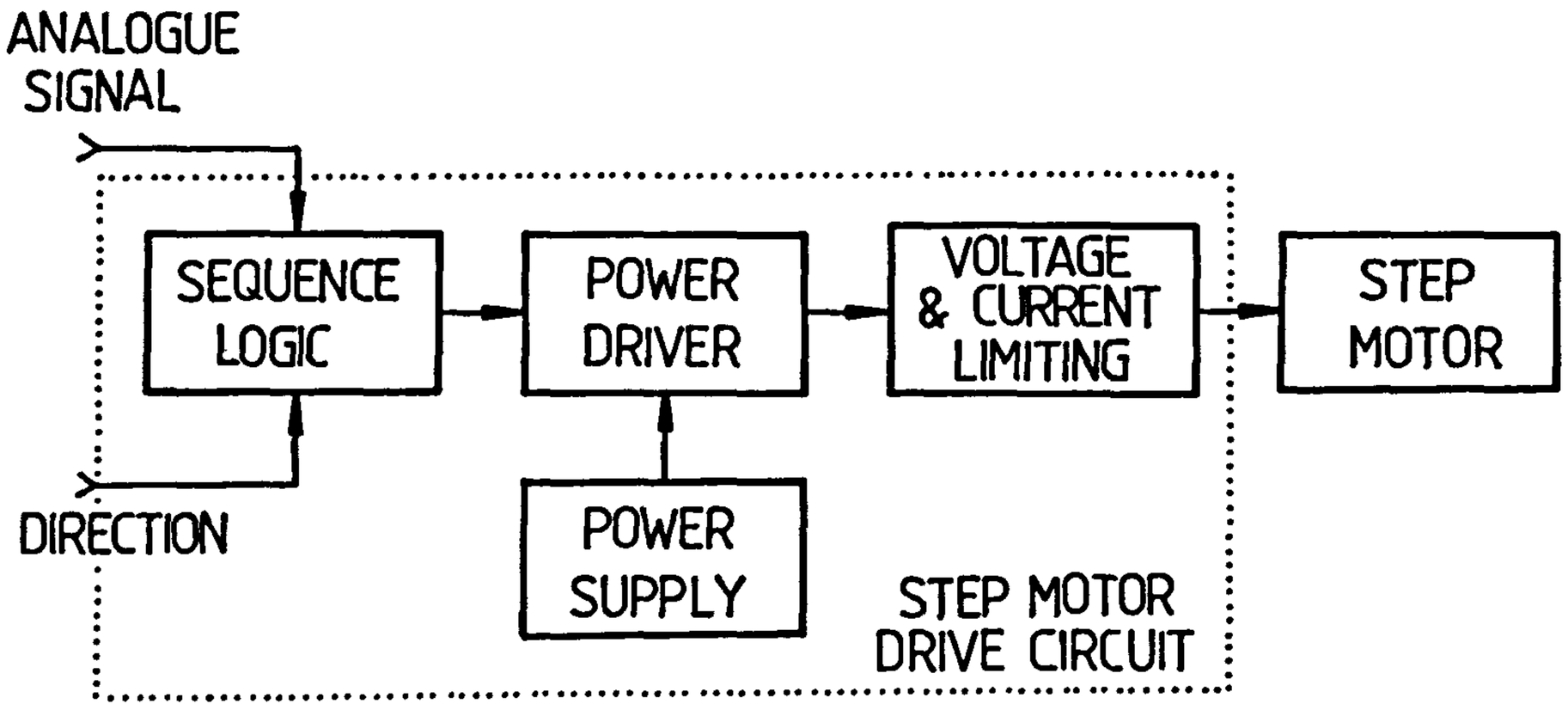

Figure 4.3 Basic Stepping Motor Circuit

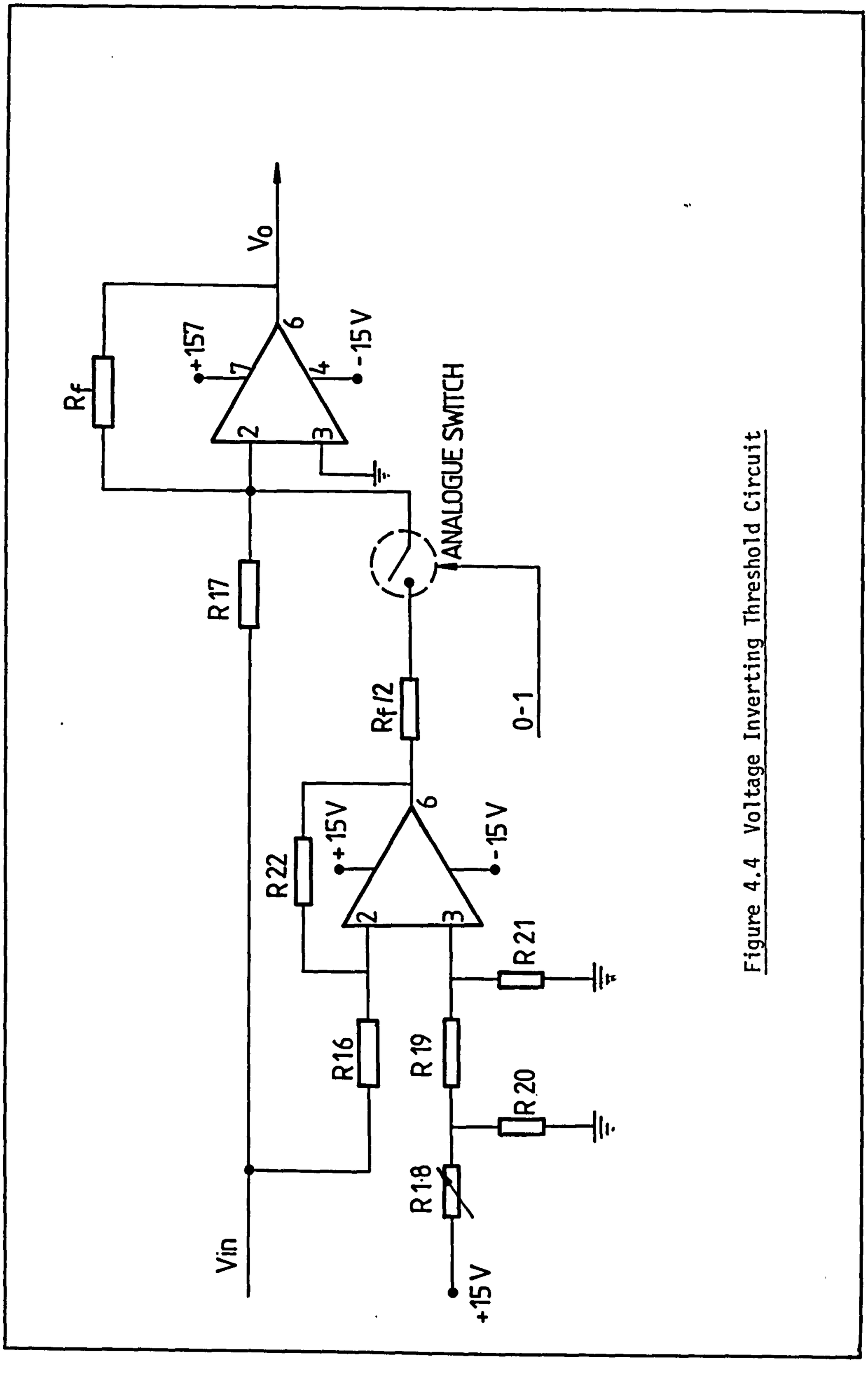

Figure 4.4 Voltage Inverting Threshold Circuit

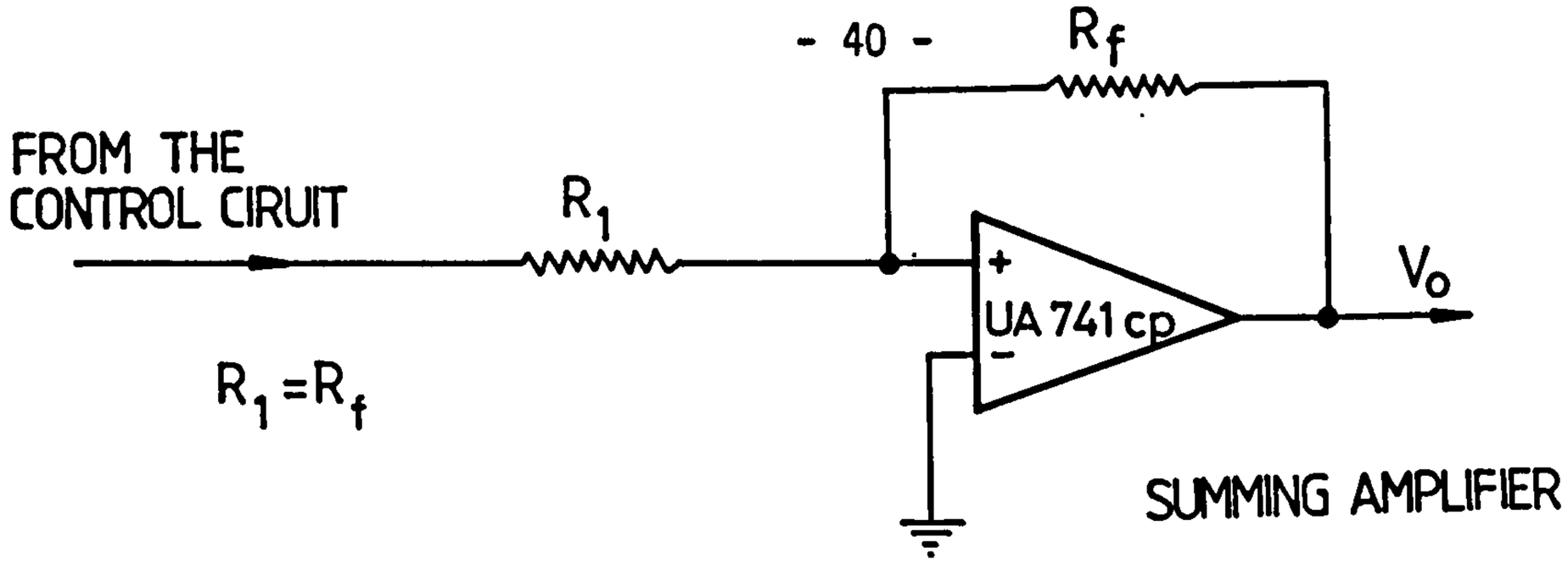

and for a signal greater than 10.5 volts the signal path is

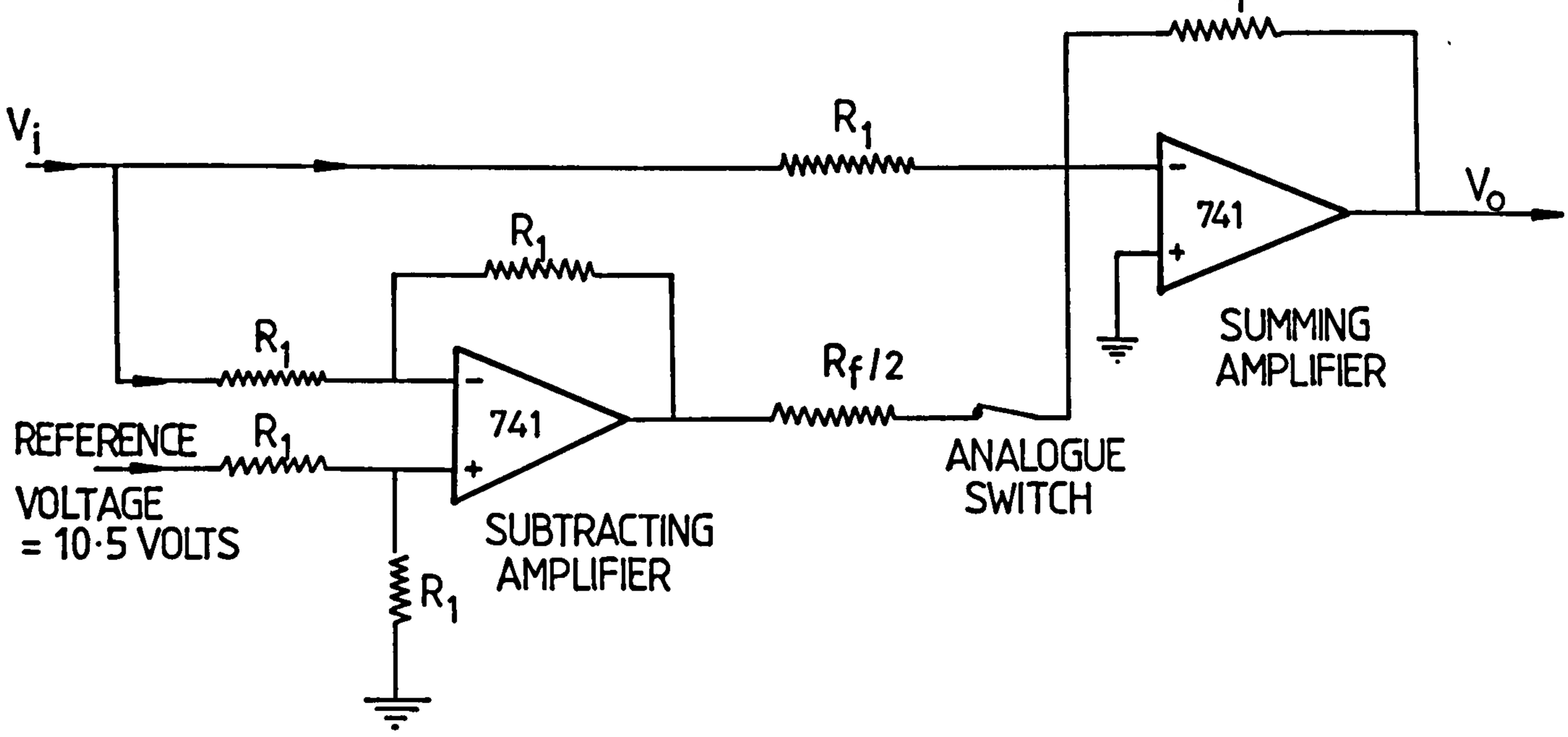

Appendix A shows the derivation and design of the control circuit which largely depends on Refs. 22-25.

4.3 STABILITY OF THE PID CONTROLLER

There are different methods to investigate the stability of a control system. One of the best and simplest ways is the Bode plot method, (Ref.24). Bode plots clearly illustrate the stability of a system. In fact, gain and phase margins are often defined in terms of Bode plots. These measures of stability can be determined for a particular system with a minimum of computational effort, especially for those cases where experimental frequency response data is available. The Bode plots consist of two curves, gain and phase, as a function of frequency in logarithmic form.

As shown in Figure 3.4 the transfer function of the Proportional-Integral and Derivative elements is

$$H_{(s)} = K_p + \frac{K_D S}{1 + 2T_D S + T_D^2 S^2} + \frac{1}{1 + 2T_I S + T_I^2 S^2} \qquad (4.1)$$

Hence $K_p = 1.2$

$K_D = 0.1$

$T_D = 3.18 \times 10^{-3}$ sec

$T_I = 3.18 \times 10^{-3}$ sec.

$$\therefore H_{(s)} = 1.2 + \frac{0.1S}{1 + 2 \times 3.18 \times 10^{-3} S + (3.18 \times 10^{-3})^2 S^2}$$

$$+ \frac{1}{1 + 2 \times 3.18 \times 10^{-3} S + (3.18 \times 10^{-3})^2 S^2}$$

$$\therefore H_{(s)} = \frac{(S + 20.5)(S + 8849)}{(S + 314)^2} \times 1.2 \qquad (4.2)$$

By substituting $S = j\omega$ (where S = frequency response = $j\omega$) as explained in Ref.24.

$$H_{(s)} = \frac{(1 + \frac{j\omega}{20.5})(1 + \frac{j\omega}{8849})}{(1 + \frac{j\omega}{314})^2} \times 2.2$$

Hence 20.5 and 314 are dominant roots with respect to S = -8849 i.e. the transfer function may be written:-

$$H_{(j\omega)} = \frac{2.2(1 + \frac{j\omega}{20.5})}{(1 + \frac{j\omega}{314})^2} \qquad (4.3)$$

There are four terms, 2.2, $(1 + j\omega/20.5)$ and $(1/(1+j\omega/314))$ twice. Figures 4.5, 4.6 and 4.7 show how each term can be plotted and added graphically to produce the straightline approximation of the Bode magnitude curve and the phase curve for this transfer function. From Figure 4.7 the gain margin and the phase margin can be estimated.

Figure 4.5 Bode Magnitude Plot

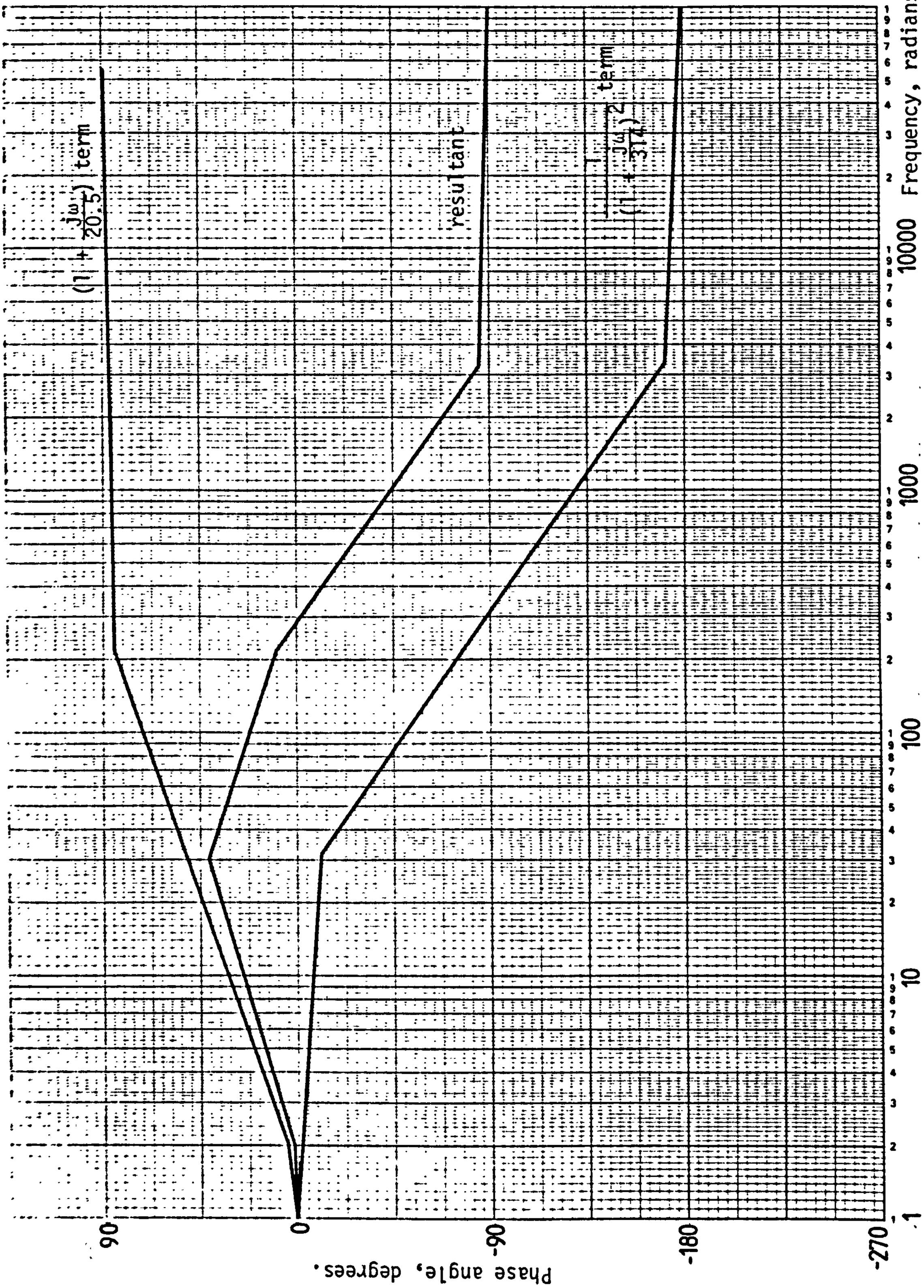

Figure 4.6 Bode Phase-angle Plot

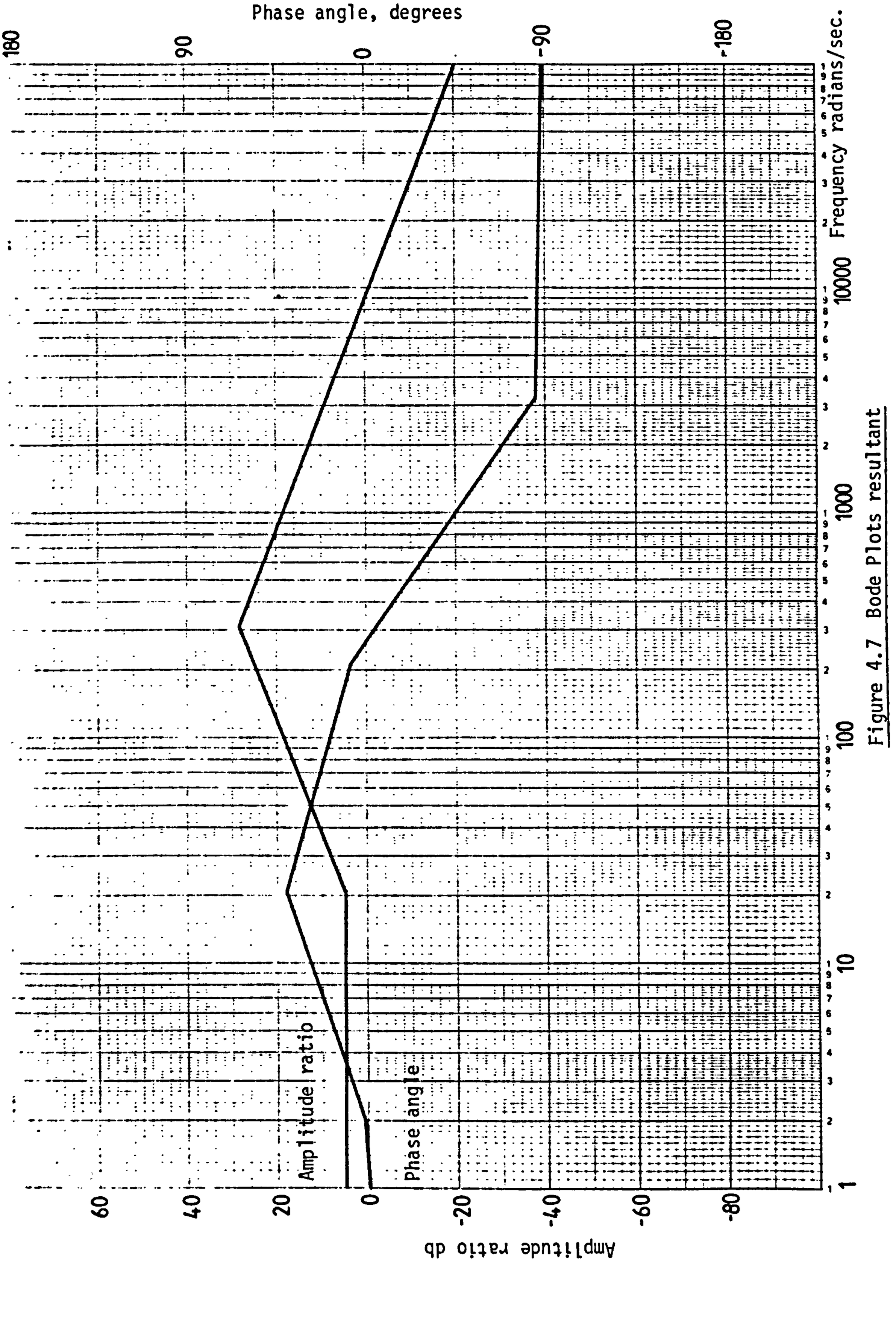

Figure 4.7 Bode Plots resultant

Gain margin $G_m = \infty$

Phase margin $\phi_n = -85^o$

i.e. the system is stable because it will never reach -180^o for any values of the frequency.

4.4 INSTRUMENTATION

4.4.1 Inlet Pressure Measurement

A pressure transducer type 4043 (Kistler Instruments Ltd. (UK)),was installed to measure the variation of pressure in the conduit upstream of the turbine. An amplifier also from Kistler Instruments Ltd., Type 4601, was used in conjunction with the transducer as its signal was not strong enough to drive the galvanometer of the UV recorder.

It was not convenient to calibrate the transducer on site, therefore a dual range dead-weight pressure gauge tester was used, Figure 4.8. The transducer was connected to the tester through the pressure circuit in Figure 4.9. The electrical circuit, also shown on this Figure, consisted of the transducer, an amplifier unit and UV recorder. Prior to calibration it was necessary to ensure the maximum UV recorder displacement for the range of pressure under consideration.

The strength of the transducer signal could be varied by adjustment of the amplifier together with a selection of a suitable galvanometer in the UV recorder and the required trace displacement was obtained.

The calibration procedure was simple. Initially the UV recorder trace position was noted for the zero signal corresponding to atmospheric pressure. Valve 'B' was closed and 'A' remained open. Using different weights at 'W' equivalent to 0 to 350 KN/m^2 the resulting displacements were measured relative to the zero signal position and corresponding to the weights at 'W'.

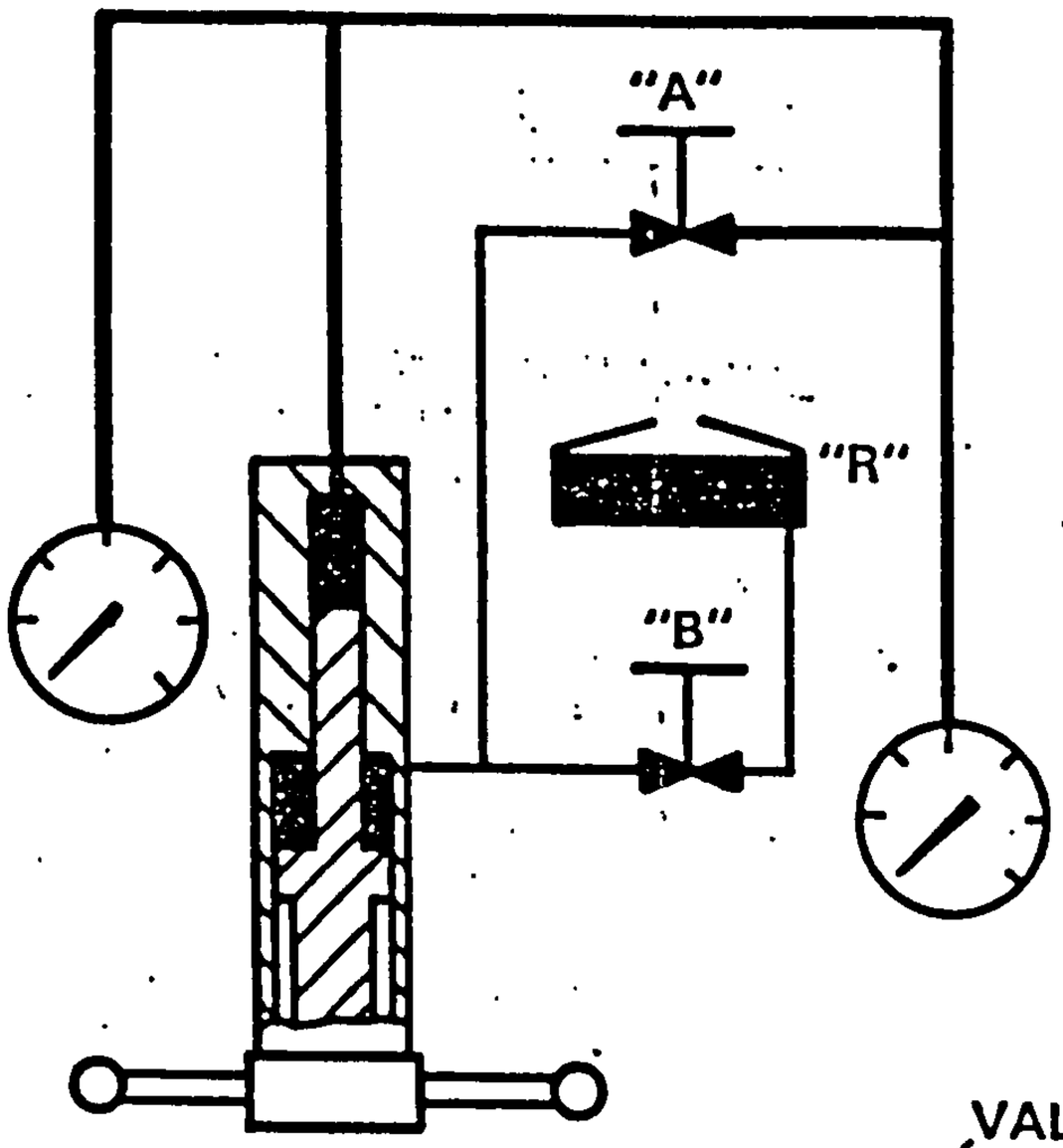

CIRCUIT DIAGRAM

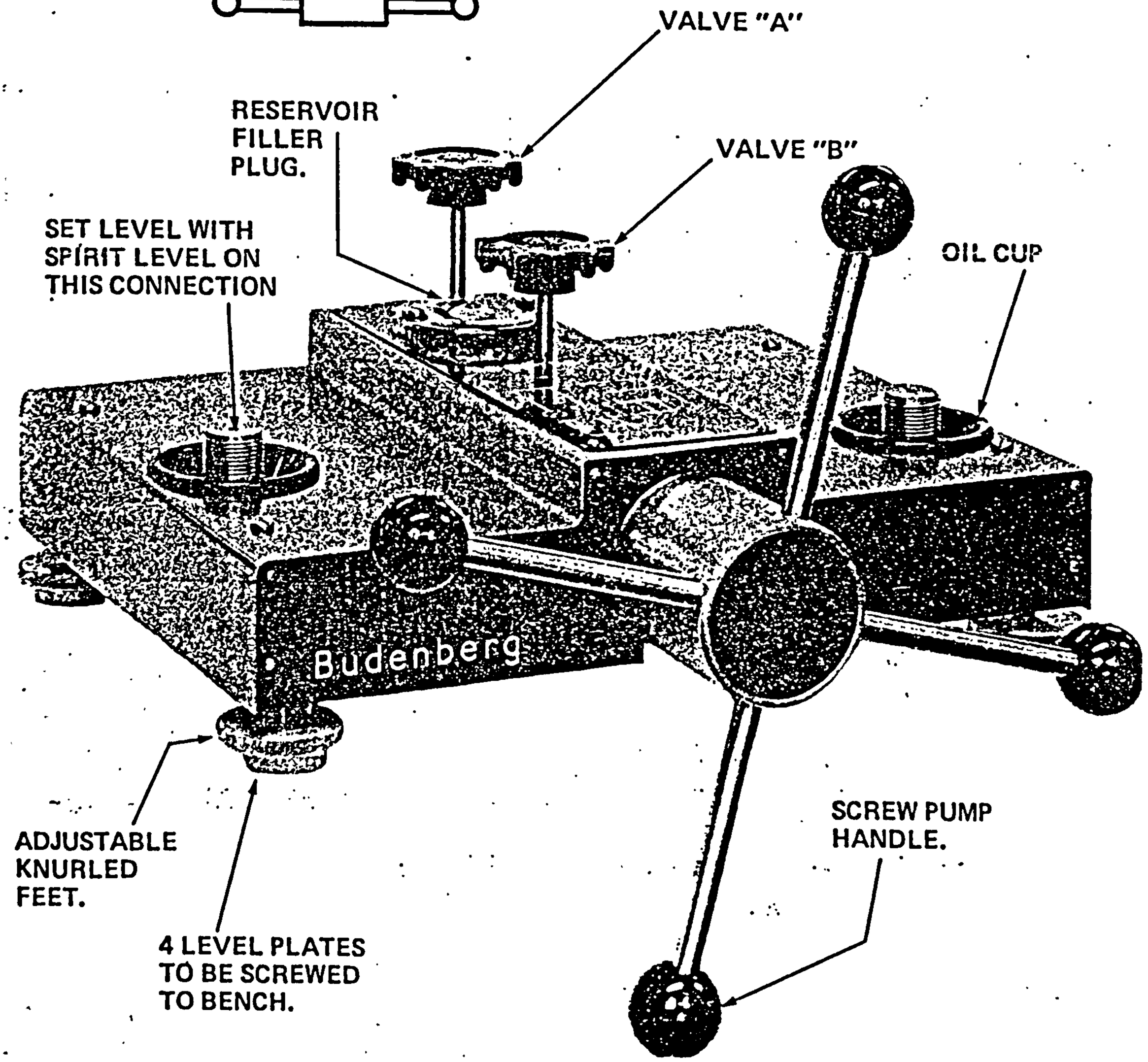

Figure 4.8 Dual range dead-weight pressure gauge tester

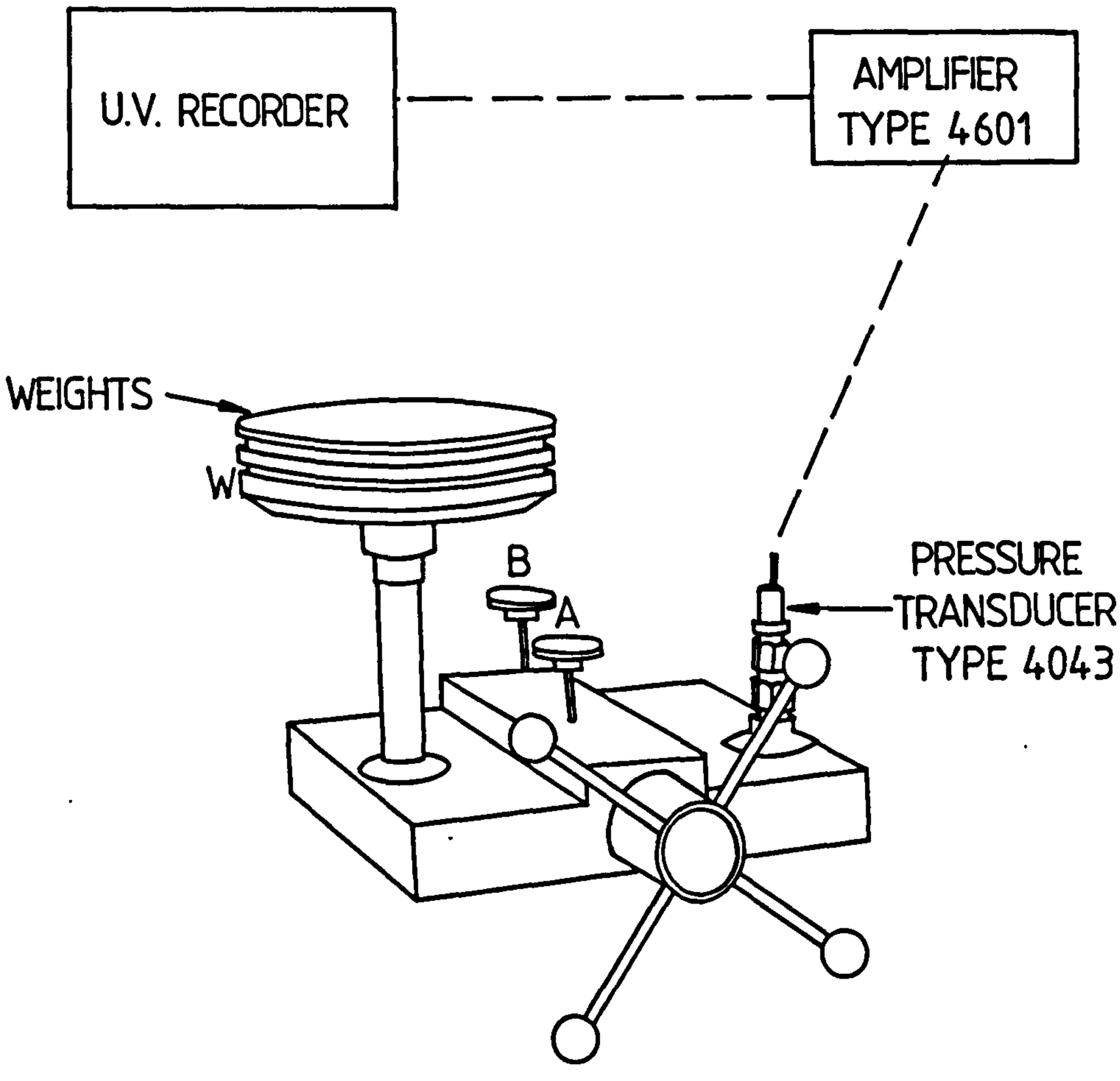

Figure 4.9 The calibration circuit of Pressure Transducer

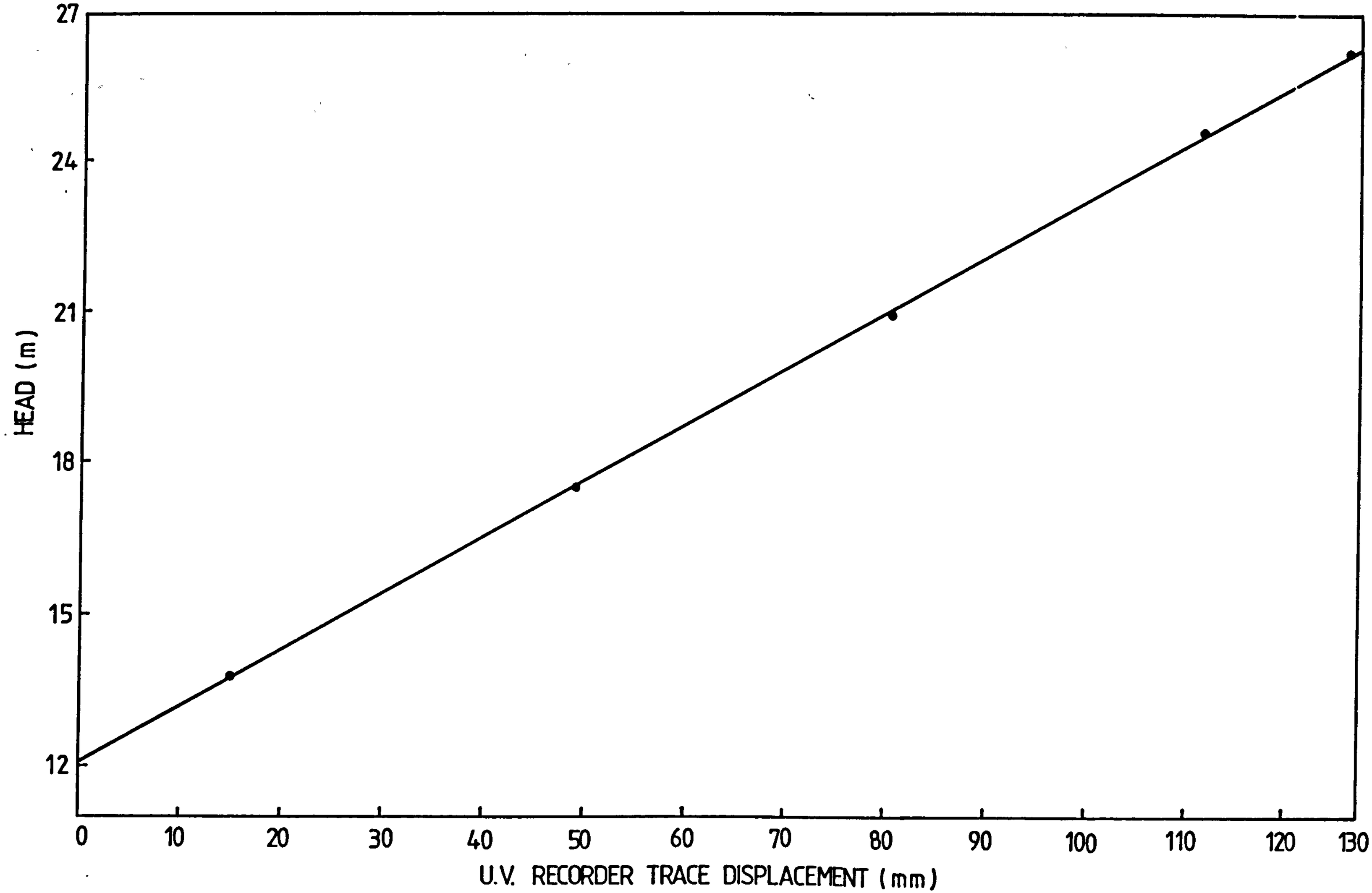

Figure 4.10 Calibration curve of the Pressure Transducer

The graph of the head ($h = P/\rho g$) against the UV recorder trace displacement was drawn for the transducer in Figure 4.10.

The estimated accuracy was to within $\pm$0.4% including translation errors, taking into consideration the error due to the calibration procedure.

4.4.2 Flowrate Measurement

As shown in Plate 3.1, a differential pressure transducer was connected across an orifice meter to measure the flowrate.

1. Orifice meter

An orifice plate with a D and D/2 tapping arrangement was used in the rig. A straight length of 21D preceded the orifice plate to provide an undistorted profile, and a 7.5D straight section followed the orifice plate downstream.

The orifice plate was made according to British Standard, (Ref.20), and it consisted of a brass plate having an axial hole (71 mm diameter) with a square edge on the upstream side and a bevelled edge on the downstream side. The pressure tappings were located at a distance of one pipe diameter upstream and one-half of the pipe diameter downstream of the plate. Figure 4.11 shows the dimensions and the constructional arrangement of this type of orifice plate.

The wall tapping holes (2.5 mm bore) were connected to a differential pressure transducer by using plastic tubing.

2. Differential pressure transducer

A differential pressure transducer type PDCR 120/WL was mounted across the orifice plate. An amplifier TYPE DPI 250 from Druck Limited (UK) was fitted in conjunction with a transducer as its signal was not strong enough to drive the galvanometer of the UV recorder. Similarly it was not convenient to calibrate the transducer on

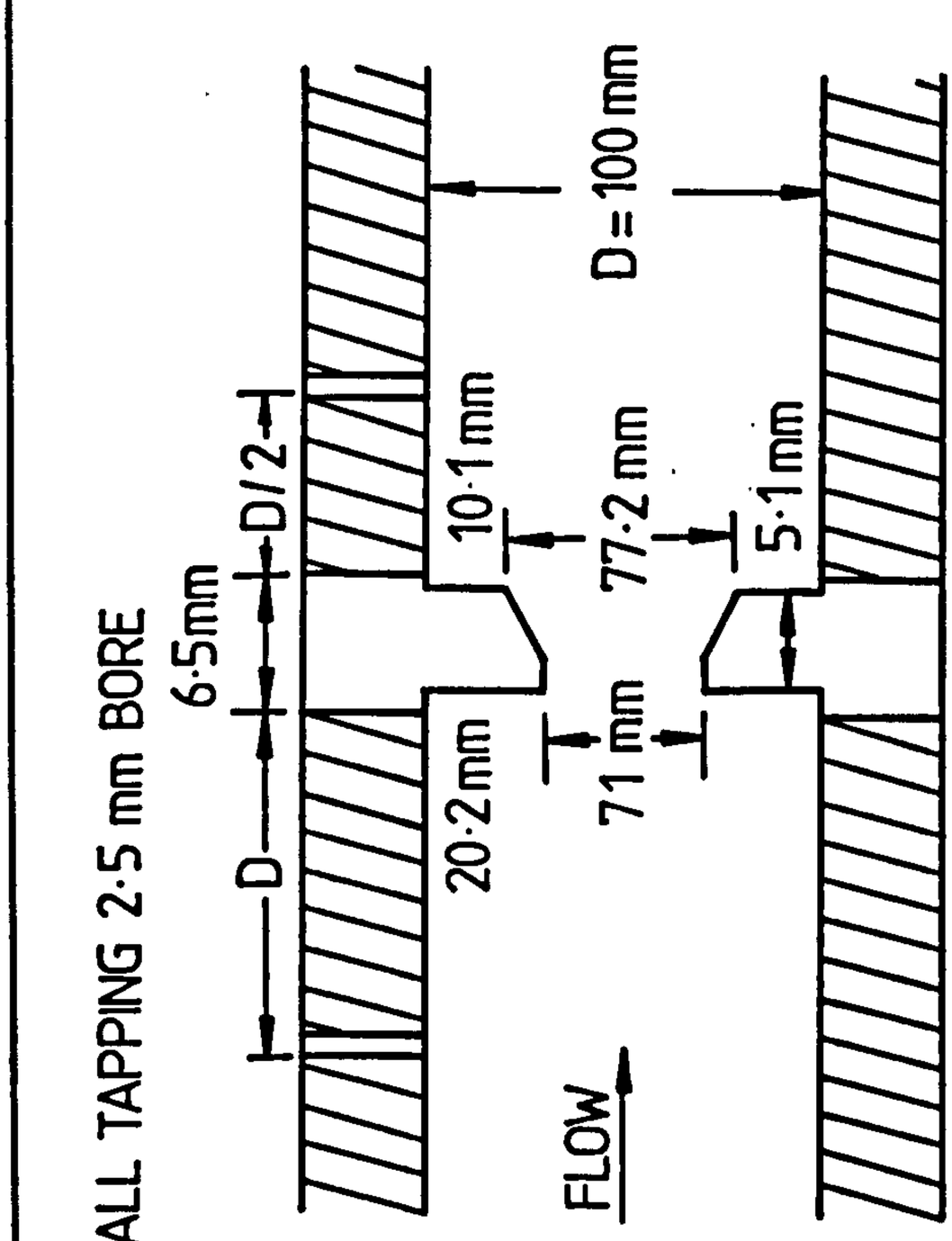

Figure 4.11 The orifice plate arrangement

site, therefore a special tester built by the BHRA Instrumentation Department was used. Figure 4.12 shows the pressure circuit. The electrical circuit, also shown on this figure, consisted of the transducer, an amplifier unit and UV recorder.

The calibration procedure was as follows. Initially the UV recorder trace position was noted for the zero signal corresponding to atmospheric pressure. The damping valve was opened to create a pressure difference in the manometer then closed. The pressure difference in the manometer is equal to the pressure difference across the transducer. By using the adjustment valve, a range of differences can be obtained.

The resulting trace displacement was measured relative to the zero signal position and the corresponding pressure difference in the manometer was found. The volume flowrate (Q) in the pipe was then related to the manometer pressure difference readings as follows:

$$Q = 0.01252\ K\sqrt{h/\rho}\ \ m^3/h \qquad (4.4)$$

where K is the product of several correction factors given in the British Standard, h is the pressure difference in mm of water and ρ is the water density (kg/cm^3). The calibration curve of the flowrate (Q) against the UV recorder trace displacement is shown in Figure 4.13.

A high natural frequency allows measuring any variation in flowrate. From the natural frequency of the differential transducer it can be estimated that the response time is about 1×10^{-5} sec. Also the response of the water in the plastic tubing was 1×10^{-5} sec. according to Brown and Nelson's formula, (Ref.26).

$$\frac{P_t}{P_i} = \text{erfc}\left|\frac{1}{2}\frac{\tau_0}{\sqrt{t - \tau_0}}\right| \qquad (4.5)$$

where P_t = the desired transducer pressure

P_i = the initial pressure

τ = dimensionless time = $t\nu/r^2$

τ_0 = dimensionless delay time = T /r^2

ν = kinematic fluid viscosity

r = pressure tubing radius

T = tubing length/acoustic velocity = L/a

erfc = the complimentary error function.

The accuracy of the measurements were subjected to many sources of systematic and random errors which are explained below.

The major source of error was the manometer reading used in calibration of the transducer. The estimated accuracy was within 0.5%. The combined errors of the transducer and the amplifier output was ±0.05%.

The total error in flowrate measurements by using the orifice plate in conjunction with a differential pressure transducer was ±0.55%.

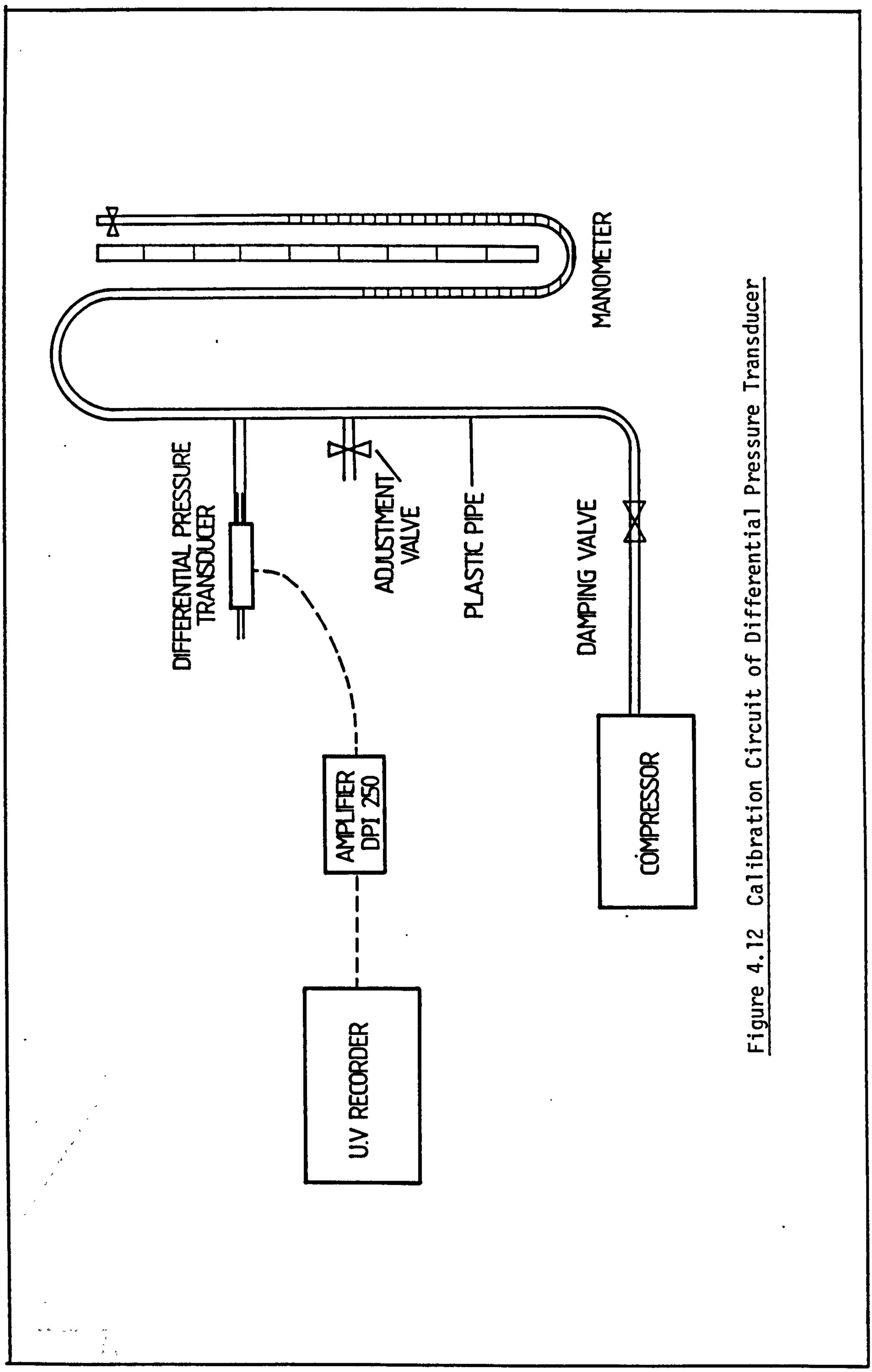

Figure 4.12 Calibration Circuit of Differential Pressure Transducer

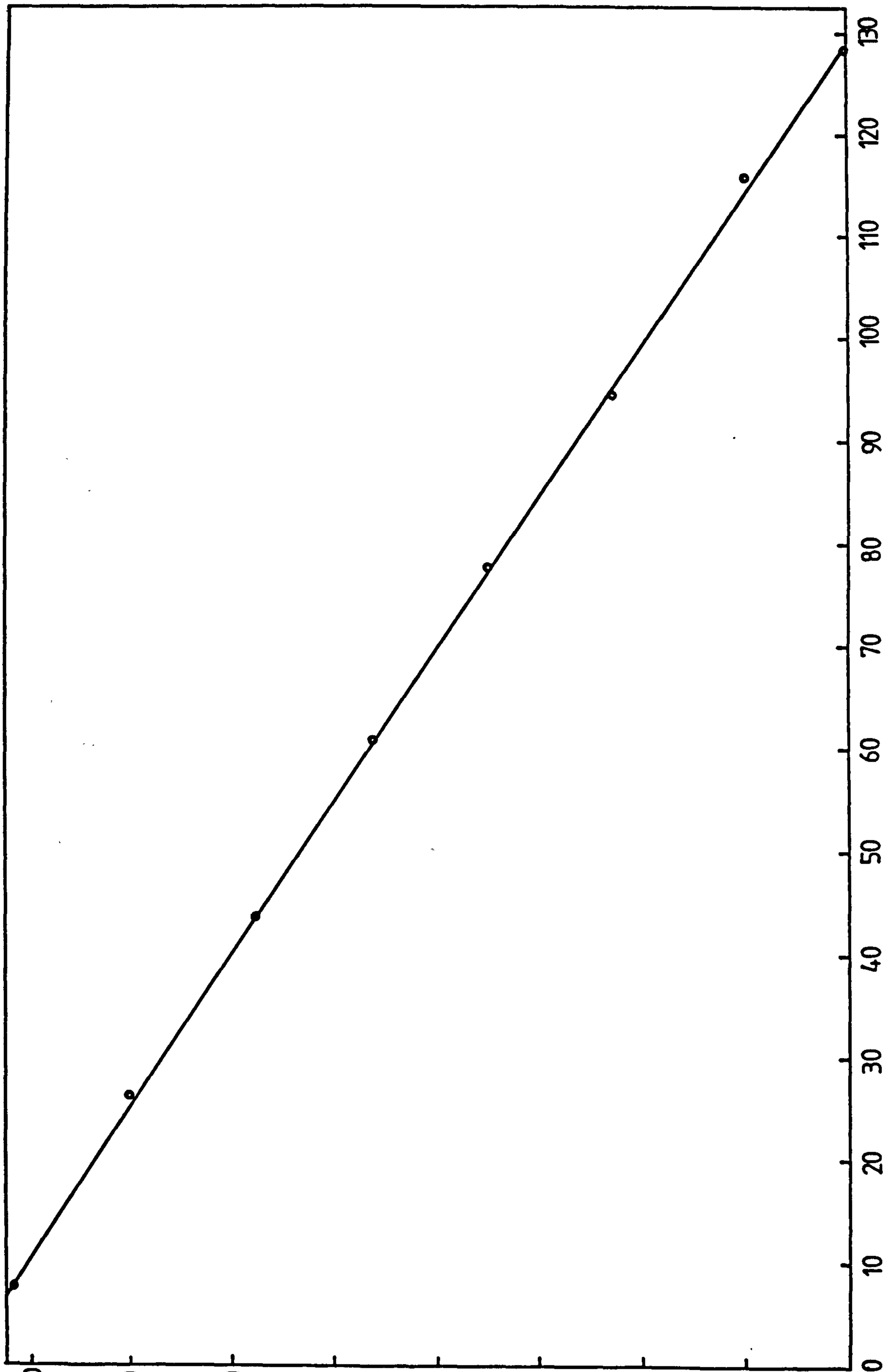

Figure 4.13 Calibration curve of Differential Pressure Transducer

4.4.3 Speed Measurement

A variable reluctance tachometer is often used to measure the speed of a shaft, (Ref.21). Tachometers using a toothed rotor made of ferromagnetic material and a transduction coil wound around a permanent magnet are the most common form of pulse output speed transducers Figure 4.14. The magnetic field surrounding the coil is distorted by the passing of a tooth carrying a pulse of output voltage in the coil. The root mean square (rms) value of the output voltage increases with a reduction in the clearance between rotor and pickup with an increase in tooth size and with an increase in rotor speed. The frequency of the output pulses is dependent on the number of teeth and the rotor speed and they are counted to determine the rms value. Usually about 60 teeth are used and clearance is about 0.3 mm,(Plate 4.2).

The output voltage is fairly sinusoidal and the peak-to-peak value proportional to the shaft speed (N rev/min).

It is easy to calibrate the tachometer on site. The output of the pickup is connected to the UV recorder. Different speeds are recorded by varying the gate opening and hence the speed of the turbine.

The calibration curve of the speed (N) against the UV recorder trace displacement is shown in Figure 4.15.

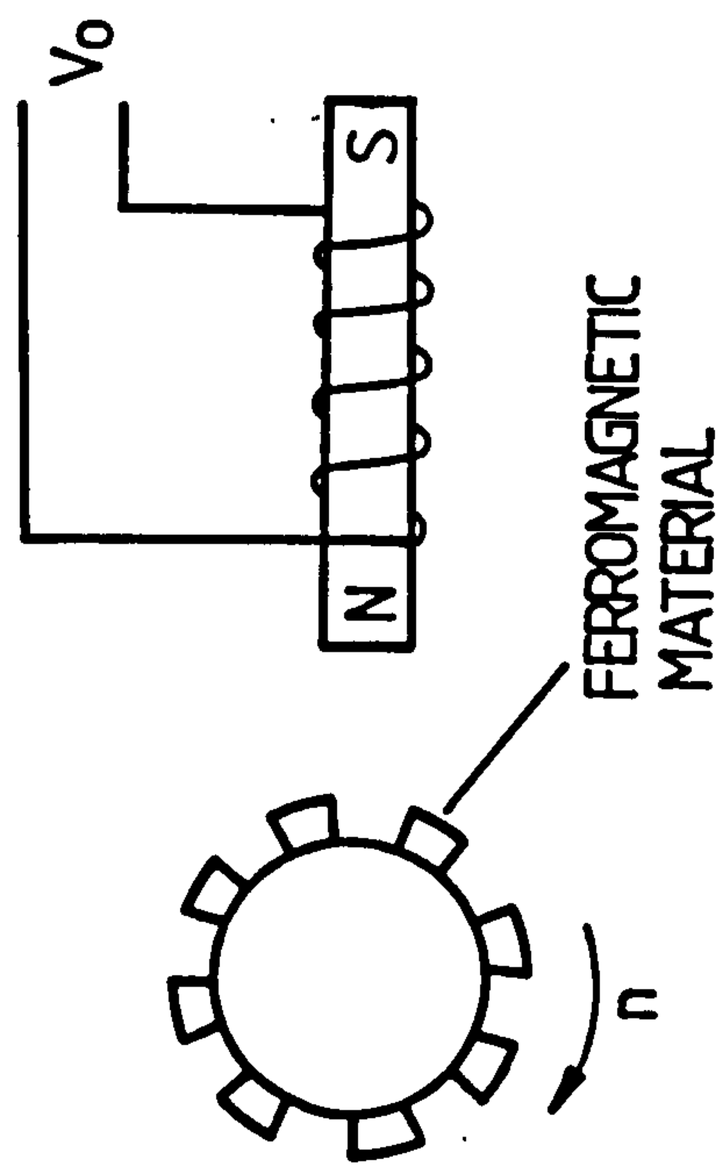

Figure 4.14 Variable Reluctance Tachometer

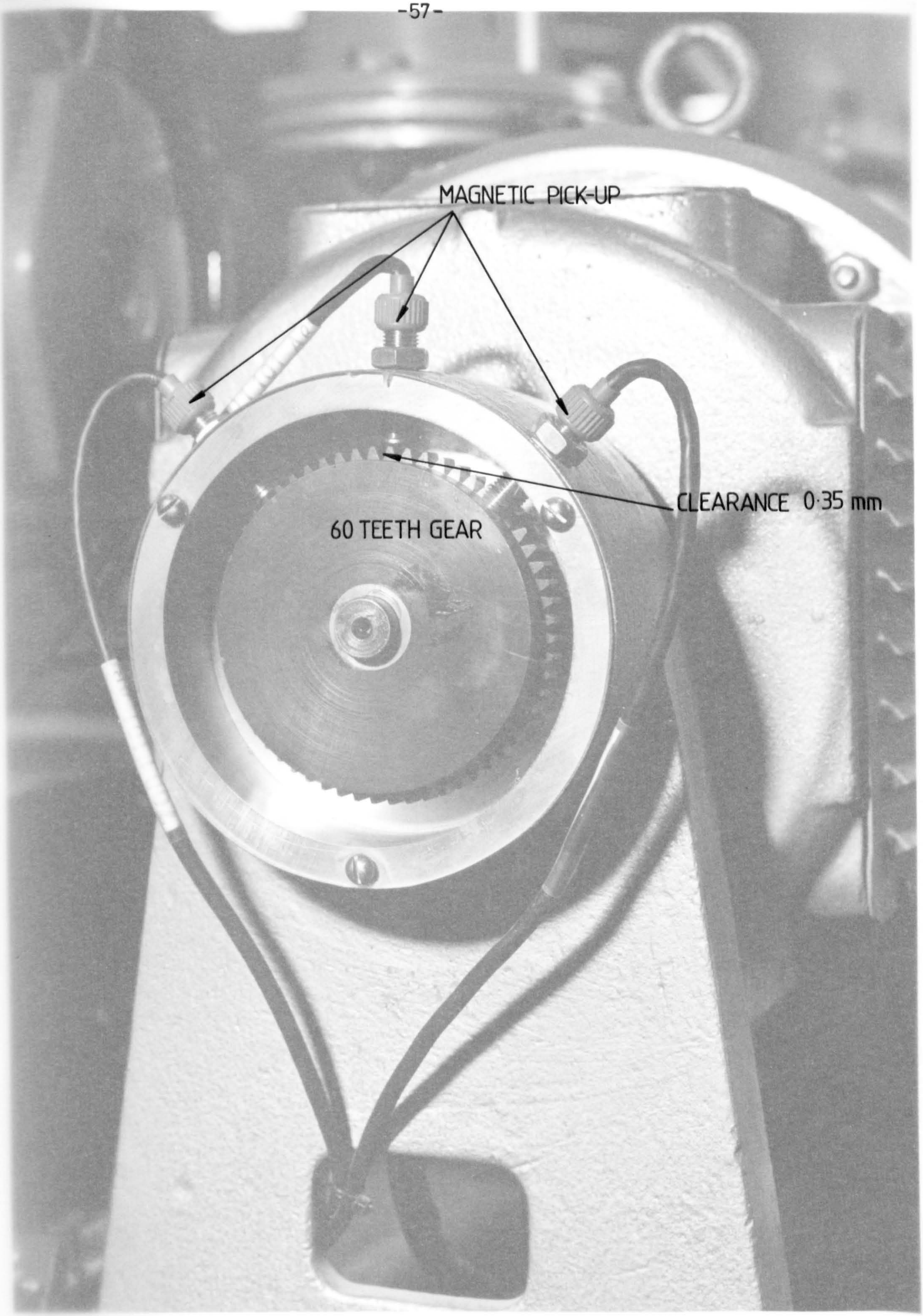

PLATE 4·2 THE TACHOMETER

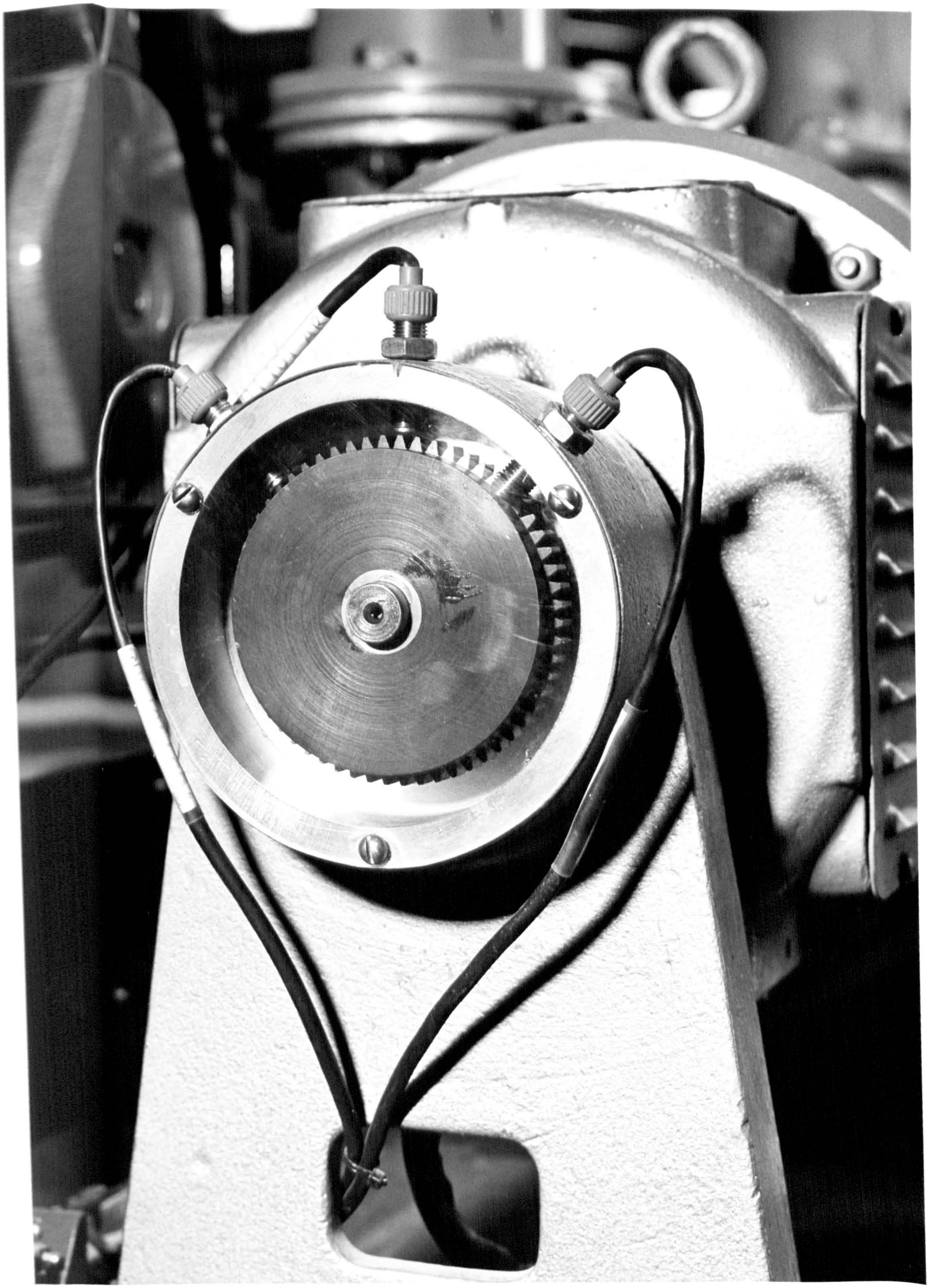

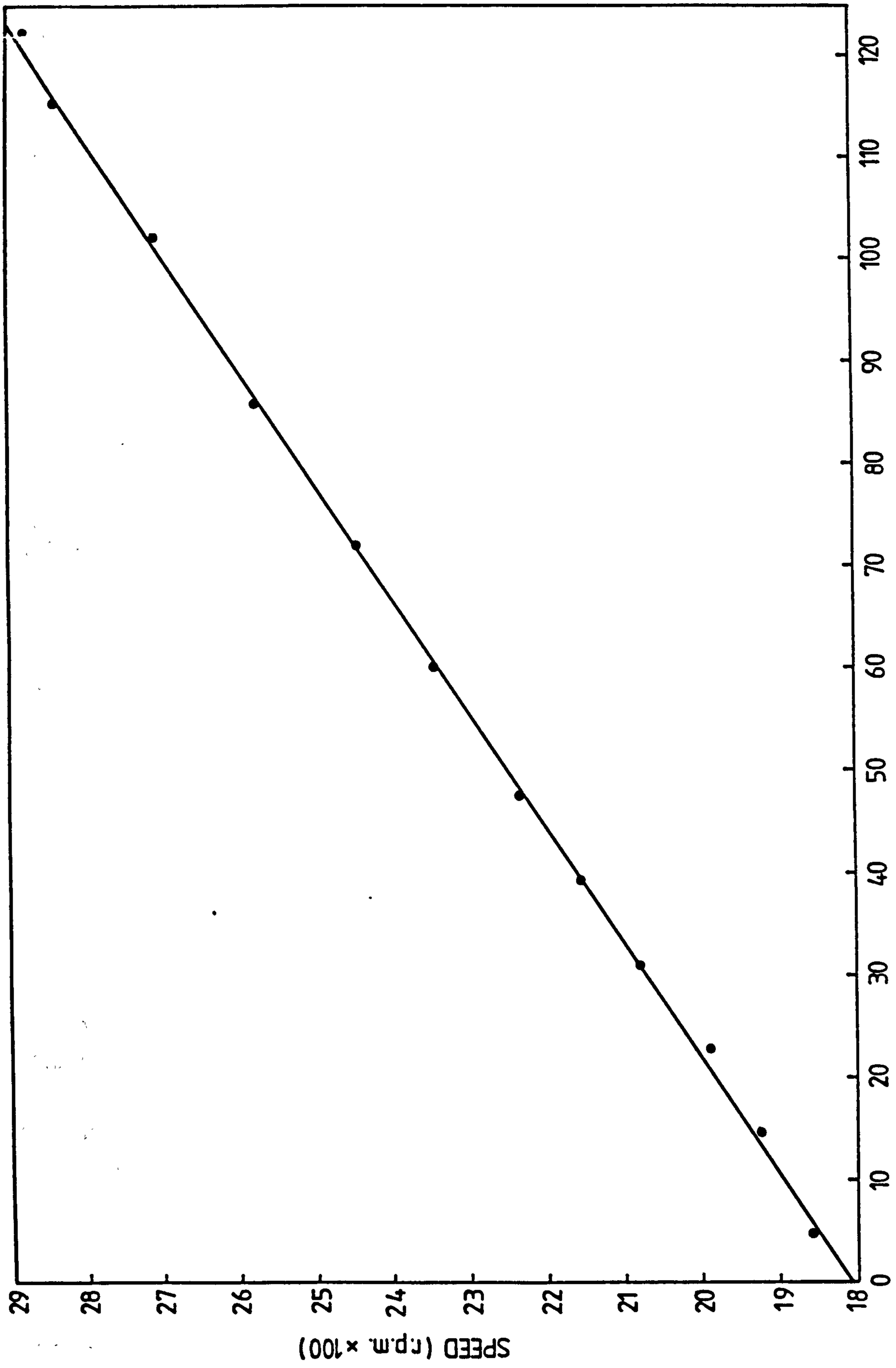

Figure 4.15 Calibration curve of the Turbine speed (rpm)

4.4.4 Gate Opening Measurement

One of the most common transducers in control systems applications is the potentiometer which converts mechanical position into an electrical voltage, (Ref.21). Figure 4.16 shows a schematic and block diagram of the relation between the input output voltage and the mechanical position of the shaft.

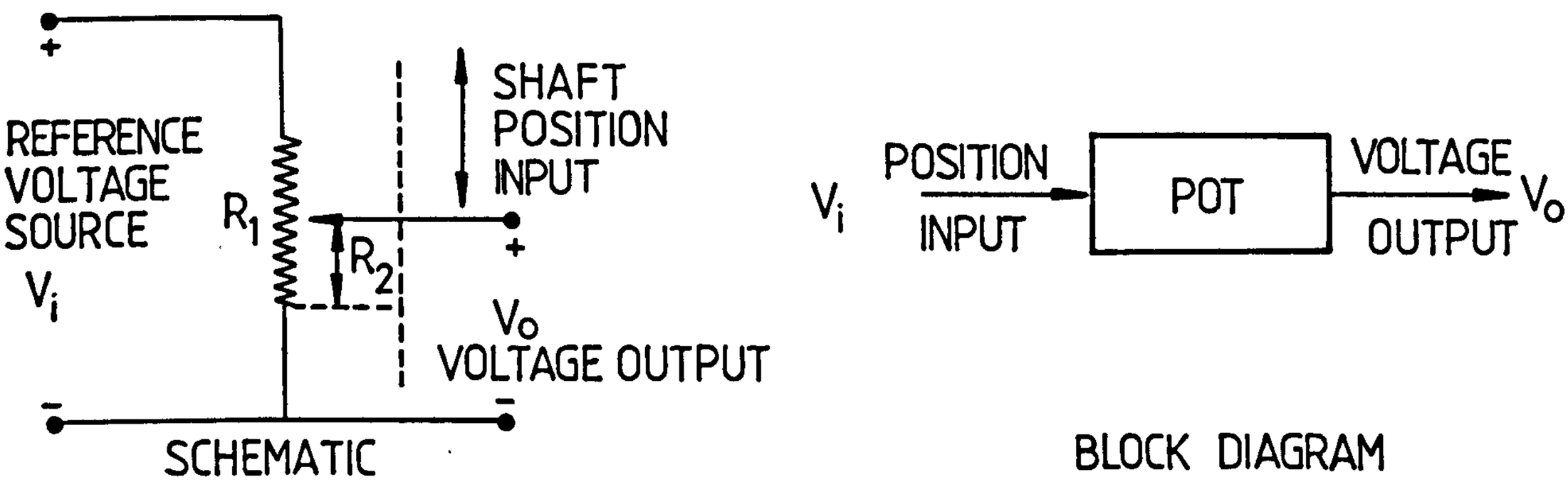

Figure 4.16 Schematic and Block Diagram of the Potentiometer

The wicket gate opening was recorded as follows.

Two gears were used with a 1 to 4 ratio, the small one connected to the stepping motor shaft and the large one connected to a potentiometer which converted the mechanical position into an electrical voltage, Plate 4.3. The relation between the mechanical position and the output voltage (V_0) is linear because both of them depend on the potentiometer position (i.e. R_2/R_1) which is varied.

The calibration of the gate opening is as follows.

When the gate is fully opened a particular signal is obtained from the potentiometer and recorded on the UV recorder. This signal

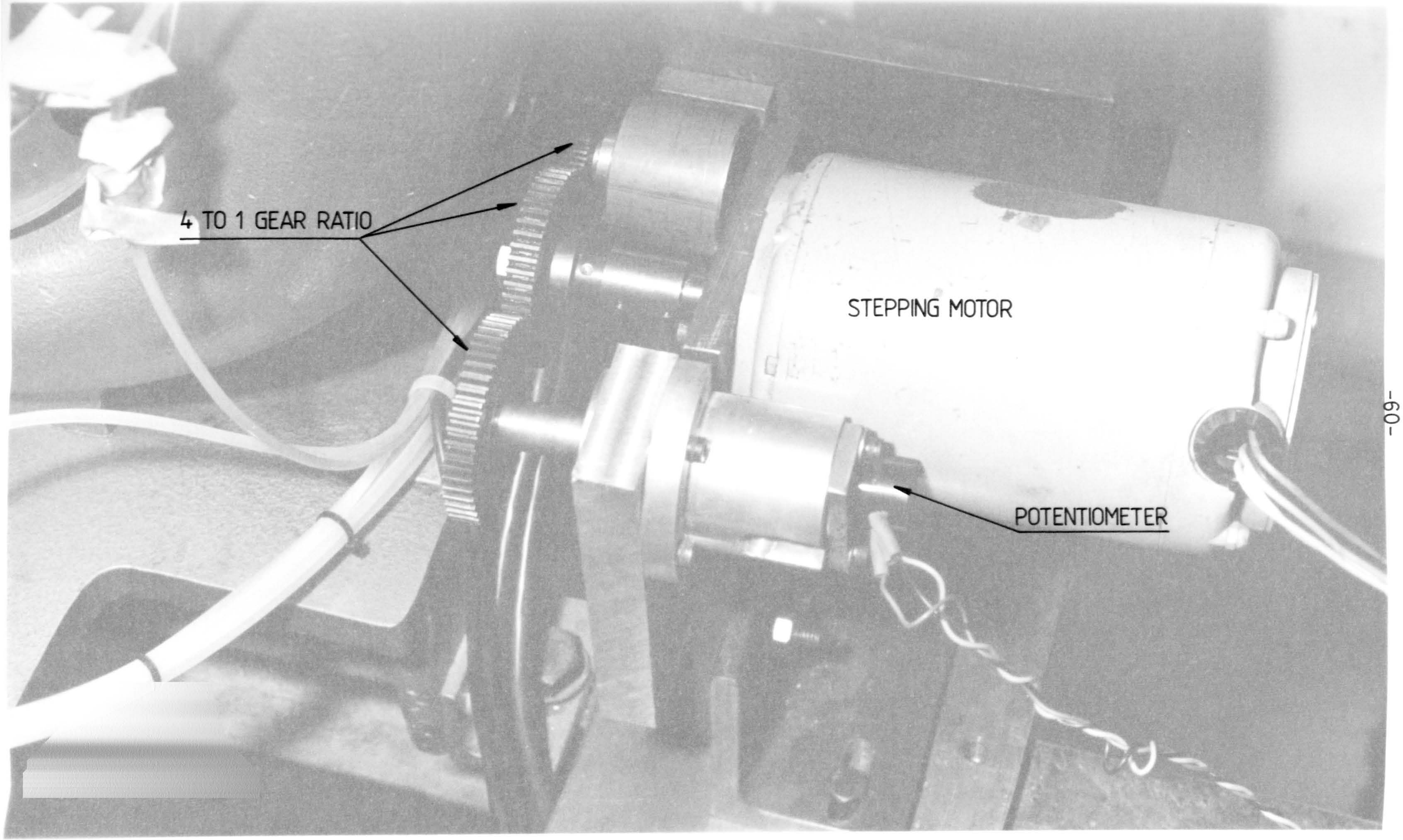

PLATE 4·3 THE STEPPING MOTOR AND POTENTIOMETER

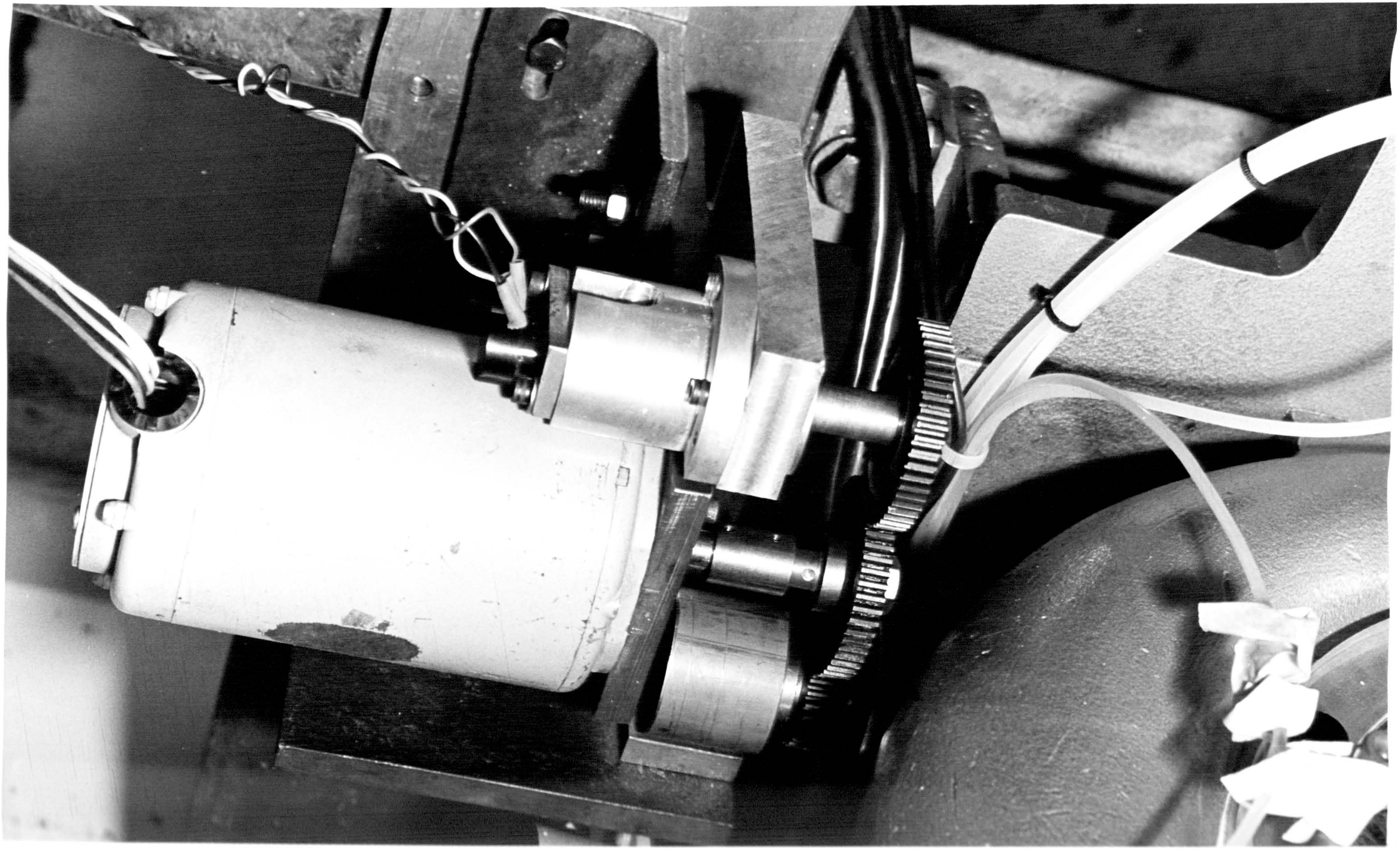

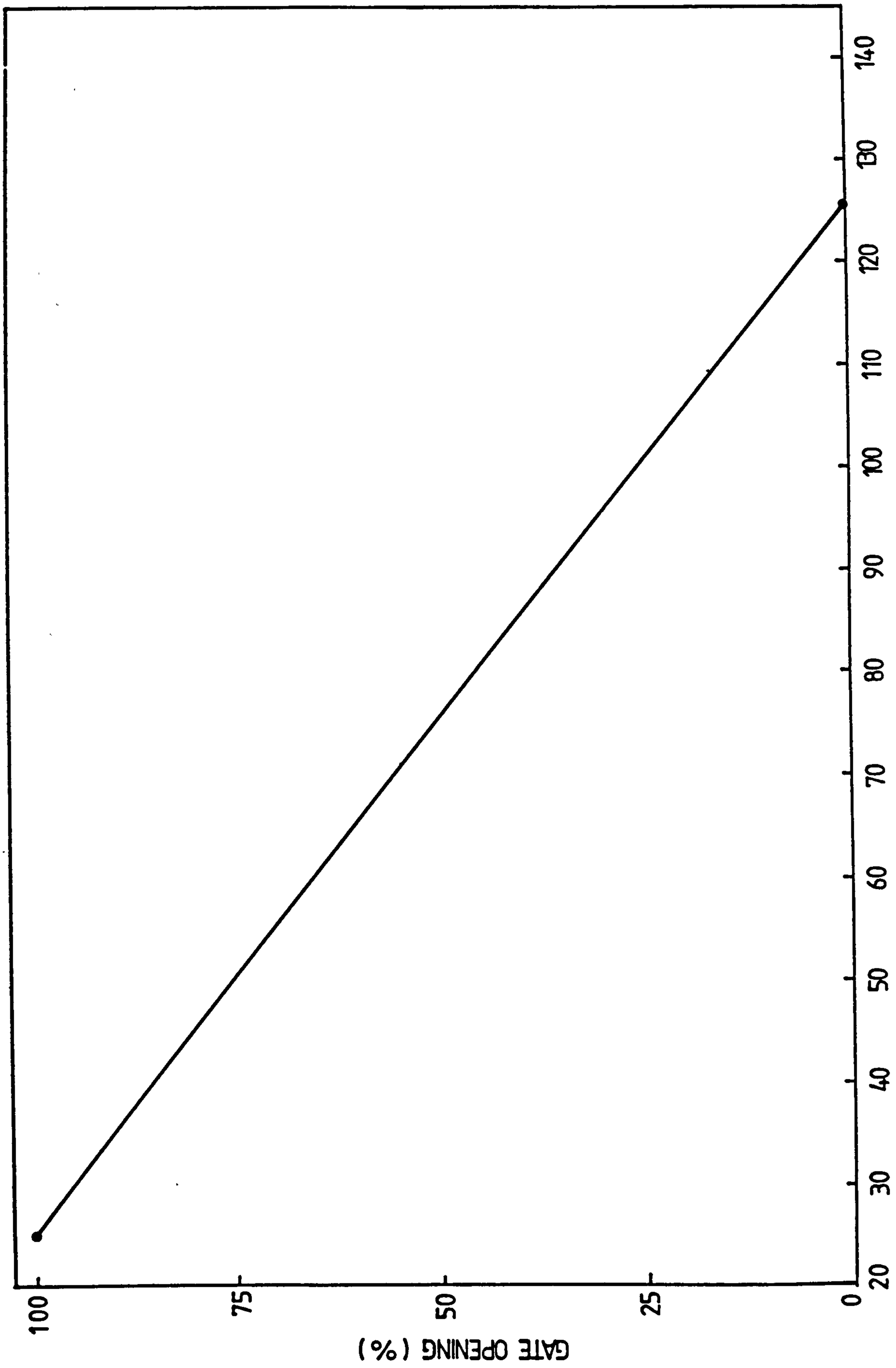

Figure 4.17 Calibration curve of the Gate opening (%)

represents 100% gate opening. The 0% gate opening is obtained by closing the gate manually and the output signal recorded also. The calibration curve of the gate opening is shown in Figure 4.17.

4.5 EXPERIMENTAL METHOD

A full set of tests were carried out for a range of partial load rejections as well as for full load rejection. Appendix B tabulates all the experimental results.

At the beginning of the experimental work on the rig it was essential to calibrate all of the instruments used for data collection. Normally one test run was carried out during a single day. The amplifiers and the UV recorder needed to be switched on one hour before the test. The experimental procedure is detailed in the following items.

1. The supply pump of the system was switched on and the required conditions of head and flow were obtained by using the gate valves.

2. The load imposed on the turbine can be fixed by using the plug in points (1-15), i.e. for full load rejection plug in points 1 and 15 were used.

3. The output of each part of the controller (PID) was checked to ensure that it was zero in each case.

4. Initially the conditions were determined in terms of the following measurements.

   (a) The speed of the turbogenerator set by recording the control console indicator on the UV recorder.

   (b) The flowrate by recording the pressure difference from the amplifier on the UV recorder.

   (c) The inlet pressure recorded on the UV recorder.

(d) The gate opening by using an avometer for the output of the potentiometer and the UV recorder

(e) The load imposed on the turbine by the generator from the voltmeter and ammeter of the control console.

5. The UV recorder and the stepping motor supply were switched on and at the same time a load rejection was done by manually switching off.

6. The speed of the turbine increased suddenly then the feedback response actuated the stepping motor to close the gate of the turbine till the speed returned to its initial value. The motor rotated clockwise,or counter clockwise when the speed was less than the demanded speed.

7. At the end of the test when the fluctuations were stopped (steady state), the stepping motor supply was switched off as well as the UV recorder.

8. Upon attaining the required steady state conditions the above procedure (Items 1 to 7) was repeated for different load rejection.

Each test was repeated many times till consistent results were achieved. This was necessary because of the sensitivity of the electronic system and due to the hysteresis in the mechanical parts.

CHAPTER 5

COMPUTATIONAL PROCEDURE

5.1 INTRODUCTION

The computer program consists of a "MAIN" program and several subroutines and functions. The main program serves primarily as a device for linking the subroutines together in proper sequence and, in addition, performs certain bookkeeping and test computations at the beginning and end of each time step. The total program is perhaps most easily described by first discussing the subroutines and functions and then showing how they are combined in the MAIN program.

5.2 FUNCTIONS (see flowcharts on pages 75-82)

5.2.1 Function FACT (I,J,K,L,PHIO)

This function is used to calculate the Lagrangean interpolation coefficients $\ell_i(x)$. Hence

$$\ell_{i(x)} = \frac{(x-x_0)(x-x_1).....(x-x_{j-1})(x-x_{j+1})....(x-x_n)}{(x_j-x_0)(x_j-x_1).....(x_j-x_{j-1})(x_j-x_{j+1})..(x_j-x_n)}$$

$$\ell_{i(x)} = \prod_{\substack{r=1 \\ r\neq j}}^{n} \left(\frac{x-x_r}{x_j-x_r}\right) \qquad (5.1)$$

By substituting $x = \phi$

$$\ell_{i(\phi)} = \prod_{\substack{r=1 \\ r\neq j \\ r\neq k \\ r\neq \ell}}^{N\phi} \left(\frac{\phi_{given} - \phi_r}{\phi_j - \phi_r}\right) \qquad (5.2)$$

where k and ℓ are the subscripts of ϕ when the function calculates the first and second derivative of Lagrangean interpolation coefficients
$\ell_{i(x)}$ and Nϕ = Number of unit speed tabulated
ϕ_{given} = The unit speed calculated.

5.2.2 Function FLAGI(N,X,I,X_0)

This function is used when all the points in the grid of the turbine characteristics are used to calculate:-

1. $\ell_{i(\tau)}$ when the general Lagrangean formula is used. Hence

$$\ell_{i(\tau)} = \prod_{\substack{r=1 \\ r\neq I}}^{N\tau} \left(\frac{\tau_{given} - \tau_r}{\tau_I - \tau_r}\right) \qquad (5.3)$$

where $X_0 = \tau$
τ_{given} = The gate opening calculated
Nτ = Number of gate openings from the turbine characteristics.

2. $\ell_{i(q)}$ when the gate opening at t=0 is calculated, i.e.

$$\tau = f(q,\phi)$$

$$\ell_{i(q)} = \prod_{\substack{r=1 \\ r\neq j}}^{Nq} \left(\frac{q_{given} - q_r}{q_j - q_r}\right) \qquad (5.4)$$

where $X_0 = q$
τ_{given} = The unit flow calculated from the initial conditions.
Nq = Number of unit flow from the turbine characteristics.

5.2.3 Function FLAG(I,J,PHIO)

This is used to calculate the Lagrangean interpolation coefficients of equation (3.44) and is the equivalent of Function FACT (I,J,0,0,PHIO) with K = L = 0.

$$\ell_{i(\phi)} = \prod_{\substack{r=1 \\ r\neq j}}^{N\phi} \left(\frac{\phi_{given} - \phi_r}{\phi_j - \phi_r}\right) \tag{5.5}$$

5.2.4 Function DLAG(I,J,PHIO)

This is used to calculate the first derivative of Langrangean interpolation coefficients of equation (3.45).

$$\frac{\partial \ell_i(x)}{\partial x} = \sum_{\substack{k=1 \\ k\neq j}}^{m} \left(\frac{1}{x_j - x_k}\right) * \prod_{\substack{r=1 \\ r\neq j \\ r\neq k}}^{m} \left(\frac{x - x_r}{x_j - x_r}\right) \tag{5.6}$$

Appendix D shows the derivation of equation (5.6).

5.2.5 Function D2LAG(I,J,PHIO)

This function in conjunction with the previous function is used to calculate the second derivative of the Lagrangean interpolation coefficients of equation (3.46).

$$\frac{\partial^2 \ell_i(x)}{\partial x} = \sum_{\substack{\ell=1 \\ \ell\neq j}}^{m} \left(\frac{1}{x_j - x_\ell}\right) * \sum_{\substack{k=1 \\ k\neq j \\ k\neq \ell}}^{m} \left(\frac{1}{x_j - x_k}\right) * \prod_{\substack{r=1 \\ r\neq j \\ r\neq k \\ r\neq \ell}}^{m} \left(\frac{x - x_r}{x_j - x_r}\right) \tag{5.7}$$

Appendix D shows the derivation of equation (5.7).

5.2.6 Function TAUF(PHIO,QI)

This is used to calculate the initial condition of the gate opening (τ at t=0) with respect to the unit flow and unit speed. The unit flow and the unit speed are calculated from the characteristics of the system.

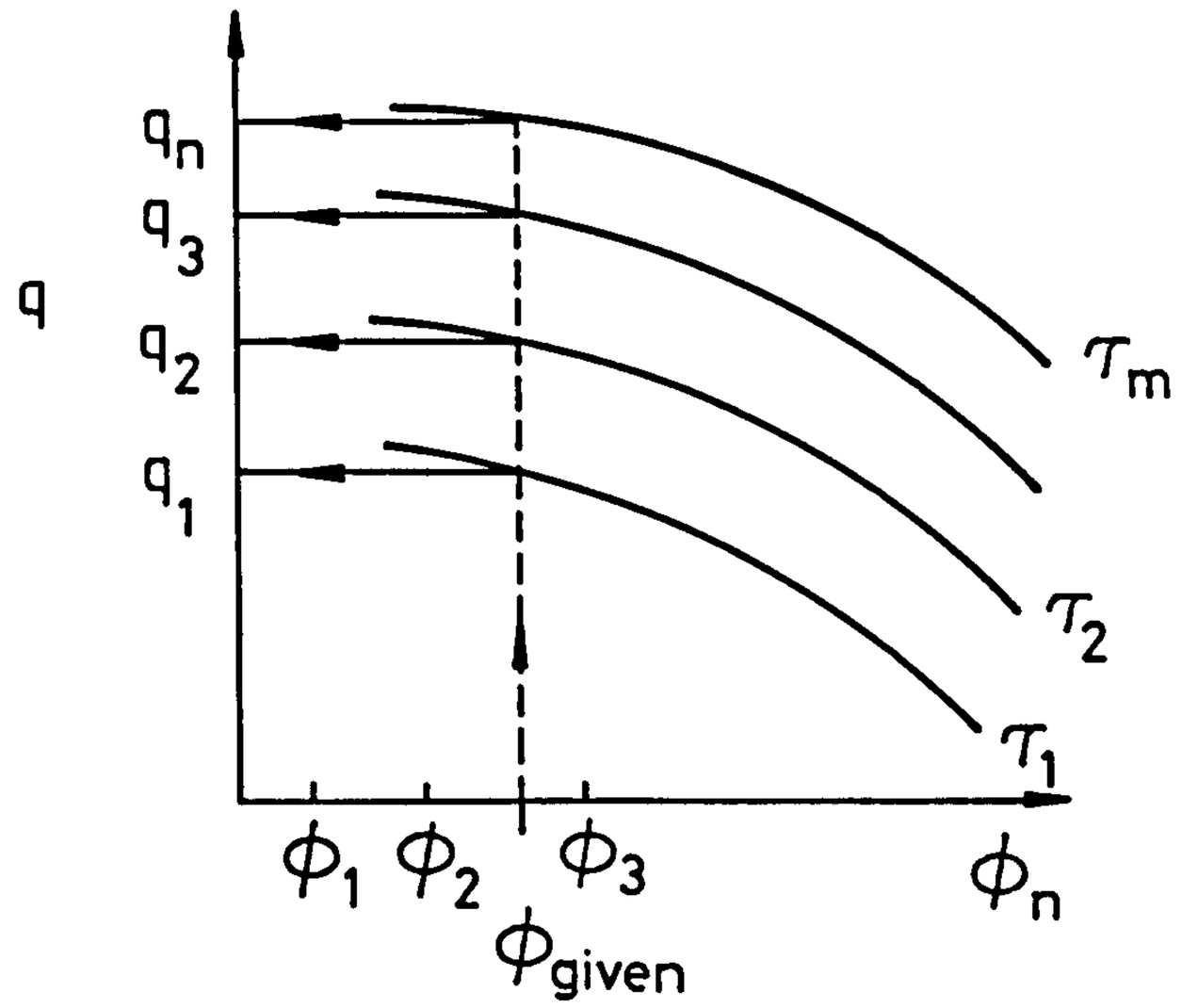

The function is worked in two steps.

1. For a given unit speed (ϕ) where $q = f(\phi,\tau)$, the unit flow can be calculated from equation (3.43).

$$q = \sum_{i=1}^{m} \prod_{\substack{r=1 \\ r\neq i}}^{m} \left(\frac{\phi_{given} - \phi_r}{\phi_i - \phi_r}\right) q(\tau_i,\phi_r) \qquad (5.8)$$

The co-ordinates at ϕ_{given} are:

$$(\tau_i,q_i) \qquad i = 1,N_\tau$$

where N_τ = Number of gate openings.

2. The previous results represent a one dimensional relation between q_i and τ_i. Then

$$\tau_{initial} = \sum_{j=1}^{Nq} \prod_{\substack{r=1 \\ r\neq j}}^{Nq} \left(\frac{q_{given} - q_r}{q_j - q_r}\right) \tau_i \qquad (5.9)$$

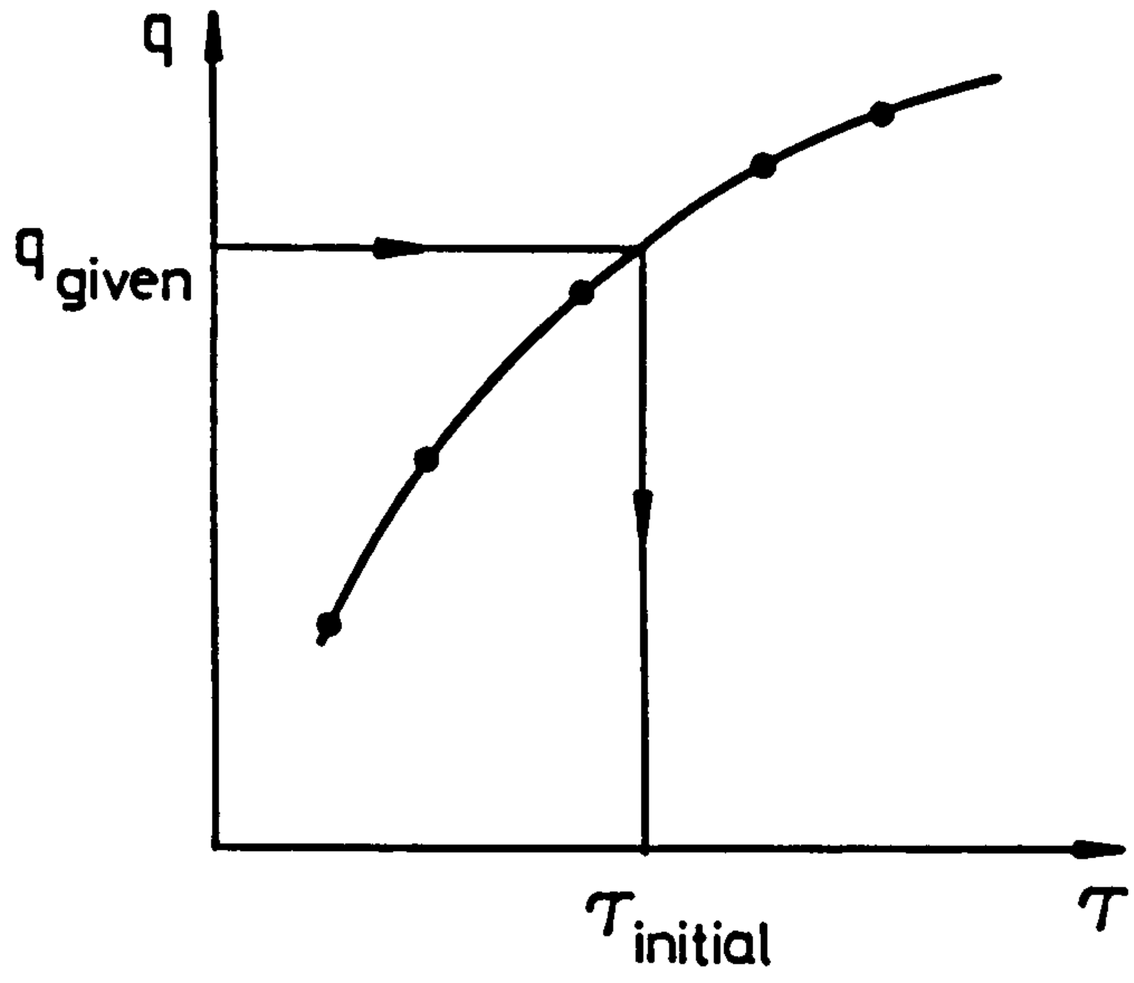

5.2.7 Function ZI(TAUI,PHII,Z,ID)

The previous functions are controlled by this function, where (Z) refers to the two dimensional performance data of the turbine and (ID) refers to the functions.

Also the function works in two steps.

1. For ϕ_{given} and τ_{given}, Z_i is calculated from equations (3.44), (3.45) and (3.46).

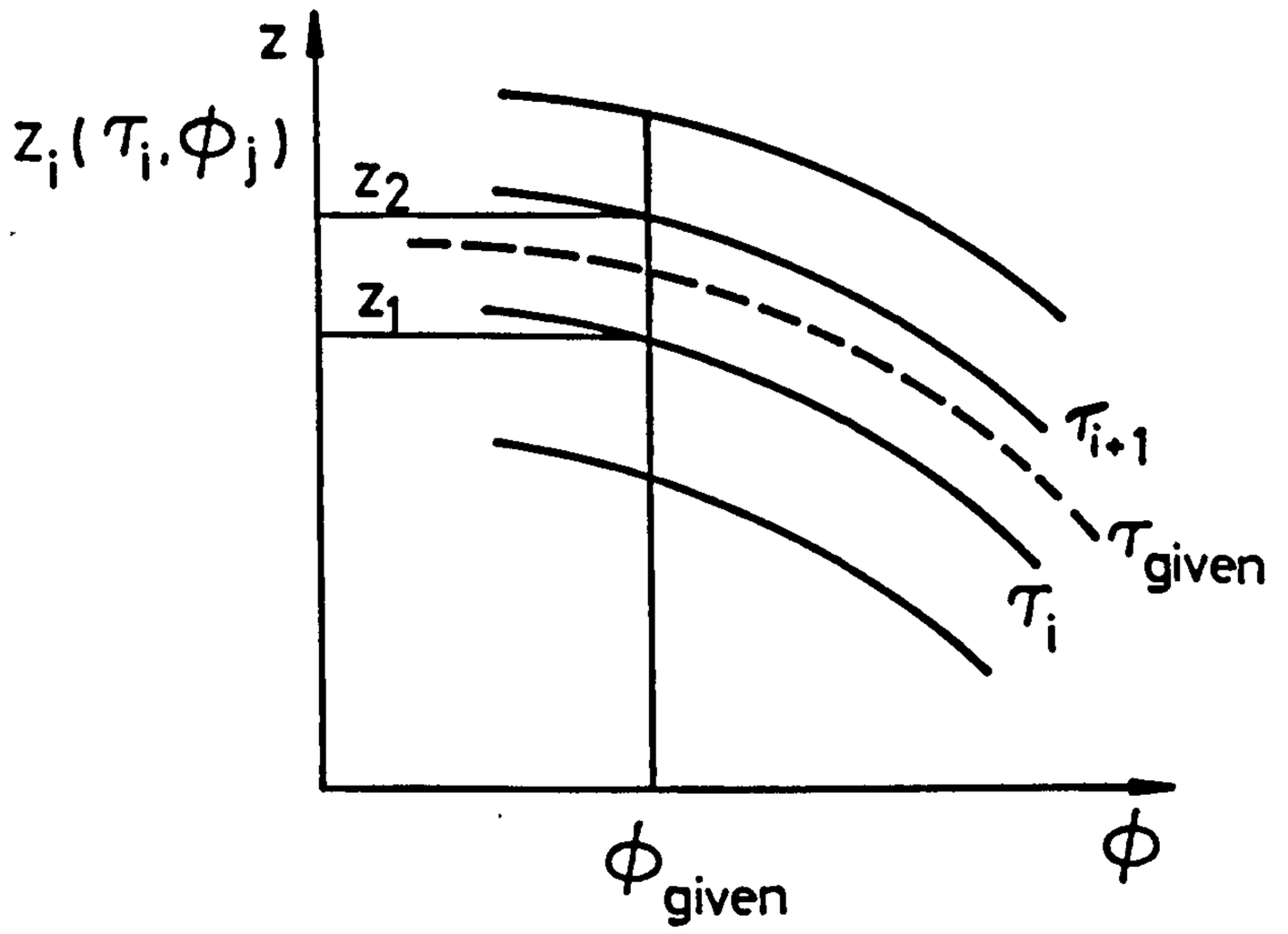

2. For Z_i calculated and τ_i defined, Z can be calculated.

$$Z = \left(\frac{Z_2 - Z_1}{\tau_2 - \tau_1}\right)(\tau_{given} - \tau_1) + Z_1 \qquad (5.10)$$

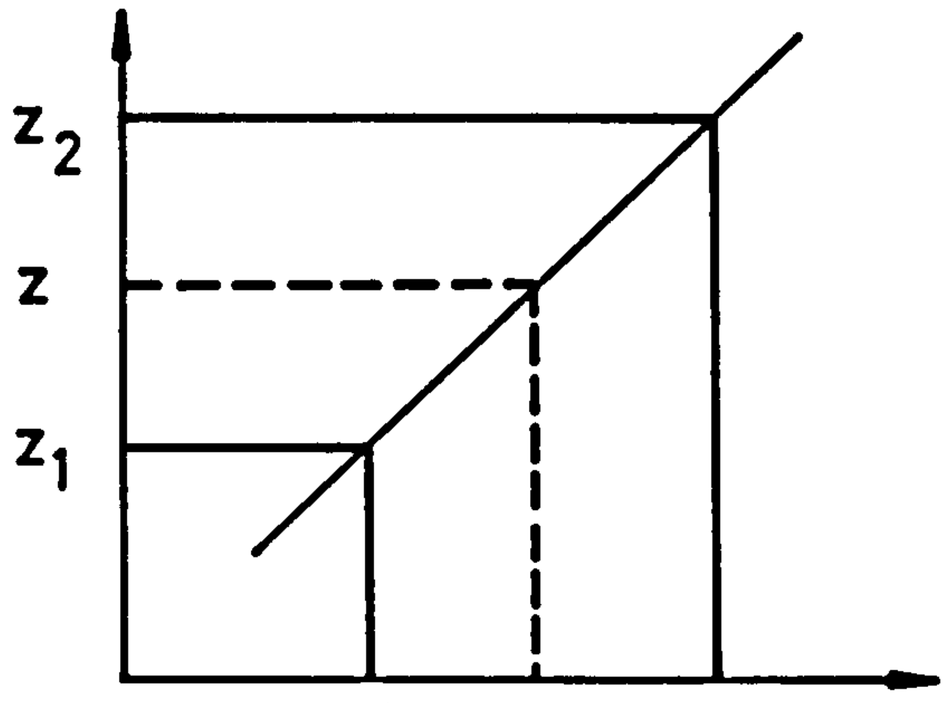

5.3 SUBROUTINES (see flowcharts on pages 83-90)

5.3.1 Subroutine DATA(IDATA)

All required data are stored by the subroutine data. It can be divided as follows:-

1. Initial conditions data (Appendix C).
2. The turbine performance data which are stored in a two dimensional table of values of unit speed vs. unit flow and unit speed vs. unit power for various gate openings (Appendix C).

5.3.2 Subroutine LINEAR(TAUI,PHII,QI,A0,A1)

The constants a_0 and a_1 of equation (3.23) are calculated as follows. By rewriting equation (3.23) with q and ϕ known

$$q = a_0 + a_1\phi \qquad (3.23)$$

Differentiate both sides of the equation with respect to ϕ.

$$\frac{dq}{d\phi} = a_1 \qquad (5.11)$$

To evaluate Function ZI(TAUI,PHII,Z,ID) for Z = Q, the data required are unit flow vs. unit speed for various gate openings and with ID = 1 which refers to the first derivative of equation (3.44), a_1 may be calculated. Hence

$$a_0 = q - a_1\phi \tag{5.12}$$

5.3.3 Subroutine PARABOLIC(TAUI,PHII,C0,C1,C2)

The constants C_0, C_1 and C_2 of equation (3.14) can be calculated as follows:

Rewriting equation (3.14)

$$p = C_0 + C_1\phi + C_2\phi^2 \tag{3.14}$$

Differentiating both sides of the equation twice with respect to ϕ

$$\frac{dp}{d\phi} = C_1 + 2C_2\phi \tag{5.13}$$

$$\frac{d^2p}{d\phi^2} = 2C_2 \tag{5.14}$$

To evaluate function ZI(TAUI,PHII,Z,ID) for Z = P, the required data are unit flow vs. unit power for various gate openings and ID=0,1,2 which refers to equations (3.44), (3.45) and (3.46). Then

$$C_2 = 0.5\,\frac{d^2p}{d\phi^2} \tag{5.15}$$

$$C_1 = \frac{dp}{d\phi} - 2C_2\phi \tag{5.16}$$

$$C_0 = p - C_1\phi - C_2\phi^2 \tag{5.17}$$

5.3.4 Subroutine ITER(N,QP,TAUI,PHII,HN,HP,CP,IC)

The aim of subroutine ITER is first to calculate the gate opening at t=0 and secondly to calculate the flowrate (QP), net head (HN) and piezometric head (HP) at the end of each time step as follows:

1. At t=0 the initial conditions of the speed (N), flowrate (Q) and net head (H_N) are known so unit flow and unit speed can be calculated. The gate opening at t=0 may be calculated from Function TAUF in conjunction with Functions FLAG and FLAG1.

2. At $t=\Delta t$, the input data are N and τ calculated by the Runge-Kutta subroutine and C_p calculated by the subroutine character. To calculate the unit speed at $t=\Delta t$, the net head is required but it is unknown. However by combining equation (3.7) and equation (3.22) and assuming $Q_{p_{t=0}} = Q_{p_{t+\Delta t}}$

$$H_N = (Q_p \cdot (S_2 \cdot Q_p - 1) + C_p)/S_1 - H_T \qquad (5.18)$$

where $$S_1 = \frac{G \times AREA}{A}$$

$$S_2 = \frac{1}{2(AREA)(A)}$$

and A = water hammer wave velocity (m/s)

AREA = cross sectional area of pipe (m^2)

Thus, the unit speed is known and the unit flow can be calculated, also the constants A_0-A_6. Then the flowrate at $t=\Delta t$ is calculated from equation (3.25) and H_N,H_p from equations (3.24) and (3.22). However, if $|Q_p - Q_{p_{assum}}| > 0.0001$ then the above procedure should be repeated to refine the solution.

3. If $t > \Delta t$, the same procedure of (2) is repeated except that

$$Q_{p_t} = Q_{p_{t-\Delta t}}$$

and $$H_N = ((Q_p - A_3)/A_2)^2$$

5.3.5 Subroutine RUNGE(PHII,TAUI,HN)

The equations (3.16),(3.33), (3.35),(3.38) and (3.41) are solved simultaneously by the fourth order Runge-Kutta method. The initial conditions of all the variables in the equations are required. N is known, τ calculated by subroutine ITER and all the governor parameters are set to zero. All the equations are non-dimensionalised by dividing all the parameters by a reference value.

N_{ref} = synchronous speed

τ_{ref} = gate opening at t=0

$(V_p, V_I, V_D, V_A)_{ref}$ = 1 (because their initial values are zero and hence could not be used).

From Runge-Kutta integration all the parameters are found at $t=\Delta t$.

5.3.6 Subroutine CHARACTER(IC,C_p)

The object of this subroutine is to calculate C_p as well as the pressure and the flowrate in the pipework. The pipework is divided into 16 reaches. The boundary conditions were derived in Chapter 3. A Newton-Raphson method was used to solve the upstream boundary condition.

Rewriting equation (3.21)

$$Q_c = \sqrt{\frac{115 - H_p}{6.2}} - \sqrt{\frac{H_p - H_s}{9.55}} \qquad (3.21)$$

assume

$$y = \sqrt{\frac{115 - H_p}{6.2}} \qquad (5.19)$$

From equations (3.21) and (3.6) with H_s = 1.0 and $C_a = S_1$ we get:-

$$G\dot{y}^4 + R\dot{y}^3 + E\dot{y}^2 + V\dot{y} + H_B = 0 \qquad (5.20)$$

where $G = (6.2 \times S_1)^2$

$R = 12.4 \times S_1$

$F = -(C_N + 115 \times S_1)$

$V = 2F$

$E = 1 + R \times F + 6.2/9.55$

$H_B = F.F - 114/9.55$

Equation (5.20) is solved by using Newton-Raphson method.

$$y_i = y_{i-1} - \frac{F(y)_{i-1}}{F'(y)_{i-1}} \qquad (5.21)$$

where $F'(y)_{i-1}$ is the differentiation of equation (5.20) with respect to (y).

5.4 THE MAIN PROGRAM

The principal functions performed by the MAIN program are listed below:

(i) The various equations generating subroutines are linked together in proper sequence.
(ii) The equation-solving iterations are controlled and tested for convergence.
(iii) Incrementing computations are performed.
(iv) Input and output are controlled.

5.5 SUMMARY OF THE COMPUTATIONAL PROCEDURE

1. Q, H_N and N are known initially so the gate opening (τ) can be found by Lagrangean interpolation (equation (3.44)) as $\tau=f(q,\phi)$.

2. The initial conditions of the variables in equations (3.16), (3.31), (3.33), (3.35) and (3.41) are required. N is known, τ calculated and all the governor parameters are set to zero.

All the equations are non-dimensionalised by dividing all the parameters by a reference value.

From Runge-Kutta integration all the parameters are found at $t=\Delta t$.

3. The method of characteristics (Ref.5), is used for calculating head and flow throughout the system.

A printout of the computer program is in Appendix E.

Flow chart of the function FACT(I,J,K,L,PHIO).
Calculation of the Lagrangean interpolation coefficient.

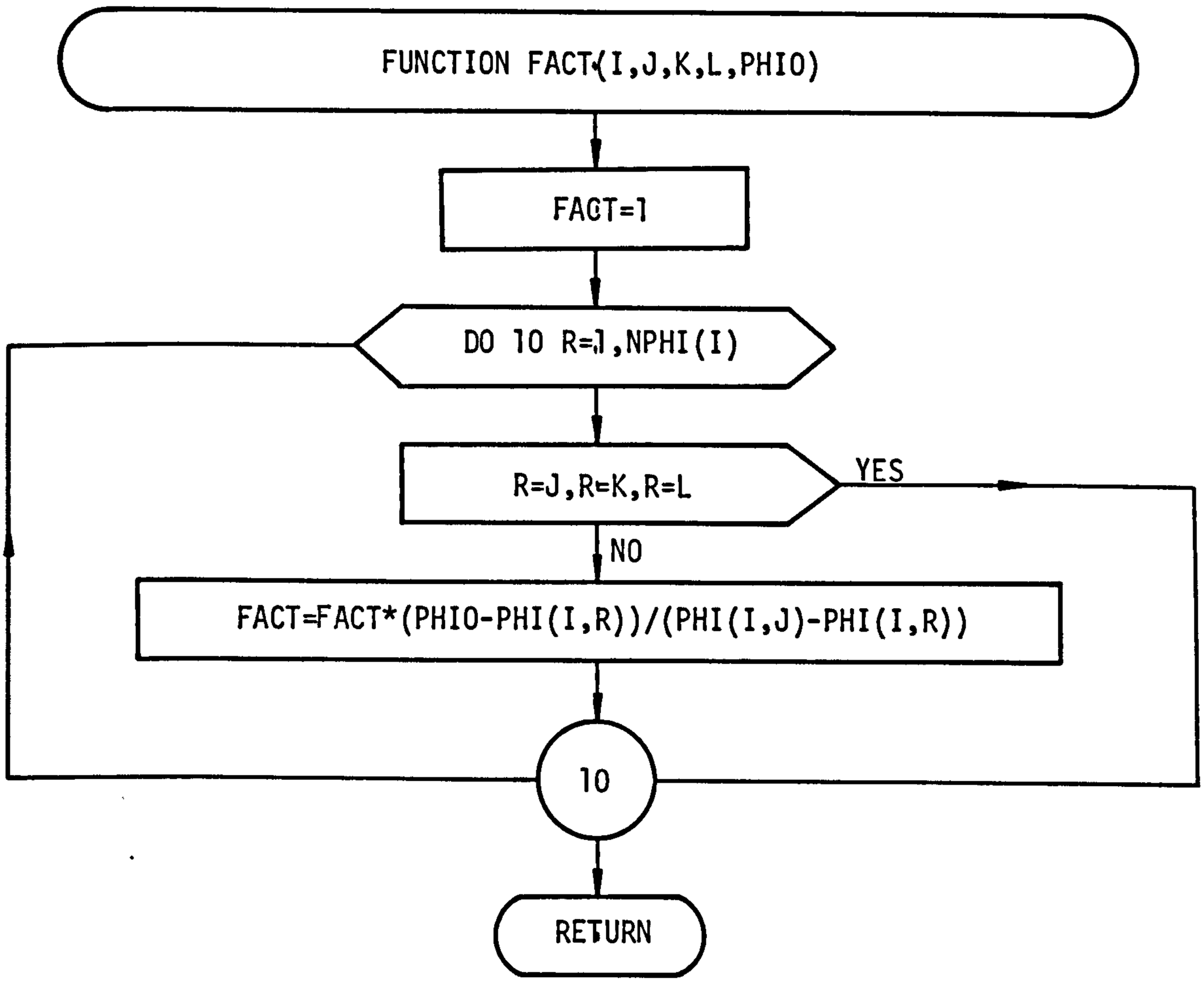

Flow chart of the function FLAG1=(N,X,I,X_0)

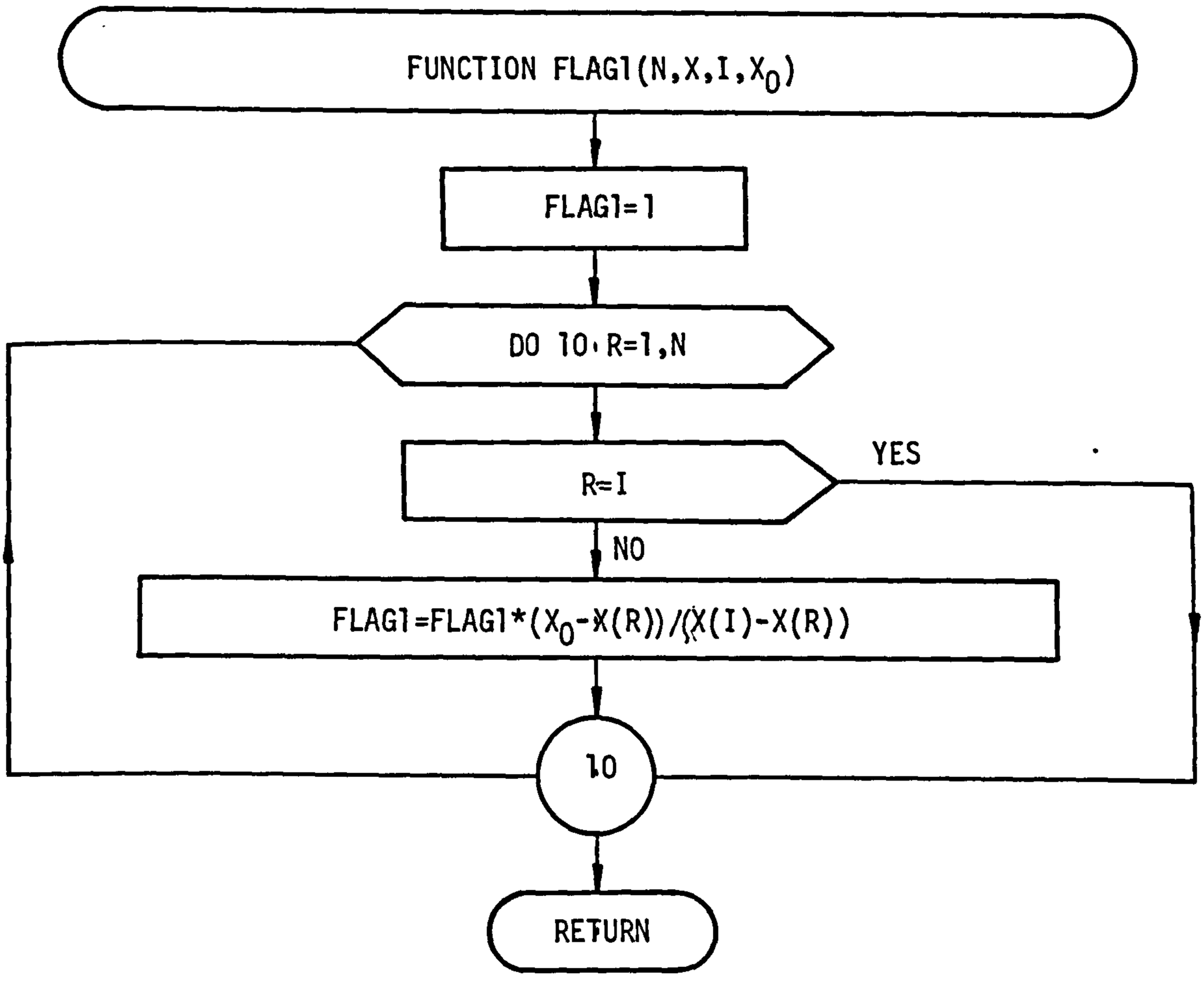

Flow chart of the function FLAG(I,J,PHIO) to calculate $\ell_i(x)$

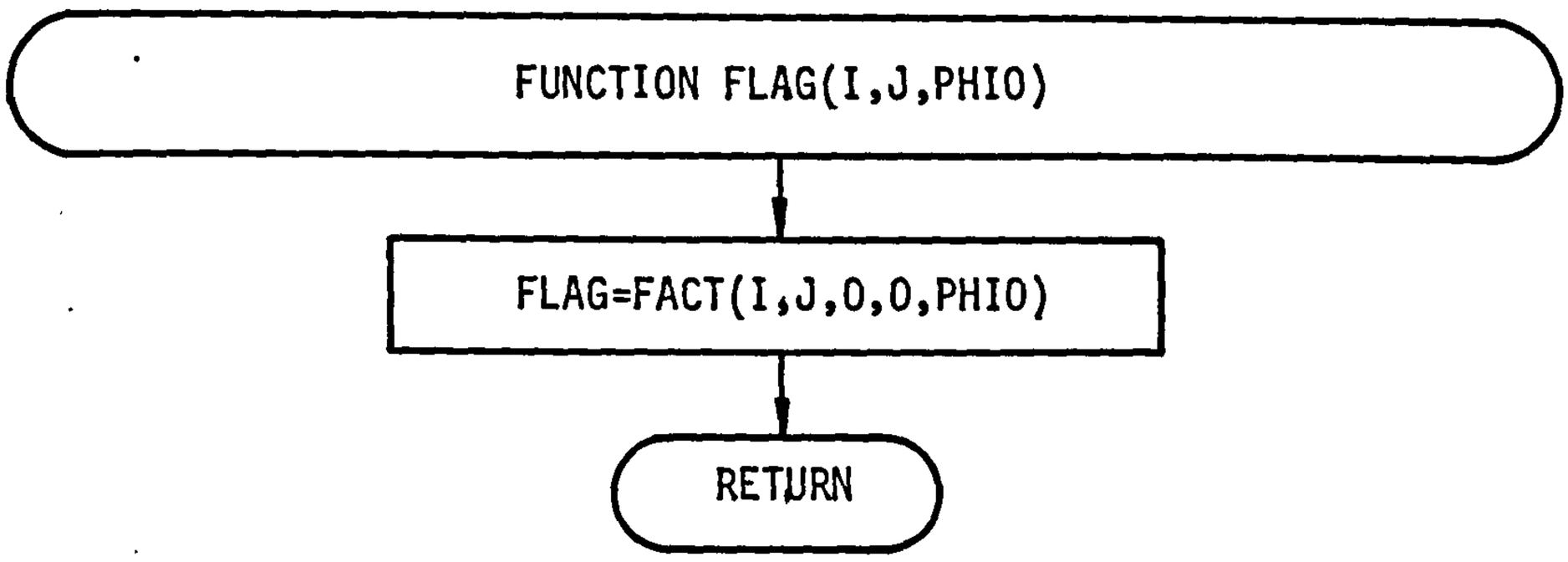

Flow chart of the function DLAG(I,J,PHIO) to calculate $\frac{\partial \ell_i(x)}{\partial x}$

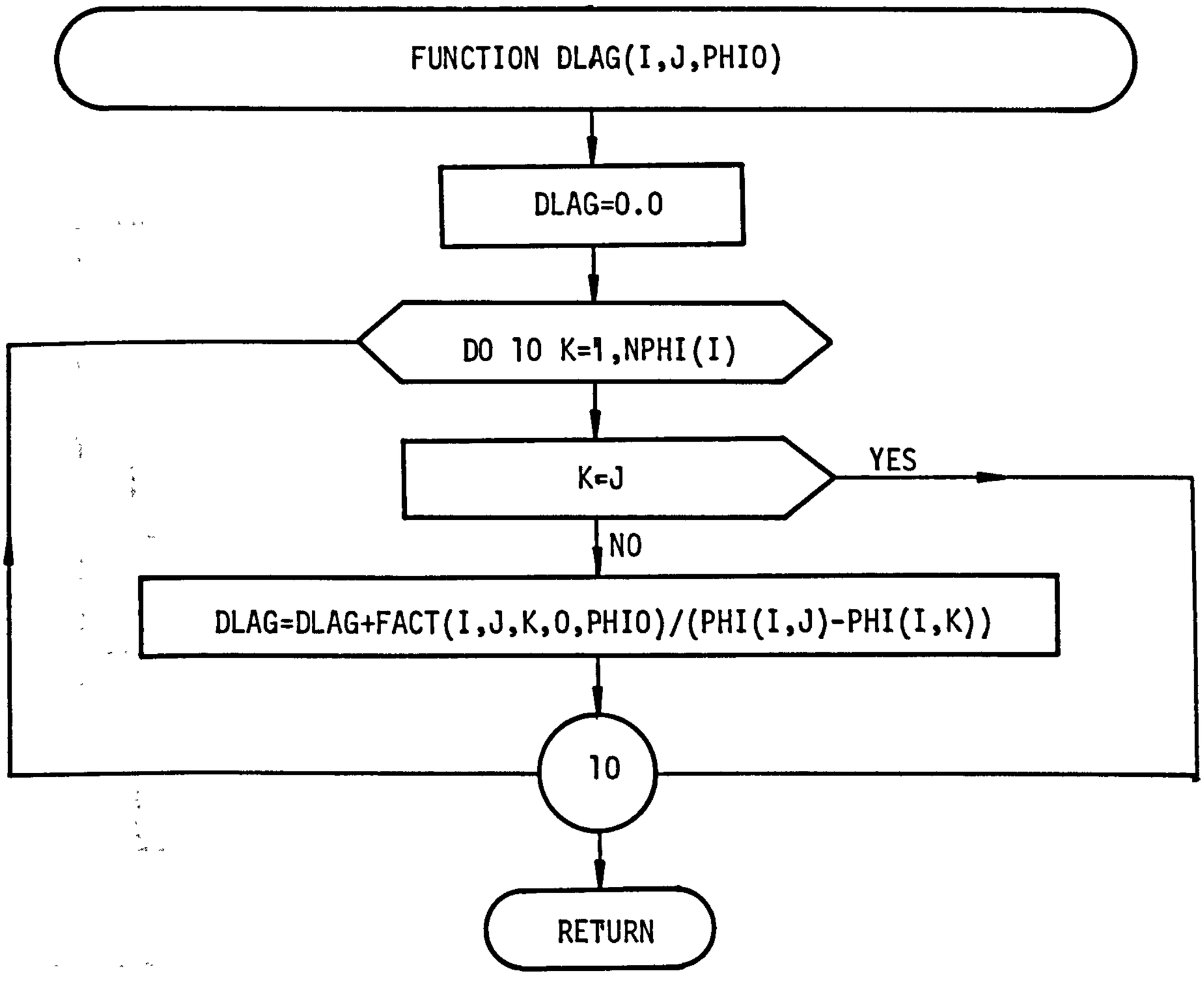

Flow Chart of the function D2LAG(I,J,PHIO) to calculate $\frac{\partial^2 \ell_i(x)}{\partial x^2}$

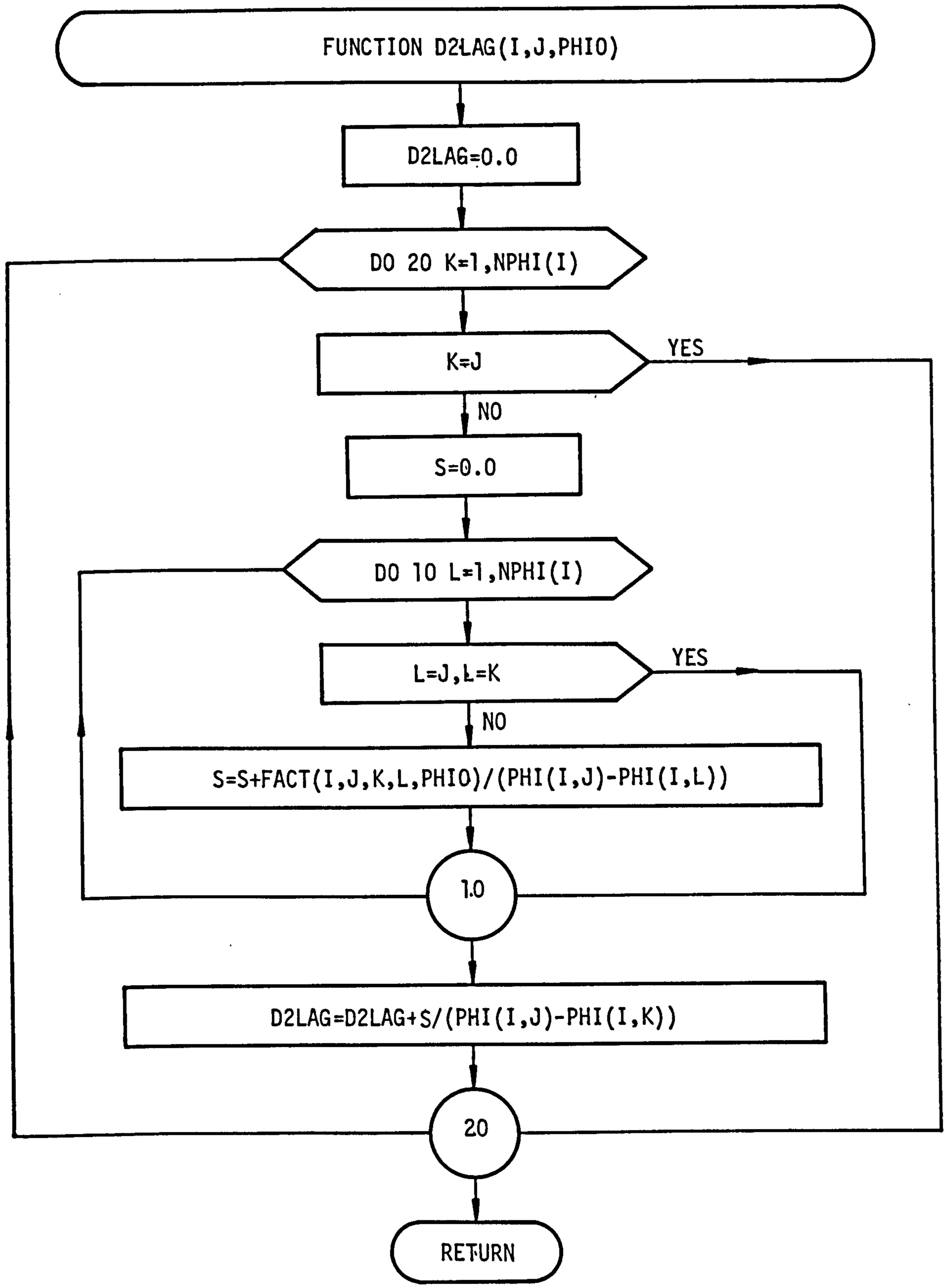

Flow chart of the function TAUF(PHII,QI).to calculate the initial condition of the gate opening (τ).

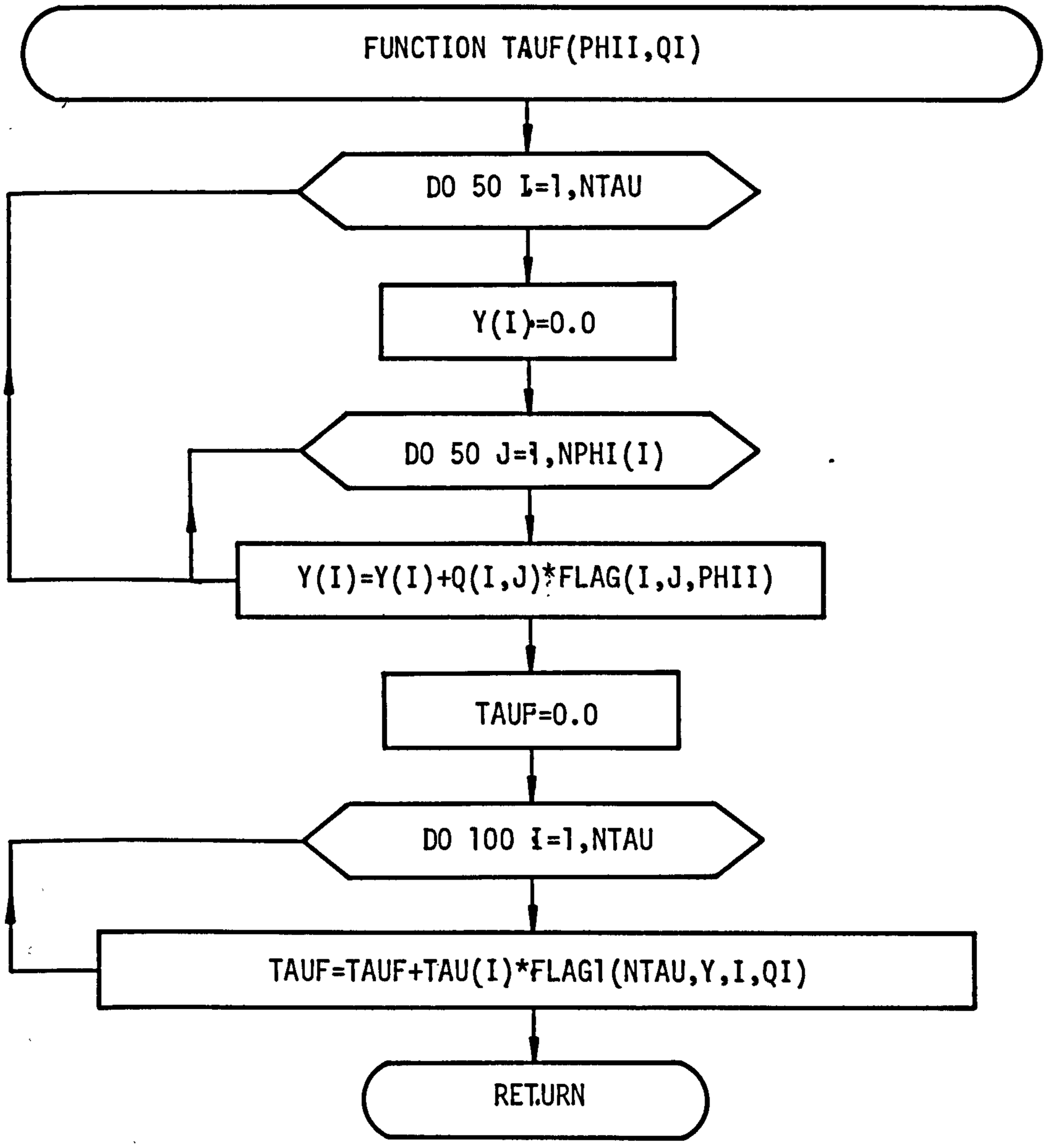

Flow Chart of the function ZI(TAUI,PHII,Z,ID)

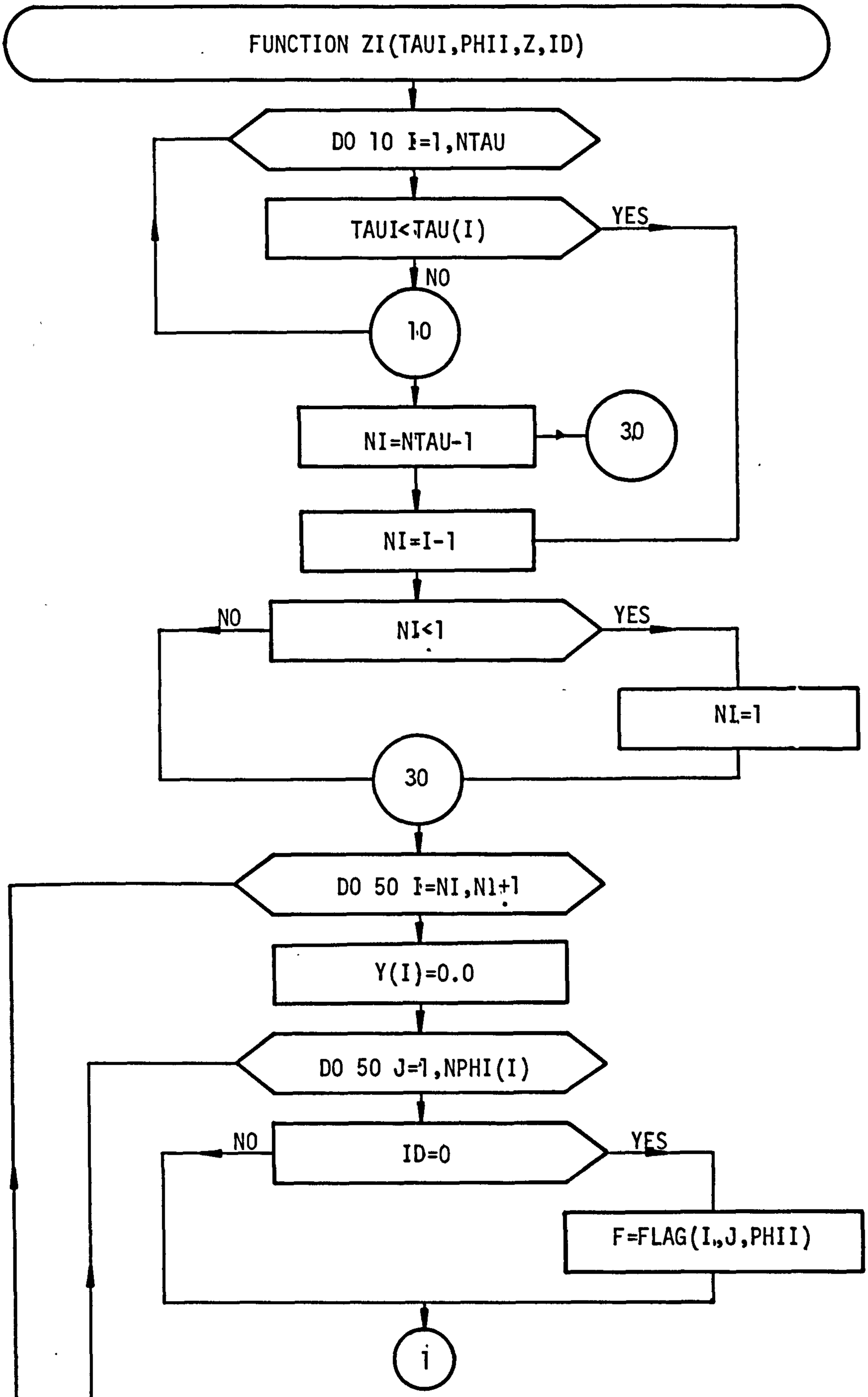

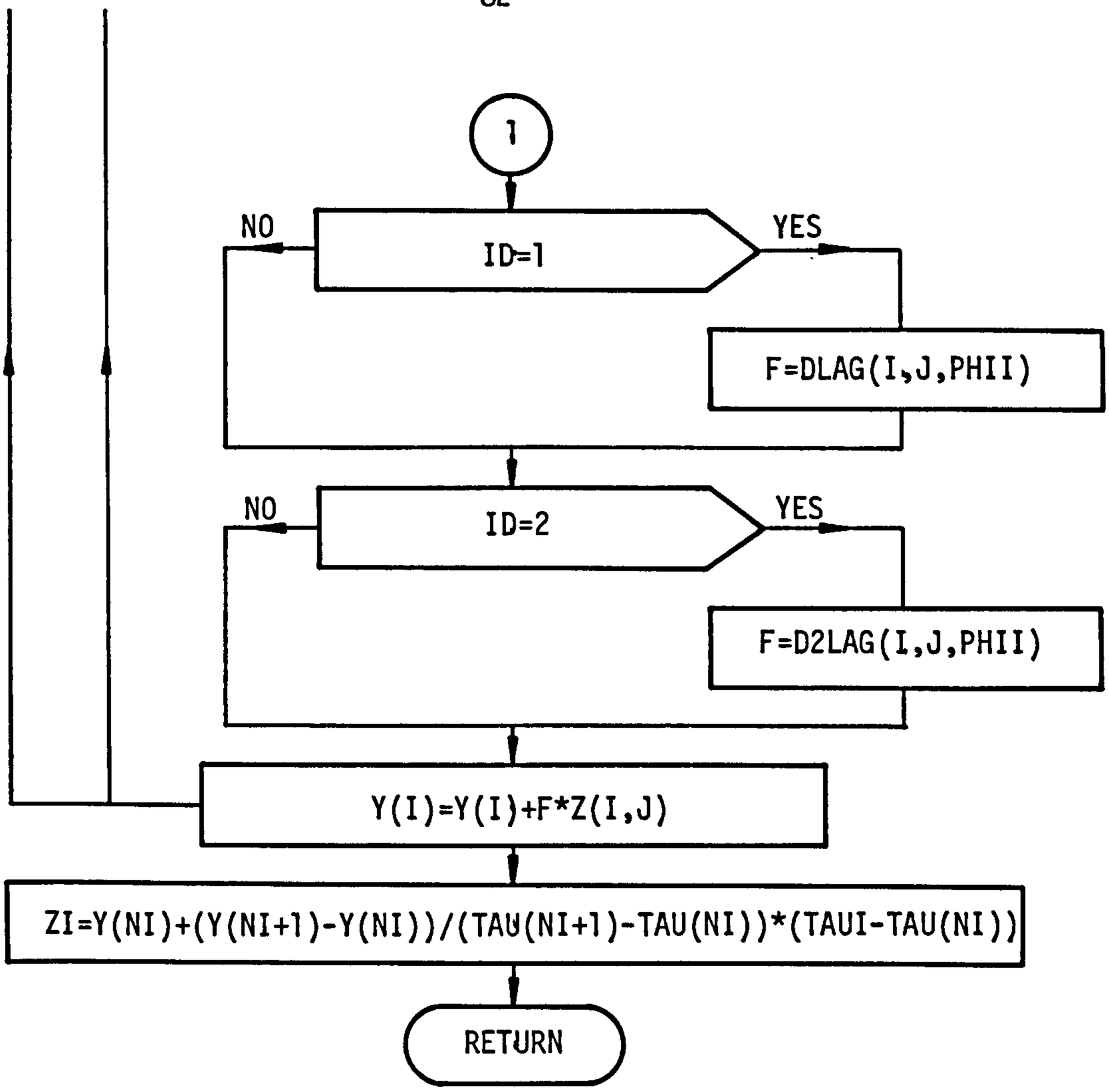
1
NO
ID=1
YES
F=DLAG(I,J,PHII)
NO
ID=2
YES
F=D2LAG(I,J,PHII)
Y(I)=Y(I)+F*Z(I,J)
ZI=Y(NI)+(Y(NI+1)-Y(NI))/(TAU(NI+1)-TAU(NI))*(TAUI-TAU(NI))
RETURN

Flow chart of the subroutine DATA(IDATA)

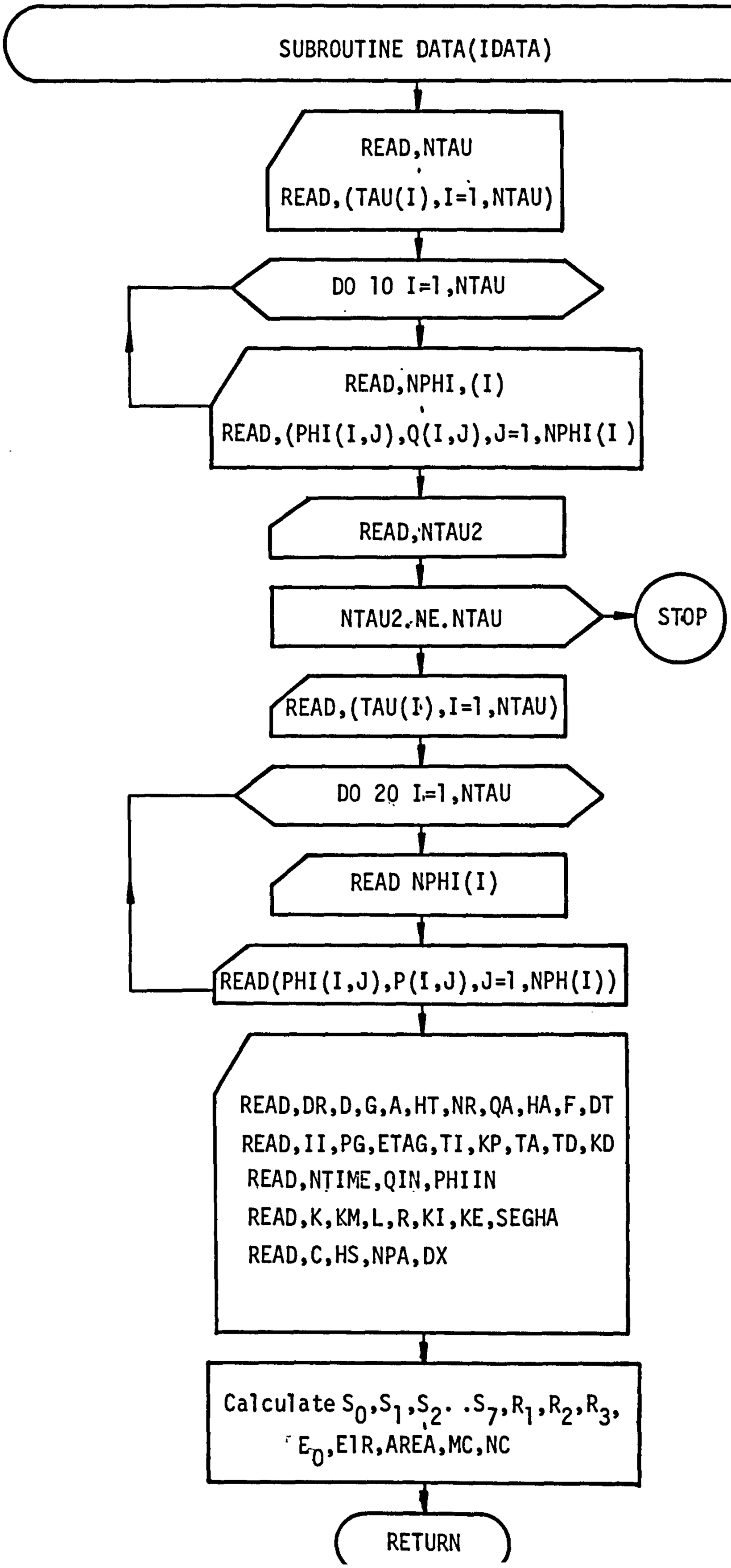

Flow chart of the subroutine LINEAR(TAUI,PHII,QI,A0,A1) to calculate a_0, a_1.

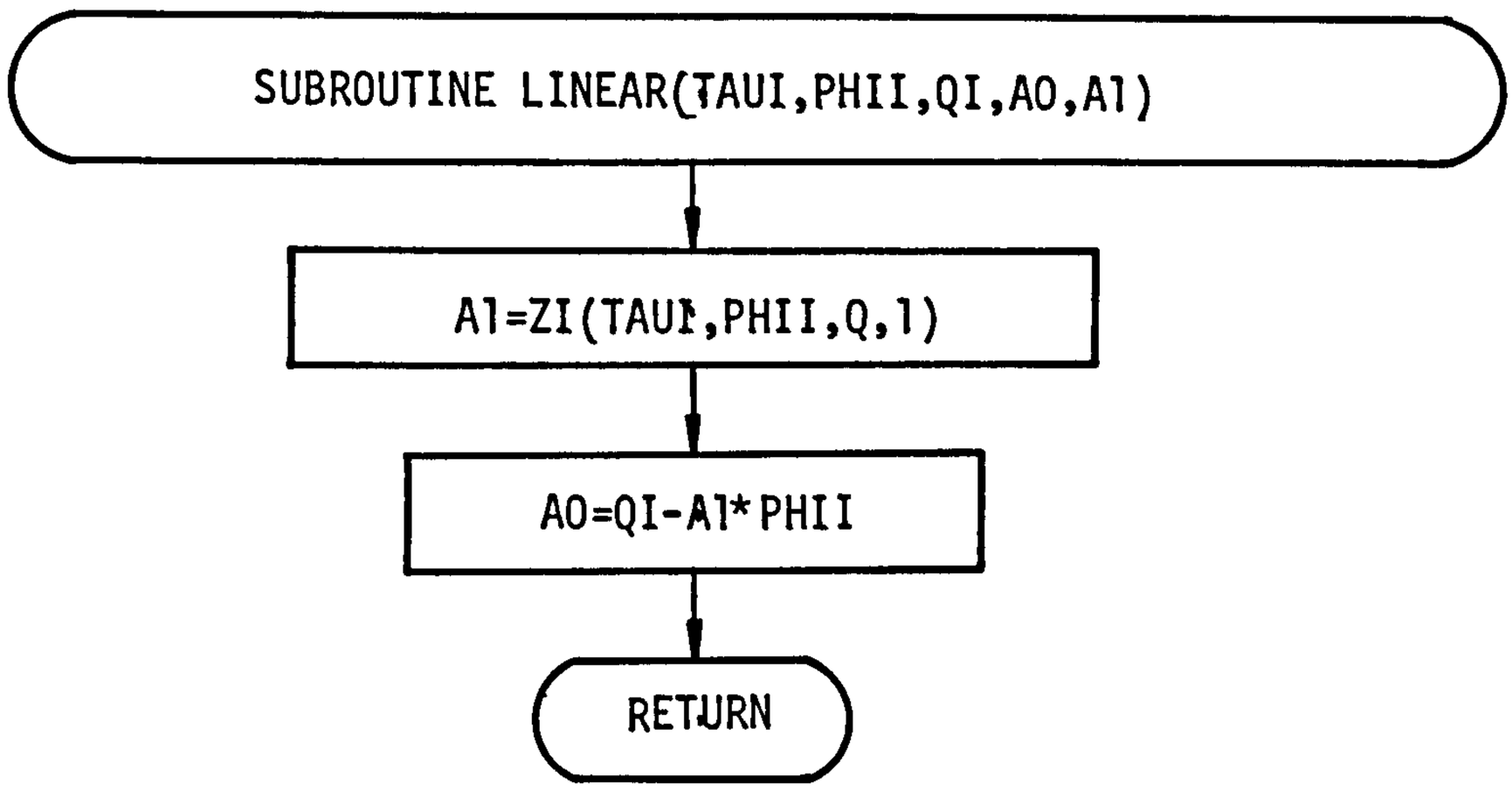

Flow chart of the subroutine PARABOLIC(TAUI,PHII,C_0,C_1,C_2) to calculate C_0,C_1,C_2.

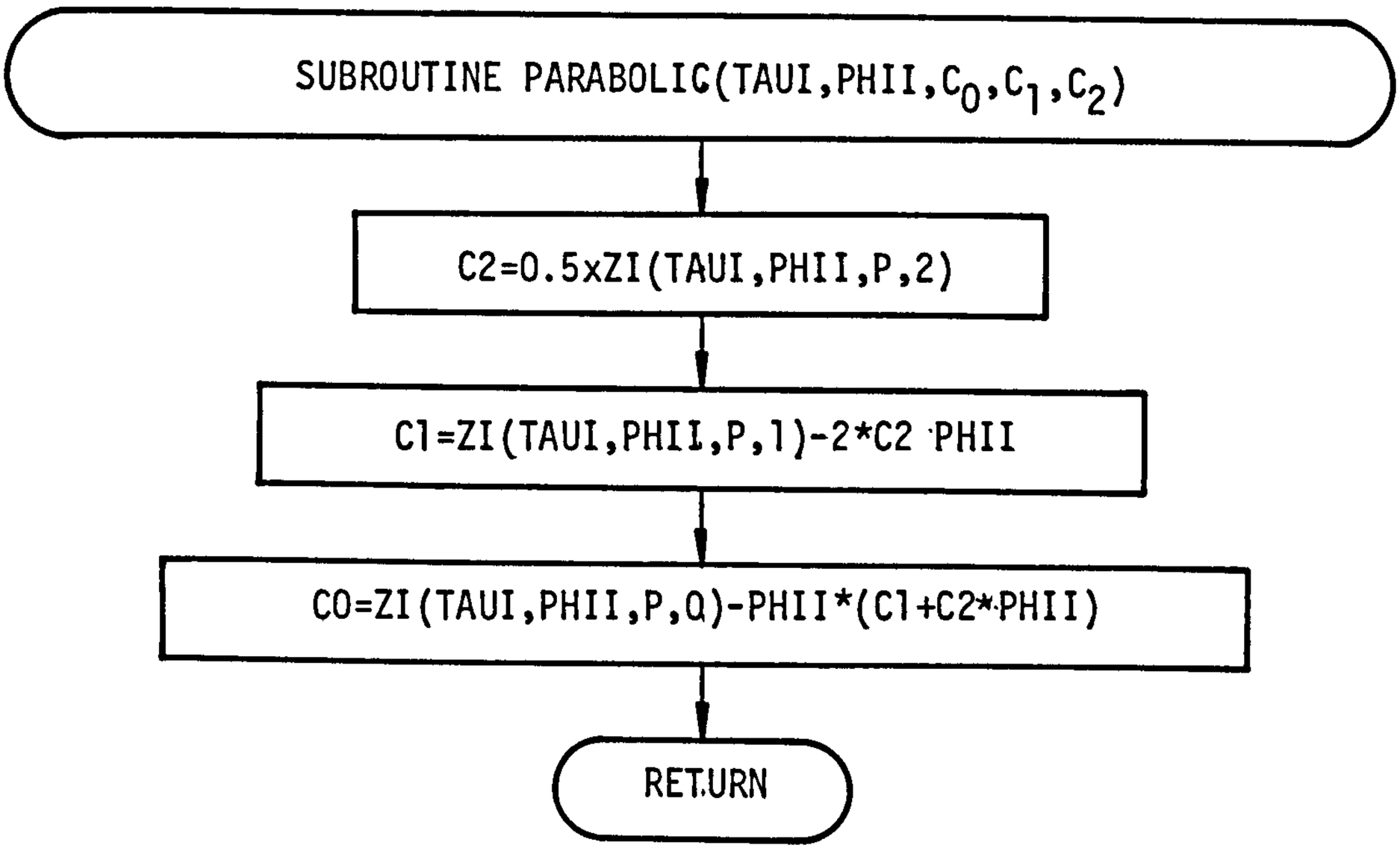

Flow chart of the subroutine ITER(N,Q_p,TAUI,PHII,HN,HP,IC,CP,YN) to calculate Q_p, H_p, H_N.

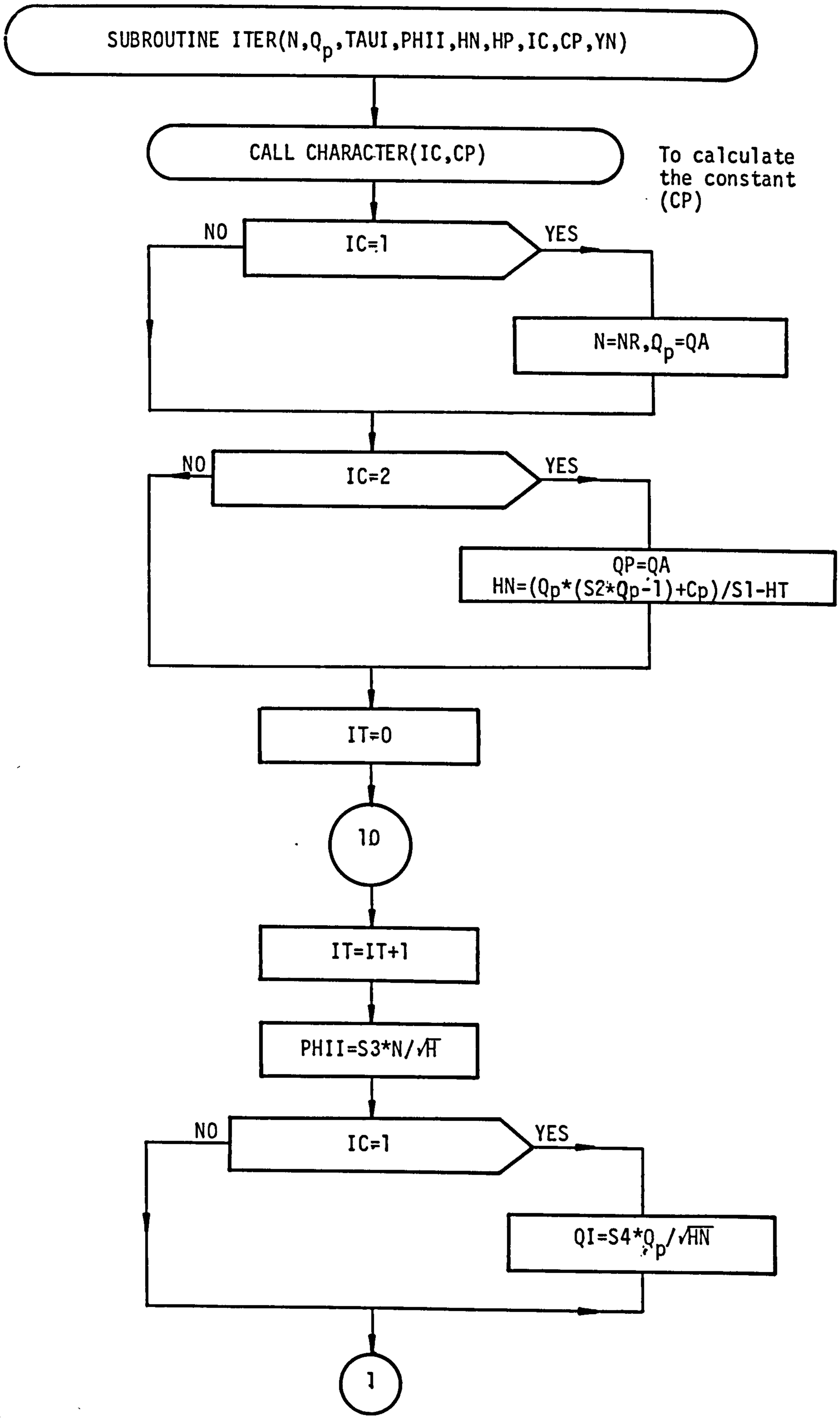

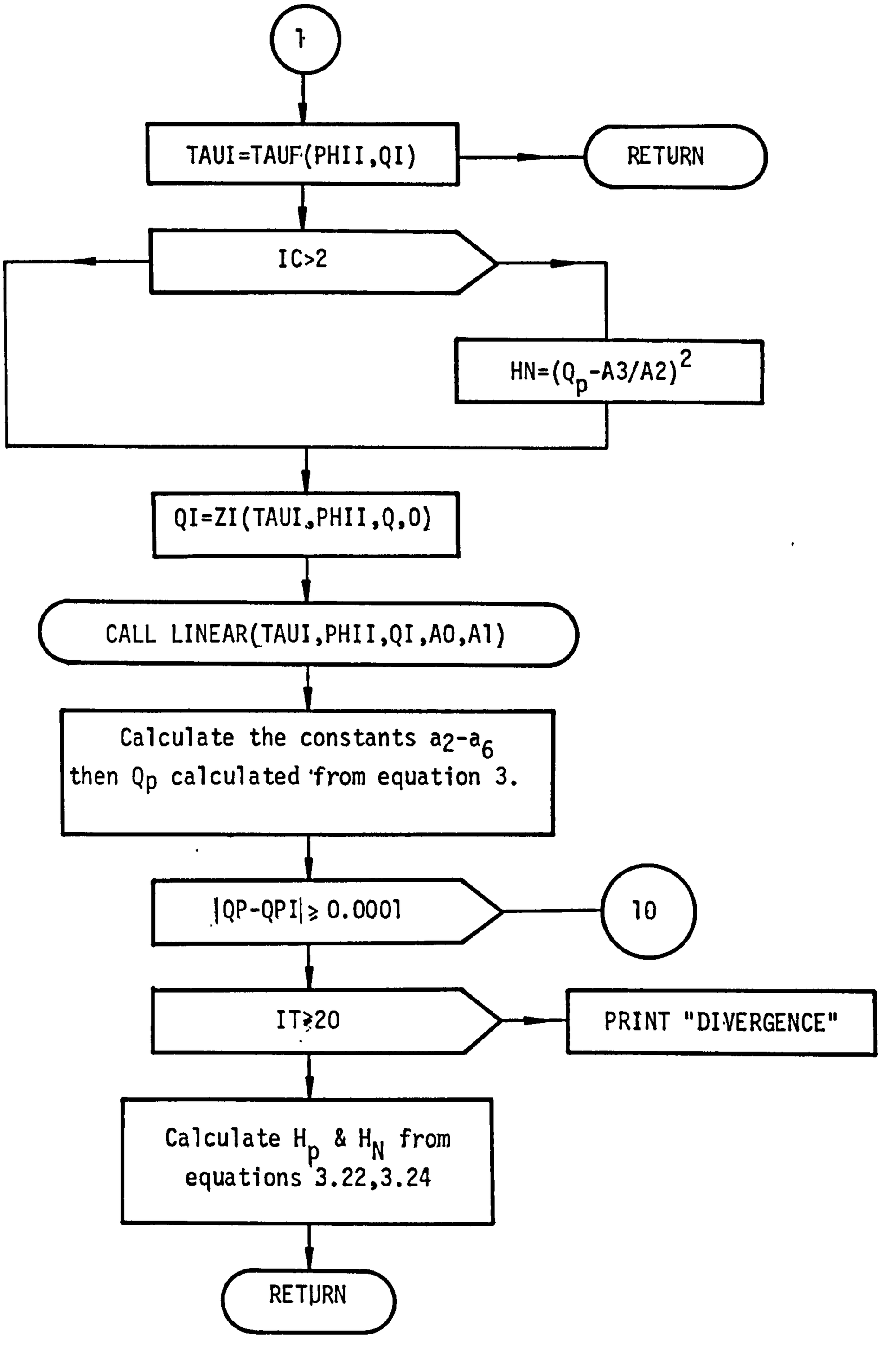
1
TAUI=TAUF(PHII,QI)
RETURN
IC>2
HN=(Qp-A3/A2)2
QI=ZI(TAUI,PHII,Q,O)
CALL LINEAR(TAUI,PHII,QI,AO,A1)
Calculate the constants a2-a6
then Qp calculated from equation 3.
|QP-QPI|≥ 0.0001
10
IT≥20
PRINT "DIVERGENCE"
Calculate Hp & HN from
equations 3.22,3.24
RETURN

Flow chart of the subroutine RUNGE(PHII,TAUI,HN)

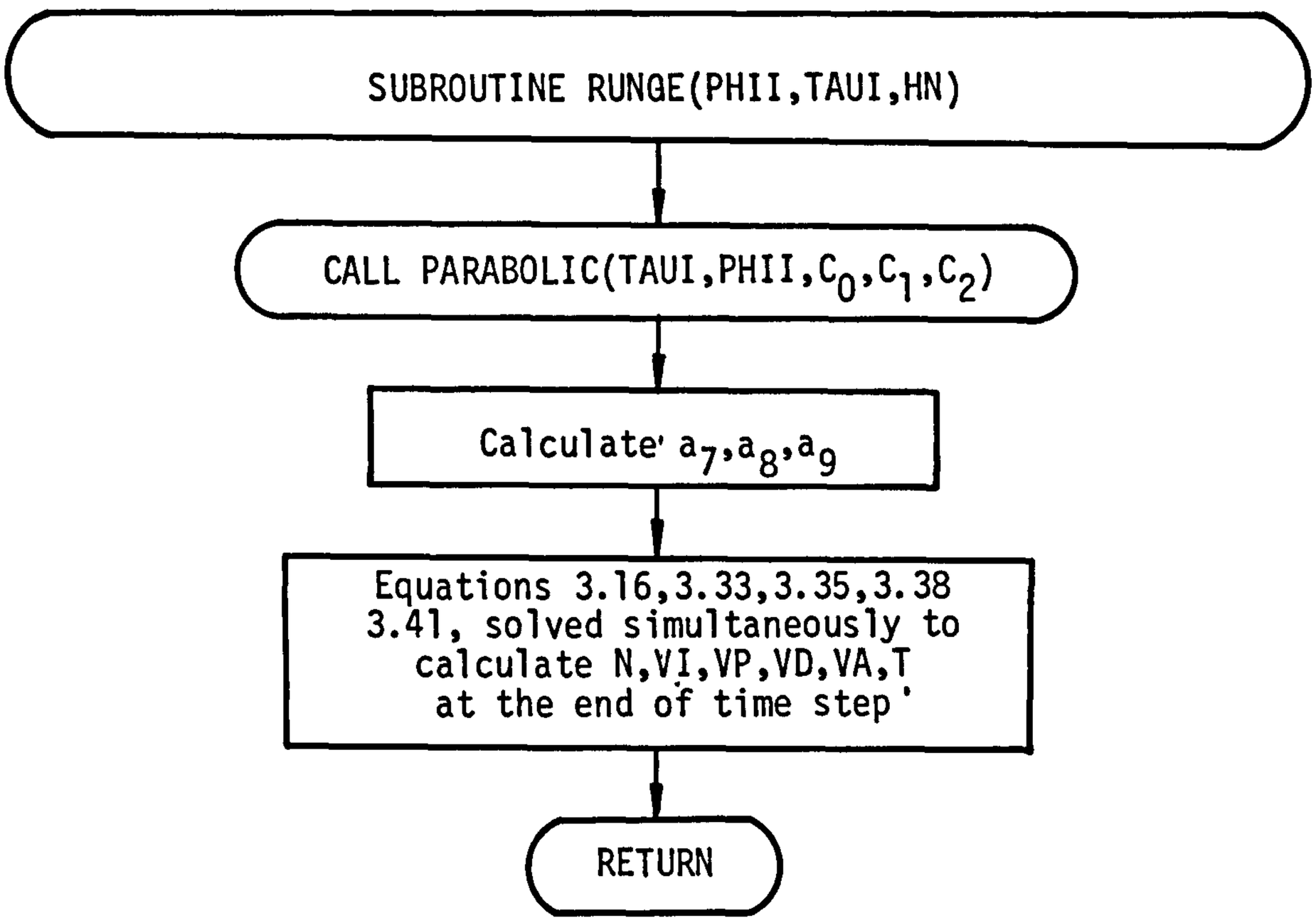

Flow chart of the subroutine CHARACTER(IC,CP)

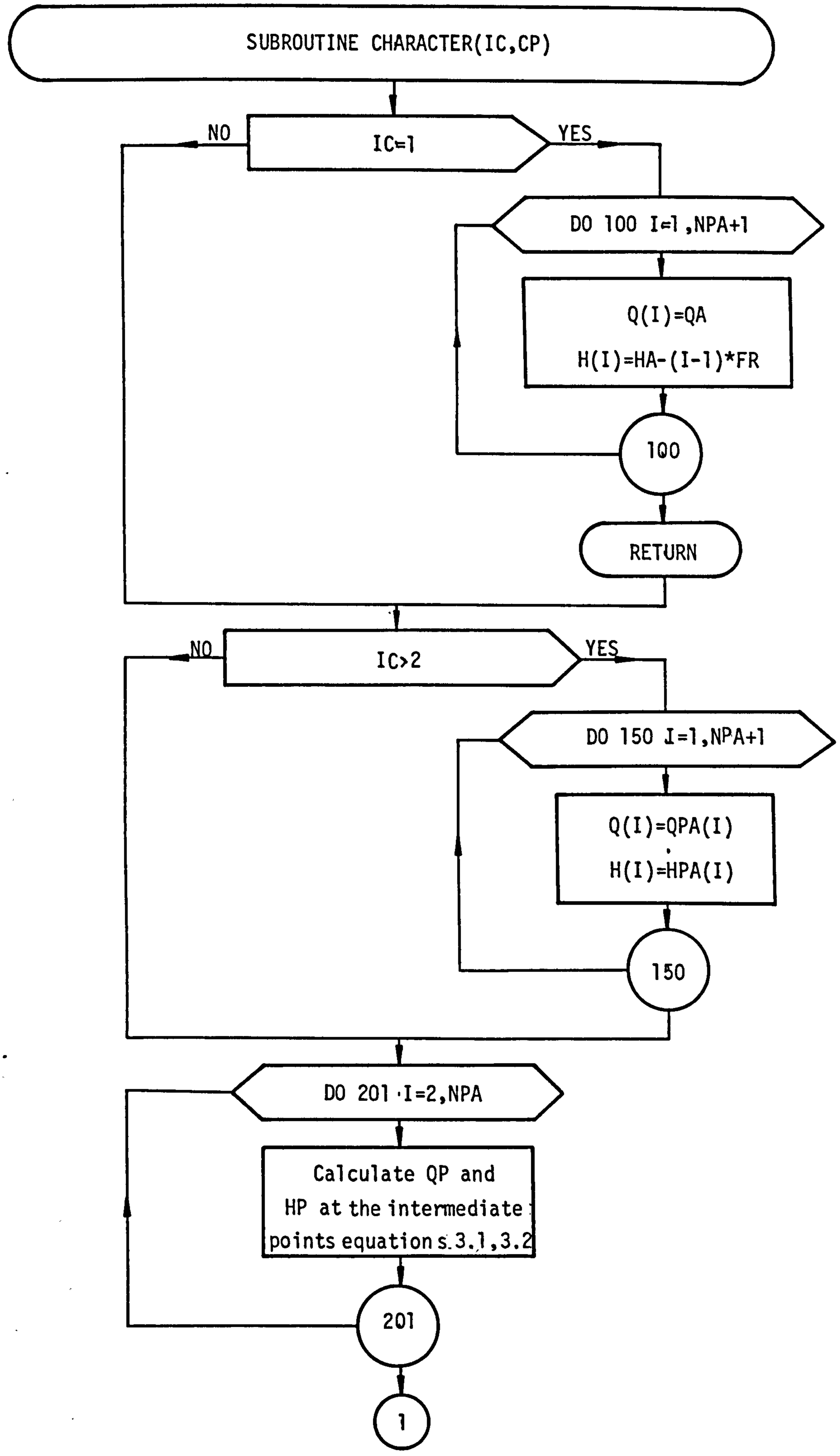

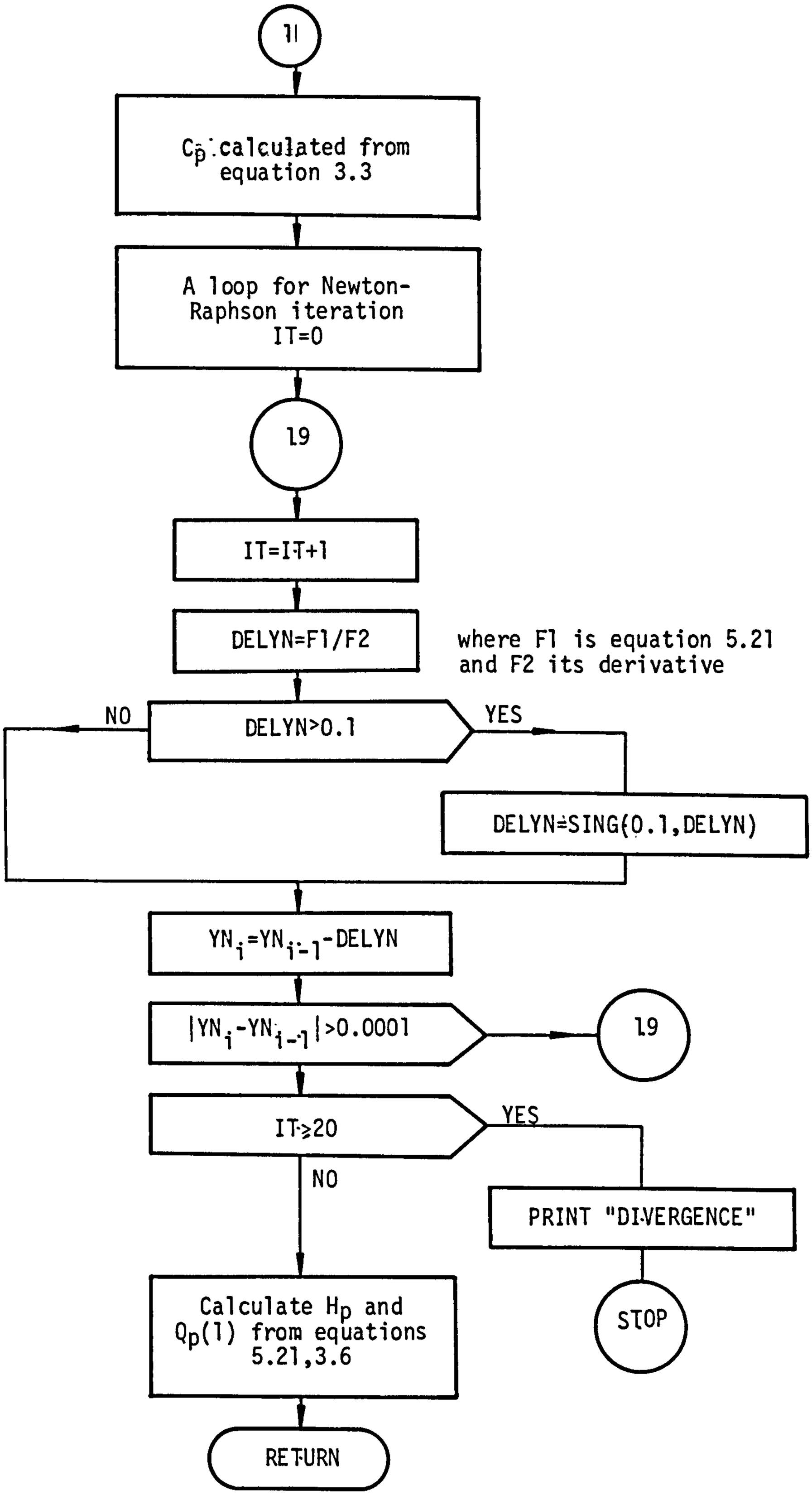
11
$C_{\bar{p}}$ calculated from equation 3.3
A loop for Newton-Raphson iteration
IT=0
19
IT=IT+1
DELYN=F1/F2
where F1 is equation 5.21 and F2 its derivative
NO
DELYN>0.1
YES
DELYN=SING(0.1,DELYN)
$YN_i=YN_{i-1}-DELYN$
$|YN_i-YN_{i-1}|>0.0001$
19
IT≥20
YES
NO
PRINT "DIVERGENCE"
STOP
Calculate H_p and $Q_p(1)$ from equations 5.21,3.6
RETURN

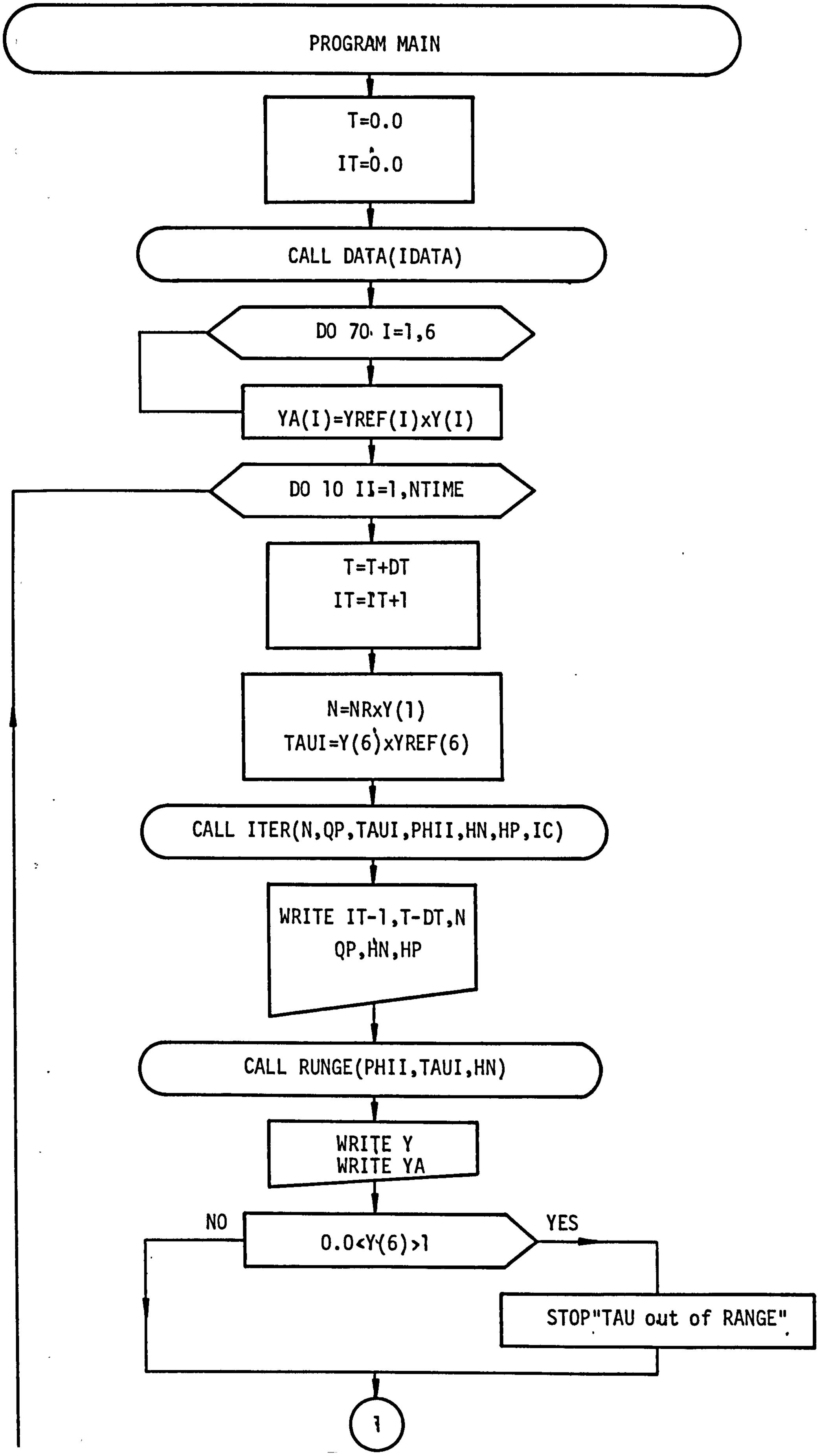
PROGRAM MAIN
T=0.0
IT=0.0
CALL DATA(IDATA)
DO 70 I=1,6
YA(I)=YREF(I)xY(I)
DO 10 II=1,NTIME
T=T+DT
IT=IT+1
N=NRxY(1)
TAUI=Y(6)xYREF(6)
CALL ITER(N,QP,TAUI,PHII,HN,HP,IC)
WRITE IT-1,T-DT,N
QP,HN,HP
CALL RUNGE(PHII,TAUI,HN)
WRITE Y
WRITE YA
NO
0.0<Y(6)>1
YES
STOP"TAU out of RANGE"
1

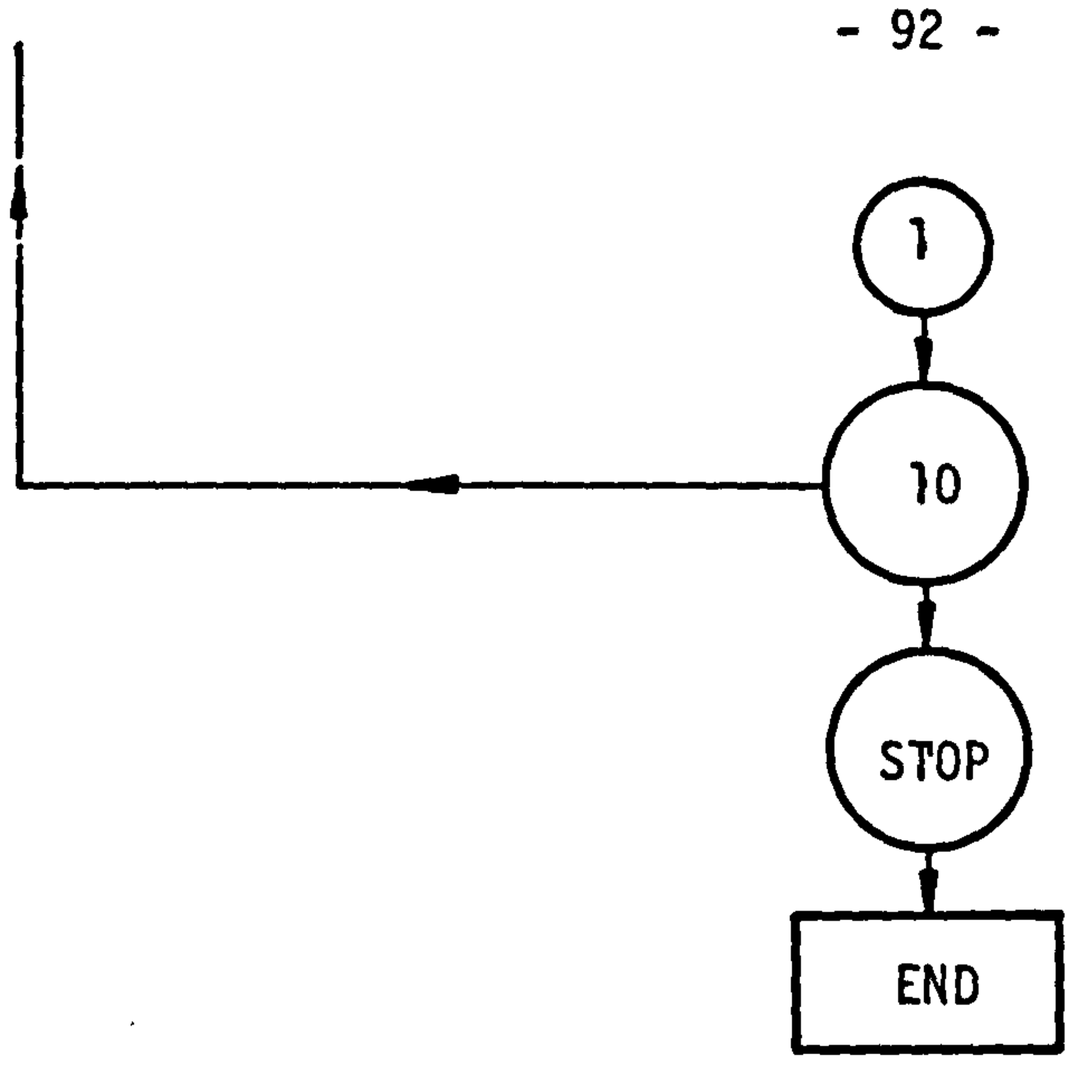
1
10
STOP
END

CHAPTER 6

COMPUTATIONAL AND EXPERIMENTAL RESULTS

6.1 INTRODUCTION

The comparisons between the computational and experimental results were made to prove the validity of the equations and assumptions on which the program is based. It was considered particularly important to verify the Lagrangean interpolation technique and the design of the proportional, integral and derivative governor. In each case instrumentation was installed for simultaneous and continuous recording of pressure, flowrate, turbine speed and gate position. Also the computed results were printed after every 10 time intervals. The various comparisons are discussed in the following sections.

6.2 FULL LOAD REJECTION

Certainly the most drastic disturbance from the point of view of economic design considerations is the full load rejection. The governor must close the gate fast enough to limit machine overspeed and yet slowly enough to limit pipework overpressures.

Load was rejected at time t=0. As a result of the load rejection the speed increased and the wicket gates were closed under governor control. Referring to equation (3.16) the incremental values of the speed are positive which means that the speed will rise, subsequently the speed reduced to speed-no-load condition; as the gate opening decreased towards the speed-no-load value, the total efficiency of the turbine approached zero. On a plot of discharge versus net head the line of zero efficiency represents the locus of steady-state speed-no load conditions. At smaller gate values it is not possible to maintain synchronous speed without the introduction of an external power source beyond that supplied by the fluid system. Therefore, the corresponding values of total efficiency must become negative, i.e. the incremental values of the speed become negative and the speed will reduce.

In the experimental work the frictional resistance and the other losses alter the speed to reduce it to speed-no-load conditions.

Computed and measured results are plotted in Figures 6.1 to 6.4. As can be seen, the experimental maximum speed is 1% greater than the computed maximum speed Figure 6.1; however, the experimental results show a faster speed reduction than that shown by the computed results. It should be noted that this deviation starts when the wicket gate opening is small. This difference may be due to lack of data for the turbine characteristics at small wicket gate openings. The computed and measured flowrate Figure 6.2, agree closely until t=1.1 seconds at which time a rapid divergence is shown in the experimental results. This difference may be due to error in the differential pressure transducer at very low pressure difference.

Several aspects of the gate time curve shown in Figure 6.3 should be noted. Very soon after rejection of the load, the gate accelerated to an almost constant velocity which was maintained until about t=1.1 seconds at which time the rate of closure was rapidly reduced. As can be seen in the Figure there is a good measure of agreement; however, the experimental results show a faster closure than the computed results. This difference may be due to the error in the estimation of the friction losses in the connecting gears and the round-off error.

The pressure rise curve due to the load rejection is shown in Figure 6.4. The agreement indicated in Figure 6.4 is excellent. The experimental pressure shows some oscillation occurring at approximately 15 per cent gate opening, at which point the rate of closure is rapidly reduced. The pressure decreases after t=1.1 seconds, when the gate variation is very small. According to Ref.3 and Ref.7 fluctuation in the pressure/time curves is greater in amplitude and takes a longer time. In our case the fluctuation is smaller and for a short period. A small error in the mathematical representation of the governor could lead to an error in the gate closure/time curve which in turn could lead to a longer error in pressure prediction especially at low gate openings.

The speed and pressure time curves, Figures 6.1 and 6.4., show that the percentage rises are 26% for the turbine speed and 22% of its net head.

Krueger, (Ref.27), in his technical publication "Selecting Hydraulic Reaction Turbines" stated that the speed rise should not exceed 60 per cent and the permissible pressure range is 25% of the design pressure. These results are therefore within these limits.

6.3 PARTIAL LOAD REDUCTION

Figures 6.5 to 6.20 show the transient response following different cases of partial load reduction. It is clear from those figures that there is a good agreement between the computed and the experimental results.

In the previous case (full load rejection) the reduction of the speed depended on the negative value of the efficiency because the final generator power was zero, but in partial load reduction cases the rise and reduction depend on the difference between the turbine power and the final generator power after partial rejection. In most cases it is noted that the gate openings reduced and then swung until the speed reached the steady state speed (synchronous speed). Figures 6.16 and 6.20 show that the swinging happens in the computational results and not in the experimental results. This difference may be due to the estimation of the actuator equation (stepping motor). It appears that the stability of the governor is greater than the estimated near the steady state conditions.

The speed time curves for all cases are shown in Figures (6.5), (6.9), (6.13) and (6.17). The experimental and the computed results agree closely except for the 31% load reduction. The experimental results show a faster speed reduction than that shown by computational results. This difference may be due to an error in recording and plotting.

The pressure rise curves show that the fluctuation at the maximum peak is reduced at 80% load and disappears in the other cases due to the difference in the gate motion. The pressure decreased very fast immediately after the gate reached the steady state position returning rapidly to its steady state condition, especially at the lower load rejection, Figures 6.15 and 6.19.

Finally Figures 6.20 to 6.24 show a typical comparison between all the load rejection tests. The closing time of the wicket gate is proportional to the load percentage reduction.

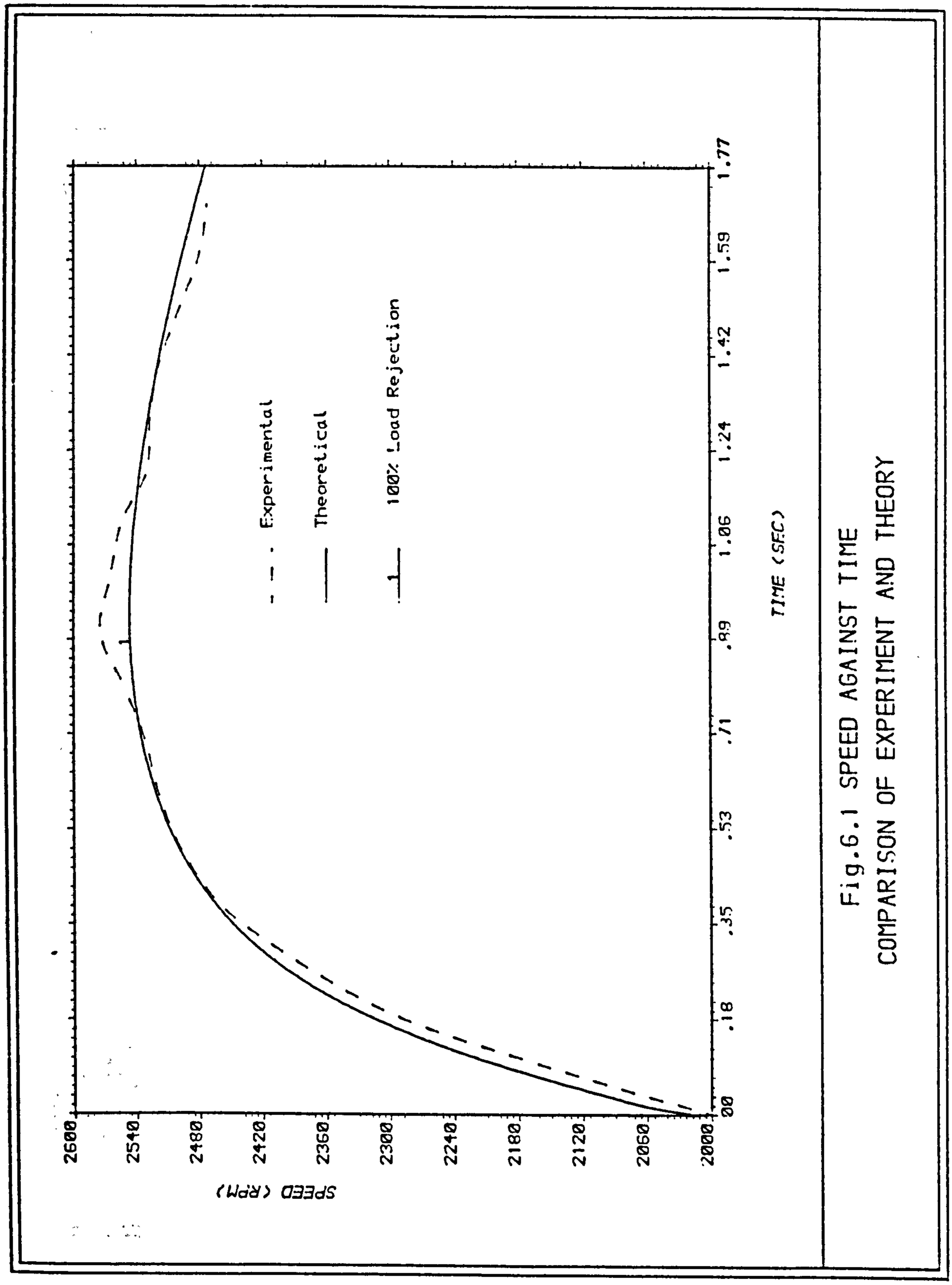

Fig.6.1 SPEED AGAINST TIME
COMPARISON OF EXPERIMENT AND THEORY

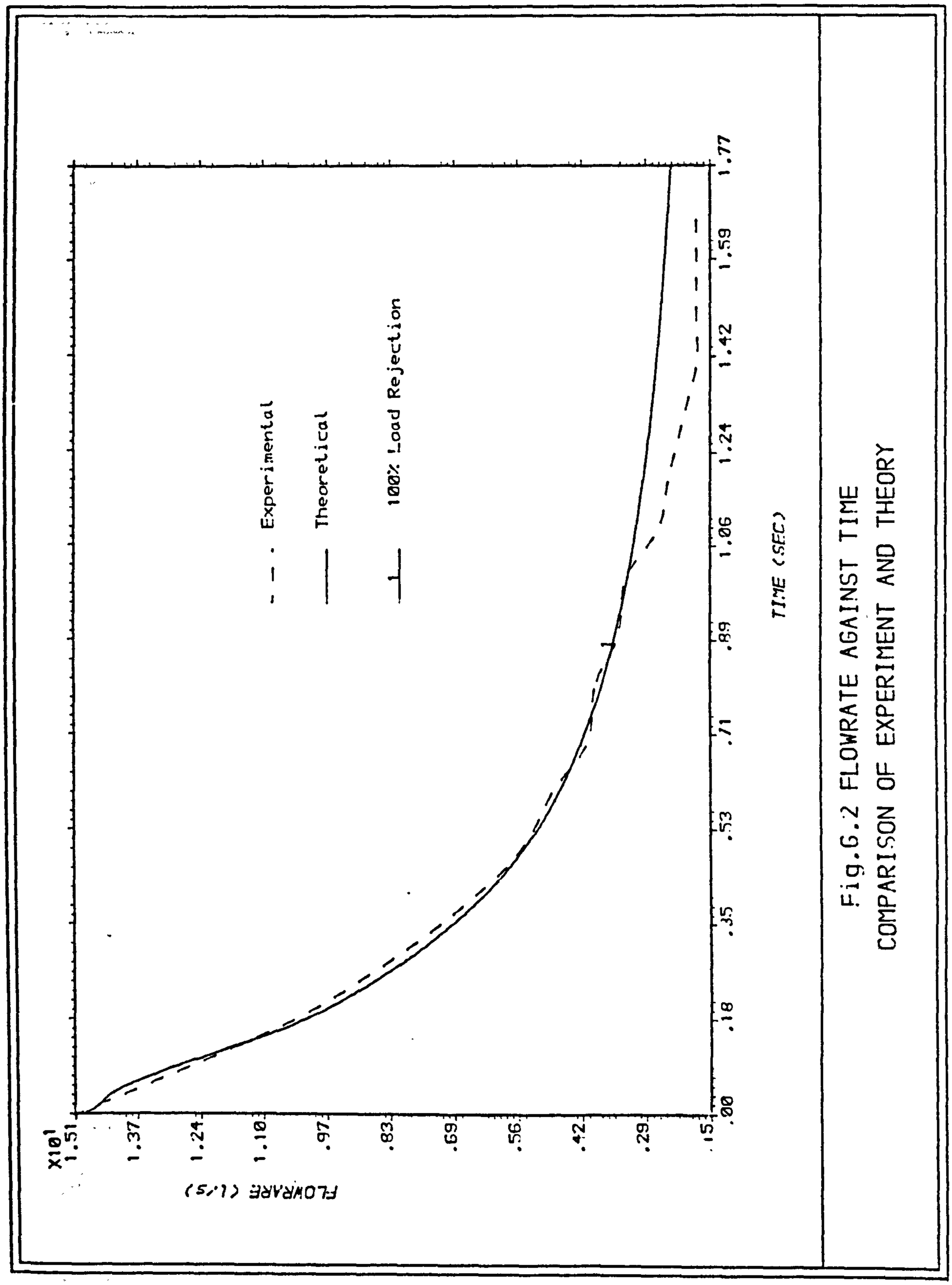

Fig.6.2 FLOWRATE AGAINST TIME
COMPARISON OF EXPERIMENT AND THEORY

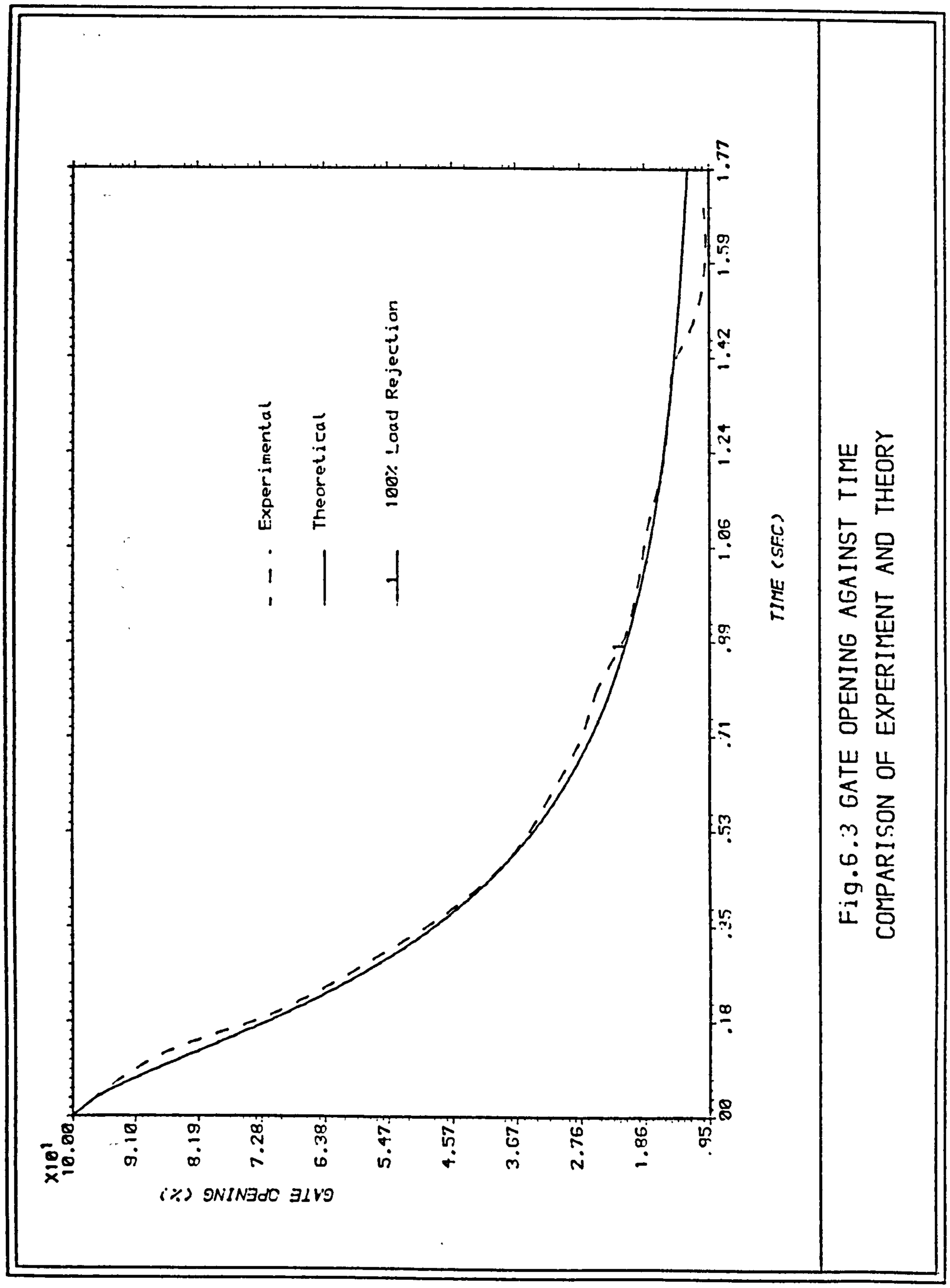

Fig.6.3 GATE OPENING AGAINST TIME
COMPARISON OF EXPERIMENT AND THEORY

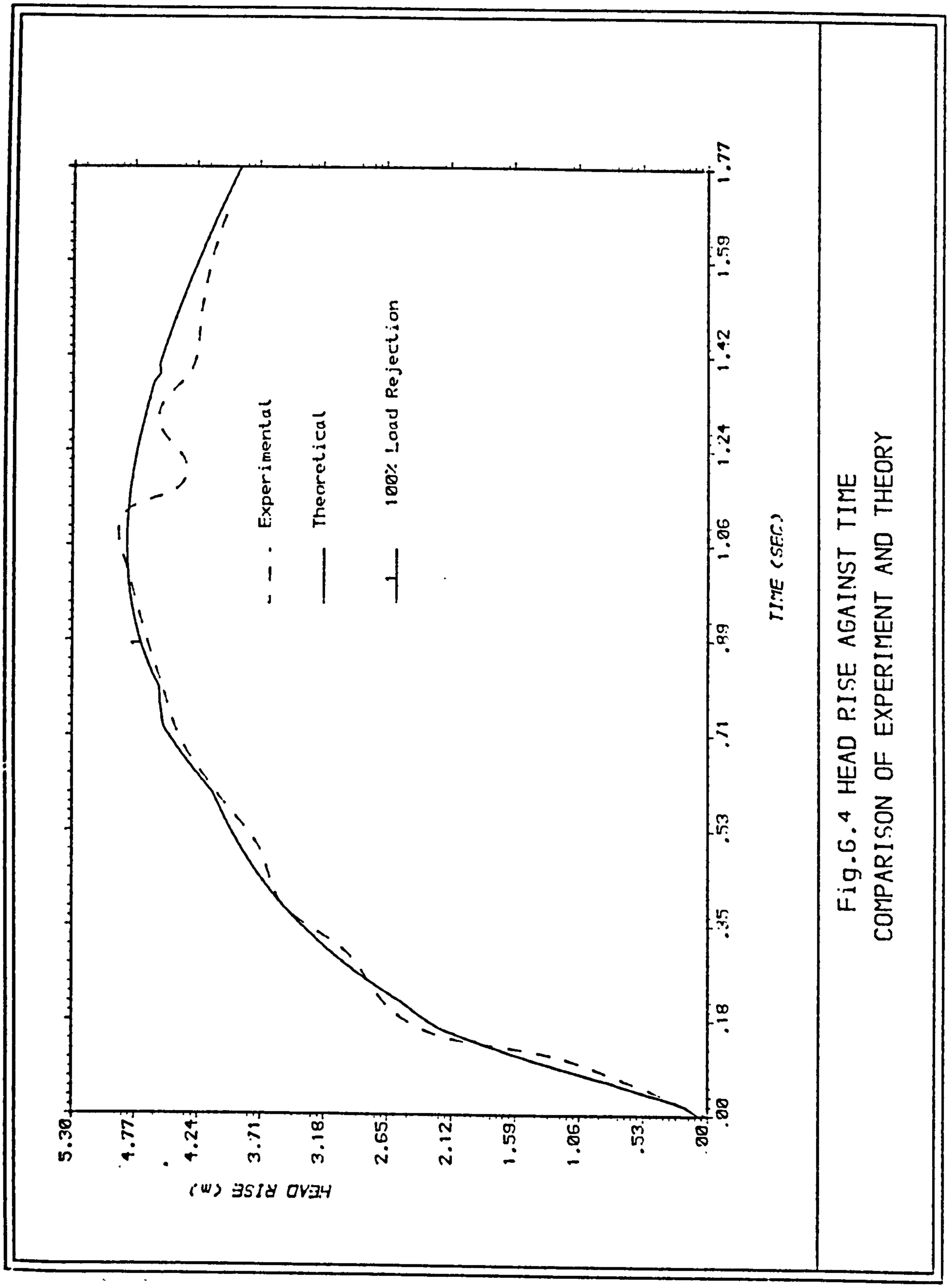

Fig.6.4 HEAD RISE AGAINST TIME
COMPARISON OF EXPERIMENT AND THEORY

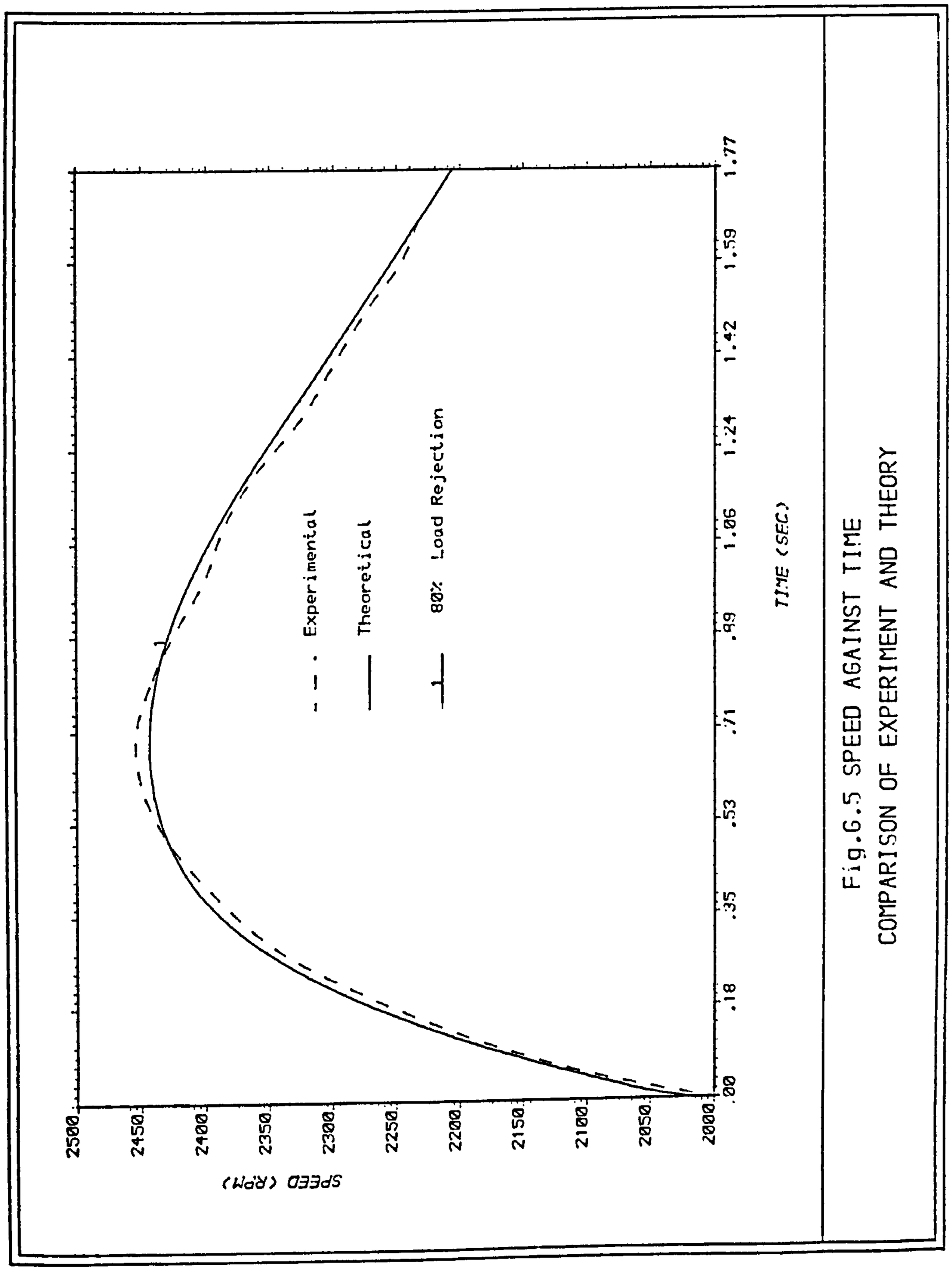

Fig.6.5 SPEED AGAINST TIME
COMPARISON OF EXPERIMENT AND THEORY

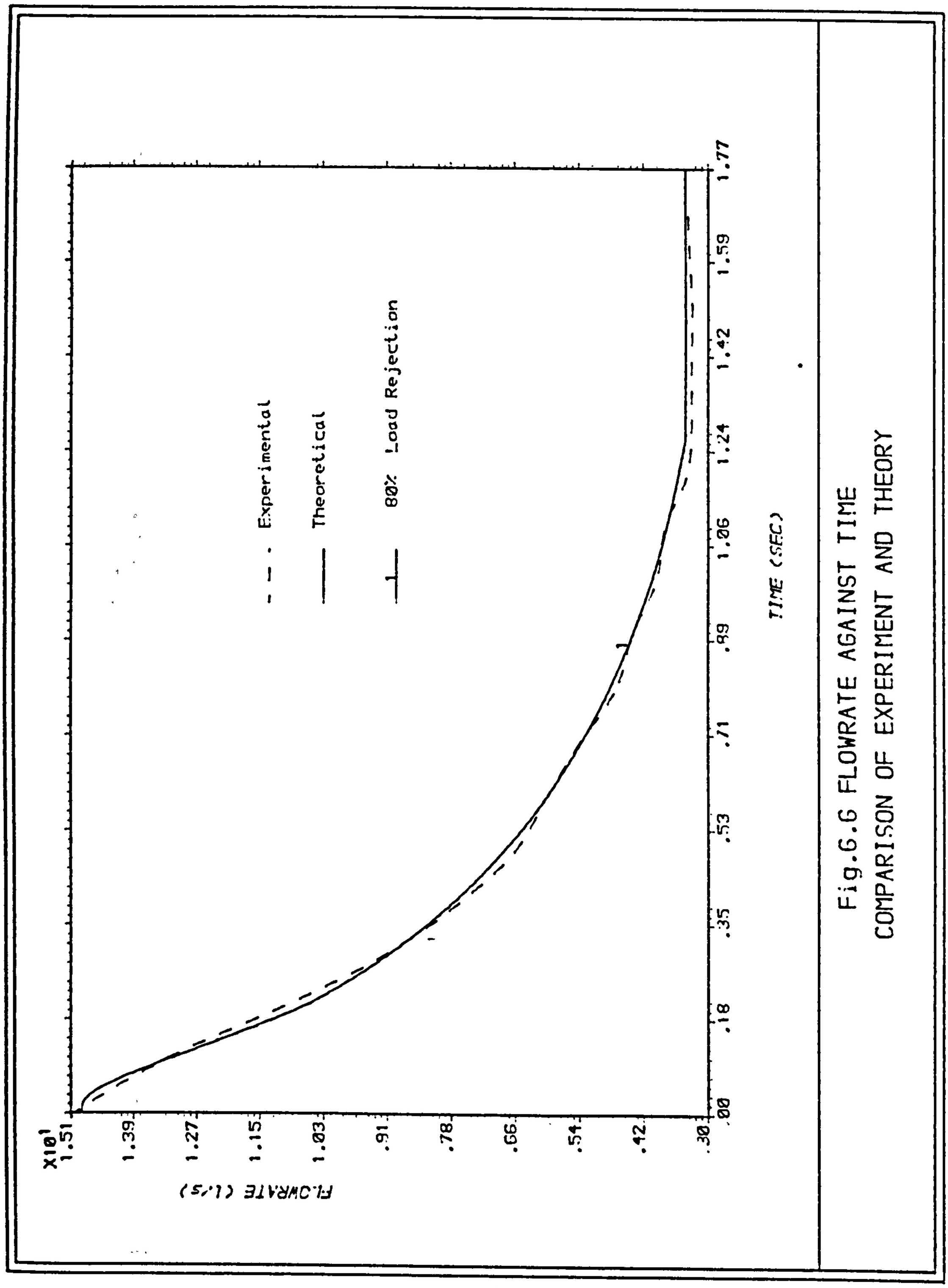

Fig.6.6 FLOWRATE AGAINST TIME
COMPARISON OF EXPERIMENT AND THEORY

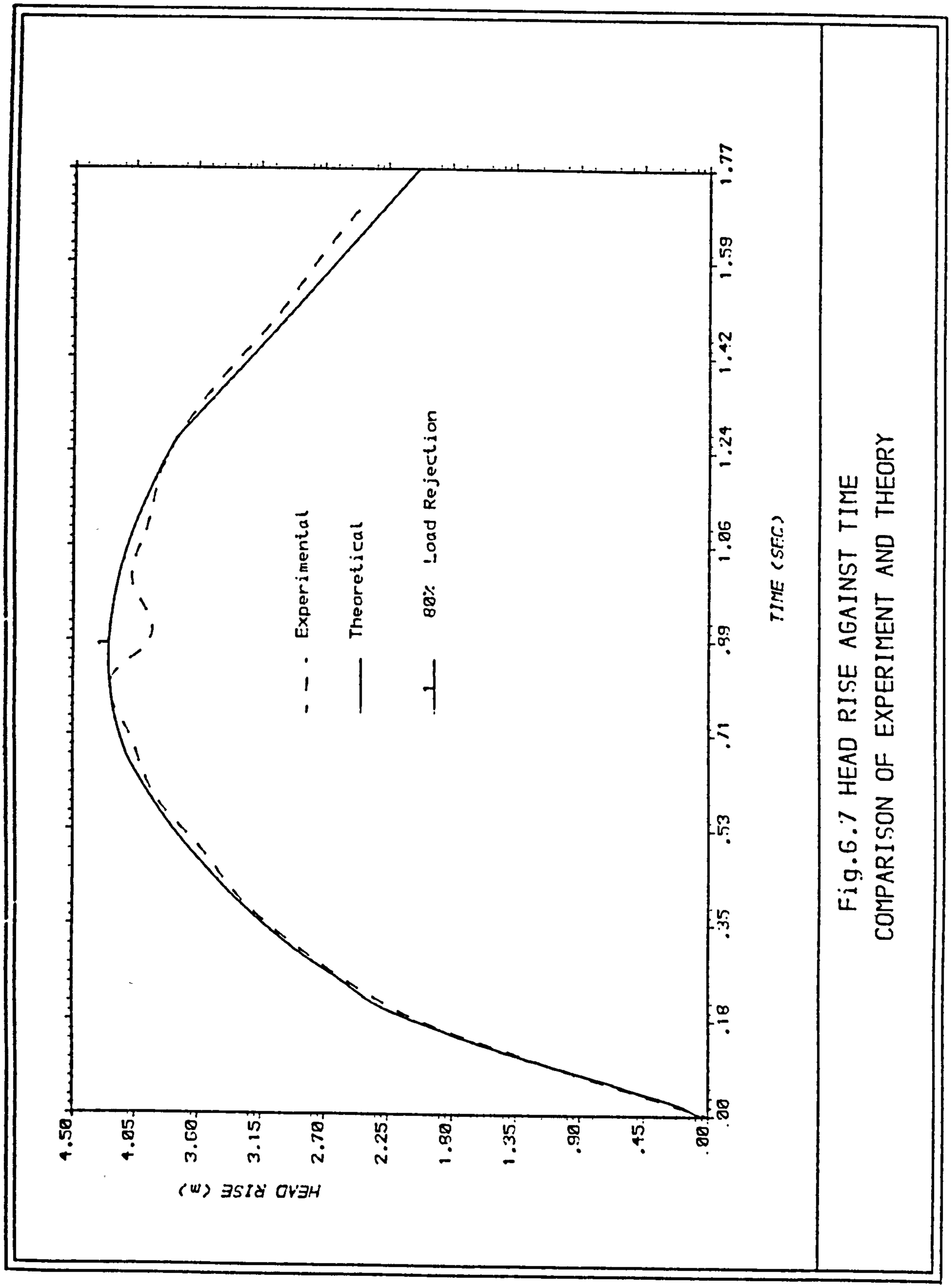

Fig.6.7 HEAD RISE AGAINST TIME
COMPARISON OF EXPERIMENT AND THEORY

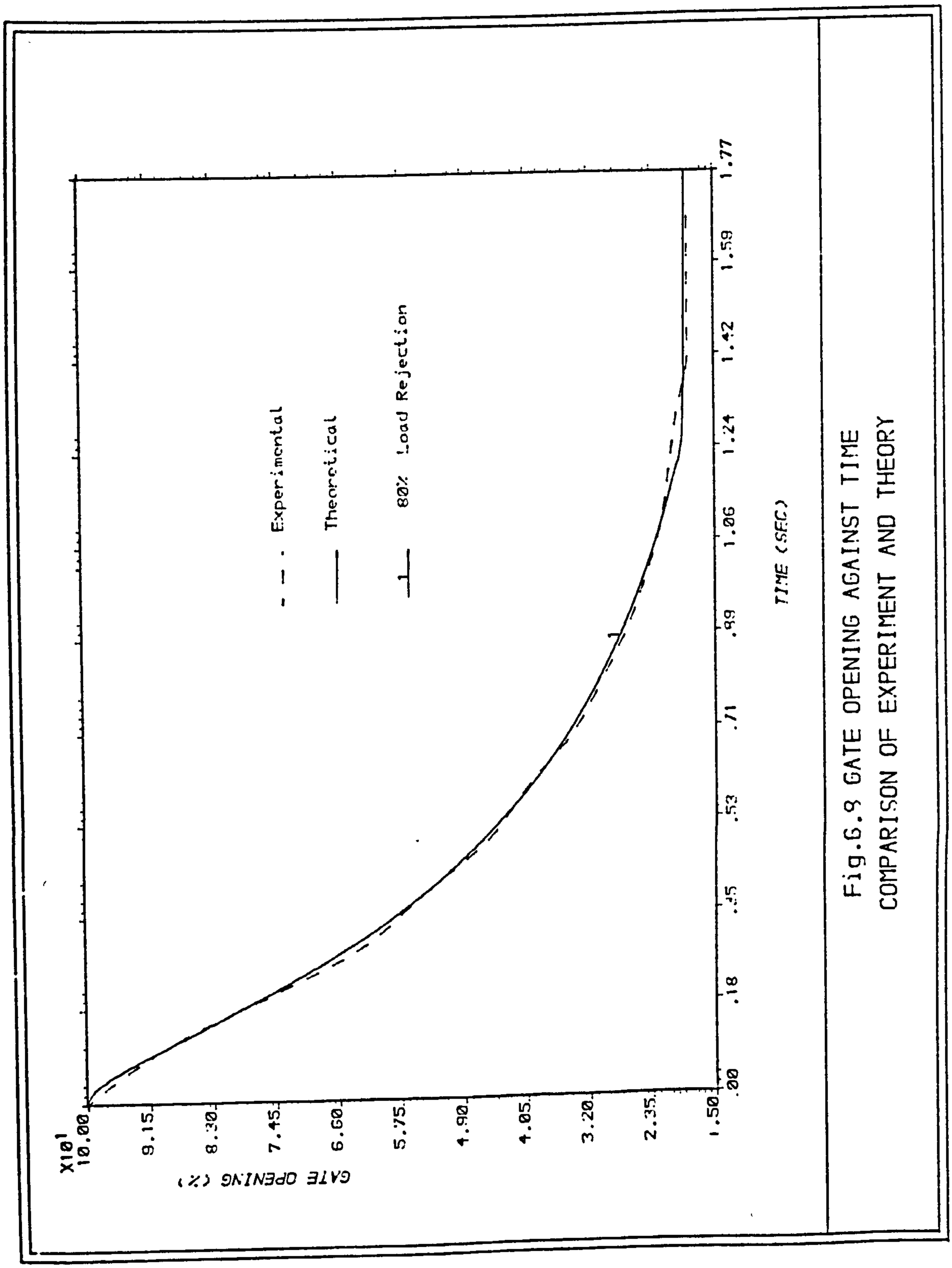

Fig.6.8 GATE OPENING AGAINST TIME
COMPARISON OF EXPERIMENT AND THEORY

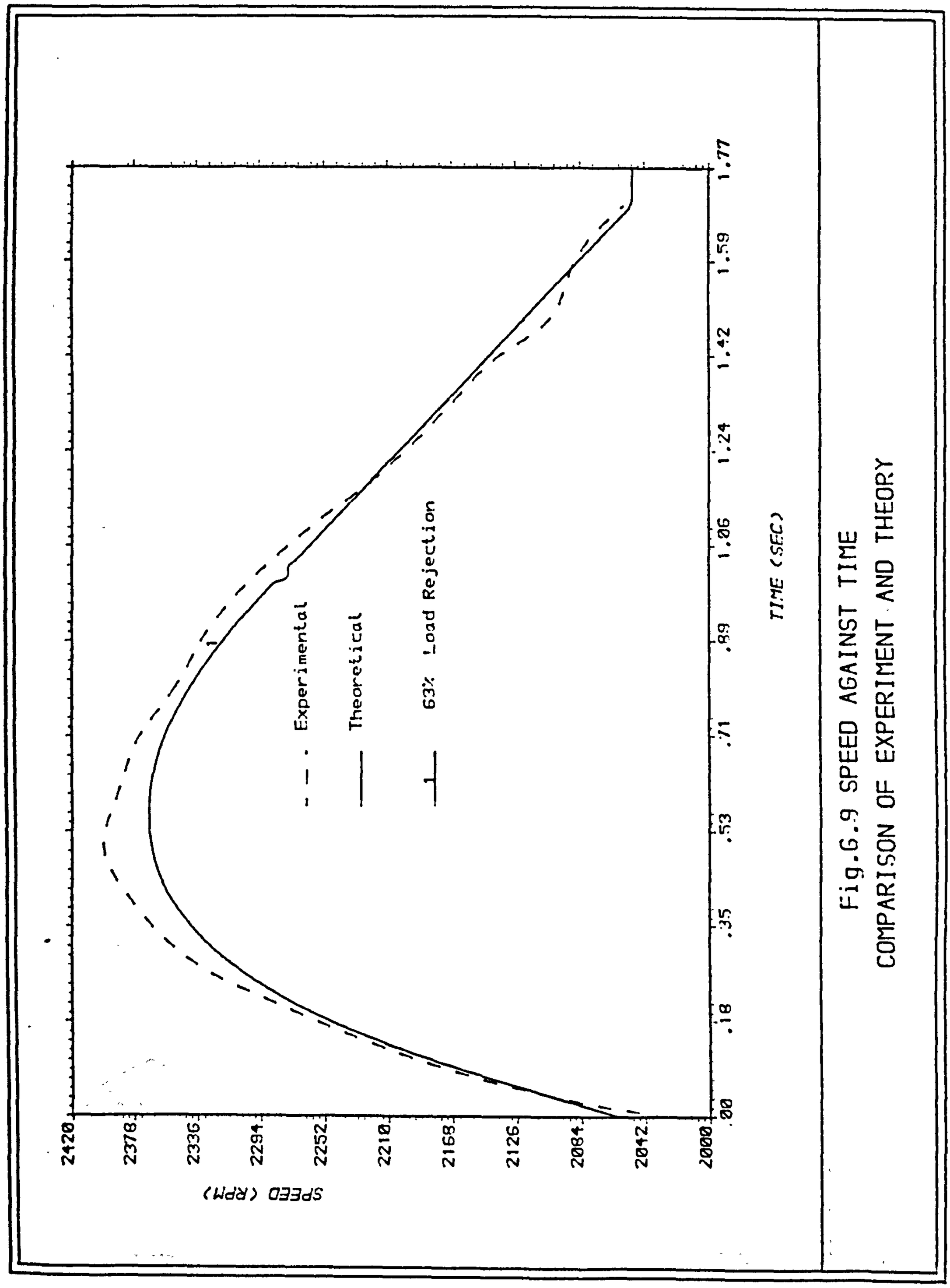

Fig.6.9 SPEED AGAINST TIME
COMPARISON OF EXPERIMENT AND THEORY

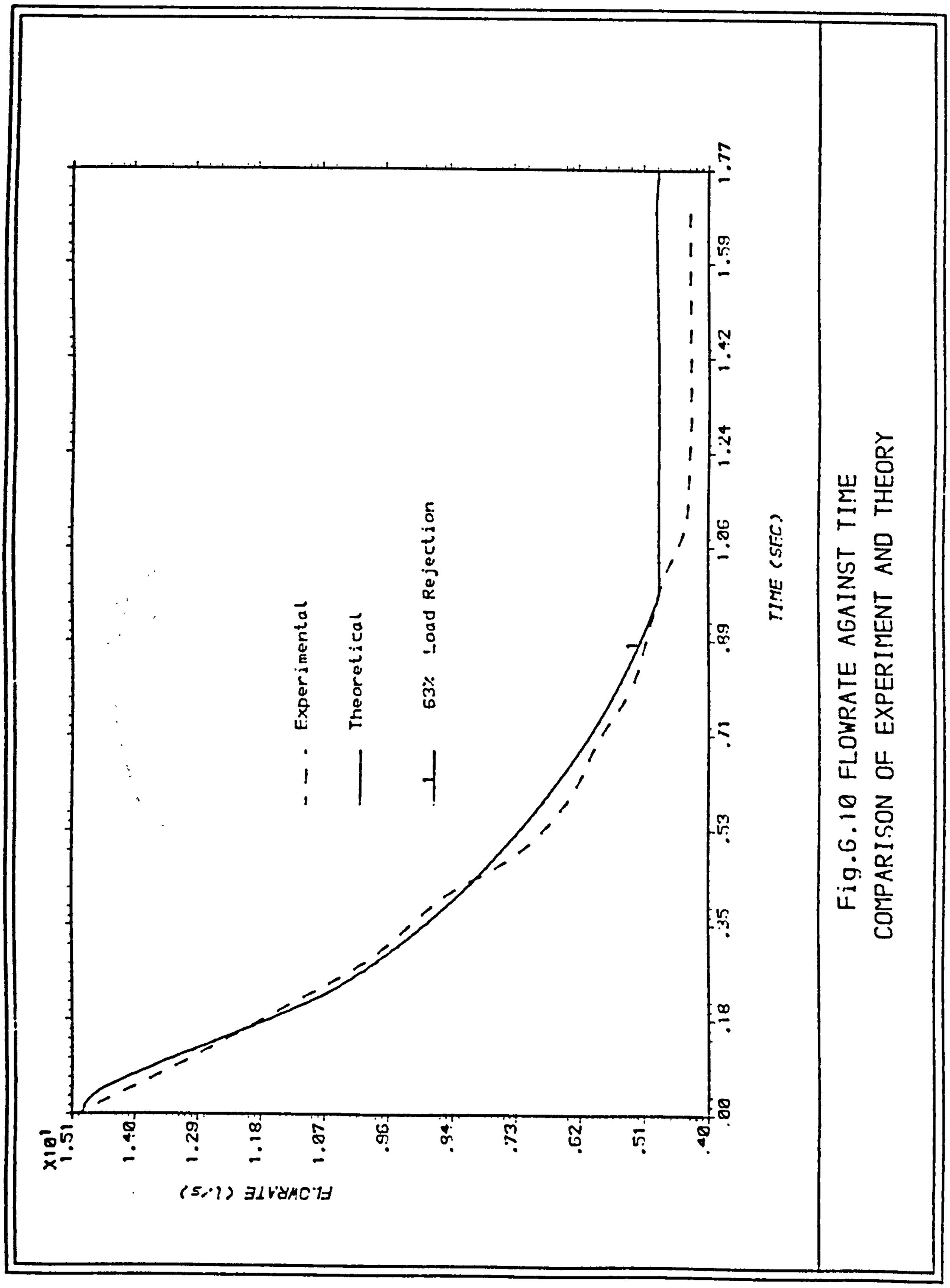

Fig.6.10 FLOWRATE AGAINST TIME
COMPARISON OF EXPERIMENT AND THEORY

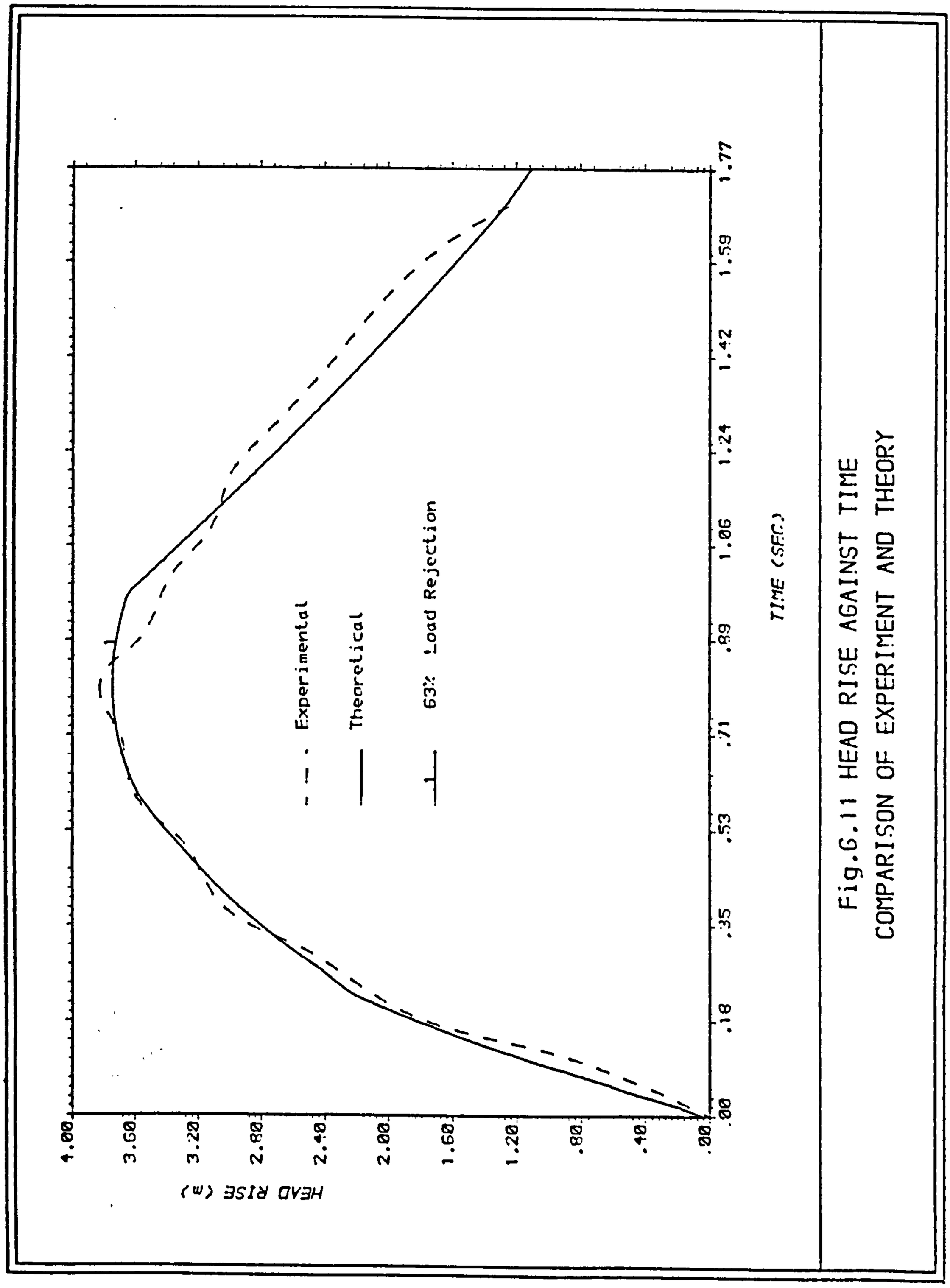

Fig.6.11 HEAD RISE AGAINST TIME
COMPARISON OF EXPERIMENT AND THEORY

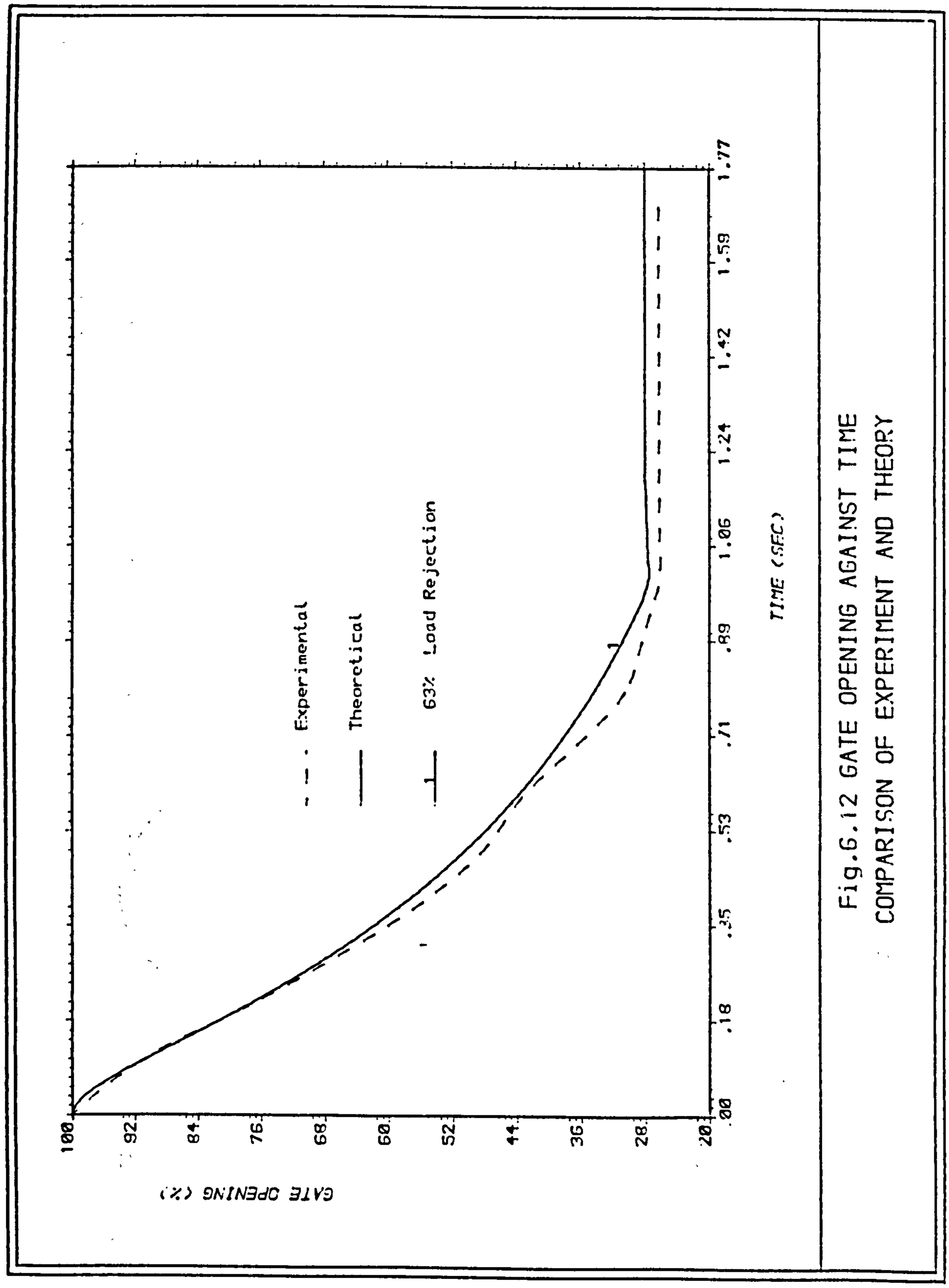

Fig.6.12 GATE OPENING AGAINST TIME
COMPARISON OF EXPERIMENT AND THEORY

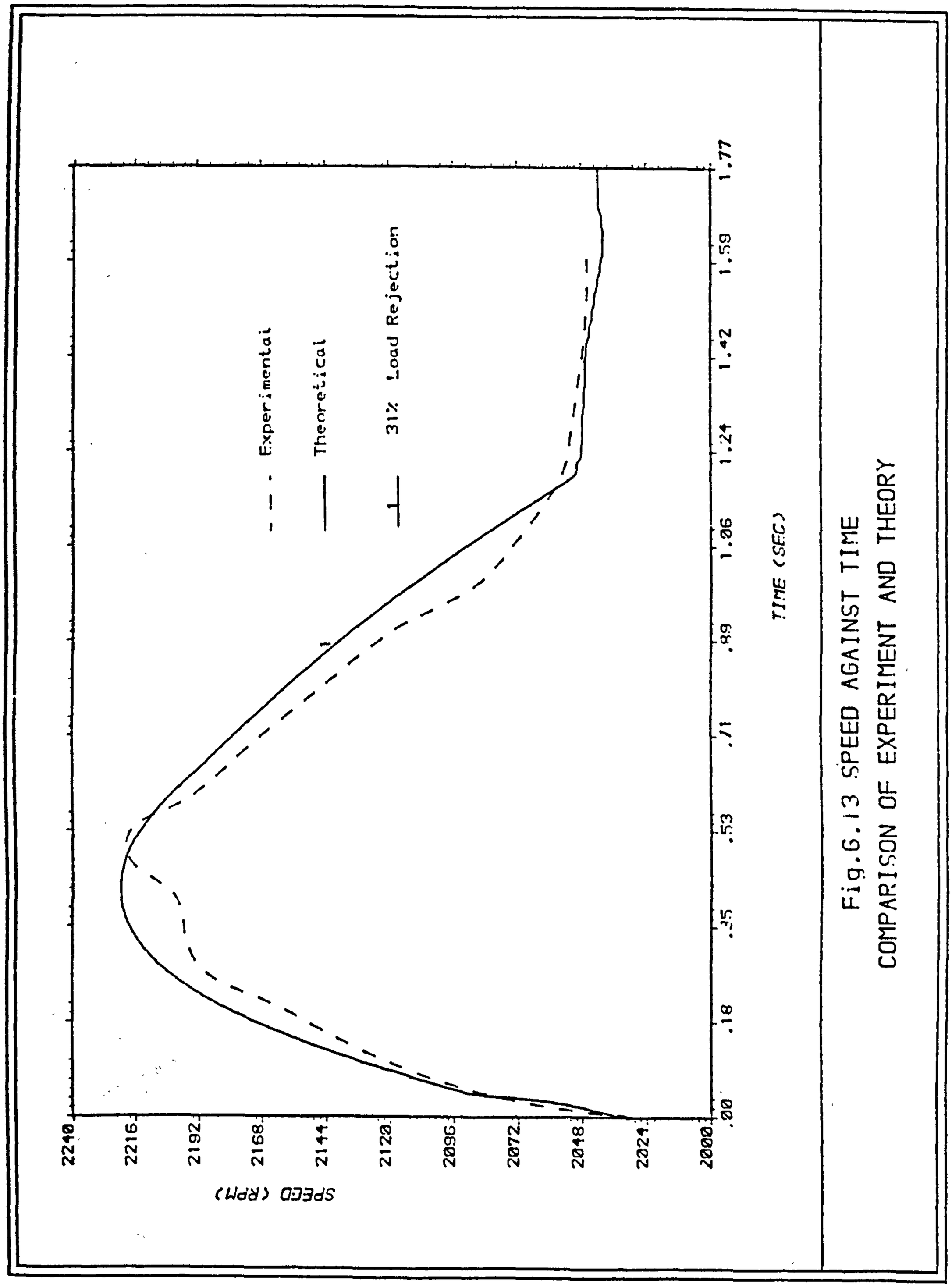

Fig.6.13 SPEED AGAINST TIME
COMPARISON OF EXPERIMENT AND THEORY

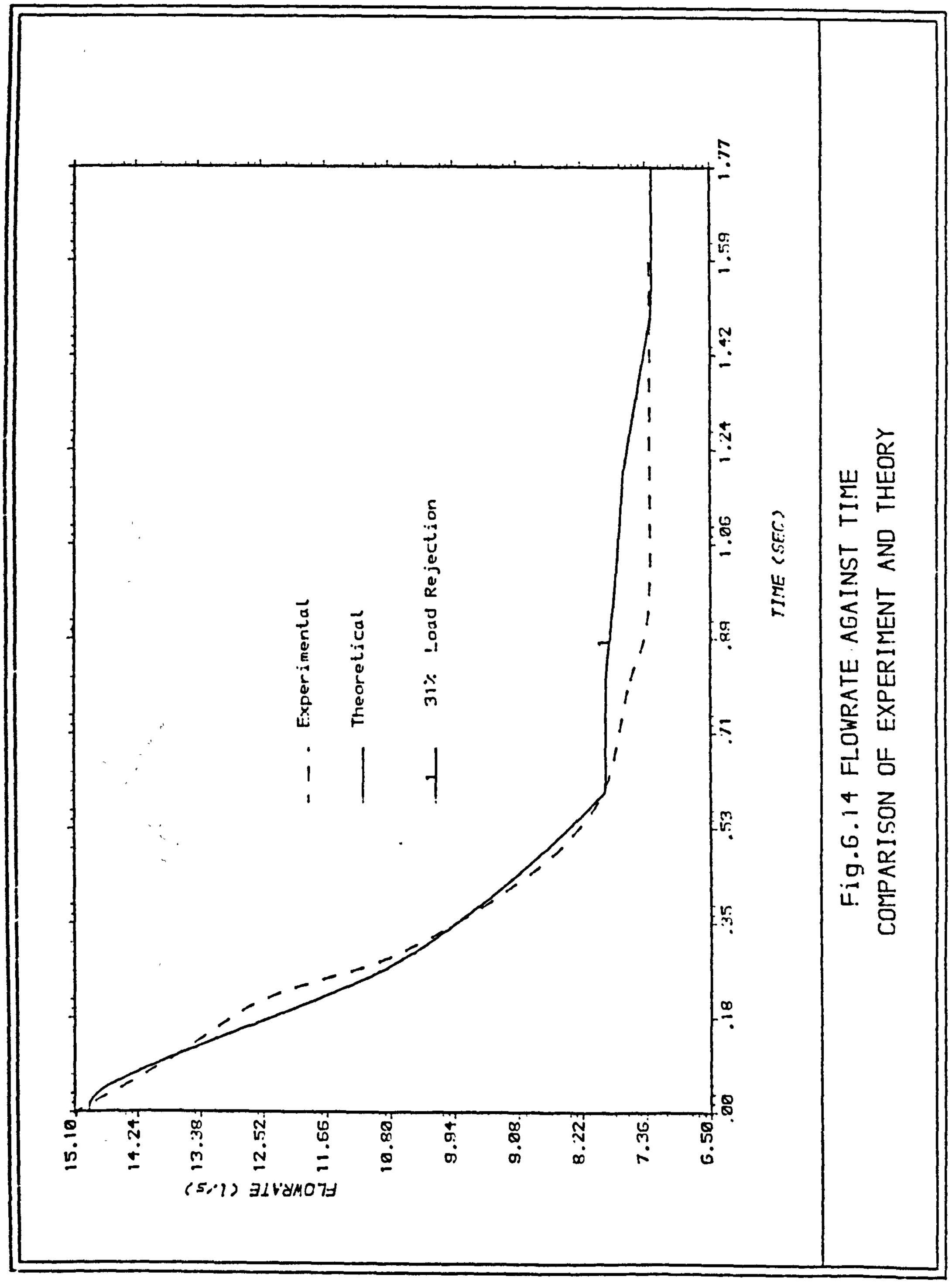

Fig.6.14 FLOWRATE AGAINST TIME
COMPARISON OF EXPERIMENT AND THEORY

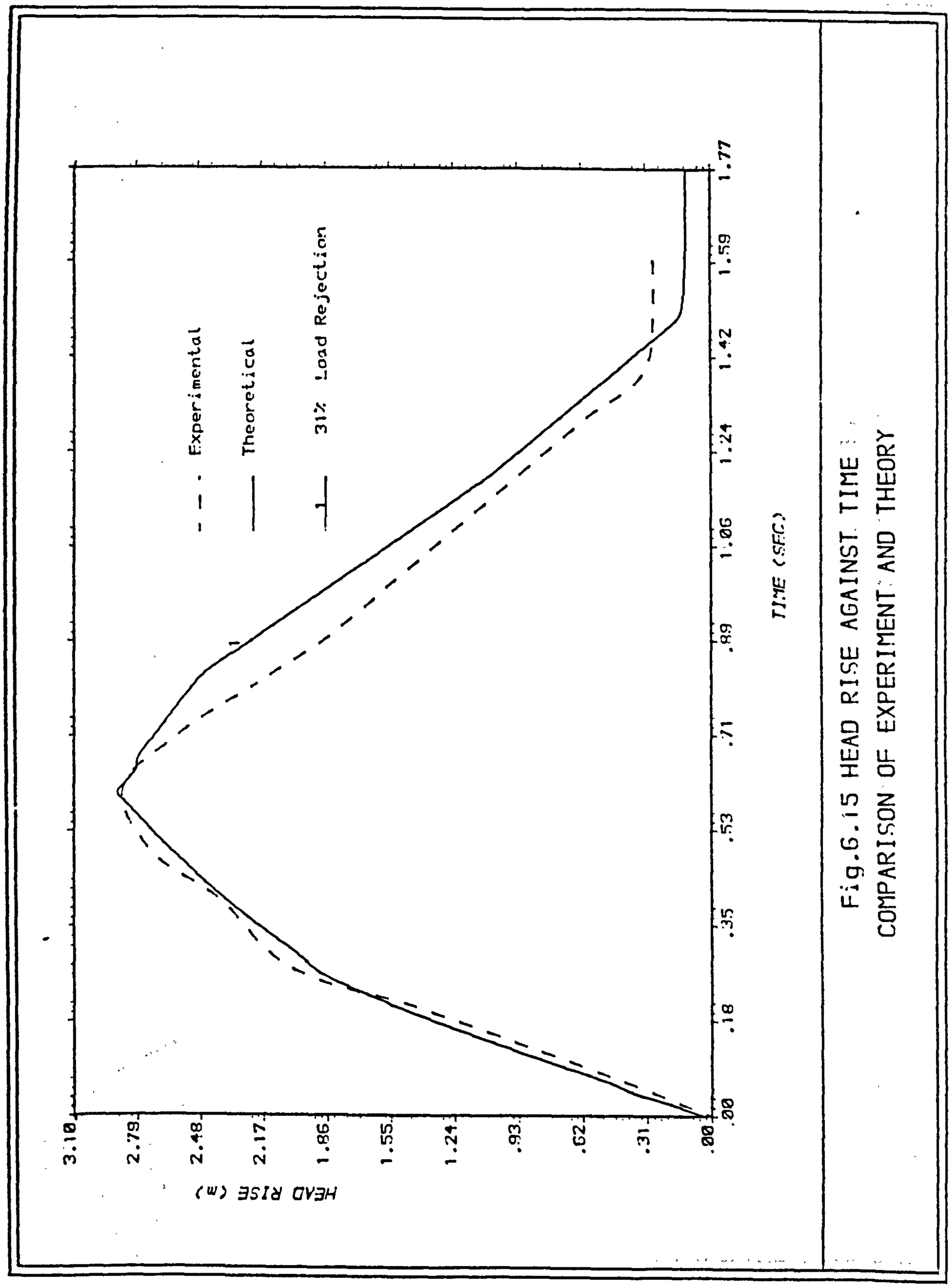

Fig.6.15 HEAD RISE AGAINST TIME
COMPARISON OF EXPERIMENT AND THEORY

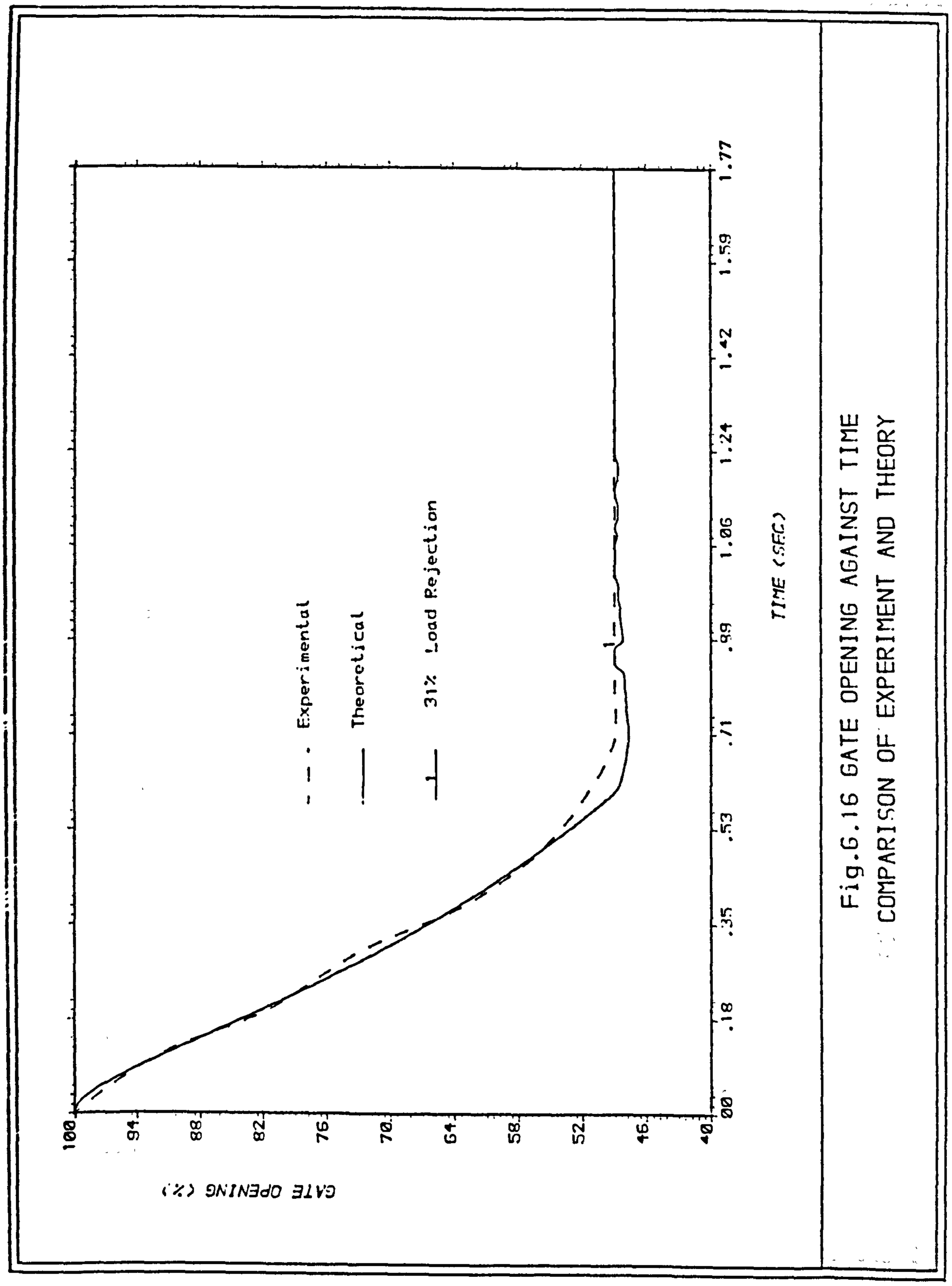

Fig.6.16 GATE OPENING AGAINST TIME
COMPARISON OF EXPERIMENT AND THEORY

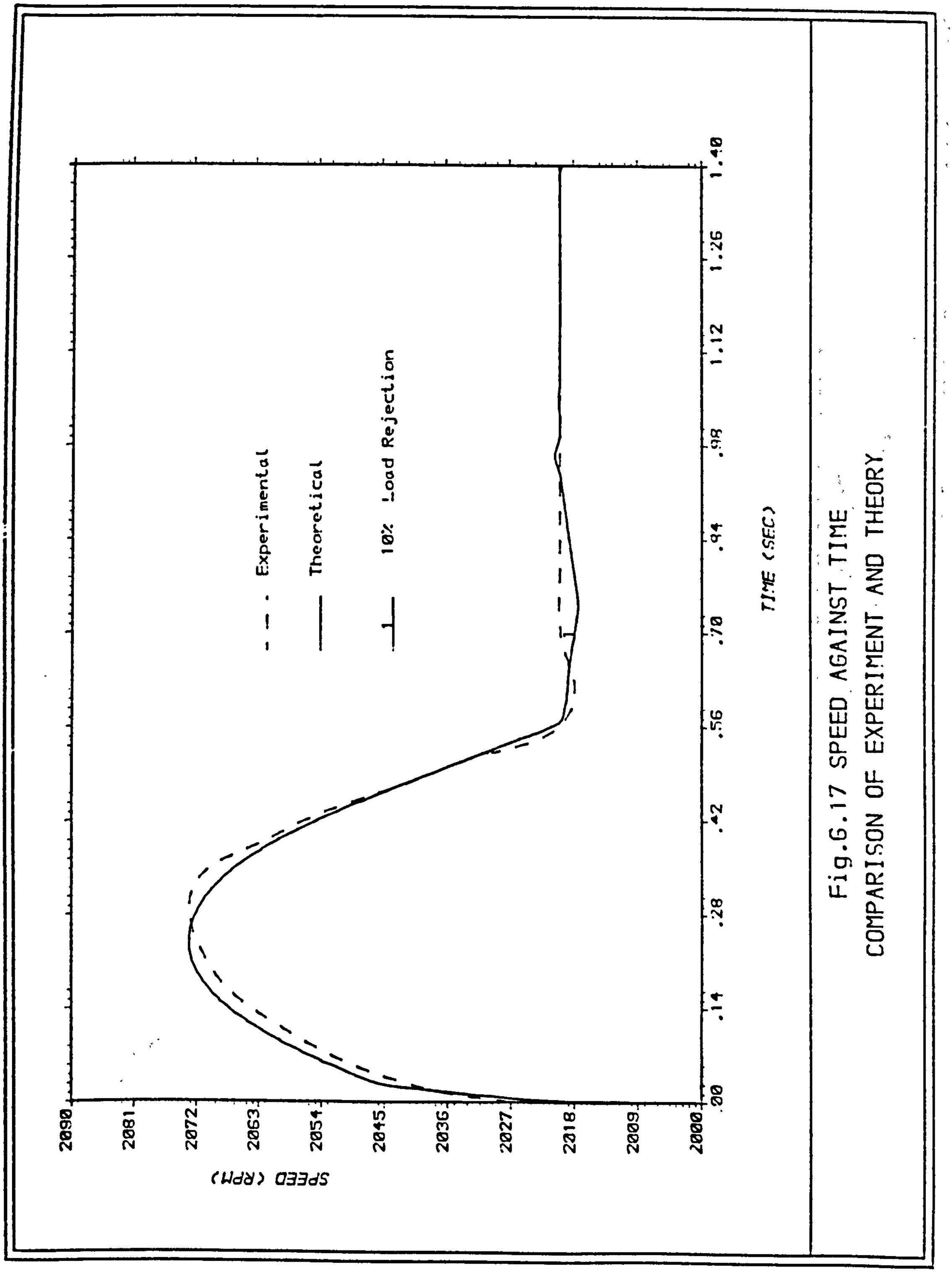

Fig.6.17 SPEED AGAINST TIME
COMPARISON OF EXPERIMENT AND THEORY

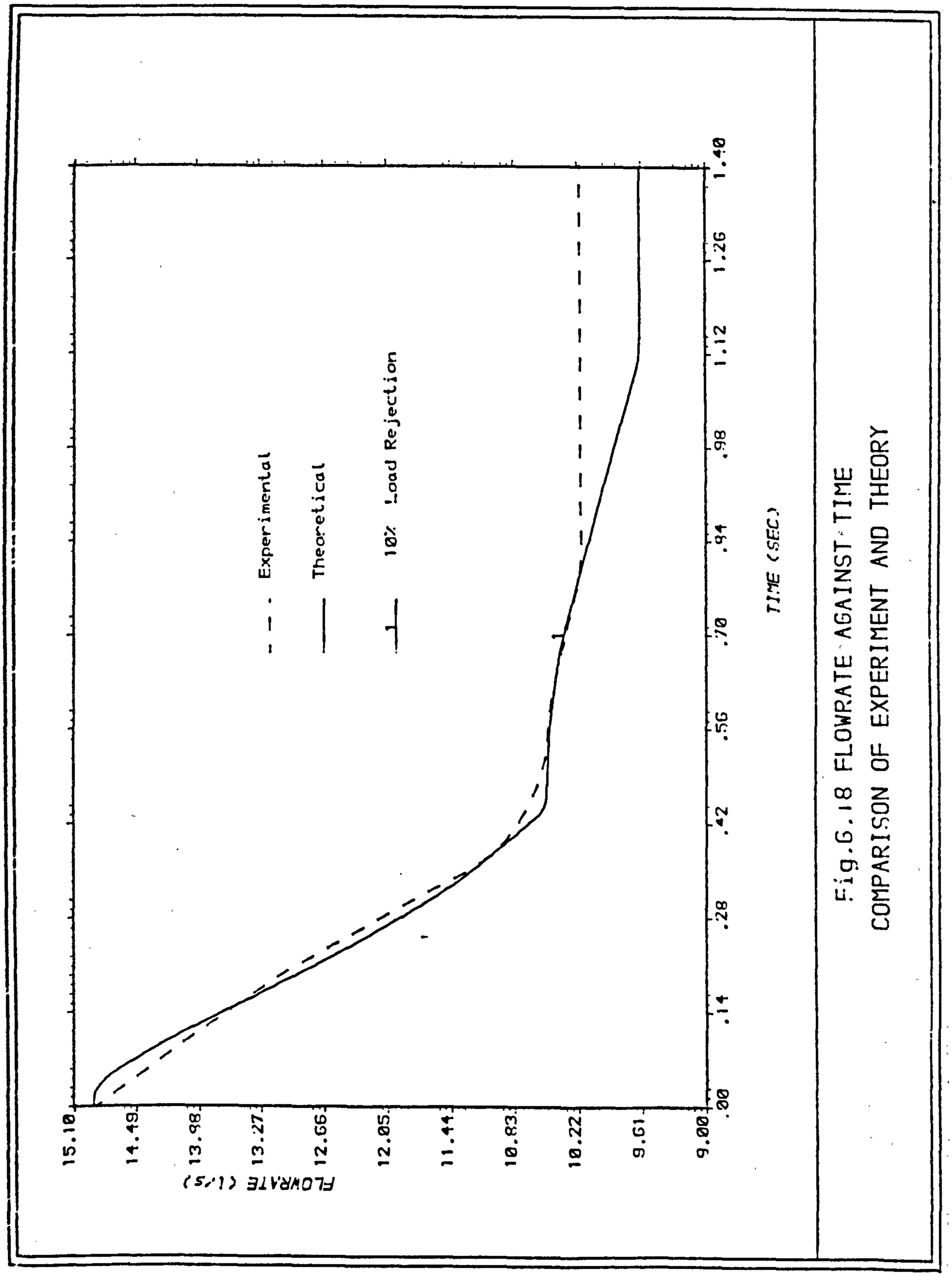

Fig.6.18 FLOWRATE AGAINST TIME
COMPARISON OF EXPERIMENT AND THEORY

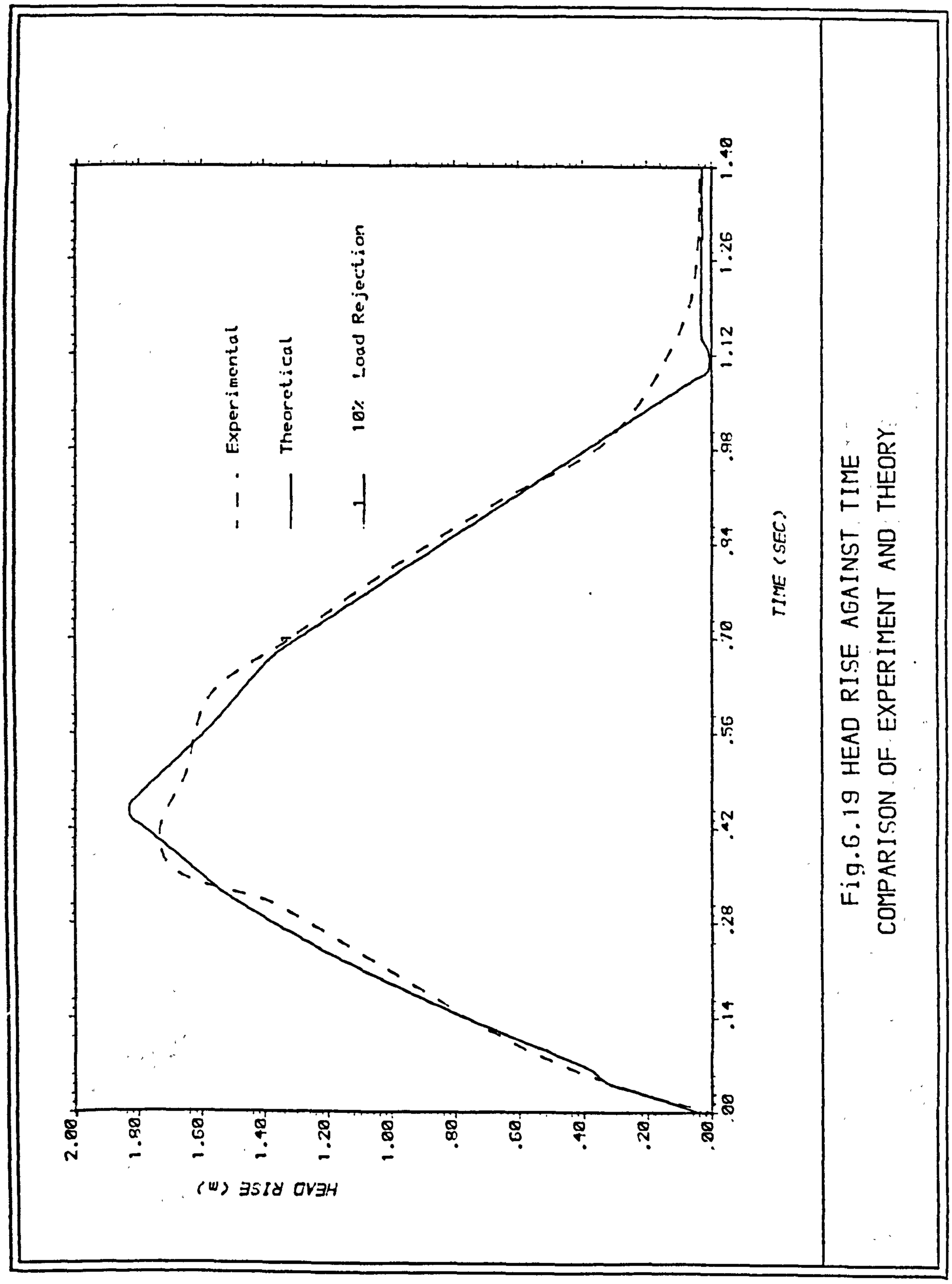

Fig.6.19 HEAD RISE AGAINST TIME
COMPARISON OF EXPERIMENT AND THEORY

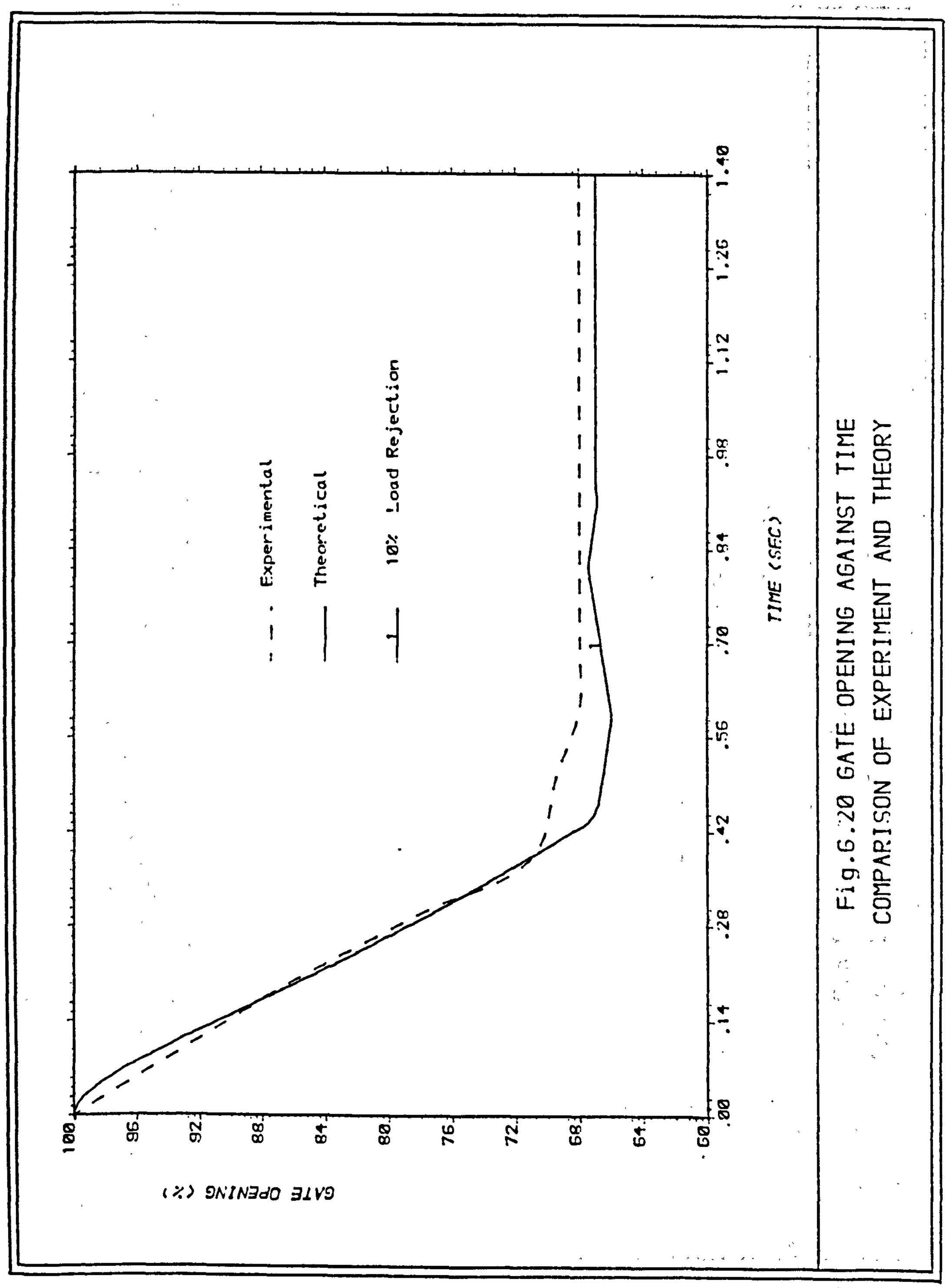

Fig.6.20 GATE OPENING AGAINST TIME
COMPARISON OF EXPERIMENT AND THEORY

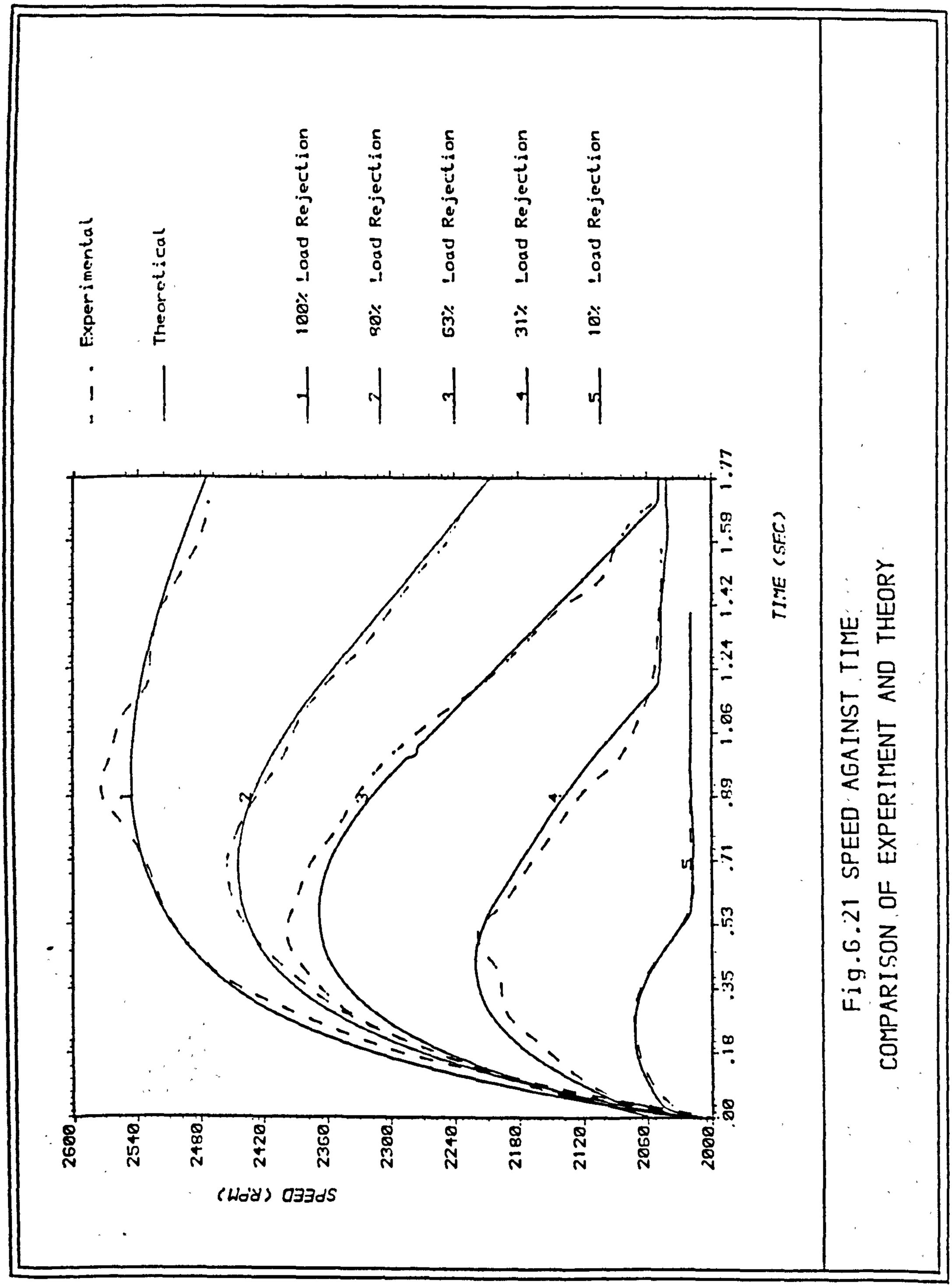

Fig.6.21 SPEED AGAINST TIME
COMPARISON OF EXPERIMENT AND THEORY

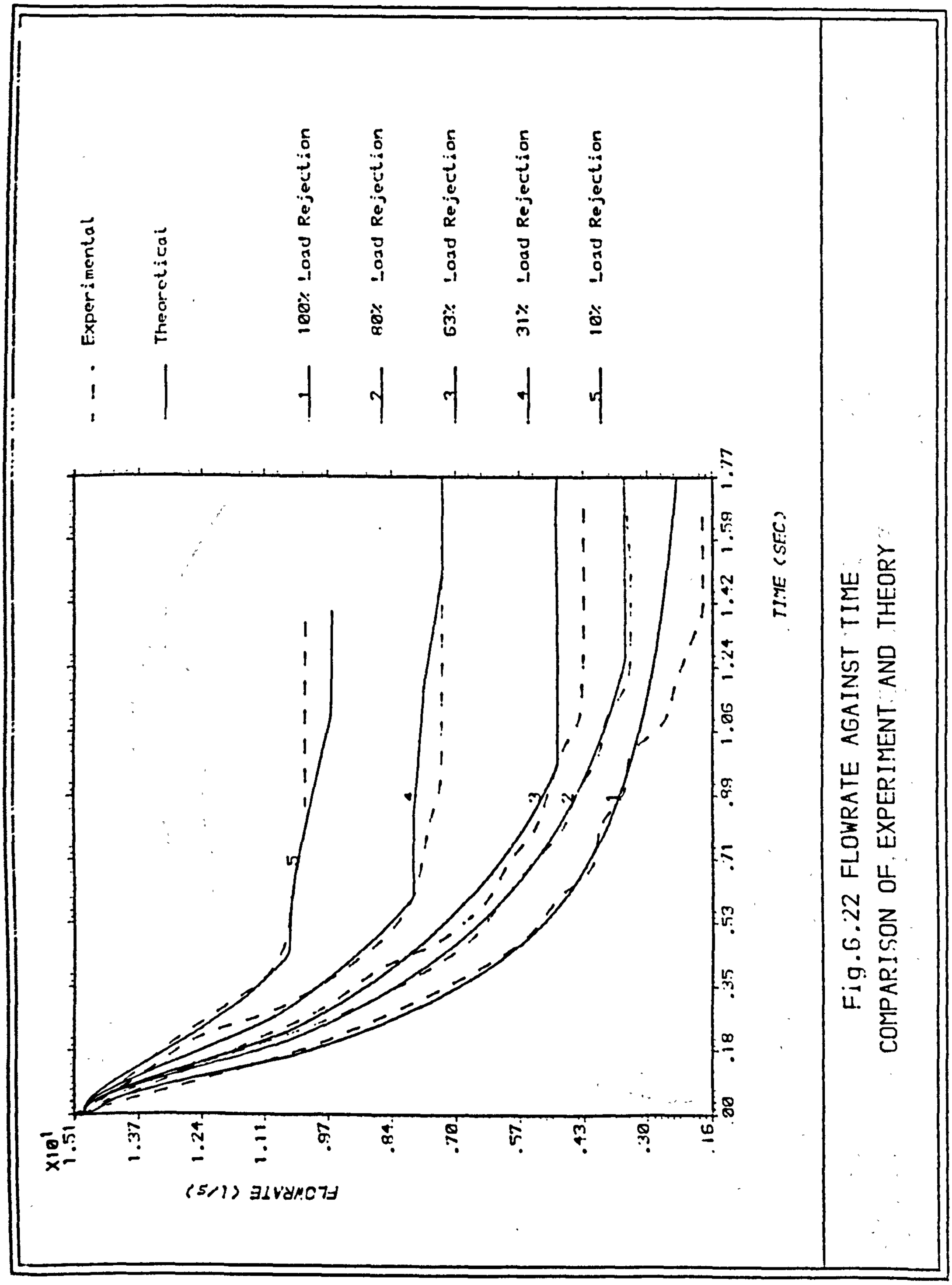

Fig.6.22 FLOWRATE AGAINST TIME
COMPARISON OF EXPERIMENT AND THEORY

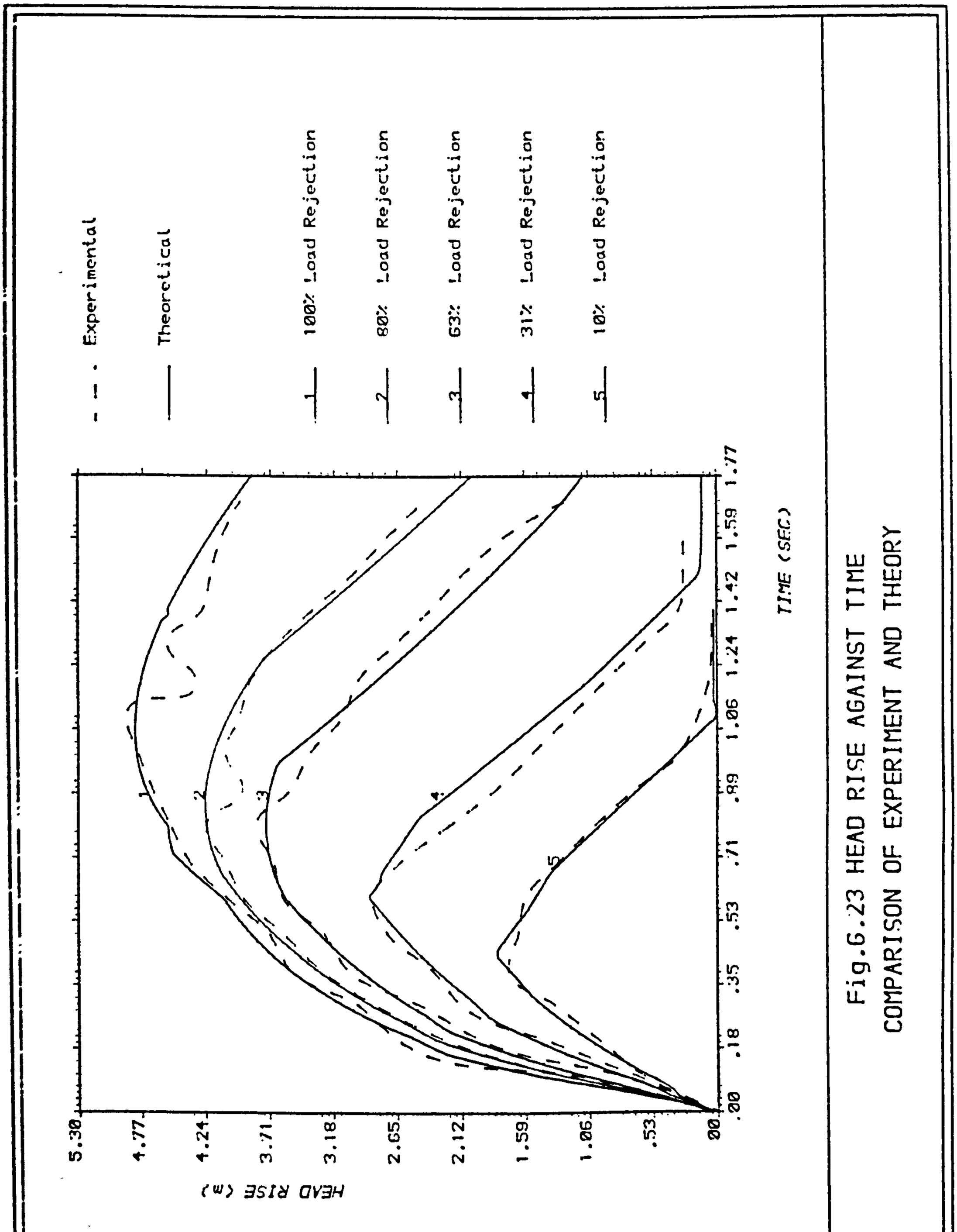

Fig.6.23 HEAD RISE AGAINST TIME
COMPARISON OF EXPERIMENT AND THEORY

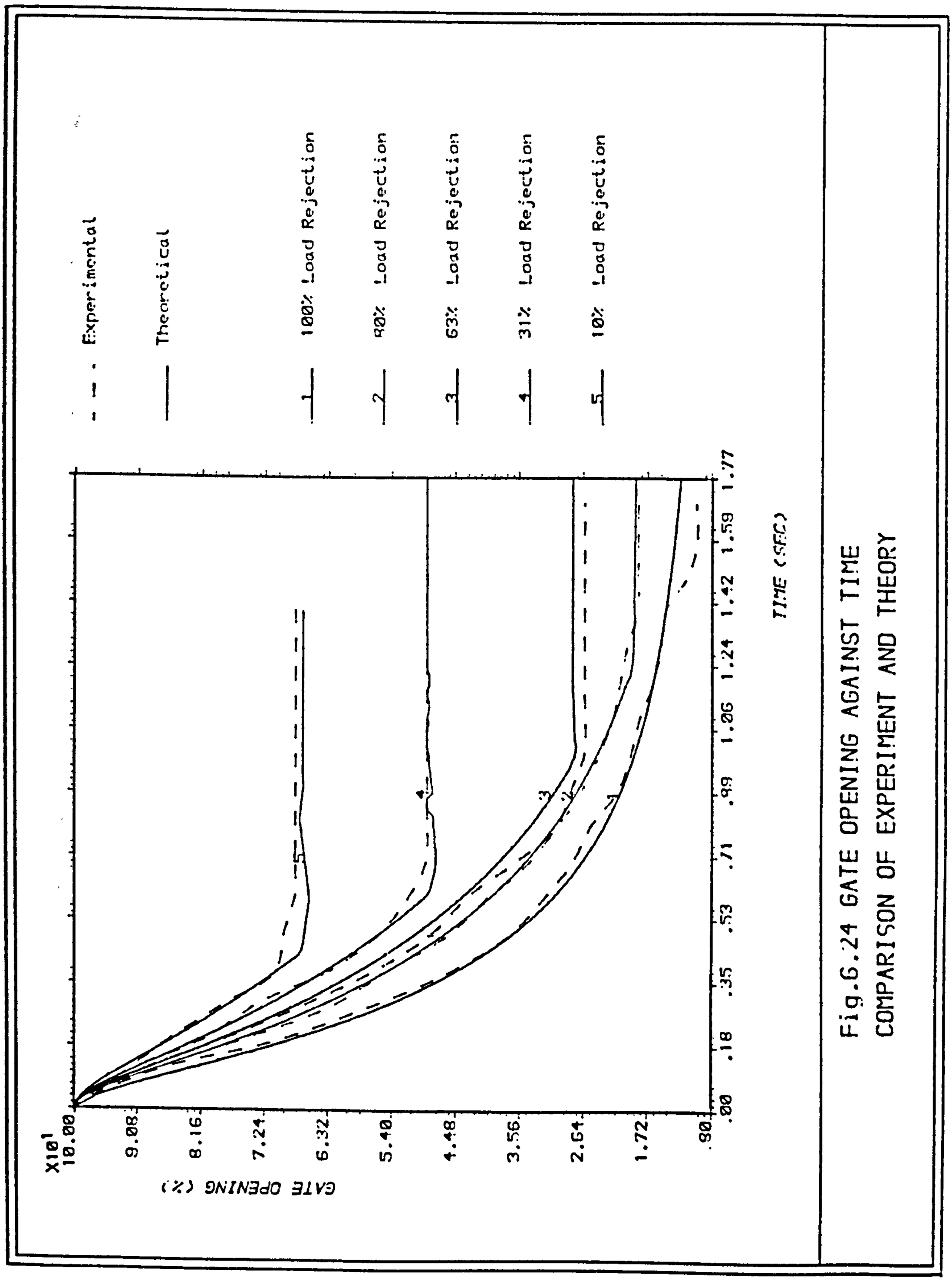

Fig.6.24 GATE OPENING AGAINST TIME
COMPARISON OF EXPERIMENT AND THEORY

CHAPTER 7

CONCLUSIONS AND FURTHER WORK

7.1 CONCLUSIONS

In the literature survey in Chapter 2 previous computational work on studying transient problems in a hydraulic power unit governed by different types of governor and the governing stability was reviewed.

The work of this thesis is mainly concerned with developing a computer program using an improved interpolation technique to deal with the turbine boundary conditions making use of piecewise Lagrangean interpolation and designing and building a proportional plus integral plus derivative (PID) governor to control a small turbine. It was found that the interpolation technique developed is more accurate than the other techniques and has many advantages which are explained in Chapter 3.

A model turbogenerator set was installed in the laboratory and a full range of tests were carried out both under full load and partial load rejection. In designing the PID governor it was found that a governor of the type described by Chaudhry, (Ref.7), with linear elements was insufficiently stable for laboratory conditions because of the higher frequencies involved when working at the smaller scale. Hence a governor using second order elements was designed. Other points to note which were introduced to give satisfactory operation are:

(i) A phase-locked loop introduced to ensure that n and n_{ref} were in phase.

(ii) A smoothing network introduced to give approximated DC input to the step motor actuator.

The stability of the system was clearly illustrated by using the Bode plot method. Figure 4.7 shows that the phase angle above minus 180 degrees means that the system is stable for all values of the frequency.

The computer program was described in Chapter 5. A flowchart for each part of the program and the main program has been drawn. The program is flexible and uses all the points in the grid of the turbine characteristic curves (general Lagrangean interpolation) or a specified subdomain which surrounds the interpolation point and contains a certain number of the grid points (piecewise Lagrangean interpolation) depending on the required accuracy.

Finally, a comparison between the computational and the experimental results has been described and presented with a plot for each test in Chapter 5. As can be seen there is a good measure of agreement particularly up to the peak of speed and pressure rise. However, the fluctuation in the experimental pressure/time curve, (Figure 6.4), was shorter and of smaller amplitude than those of previous researchers, (Refs. 3,7).

7.2 SUGGESTIONS FOR FURTHER WORK

1. The computer program developed for studying the transients caused by load changes could be used for studying the transient behaviour when a fluctuating load is imposed on the system. In this case the power of the generator integrated with time would be used instead of the final generator power used when assuming a step change.

2. The PID governor presented in this thesis was an analogue governor. It would be worthwhile to develop a new digital governor, for example an adaptive control governor which changes the governor parameters with relation to the gate opening,and compare its result with the PID governor.

APPENDIX A

A.1 PHASE LOCK LOOP

A typical connection diagram is shown in Figure A.1.

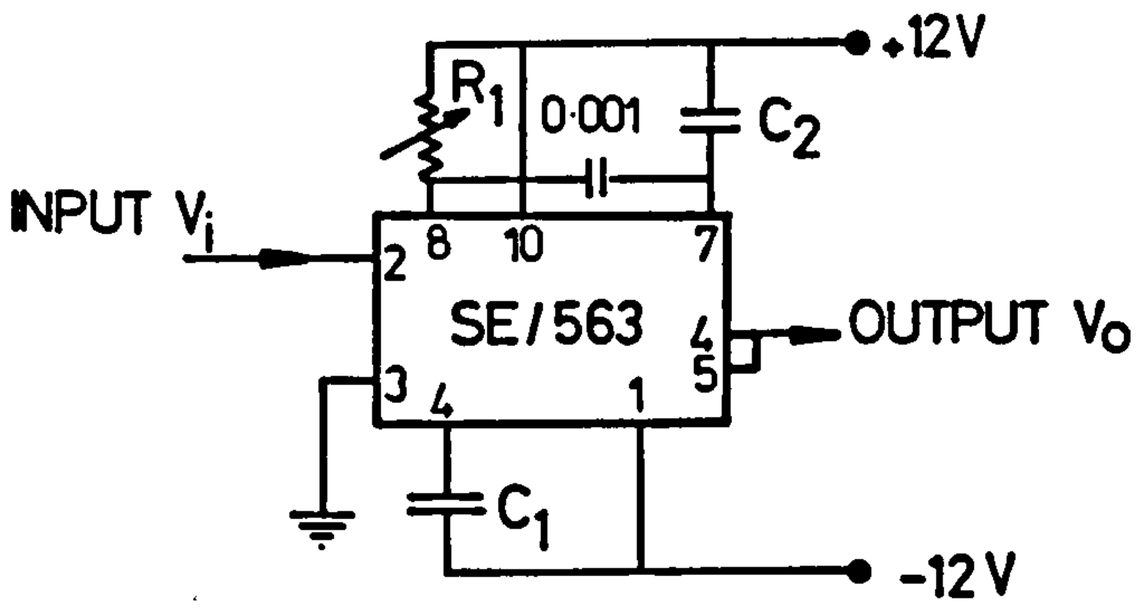

Figure A.1

The voltage controlled oscillator (VCO) free running frequency is given approximately by

$$f_o = \frac{1.2}{4 R_1 C_1} \qquad (A.1)$$

and should be adjusted to be at the centre of the input signal frequency range. C_1 can be any value but R_1 should be within the range of 2000 to 20,000 ohms with an optimum value of the order of 4,000 ohms, i.e.

The reference speed of the system = 2,000 rpm.

$$f = \frac{N}{P} \text{ where P is the number of poles}$$

$$\therefore f_o = \frac{2000}{60} = 33.3 \text{ Hz}$$

Hence R_1 = 4,000 ohms

$\therefore C_1 = 2.2\ \mu F$

Lock range:

$$f_L = \pm \frac{8 f_o}{V_{cc}} \qquad (A.2)$$

where V_{cc} = 6 volts

$$\therefore f_L = \pm 44.4 \text{ Hz}$$

Capture range:

$$f_c = \pm \frac{1}{2\pi}\sqrt{\frac{2 f_L}{\tau}}$$

where $\tau = (3.6 \times 10^3) \times C_2$ and $C_2 = 2.4\ \mu F$

$$\therefore f_c = \pm 16 \text{ Hz.}$$

Practically it was found that the capture range is = ±20 Hz.

A.2 PROPORTIONAL ELEMENT

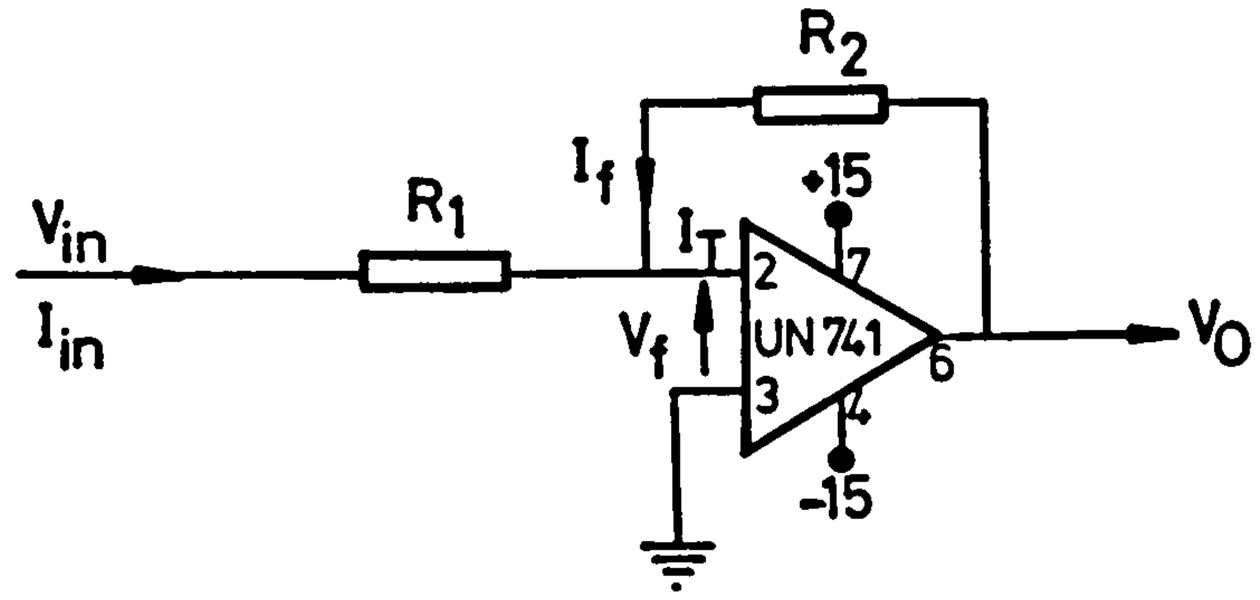

Figure A.2

In Figure A.2, the circuit inverts the polarity of the applied input signal but the gain of the feedback circuit is determined by the value of the external elements. The following relationships are established.

The current supplied by the input signal is:

$$I_{in} = \frac{V_{in} - V_f}{R_1}$$

since V_f is virtual earth i.e. $V_f = 0$

$$\therefore I_{in} = \frac{V_{in}}{R_1}$$

The effective nput resistance of the circuit is thus R_1. The output voltage causes I_f to flow through resistor R_2 and

$$I_{in}+I_f = I_T$$

since $Z_{in} = \infty$

$$\therefore I_T = 0$$

$$\therefore I_{in} = - I_f$$

$$\therefore \frac{V_{in}}{R_1} = I_{in} = -I_f = - \frac{V_0}{R_2}$$

$$\boxed{\therefore V_0 = - \frac{R_2}{R_1} V_{in}}$$

where $R_2/R_1 = K_p$, the gain of the proportional elements.

A.3 INTEGRATOR CIRCUIT

The basic diagram of the second order system is shown below.

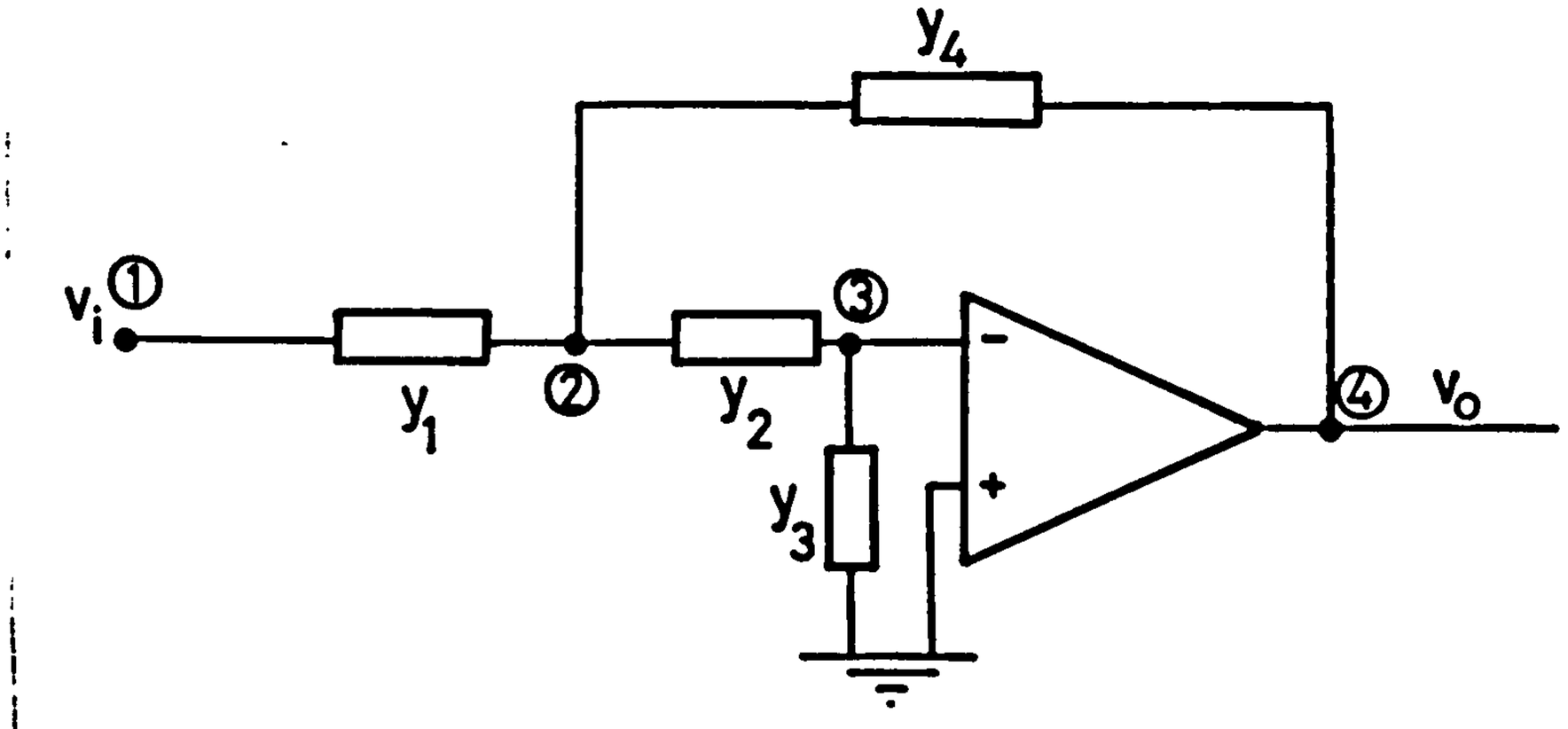

Figure A.3

$$|I| = |Y||V|$$

$$Y = \begin{vmatrix} Y_{11} & Y_{12} & Y_{13} & Y_{14} \\ Y_{21} & Y_{22} & Y_{23} & Y_{24} \\ Y_{31} & Y_{32} & Y_{33} & Y_{34} \\ Y_{41} & Y_{42} & Y_{43} & Y_{44} \end{vmatrix}$$

$$= \begin{array}{c} \begin{matrix} 1 & 2 & 3 & 4 \end{matrix} \\ \begin{vmatrix} Y_1 & -Y_1 & 0 & 0 \\ -Y_1 & Y_1+Y_2+Y_4 & -Y_2 & -Y_4 \\ 0 & -Y_2 & Y_2+Y_3 & 0 \\ 0 & -Y_4 & 0 & Y_4 \end{vmatrix} \end{array} \begin{matrix} 1 \\ 2 \\ 3 \\ 4 \end{matrix}$$

The gain of the operational amplifier is very high and the output is limited, i.e. the input voltage = 0.

Column 3 can be added to column 4 and since the output impedance of the operational amplifier is equal to zero row 4 can be cancelled.

The input impedance $Z_{in} = \frac{\Delta 11}{\Delta}$

The output impedance $Z_0 = \frac{\Delta 44}{\Delta}$

i.e. the transfer function is

$$H_{(s)} = \frac{Z_0}{Z_{in}} \times \frac{I_0}{I_{in}}$$

$$H_{(s)} = \frac{\Delta 14}{\Delta 11} \times (-1)^{1+4}$$

$\Delta 14 = Y_1 Y_2$ (i.e. by deleting row 1 and column 4)

$$\Delta 11 = |(Y_1+Y_2+Y_4)(Y_2+Y_3) - Y_2(Y_2+Y_4)|$$

$$\Delta 11 = Y_1Y_2 + Y_1Y_3 + Y_2Y_3 + Y_4Y_3$$

$$\therefore H_{(s)} = \frac{-1}{\frac{Y_1Y_3 + Y_3Y_2}{Y_1Y_2} + \frac{Y_4Y_3}{Y_1Y_2}}$$

Y_1Y_2 should be independent of frequency, i.e. resistors.

$$\therefore Y_1 = \frac{1}{R_1} \quad \text{and} \quad Y_2 = \frac{1}{R_2}$$

$$Y_3 = SC_3 \qquad Y_4 = SC_4$$

$$\therefore H_{(s)} = \frac{-1}{1 + SC_3(R_1+R_2) + S^2(R_1R_2C_3C_4)}$$

But the general transfer function of second order systems is:-

$$H(s) = \frac{K_0}{1 + \frac{2\zeta}{\omega_0} S + \frac{1}{\omega_0^2} S^2}$$

$$\therefore \omega_n^2 = \frac{1}{R_1R_2C_3C_4}$$

For simplicity $R_1 = R_2 = R$

$C_3 = C_4 = C$

$$\therefore \omega_n = \frac{1}{RC}$$

and

$$\frac{2\zeta}{\omega_n} = C_3(R_1+R_2)$$

$$\frac{2\zeta}{\omega_n} = 2RC$$

$$\therefore \zeta = 1$$

Since the output frequency of the system is proportional to the speed of the turbine and the runaway speed of the turbine is equal to 3,000 rpm.

$$f = \frac{N}{P} = \frac{3000}{60} = 50 \text{ Hz}$$

and

$$\omega_0 = 2\pi f$$

$$\therefore f = \frac{1}{2\pi RC}$$

Thus C can be assumed because capacitors are available only in limited values in the laboratory.

$$C = 0.02 \ \mu F$$
$$R = 159 \ K\Omega$$
$$T_I = RC = 3.18 \times 10^{-3} \text{ sec.}$$

A.4 DERIVATIVE CIRCUIT

The general diagram of the derivative circuit is shown below.

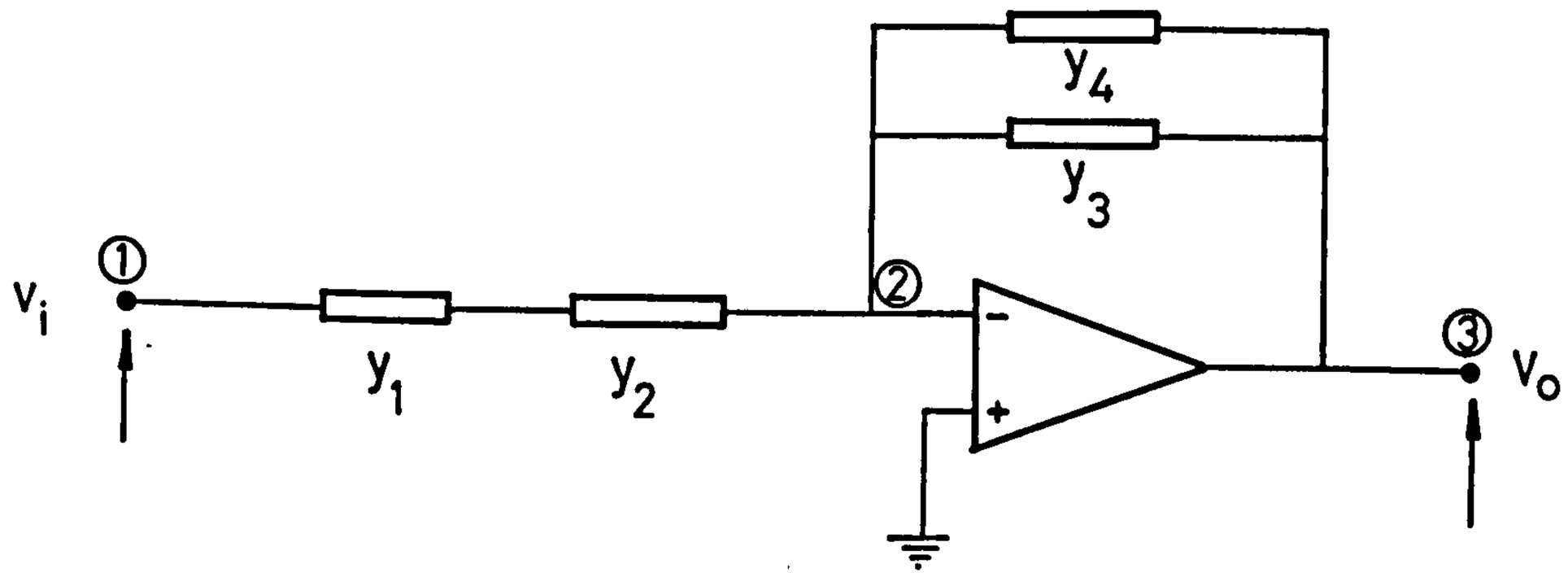

$$|I| = |V||Y|$$

Y_1 and Y_2 are in series. To simplify the solution put

$$Y_s = \frac{Y_1 Y_2}{Y_1 + Y_2}$$

$$\therefore Y = \begin{vmatrix} Y_{11} & Y_{12} & Y_{13} \\ Y_{21} & Y_{22} & Y_{23} \\ Y_{31} & Y_{32} & Y_{33} \end{vmatrix}$$

$$= \begin{array}{c} \begin{vmatrix} Y_s & -Y_s & 0 \\ -Y_s & Y_s+Y_3+Y_4 & -(Y_3+Y_4) \\ 0 & -(Y_3+Y_4) & Y_3+Y_4 \end{vmatrix} \\ \begin{array}{ccc} 1 & 2 & 3 \end{array} \end{array}$$

Since the output impedance of the operational amplifier is equal to zero, column 2 and row 3 can be deleted.

$$\therefore Y = \begin{vmatrix} Y_s & 0 \\ -Y_s & -(Y_3+Y_4) \end{vmatrix}$$

Similarly the transfer function is

$$H_{(s)} = \frac{\Delta 13}{\Delta 11} (-1)^{1+3}$$

and

$$\Delta 13 = -Y_s = \frac{-Y_1 Y_2}{Y_1+Y_2}$$

$$\Delta 11 = -(Y_3 + Y_4)$$

$$\therefore H_{(s)} = \frac{Y_1 Y_2}{(Y_1+Y_2)(Y_3+Y_4)}$$

where $Y_1 = \frac{1}{R_1}$, $Y_2 = SC_1$, $Y_3 = \frac{1}{R_2}$, $Y_4 = SC_2$

$$\therefore H_{(s)} = \frac{R_2 C_1 S}{1 + (R_1 C_1 + R_2 C_2)S + (R_1 R_2 C_1 C_2)S^2}$$

For simplicity take $R_1 C_1 = R_2 C_2 = T_D$

and $R_2 C_1 = K_D$

$$\therefore H_{(s)} = \frac{K_D S}{1 + 2T_D S + T_D^2 S^2}$$

$$\therefore \frac{V_{D(s)}}{Z_{(s)}} = \frac{K_D S}{1 + 2T_D S + T_D^2 S^2}$$

Hence $f_0 = \frac{1}{2\pi R_1 C_1}$

if $C_1 = 1.0\ \mu F$
$\therefore R_1 = 3.18\ K\Omega$
$\therefore T_D = 3.18 \times 10^{-3}$ sec.

Also

$C_2 = 32\ nF$
$R_2 = 100\ K\Omega$

A.5 SMOOTHING NETWORK

This is a second order low pass filter. The derivation of a second order system was shown in Section A.3. It was found that an approximated DC output can be obtained when $\omega_0 = 10$ Hz i.e.

Referring to equation

$$f = \frac{\omega_0}{2\pi}$$

$$\therefore f = \frac{1}{2\pi RC}$$

Similarly C can be assumed e.g. $C = 0.47\ \mu F$.

$\therefore R = 33\ K\Omega$

$\therefore T_A = 0.015$ sec.

****
APPENDIX (B)
****

EXPERIMENTAL RESULTS

C*** FULL LOAD REJECTION 100% ***
C*** FINAL GENERATOR LOAD PG=0.0
C*** RATED HEAD HN=21.0 (m)
C*** SYNCHRONOUS SPEED NR=2000.0 RPM

TIME T(SEC)	SPEED N(RPM)	FLOWRATE Q(l/s)	HEAD RISE PR(m)	GATE OPENING (%)
0.00000E+00	0.20000E+04	0.13056E+02	0.00000E+00	0.10000E+03
0.10000E+00	0.21700E+04	0.12295E+02	0.11156E+01	0.89436E+02
0.20000E+00	0.23130E+04	0.98587E+01	0.26396E+01	0.69813E+02
0.30000E+00	0.24000E+04	0.80960E+01	0.29779E+01	0.56127E+02
0.40000E+00	0.24660E+04	0.66052E+01	0.35538E+01	0.44625E+02
0.50000E+00	0.25000E+04	0.54716E+01	0.37271E+01	0.36625E+02
0.60000E+00	0.25200E+04	0.48631E+01	0.40802E+01	0.31938E+02
0.70000E+00	0.25330E+04	0.40903E+01	0.43891E+01	0.27812E+02
0.80000E+00	0.25530E+04	0.39487E+01	0.45415E+01	0.25250E+02
0.90000E+00	0.25750E+04	0.34332E+01	0.46939E+01	0.21250E+02
0.10000E+01	0.25650E+04	0.33022E+01	0.48158E+01	0.19450E+02
0.11000E+01	0.25550E+04	0.29747E+01	0.49073E+01	0.18220E+02
0.12000E+01	0.25300E+04	0.23575E+01	0.43282E+01	0.16250E+02
0.13000E+01	0.25270E+04	0.20743E+01	0.45720E+01	0.15250E+02
0.14000E+01	0.25180E+04	0.17910E+01	0.42672E+01	0.14550E+02
0.15000E+01	0.24990E+04	0.17910E+01	0.42062E+01	0.11250E+02
0.16000E+01	0.24800E+04	0.17910E+01	0.41148E+01	0.10000E+02
0.17000E+01	0.24720E+04	0.17910E+01	0.39624E+01	0.10250E+02

C*** PARTIAL LOAD REDUCTION 60% ***
C*** FINAL GENERATOR LOAD PG=0.44 KW
C*** RATED HEAD HN=21.0 (m)
C*** SYNCHRONOUS SPEED NR=2000.0

TIME T(SEC) **********	SPEED N(RPM) **********	FLOWRATE Q(l/s) **********	HEAD RISE PR(m) **********	GATE OPENING (%) **********
0.00000E+00	0.20000E+04	0.15038E+02	0.00000E+00	0.10000E+03
0.10000E+00	0.21700E+04	0.13310E+02	0.11897E+01	0.90000E+02
0.20000E+00	0.22750E+04	0.11045E+02	0.22250E+01	0.75300E+02
0.30000E+00	0.23500E+04	0.90624E+01	0.28224E+01	0.62000E+02
0.40000E+00	0.23950E+04	0.76464E+01	0.32918E+01	0.54000E+02
0.50000E+00	0.24300E+04	0.65835E+01	0.35965E+01	0.45300E+02
0.60000E+00	0.24500E+04	0.60088E+01	0.39319E+01	0.40000E+02
0.70000E+00	0.24550E+04	0.53808E+01	0.40843E+01	0.34000E+02
0.80000E+00	0.24430E+04	0.47144E+01	0.42367E+01	0.30000E+02
0.90000E+00	0.24230E+04	0.44096E+01	0.39319E+01	0.26500E+02
0.10000E+01	0.24000E+04	0.39648E+01	0.40843E+01	0.24000E+02
0.11000E+01	0.23850E+04	0.38032E+01	0.39624E+01	0.22000E+02
0.12000E+01	0.23600E+04	0.33784E+01	0.38710E+01	0.21000E+02
0.13000E+01	0.23250E+04	0.32984E+01	0.36576E+01	0.20000E+02
0.14000E+01	0.23000E+04	0.33084E+01	0.33528E+01	0.18500E+02
0.15000E+01	0.22750E+04	0.32884E+01	0.30175E+01	0.18500E+02
0.16000E+01	0.22450E+04	0.33484E+01	0.27432E+01	0.18500E+02
0.17000E+01	0.22300E+04	0.33884E+01	0.24384E+01	0.18500E+02

C*** PARTIAL LOAD REJECTION 63% ***
C*** FINAL GENERATOR LOAD PG=0.9 KW
C*** RATED HEAD HN=21.0 (m)
C*** SYNCHRONOUS SPEED NR=2000.0 RPM

TIME T(SEC)	SPEED N(RPM)	FLOWRATE Q(l/s)	HEAD RISE PR(m)	GATE OPENING (%)
0.00000E+00	0.20320E+04	0.14986E+02	0.00000E+00	0.10000E+03
0.10000E+00	0.21850E+04	0.13092E+02	0.78029E+00	0.91375E+02
0.20000E+00	0.22760E+04	0.11359E+02	0.19507E+01	0.78112E+02
0.30000E+00	0.23460E+04	0.97449E+01	0.24689E+01	0.66250E+02
0.40000E+00	0.23800E+04	0.85724E+01	0.30785E+01	0.55750E+02
0.50000E+00	0.23990E+04	0.71681E+01	0.32736E+01	0.48000E+02
0.60000E+00	0.23890E+04	0.63468E+01	0.36119E+01	0.43120E+02
0.70000E+00	0.23760E+04	0.59076E+01	0.36881E+01	0.36000E+02
0.80000E+00	0.23500E+04	0.53213E+01	0.38283E+01	0.30125E+02
0.90000E+00	0.23300E+04	0.50410E+01	0.35357E+01	0.28120E+02
0.10000E+01	0.23000E+04	0.47861E+01	0.33833E+01	0.26250E+02
0.11000E+01	0.22600E+04	0.43924E+01	0.31090E+01	0.26240E+02
0.12000E+01	0.22140E+04	0.43301E+01	0.29870E+01	0.26260E+02
0.13000E+01	0.21780E+04	0.43046E+01	0.26822E+01	0.26260E+02
0.14000E+01	0.21450E+04	0.43046E+01	0.23774E+01	0.26260E+02
0.15000E+01	0.21000E+04	0.43046E+01	0.21031E+01	0.26260E+02
0.16000E+01	0.20860E+04	0.43046E+01	0.17678E+01	0.26260E+02
0.17000E+01	0.20550E+04	0.43046E+01	0.12497E+01	0.26260E+02

[*** PARTIAL LOAD REJECTION 31% ***
[*** FINAL GENERATOR LOAD PG=1.5 KW
[*** RATED HEAD HN=21(m)
[*** SYNCHRONOUS SPEED NR=2000.0 RPM

TIME T(SEC)	SPEED N(RPM)	FLOWRATE Q(l/s)	HEAD RISE PR(m)	GATE OPENING (%)
0.00000E+00	0.20000E+04	0.15083E+02	0.00000E+00	0.10000E+03
0.10000E+00	0.21200E+04	0.13772E+02	0.67056E+00	0.92800E+02
0.20000E+00	0.21600E+04	0.12665E+02	0.14021E+01	0.80920E+02
0.30000E+00	0.21950E+04	0.10643E+02	0.21336E+01	0.73180E+02
0.40000E+00	0.22000E+04	0.93966E+01	0.23774E+01	0.62250E+02
0.50000E+00	0.22200E+04	0.84648E+01	0.27432E+01	0.55500E+02
0.60000E+00	0.21930E+04	0.79296E+01	0.28651E+01	0.51500E+02
0.70000E+00	0.21700E+04	0.77314E+01	0.26213E+01	0.49000E+02
0.80000E+00	0.21450E+04	0.75898E+01	0.22250E+01	0.49000E+02
0.90000E+00	0.21200E+04	0.73604E+01	0.18288E+01	0.49000E+02
0.10000E+01	0.20850E+04	0.73066E+01	0.15240E+01	0.49000E+02
0.11000E+01	0.20680E+04	0.73066E+01	0.12192E+01	0.49000E+02
0.12000E+01	0.20550E+04	0.73066E+01	0.91440E+00	0.49000E+02
0.13000E+01	0.20510E+04	0.73066E+01	0.60960E+00	0.49000E+02
0.14000E+01	0.20480E+04	0.73066E+01	0.30480E+00	0.49000E+02
0.15000E+01	0.20460E+04	0.73066E+01	0.27432E+00	0.49000E+02

C*** PARTIAL LOAD REJECTION 10% ***
C*** FINAL GENERATOR LOAD PG=2.1 KW
C*** RATED HEAD HN=21.0 (m)
C*** SYNCHRONOUS SPEED NR=2000.0 RPM

TIME T(SEC)	SPEED N(RPM)	FLOWRATE Q(l/s)	HEAD RISE PR(m)	GATE OPENING (%)
0.00000E+00	0.20200E+04	0.14885E+02	0.00000E+00	0.10000E+03
0.10000E+00	0.20580E+04	0.13982E+02	0.60960E+00	0.93000E+02
0.20000E+00	0.20700E+04	0.13027E+02	0.97536E+00	0.86000E+02
0.30000E+00	0.20730E+04	0.11894E+02	0.13411E+01	0.78000E+02
0.40000E+00	0.20600E+04	0.10895E+02	0.17374E+01	0.70500E+02
0.50000E+00	0.20360E+04	0.10563E+02	0.16490E+01	0.69500E+02
0.60000E+00	0.20160E+04	0.10478E+02	0.15911E+01	0.68000E+02
0.70000E+00	0.20200E+04	0.10337E+02	0.13105E+01	0.68000E+02
0.80000E+00	0.20200E+04	0.10195E+02	0.10058E+01	0.68000E+02
0.90000E+00	0.20200E+04	0.10195E+02	0.67056E+00	0.68000E+02
0.10000E+01	0.20200E+04	0.10195E+02	0.30528E+00	0.68000E+02
0.11000E+01	0.20200E+04	0.10195E+02	0.15336E+00	0.68000E+02
0.12000E+01	0.20200E+04	0.10195E+02	0.60960E-01	0.68000E+02
0.13000E+01	0.20200E+04	0.10195E+02	0.36576E-01	0.68000E+02
0.14000E+01	0.20200E+04	0.10195E+02	0.36576E-01	0.68000E+02

****

APPENDIX (C)

****

INITIAL CONDITION DATA

6. 4. 32.2 1104.0 0.0 2000. 0.531 70.0 0.015 0.0015

0.987874319 0.0 0.96 0.00318 1.2 0.015 0.00318

1200 0.27899999 0.78034512

1.0 0.6 0.0023 0.27 0.0173 0.47 0.02

1. 0.0 0.0 0.0 1.

1. 1. 1. 1. 1. 1.

9.5 1.0 16 1.6

**** TURBINE CHARACTERISTIC DATA ***

UNIT SPEED VS UNIT FLOW DATA

NUMBER OF GATE OPENING

4

0.2500000 0.5000000 0.7500000 1.000000

NUMBER OF UNIT SPEED VS UNIT FLOW PONITS

10

UNIT SPEED	UNIT FLOW
0.1011900	0.1080700
0.1762800	0.1080700
0.2529900	0.1080700
0.3525600	0.1070000
0.4765500	9.8439999E-02
0.6855000	9.4159998E-02
0.7932000	8.5599996E-02
0.8487000	8.0250002E-02
0.8911800	7.4900001E-02

0.9466801	6.7410000E-02
14	
8.1615001E-02	0.1819000
0.1550550	0.1808300
0.2285100	0.1797600
0.3100500	0.1781500
0.3917250	0.1765502
0.4696600	0.1733400
0.5875950	0.1679900
0.7181700	0.1562200
0.7998000	0.1465900
0.8846551	0.1348200
0.9287250	0.1273300
0.9662700	0.1187700
1.002150	0.1123500
1.031550	0.1016500
17	
8.1615001E-02	0.2430556
0.1632000	0.2396800
0.2350500	0.2386101
0.3231750	0.2364700
0.4015500	0.2354000
0.4815000	0.2327250
0.5451600	0.2300500
0.6349500	0.2257700
0.7018500	0.2193500
0.7704000	0.2107900
0.8586000	0.1979500
0.9060000	0.1872500
0.9630001	0.1722700
0.9956400	0.1626400
1.028250	0.1524750
1.054500	0.1433800
1.083750	0.1316100
17	
0.1060950	0.3081600
0.1926000	0.3060200
0.2774745	0.3049500
0.3623505	0.3038800
0.4570200	0.3006711
0.5549505	0.2974600

0.6153427	0.2942500
0.7018500	0.2889000
0.7834650	0.2803400
0.8487480	0.2717800
0.9271500	0.2546600
0.9793260	0.2396800
1.028295	0.2268400
1.051140	0.2097200
1.077258	0.1958098
1.096875	0.1829698
1.113165	0.1690600

UNIT SPEED VS UNIT POWER DATA

NUMBER OF GATE OPENING

4

0.2500000 0.5000000 0.7500000 1.000000

NUMBER OF UNIT SPEED VS UNIT POWER POINTS

10

UNIT SPEED	UNIT POWER
0.1011900	1.2475353E-03
0.1762600	2.4950707E-03
0.2529900	3.7426064E-03
0.3525600	4.9407338E-03
0.4765500	5.6818440E-03
0.6855000	5.4348069E-03
0.7932000	3.9525875E-03
0.8487000	2.7791630E-03
0.8911600	1.7292569E-03
0.9466801	7.7816559E-04

14

8.1615001E-02	2.0998120E-03
0.1550550	4.1749203E-03
0.2285100	6.2253247E-03
0.3100500	8.2263229E-03
0.3917250	1.0190264E-02
0.4896600	1.2005984E-02
0.5875950	1.2605048E-02

0.7181700	1.1721891E-02
0.7998000	1.0153209E-02
0.8846551	7.7816565E-03
0.9287250	5.8794734E-03
0.9662700	4.1131615E-03
1.002150	2.5938854E-03
1.031550	1.1734243E-03

17

8.1615001E-02	2.7791630E-03
0.1532000	5.5336226E-03
0.2350500	8.2633775E-03
0.3231750	1.0919022E-02
0.4015500	1.3587018E-02
0.4815000	1.6119147E-02
0.5451600	1.7261691E-02
0.6349500	1.8243661E-02
0.7018500	1.8099729E-02
0.7704000	1.7033182E-02
0.8586000	1.4853082E-02
0.9060000	1.2969427E-02
0.9630001	9.9432273E-03
0.9956400	7.5099203E-03
1.028295	5.2804099E-03
1.054500	3.3102920E-03
1.083750	1.5192757E-03

17

0.1060950	3.5573286E-03
0.1926000	7.1146232E-03
0.2774745	1.0560819E-02
0.3523505	1.4031685E-02
0.4570200	1.7354328E-02
0.5549505	2.0602861E-02
0.6153427	2.2078905E-02
0.7018500	2.3344969E-02
0.7834650	2.3138694E-02
0.8487480	2.1961564E-02
0.9271500	1.9108290E-02
0.9793260	1.6600868E-02
1.028295	1.3092945E-02
1.051140	9.6838381E-03
1.077258	6.7811576E-03
1.096845	4.2243279E-03
1.113165	1.9515899E-03

APPENDIX D

D.1 Derivation of equation (5.6).

Let $\ell_{i(x)} = z$, $y_r = \frac{x-x_r}{x_j-x_r}$, $y_k = \frac{x-x_k}{x_j-x_k}$

and $z = y_1\, y_2\, y_3 \ldots\ldots y_r$

Then $\log z = \log y_1 + \log y_2 + \log y_3 \,,\ldots\ldots, + \log y_r$

Differentiate both sides of the equation with respect to x.

$$\frac{1}{z}\frac{\partial z}{\partial x} = \frac{1}{y_1}\ \frac{\partial y_1}{\partial x} + \frac{1}{y_2}\frac{\partial y_2}{\partial x} + \frac{1}{y_3}\frac{\partial y_3}{\partial x} \ldots\ldots + \frac{1}{y_r}\frac{\partial y_r}{\partial x}$$

Multiply both sides by z and let dy/dx = y'

$$\frac{\partial z}{\partial x} = y_1'\, y_2\, y_3 \ldots\ldots y_r + y_1\, y_2'\, y_3 \ldots\ldots y_r + y_1\, y_2\, y_3' \ldots y_r$$
$$+ y_1\, y_2\, y_3 \ldots\ldots y_r'$$

$$= \frac{\partial}{\partial x}\left(\prod_{r=1}^{m} y_r\right)$$

$$= \sum_{k=1}^{m}\left(\prod_{\substack{r=1\\ r\neq k}}^{m} y_r\right)\frac{\partial y_k}{\partial x}$$

But $y_k = \frac{x-x_k}{x_j-x_k}$

and $\frac{\partial y_k}{\partial x} = \frac{1}{x_j-x_k}$

$$\therefore \frac{\partial \ell_{i(x)}}{\partial x} = \sum_{\substack{k=1\\ k\neq j}}^{m}\left(\frac{1}{x_j-x_k}\right)\prod_{\substack{r=1\\ r\neq j\\ r\neq k}}^{m}\frac{x-x_r}{x_j-x_r} \qquad (5.6)$$

D.2 Derivation of equation (5.7).

By the previous method the second derivative of equation (3.43) can be derived.

Then

$$\frac{\partial}{\partial x}\left(\frac{\partial \ell_{i(x)}}{\partial x}\right) = \sum_{\substack{k=1\\k\neq j}}^{m} \left(\frac{1}{x_j - x_k}\right)\left(\frac{\partial}{\partial x}\left(\prod_{\substack{r=1\\r\neq j\\r\neq k}}^{m} \frac{x-x_r}{x_j-x_r}\right)\right)$$

Substitute equation (5.6)

$$\frac{\partial^2 \ell_{i(x)}}{\partial x^2} = \sum_{\substack{\ell=1\\\ell\neq j}}^{m} \left(\frac{1}{x_j - x_\ell}\right) \sum_{\substack{k=1\\k\neq j\\k\neq \ell}}^{m} \left(\frac{1}{x_j-x_k}\right) \prod_{\substack{r=1\\r\neq j\\r\neq k\\r\neq \ell}}^{m} \frac{x-x_r}{x_j-x_r} \qquad (5.7)$$

```
C*********************     APPENDIX  E  ***********************
C*************************************************************
C
C          TRANSIENTS CAUSED BY LOAD CHANGES ON
C                      TURBOGENERATOR SET
C
C*************************************************************
C*************************************************************
C
                          PROGRAM MAIN
C*************************************************************
C*************************************************************
C   N=ROTATIONAL SPEED (RPM)  NR=RATED SPEED (RPM)
C   AREA=CROSS-SECTIONAL AREA OF PIPE (M**2)
C   A=WATERHAMMER WAVE VELOCITY (m/s) D=PIPE DIAM-
C   ETEP (m) DR=TURBINE RUNNER DIAMETER (m) F=DAR-
C   CY-WEISBACH FRICTION FACTOR G=ACCELERATION DUE TO
C   GRAVITY (M/S**2) n=N/NR PHI=UNIT SPEED QI=UNIT FLOW
C   P=UNIT POWER PG=POWER OF GENERATOR (KW) ETAG=GENERATOR
C   EFFICIENCY SEGMA=PERMANENT SPEED DROOP NTAU=NUMBER OF
C   GATE OPENING CURVES FROM TURBINE CHARACTERISTICS
C   NPHI=NUMBER OF UNIT SPEED HA=PIEZOMETRIC HEAD AT
C   BEGIVING OF TIME STEP HN=NET HEAD(m) HP=PIEZOMETRIC
C   HEAD AT END OF TIME STEP HT=TAILWATER LEVEL ABOVE THE
C   DATUM (m) II=MOMENT OF INERTIA OF ROTATIONAL PARTS
C   (KG.M**2) KD=GAIN OF DERIVATIVE ELEMENT KE=VOLTAGE
C   CONSTANT OF STEP MOTOR (VOLTS/RADIAN) KI=MAGNETIC NULL
C   DISPLACEMENT CONSTAN OF STEP MOTOR (RADIANS/AMP)
C   KM=CONSTANT OF ANALOGUE MULTIPLIER KP=GAIN OF PROPOR-
C   IONAL ELEMENT QA=FLOW AT BEGINNING OF TIME STEP (1/s)
C   QP=FLOW AT THE END TIME STEP (1/s)
C   R=RESISTANSE OF STEP MOTOR WINDINGS TA=SMOOTHING NET-
C   WORK TIME CONSTANT TD=TIME CONSTANT OF THE DERIVATIVE
C   ELEMENT TI=TIME CONSTANT OF THE INTEGRAL ELEMENT
C   TS=TIME CONSTANT OF STEP MOTOR WINDING VA=SMOOTHING
C   NETWORK OUTPUT VD=OUTPUT OF DERIVATIVE ELEMENT VI=
C   OUTPUT OF INTEGRAL ELEMENT VP=OUTPUT OF PROPORTIONAL
C   ELEMENT Z=INPUT TO DERIVATIVE,INTEGRAL AND PROPORTIONAL
C   ELEMENTS NPA=NUMBER OF PARTS INTO WHICH PIPE IS DIVIDED
C*************************************************************


      REAL N,NR,YA(6)
      COMMON /RC/NR/RUNGEC/NTIME,DT,Y(6),DY(6)/INITIALC/YREF(6)
      COMMON/ITERC3/QPA(100),HPA(100)
      CHARACTER* 3 CASE,FN*1,FILE*7
      READ(1,'(A3,1X,A1)') CASE,FN
      IF(CASE.NE.'NEW'.AND.CASE.NE.'OLD') STOP 'UNDEFIND CASE!'
      FILE='MP'//FN//'.PLO'
```

```
      IF(CASE.EQ.'OLD') THEN
      OPEN(14,ACCESS='DIRECT',RECL=60,NAME=FILE,STATUS='OLD',
     X      FORM='FORMATTED')
      READ(14,'(I5)',REC=1) IREC
      CALL DATA(1)
      READ(55,REC=1) T,IT,QP,PHII,HN,HP,Y,DY,CP,YN
      READ(55,REC=2)QPA
      READ(55,REC=3)HPA
      GO TO 80
      END IF
      OPEN(14,ACCESS='DIRECT',RECL=60,NAME=FILE,STATUS='NEW',
     X      FORM='FORMATTED')
      WRITE(14,'(5E12.5)',REC=1000.)0.0,0.0,0.0,0.0,0.0
      IREC=1
      T=0.0
      IT=0
      CALL DATA(0)
      WRITE(2,30)
      WRITE(2,50)Y
      DO 70 I=1,6
 70   YA(I)=YREF(I)*Y(I)
      WRITE(2,50) YA
 80   DO 10 II=1,NTIME
      T=T+DT
      IT=IT+1
      N=NR*Y(1)
      TAUI=Y(6) *YREF(6)
      CALL ITER(N,QP,TAUI,PHII,HN,HP,IT,PR,CP,YN)
      IF(((IT-1)/10)*10.EQ.IT-1) WRITE(2,60)IT-1,T-DT,N,QP,HN,HP
C     WRITE(2,60)IT-1,T-DT,N,QP,HN,HP
      IF(((IT-2)/10)*10.EQ.IT-2) THEN
      IREC=IREC+1
      WRITE(14,'(5E12.5)',REC=IREC) T-DT,N,QP,PR,Y(6)
      END IF
      END IF
      CALL RUNGE(PHII,TAUI,HN)
      IF((C(IT-1)/10)*10.EQ.IT-1) WRITE(2,50)Y
C     WRITE(2,50)Y
      DO 75 I=1,6
 75   YA(I)=YREF(I)*Y(I)
      IF(((IT-1)/10)*10.EQ.IT-1) WRITE(2,50) YA
C     WRITE(2,50)YA
      IF(Y(6).LT.0.0.OR.Y(6).GT.1)STOP'TAU OUT OF RANGE'
 10   CONTINUE
 30   FORMAT(3X,'IT,T,N,QP,HN,HP,N/NR,VI,VA,VD,VP,TAU:'/)
 50   FORMAT(60X,6G11.4)
 60   FORMAT(1H+,I4,6G11.4)
      WRITE(55,REC=1) T,IT,QP,PHII,HN,HP,Y,DY,CP,YN
      WRITE(55,REC=2)QPA
      WRITE(55,REC=3)HPA
```

```
      WRITE(14,'(I5)',REC=1) IREC
      STOP'O.K.'
      END


      SUBROUTINE DATA (IDATA)
      COMMON/INITIALC/YREF(6),SEGMA
      REAL NR,NREF,KP,II,K,KM,L,KI,KE,MC,NC,KD
      COMMON/TAUC/NTAU,TAU(40)/PHIC/NPHI(40),PHI(40,40)
     1 /ITERC/HT,S0,S1,S2,S3,S4,S5,S6/RC/NR,QA,R1,R2,R3,HA,HAA
     3 /DEC/E0,E1R,K,KM,NREF,TD,TI,TA,KP,MC,NC,KD
     4 /RUNGEC/NTIME,DT,Y(6),DY(6)/POINTS/Q(40,40),P(40,40)
     5 /ITERC2/S7,NPA,AREA,A,C,HS
      READ(10,*)NTAU
      READ(10,*)(TAU(I),I=1,NTAU)
      DO 10 I=1,NTAU
      READ(10,*)NPHI(I)
10    READ(10,*)(PHI(I,J),Q(I,J),J=1,NPHI(I))
      READ(20,*)NTAU2
      IF(NTAU2.NE.NTAU)STOP'CHARTS DATA ERROR'
      READ(20,*)(TAU(I),I=1,NTAU)
      DO 20 I=1,NTAU
      READ(20,*)NPHI(I)
20    READ(20,*)(PHI(I,J),P(I,J),J=1,NPHI(I))
      IF(IDATA.EQ.1)GO TO 50
      OPEN(55,ACCESS= 'DIRECT', STATUS= 'NEW',RECL=100)
      WRITE(2,22)
22    FORMAT(/5X,'DATA PARAMETERS'/5X,15(1H-))
      READ(1,*)DR,D,G,A,HT,NR,QA,HA,F,DT
      PI4=ATAN(1.0)
      AREA=PI4*D*D/144.
      R1=(DR/12.)**2
      S0=F*DT/(2.*AREA*D/12.)
      S1=G*AREA/A
      S2=0.5/AREA/A
      S3=DR/1836.
      S4=1.0/R1
      S5=DR**3/1838./144.
      S6=0.5/G/AREA**2
      R2=DR**3*NR/264672.
      R3=(R1*NR)**2/23460.
      READ(1,*)II,PG,ETAG,TI,KP,TA,TD,KD
      READ(1,*)NTIME,QIN,PHIIN
      READ(1,*)K,KM,L,R,KI,KE,SEGMA
      MC=(L+KE*KI)/R
      NC=KI/R
      E0=91.19*550.0*32.2/II/(NR**2)
      E1R=E0*PG/ETAG
      TAUIN=TAUF(PHIIN,QIN)
      NREF=1.0
```

```
C       INITIAL AND REFERANCE VALUES
          READ(1,*)(YREF(I),I=2,6)
          READ(1,*)(Y(I),I=1,6)
          READ(1,*)C,HS,NPA,DX
          S7=6263.8*F*DX/(D**5)
          YREF(6)=TAUIN
          DY(1)=0.0
          DY(5)=0.0
          DY(6)=0.0
          DY(2)=DY(2)*DT
          DY(3)=DY(3)*DT
          DY(4)=DY(4)*DT
          YREF(1)=NR
          WRITE(50,*) YREF,SEGMA
          WRITE(50,*) HT,S0,S1,S2,S3,S4,S5,S6,S7
          WRITE(50,*) NR,CA,R1,R2,R3,HA,HAA
          WRITE(50,*) E0,E1R,K,KM,NREF,TD,TI,TA,KP,MC,NC
          WRITE(50,*) NTIME,DT
          WRITE(50,*) C,HS,NPA,DX
          RETURN
   >0     READ(>0,*) YREF,SEGMA
          READ(50,*) HT,S0,S1,S2,S3,S4,S5,S6,S7
          READ(50,*) NR,CA,R1,R2,R3,HA,HAA
          READ(50,*) E0,E1R,K,KM,NREF,TD,TI,TA,KP,MC,NC
          READ(50,*) NTIME,DT
          READ(50,*) C,HS,NPA,DX
          RETURN
          END

          FUNCTION FACT(I,J,K,L,PHID)
          COMMON/PHIC/NPHI(40),PHI(40,40)
          INTEGER R
          FACT=1
          DO 10 R=1,NPHI(I)
          IF(R.EQ.J.OR.R.EQ.K.OR.R.EQ.L)GO TO 10
          FACT=FACT*(PHID-PHI(I,R))/(PHI(I,J)-PHI(I,R))
   10     CONTINUE
          RETURN
          END

          FUNCTION FLAG1(N,X,I,X0)
          DIMENSION X(N)
          INTEGER R
          FLAG1=1
          DO 10 R=1,N
          IF(R.NE.I)FLAG1=FLAG1*(X0-X(R))/(X(I)-X(R))
   10     CONTINUE
          RETURN
          END
```

```
      FUNCTION FLAG(I,J,PHID)
      FLAG=FACT(I,J,0,0,PHID)
      RETURN
      END

      FUNCTION DLAG(I,J,PHID)
      COMMON/PHIC/NPHI(40),PHI(40,40)
      DLAG=0.0
      DO 10 K=1,NPHI(I)
      IF(K.NE.J)DLAG=DLAG+FACT(I,J,K,0,PHID)/(PHI(I,J)-PHI(I,K))
10    CONTINUE
      END

      FUNCTION D2LAG(I,J,PHID)
      COMMON/PHIC/NPHI(40),PHI(40,40)
      D2LAG=0.0
      DO 20 K=1,NPHI(I)
      IF(K.EQ.J)GO TO 20
      S=0.0
      DO 10 L=1,NPHI(I)
      IF(L.EQ.J.OR.L.EQ.K)GO TO 10
      S=S+FACT(I,J,K,L,PHID)/(PHI(I,J)-PHI(I,L))
10    CONTINUE
      D2LAG=D2LAG+S/(PHI(I,J)-PHI(I,K))
20    CONTINUE
      RETURN
      END

      FUNCTION TAUF(PHII,QI)
      COMMON/TAUC/NTAU,TAU(40)/PHIC/NPHI(40)/POINTS/Q(40,40)
      DIMENSION Y(40)
      DO 50 I=1,NTAU
      Y(I)=0.0
      DO 50 J=1,NPHI(I)
50    Y(I)=Y(I)+Q(I,J)*FLAG(I,J,PHII)
      TAUF=0.0
      DO 100 I=1,NTAU
100   TAUF=TAUF+TAU(I)*FLAG1(NTAU,Y,I,QI)
      RETURN
      END

      FUNCTION ZI(TAUI,PHII,Z,ID)
      DIMENSION Z(40,40),Y(40)
      COMMON/TAUC/NTAU,TAU(40)/PHIC/NPHI(40)
C*** PIECEWISE LAGRANGEAN INTERPOLATION ***
      DO 10 I=1,NTAU
      IF(TAUI.LT.TAU(I)) GO TO 20
10    CONTINUE
      NI=NTAU-1
      GO TO 30
```

```
20      NI=I-1
        IF(NI.LT.1) NI=1
30      DO 50 I=NI,NI+1
        Y(I)=0.0
        DO 50 J=1,NPHI(I)
        IF(ID.EQ.0)F=FLAG(I,J,PHII)
        IF(ID.EQ.1)F=DLAG(I,J,PHII)
        IF(ID.EQ.2)F=D2LAG(I,J,PHII)
 50     Y(I)=Y(I)+F*Z(I,J)
        ZI=Y(NI)+(Y(NI+1)-Y(NI))/(TAU(NI+1)-TAU(NI))*(TAUI-TAU(NI))
C*** GENERAL LAGRANGEAN INTERPOLATION ***
C       DO 50 I=1,NTAU
C       Y(1)=0.0
C       DO 50 J=1,NPHI(I)
C       IF(ID.EQ.0)F=FLAG(I,J,PHII)
C       IF(ID.EQ.1)F=DLAG(I,J,PHII)
C       IF(ID.EQ.2)F=D2LAG(I,J,PHII)
C 50    Y(I)=Y(I)+F*Z(I,J)
C       ZI=0.0
C       DO 100 I=1,NTAU
C 100   ZI=ZI+Y(I)*FLAG1(NTAU,TAU,I,TAUI)
        RETURN
        END

        SUBROUTINE LINEAR(TAUI,PHII,QI,A0,A1)
        COMMON/POINTS/C(40,40)
        A1=ZI(TAUI,PHII,C,1)
        A0=QI-A1*PHII
        RETURN
        END

        SUBROUTINE PARABOLIC(TAUI,PHII,C0,C1,C2)
        COMMON/POINTS/C(40,40),P(40,40)
        C2=0.5*ZI(TAUI,PHII,P,2)
        C1=ZI(TAUI,PHII,P,1)-2.*C2*PHII
        C0=ZI(TAUI,PHII,P,0)-PHII*(C1+C2*PHII)
        RETURN
        END

        SUBROUTINE ITER(N,QP,TAUI,PHII,HN,HP,IC,PR,CP,YN)
        REAL N,NR
        DATA ICOND/1/
        COMMON/POINTS/Q(40,40)/ITERC/HT,S0,S1,S2,S3,
     1  S4,S5,S6/RC/NR,QA,R1,R2,R3,HA,HAA
     2  /ITERC3/QPA(100),HPA(100)
     3  /ITERC2/S7,NPA
        CALL CHARACTER(IC,CP,YN)
        IF(IC.EQ.1)THEN
        N=NR
        QP=QA
```

```
      HN=4A-0.7
      END IF
      IF(IC.EC.2)THEN
      CP=QA
      HN=(CP*(S2*QP-1)+CP)/S1-HT
      END IF
      IT=0
10    IT=IT+1
      SQHN=SQRT(HN)
      PHII=S3*N/SQHN
      IF(IC.EC.1)RETURN
      IF(IC.GT.2.AND.IT.GT.5) THEN
      HN=((CP-A3)/A2)**2
      END IF
      PHII=S3*N/SQRT(HN)
      QI=ZI(TAUI,PHII,U,0)
      CALL LINEAR(TAUI,PHII,QI,A0,A1)
      A2=A0*R1
      A3=A1*N*S5
      A4=S2-S1/A2/A2
      A5=2.*S1*A3/A2/A2-1.
      A6=CP-S1*(HT+(A3/A2)**2)
      DD=A5*A5-4.*A4*A6
      IF(A4.EC.0.0)GO TO 200
      IF(DD.LT.0.0)GO TO 200
      DQP=((-A5-SQRT(DD))/A4/2.-QP)
      QP=QP+DQP
      IF(ABS(DQP).LE.0.0001)GO TO 30
      IF(IT.GE.20)GO TO 20
      GO TO 10
20    PRINT*,'***DIVERGENCE'
      WRITE(2,50)'A0,A1,A2,A3,A4,A5,A6,DQP,QP=',
     1  A0,A1,A2,A3,A4,A5,A6,DQP,QP
      STOP
   30 HN=((QP-A3)/A2)**2
      HP=HN+HT-S6*QP*QP
      PR=HP-HAA
      QPA(NPA+1)=QP
      HPA(NPA+1)=HP
      RETURN
200   WRITE(2,50)'A0,A1,A2,A3,A4,A5,A6,DQP,QP=',
     1  A0,A1,A2,A3,A4,A5,A6,DQP,QP
      STOP'ITERATION ERROR'
50    FORMAT(A30/9G12.4/)
      END

      SUBROUTINE RUNGE(PHII,TAUI,HN)
      DIMENSION ICOND(6)
      REAL K,KM,NREF,KP,MC,N1,N2,N3,N4,NC,KD
      DATA ICOND/6*1/
```

```
      COMMON/INITIALC/YREF(6),SEGMA
      COMMON/FC/NR,GA,R1,R2,R3/DEC/E0,E1R,K,KM,NREF,TD,TI
     1   ,TA,KP,MC,NC,KD/RUNGEC/NTIME,DT,Y(6),DY(6)
C*************************************************************
      DN(Y)=(E1/Y+E2+E3*Y)*DT
      DG(VA,G)=(NC*VA*(YREF(3)/YREF(6))-G)/MC*DT
      DZ(DY,DGT)=KM/YREF(5)*(K*DY+SEGMA*DGT*YREF(6))*NREF
      D2VD(DZT,DVD,VD)=(KD*DZT*(YREF(5)/YREF(4))-2.0*TD*DVD-VD)/
     1                  TD**2*DT2
      D2VI(DVIT,VI,Z)=(Z*(YREF(5)/YREF(2))-VI-2*TI*DVIT)
     1                 /TI**2*DT2
      D2VA(VA,VI,VD,Z,DVA)=(VI*(YREF(2)/YREF(3))+VD*(YREF(4)
     1  /YREF(3))+KP*Z*(YREF(5)/YREF(3))-VA-2*TA*DVA)/TA**2*DT2

      ZF(Y,G)=KM/YREF(6)*(K*Y+SEGMA*G*YREF(6))*NREF
      CALL PARABOLIC(TAUI,PHII,C0,C1,C2)
      A7=R1*C0*HN**1.5
      A8=R2*C1*HN
      A9=R3*C2*SQRT(HN)
      E1=E0*A7-E1R
      E2=E0*A8
      E3=EC*A9
      DT2=DT*DT/2.
C*************************************************************
      N1=Y(1)
      DN1=DN(N1)
      G1=Y(6)
      VA1=Y(3)
      DG1=DG(VA1,G1)
      DZ1=DZ(DN1,DG1)
      DVD1=DY(4)
      VD1=Y(4)
      D2VD1=D2VD(DZ1,DVD1,VD1)
      DVI1=DY(2)
      VI1=Y(2)
      D2VI1=D2VI(DVI1,VI1,DZ1)
      Z1=ZF(N1,G1)
      DVA1=DY(3)
      D2VA1=D2VA(VA1,VI1,VD1,Z1,DVA1)
C*************************************************************
      N2=Y(1)+DN1/2
      DN2=DN(N2)
      G2=Y(6)+DG1/2
      VA2=Y(3)+DY(3)/2+D2VA1/4
      DG2=DG(VA2,G2)
      DZ2=DZ(DN2,DG2)
      DVD2=DY(4)+D2VD1
      VD2=Y(4)+DY(4)/2+D2VD1/4
      D2VD2=D2VD(DZ2,DVD2,VD2)
      DVI2=DY(2)+D2VI1
```

```
      VI2=Y(2)+DY(2)/2+D2VI1/4
      D2VI2=D2VI(DVI2,VI2,DZ2)
      Z2=ZF(N2,G2)
      DVA2=DY(3)+D2VA1
      D2VA2=D2VA(VA2,VI2,VD2,Z2,DVA2)
C*****************************************************
      N3=Y(1)+DN2/2
      DN3=DN(N3)
      G3=Y(6)+DG2/2
      VA3=Y(3)+DY(3)/2+D2VA1/4
      DG3=DG(VA3,G3)
      DZ3=DZ(DN3,DG3)
      DVD3=DY(4)+D2VD2
      VD3=Y(4)+DY(4)/2+D2VD1/4
      D2VD3=D2VD(DZ3,DVD3,VD3)
      DVI3=DY(2)+D2VI2
      VI3=Y(2)+DY(2)/2+D2VI1/4
      D2VI3=D2VI(DVI3,VI3,DZ3)
      Z3=ZF(N3,G3)
      DVA3=DY(3)+D2VA2
      D2VA3=D2VA(VA3,VI3,VD3,Z3,DVA3)
C*****************************************************
      N4=Y(1)+DN3
      DN4=DN(N4)
      G4=Y(6)+DG3
      VA4=Y(3)+DY(3)+D2VA3
      DG4=DG(VA4,G4)
      DZ4=DZ(DN4,DG4)
      DVD4=DY(4)+2*D2VD3
      VD4=Y(4)+DY(4)+D2VD3
      D2VD4=D2VD(DZ4,DVD4,VD4)
      DVI4=DY(2)+2*D2VI3
      VI4=Y(2)+DY(2)+D2VI3
      D2VI4=D2VI(DVI4,VI4,DZ4)
      Z4=ZF(N4,G4)
      DVA4=DY(3)+2*D2VA3
      D2VA4=D2VA(VA4,VI4,VD4,Z4,DVA4)
C*****************************************************
      Y(1)=Y(1)+(DN1+2*DN2+2*DN3+DN4)/6*0.92
      Y(6)=Y(6)+(DG1+2*DG2+2*DG3+DG4)/6
      Y(5)=ZF(Y(1),Y(6))*KP
      Y(4)=Y(4)+(D2VD1+D2VD2+D2VD3)/3
      DY(4)=DY(4)+(D2VD1+2*D2VD2+2*D2VD3+D2VD4)/3
      Y(2)=Y(2)+(D2VI1+D2VI2+D2VI3)/3
      DY(2)=DY(2)+(D2VI1+2*D2VI2+2*D2VI3+D2V4)/3
      Y(3)=Y(3)+(D2VA1+D2VA2+D2VA3)/3
      DY(3)=DY(3)+(D2VA1+2*D2VA2+2*D2VA3+D2VA4)/3
      IF(Y(1).LT.0.99999999) NREF=-1.
      IF(Y(1).GT.1.0000001) NREF=1.
      RETURN
```

```
      END


      SUBROUTINE CHARACTER(IC,CP)
      DIMENSION  Q(100),H(100)
      COMMON /ITERC/HT,S0,S1/RC/NR,QA,R1,R2,R3,HA/ITERC2/S7,
     1 NPA,AREA,A,C,HS/ITERC3/QPA(100),HPA(100)
C***  COMPUTE STEADY-STATE CONDITIONS
      IF(IC.EQ.1)THEN
      FR=S7*QA**2
      DO 100 I=1,NPA+1
      Q(I)=QA
      H(I)=HA-(I-1)*FR
  100 CONTINUE
      RETURN
      END IF
C***  INITILIZATION
      IF(IC.GT.2)THEN
      DO 150 I=1,NPA+1
      Q(I)=QPA(I)
      H(I)=HPA(I)
  150 CONTINUE
      END IF
C***  COMPUTE H AND Q AT THE INTERIOR NODES ***
      DO 201 I=2,NPA
      CP=Q(I-1)+S1*H(I-1)-S0*Q(I-1)*ABS(Q(I-1))
      CN=Q(I+1)-S1*H(I+1)-S0*Q(I+1)*ABS(Q(I+1))
      QPA(I)=0.5*(CP+CN)
      HPA(I)=0.5*(CP-CN)/S1
  201 CONTINUE
C***  COMPUTE CP AT A DISTANCE DX FROM THE INLET
C                  OF THE TURBINE
      CP=Q(NPA)+S1*H(NPA)-S0*Q(NPA)*ABS(Q(NPA))
C***  COMPUTE H AND Q AT UPSTREAM END  ***
      CN=Q(2)-S1*H(2)-S0*Q(2)*ABS(Q(2))
      G=(20.3*S1)**2
      R=40.6*S1
      F=-(CN+96.0*S1)
      V=2*F
      E=1.0+R*F+20.3/85.0
      HB=F*F-95.0/85.0
      IT=0
      IF(YN.EQ.0.0) YN=1.3549
   19 IT=IT+1
      PYN=YN
      F1=3*PYN**4+R*PYN**3+E*PYN**2+V*PYN+HB
      F2=4.*G*PYN**3+3.*R*PYN**2+2.*E*PYN+V
      DELYN=F1/F2
      IF(ABS(DELYN).GT.0.001)DELYN=SIGN(0.001,DELYN)
      YN=PYN-DELYN
```

```
      IF(ABS(YN-PYN).LE.0.0001)GO TO 31
      IF(IT.GE.20)GO TO 21
      GO TO 19
21    PRINT*,'***DIVERGENCE'
      STOP
31    HPA(1)=96.0-20.3*YN*YN
      QPA(1)=CN+S1*HPA(1)
      RETURN
      END
```

REFERENCES

1. JAEGER, C. — "Engineering Fluid Mechanics". Blackie and Son Ltd., London. 1960.

2. SWIECICKI, I. — "Regulation of a hydraulic turbine calculated by step-by-step method". Journal of Basic Engineering, September, 1961/445.

3. PERKINS, F.E. TEDROW, A.C. EAGLESON, P.W. IPPEN, A.T. — "Hydropower plant transients" Dept. of Civil Engineering, Hydrodynamics Lab., Report No. 71, Part II-III. Massachusetts Institute of Technology, September, 1964.

4. WOZNIAK, L. FETT, G.H. — "Conduit representation in closed loop simulation of hydroelectric system". Journal of Basic Engineering, American Society of Mechanical Engineers, pp. 599-604, September, 1972.

5. WYLIE, E.B. STREETER, V.L. — "Fluid Transients". McGraw-Hill Inc., New York, 1978.

6. CHAUDHRY, M.H. — "Applied Hydraulic Transients". Van Nostrand Reinhold Ltd., Canada, 1977.

7. CHAUDHRY, M.H. — "A non linear mathematical model for analysis of transients caused by a governed Francis turbine". 3rd International Conference on Pressure Surge, Canterbury, England, (Published by BHRA), March 25-27, 1980.

8. PAYNTER, H.M. — "A palimpsest on the electronic analogue act". A. Philbrick Researches Inc., Massachusetts, 1955.

9. HOVEY, H.M. — "Optimum adjustment of governors in Hydro generating stations". Engineering Journal, Engineering Inst. of Canada, pp.64-71, November, 1960.

10. CHAUDHRY, M.H. — "Governing stability of a hydroelectric power plant". Water power, London, pp.131-136, April, 1970.

11. THORNE, D.H. HILL, E.F. — "Extension of stability boundaries of hydraulic turbine generating unit". Trans. on Power Apparatus and systems, American Inst. of Electrical and Electronic Engineers, Aps.94, No.4, pp.1401-1409, July/August, 1975.

12. DHALIWAL, N.S.
WICHERT, H.E.
"Analysis of PID governors in Multimachine system".
IEEE Trans. Vol.PAS-77, March/April, pp. 456-463, 1978.

13. HAGIHORA, S.
YOKOTA, H.
GODA, K.
ISOBE, K.
"Stability of hydraulic turbine generating unit controlled by PID Governor".
IEE Trans. Vol.PAS-98, No.6, pp.2294-2298, November/December, 1979.

14. PHI, D.T.
BOURQUE, E.T.
THORNE, D.H.
HILL, E.F.
"Analysis and application of the stability limits of hydro-generating unit".
IEEE PES Winter meeting, Atlanta, Georgia, February, 1-6, 1981.

15. COLLATZ, L.
"The numerical treatment of differential equations".
3rd Edition, New York, 1966.

16. DELGADO, N.A.
"Mathematical model of a stepping motor".
Trans. IEEE, Vol.AC14, August, 1969.

17. PRENTER, P.M.
"Splines and variational methods".
John Wiley and Sons, New York, 1975.

18. ODEN, J.T.
REDDY, J.N.
"An introduction to the mathematical theory of finite elements".
John Wiley and Sons, 1976.

19. WOZNIAK, L.
FEFF, G.H.
"Representation of pump-turbine characteristics".
ASME paper No.69-FE-7, June 16, 1969.

20. BRITISH STANDARD 1042
"Methods of measurement of fluid flow in closed conduits".
Part 1. Pressure differential devices, Section 1.1, BSI, London, 1981.

21. JONES, E.B.
"Instrumentation, Measurement and feedback".
McGraw-Hill, London. 1977.

22. JONES, M.H.
"A practical introduction to electronic circuits".
Cambridge University Press, London, 1982.

23. CLAYTON, G.B.
"Experiments with operational amplifiers; learning by doing".
MacMillan Press Ltd., 1978.

24. DOEBELIN, E.O.
"Dynamic analysis and feedback control".
McGraw-Hill, London, 1962.

25. RAVEN, F.H.
"Automatic control engineering".
McGraw-Hill Kogakusha Ltd. London. 1978.

26. BENEDICT, R.P. "Fundamentals of temperature, pressure and flow measurements". John Wiley and Sons, London, 1976.

27. KRUGER, R.E. "Selecting hydraulic reaction turbines". Engineering Monograph No.20, United States Department of the Interior, Bureau of Reclamation. 1980.